UNIVERSITY OF BIRMINGHAM

Fuel Production and Optimisation from Mixed Plastic Waste

By

Konstantina Stamouli

A thesis submitted to

The University of Birmingham

for the degree of

DOCTOR OF PHILOSOPHY

School of Chemical Engineering

College of Engineering and Physical Sciences

University of Birmingham

September 2017

Abstract

Increasing plastic consumption has created an alerting problem with waste disposal of the mixed waste plastics once the recyclable fractions have been recovered. The percentage sent to landfill of the generated mixed plastic waste amounts to one third of the total. Liquid fuel recovery from mixed plastic waste is possible using pyrolysis as a tertiary recycling process.

The focus of this study was to obtain useful liquid product recovered from the pyrolysis of a variety of commercial mixed plastic waste utilising a pilot scale fluidised bed reactor of 1kg/hr processing capacity. The influence of residence time (1.78 to 2.74s), feedstock variation and reaction temperature (500 – 550^{o}C) were investigated to optimise the quality of the wax products. Characterisation of the mixed plastic feedstocks through TGA, DSC and FTIR analysis was carried out to lay the foundation of the pyrolysis conditions. Understanding the fuel quality and product distribution was essential in assessing the key properties such as melting point and viscosity in the optimisation process.

Key findings of the research concluded that increasing residence time has the strongest effect on reducing the melting point (up to 14^{o}C) of the liquid product across all studied feedstocks although the magnitude of the effect greatly depends upon the initial feedstock composition. Changes is the average melting point correspond to a shift in the average carbon number distribution of the product. Feedstock and process parameters variability were also found to greatly affect the final product quality resulting

in a versatile product composition as well as the product yields that varied between 27 and 60% w.t.

Dedication

I would like to dedicate this thesis to my grandmother Siragoula who taught me to be strong and positive and has always been my inner strength.

Acknowledgements

I would like to extend my gratitude to the company that has engaged me in this project and has funded the largest part of my research. I am especially grateful to: Prof. Joseph Wood for his guidance, supervision, constructive comments and overall support and patience. I would also like to thank Dr. Gary A. Leeke for his input, challenges and support that have helped me overcome any setbacks.

If it hadn't been for Dr. Angela Fivga who I am also proud to think as my best friend I would have never embarked on this project and be inspired therefore I am deeply thankful. Without Nigel during my experiments all this work would not have been possible and enjoyable so thank you very much. Bill and Bob from the Chemical Engineering workshop have worked miracles on manufacturing parts in such a short time and always fuelled with a positive attitude. Lynn Draper has been an invaluable source of support and encouragement at times when it was most needed and for that I am extremely appreciative and would like to extend my gratitude.

Although a few lines are not enough to express that, without Ioanna this journey would have been less fun and meaningful, Annie has been there nearly every other day, Davidson has picked my moral up countless times, Flora had her hug open always, Abdulah had this strong faith in me and an amazing work ethic and George has always supported me in good and bad times. Saboor has been an inseparable part of this journey and I have been very happy and lucky to have him by my side.

Completion of this work would not have been possible if I didn’t have the support and motivation from my family and network of friends who have invested their time and patience during the past four years.

Contents

List of Figures

List of Tables

Chapter 1

Introduction

1. Background

The unique qualities of polymers and plastics in combination with their low value have created an exploding expansion for this material since it was first discovered in 1862 (Brydson 1999). Some of the key characteristics of plastics that have aided to their widespread use include their lightweight and flexible structure that can create a variety of products ranging from packing films to durable frames and pipes as well as building materials requiring less energy during the manufacturing process in comparison to glass or metal (North and Halden 2013). These properties in combination with their inexpensive quality have created a dominating reliance on this material worldwide over the past decades. Classification of the different plastic materials can be based either on their chemical structure, synthesis process or specific properties such as density and according to the resin identification code (RIC) set by the Society of Plastic Industry to facilitate recycling of plastic waste seven main plastic groups stated in Figure 1 have been identified based on their applications and properties (White 2013):

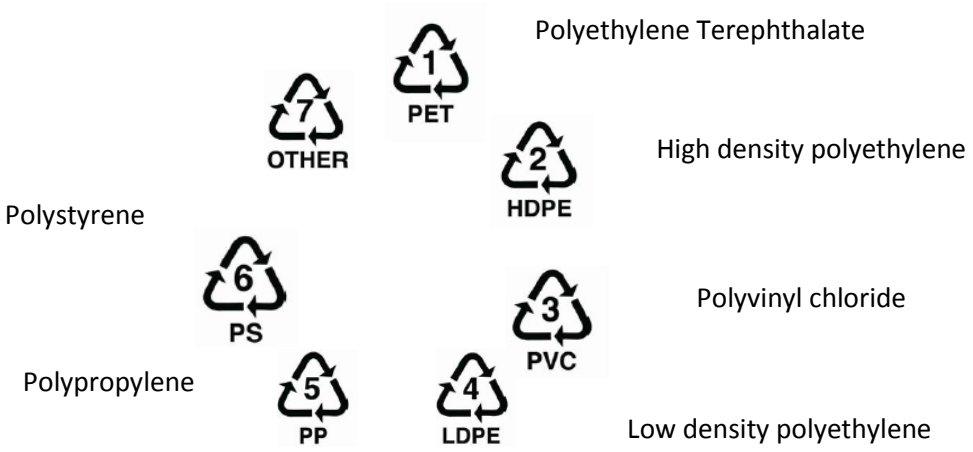

Figure 1: Main plastic group classification (Industry 1988).

The wider family of plastic materials are derived from organic products such as cellulose, coal, gas and crude oil. As shown in Figure 2 only 4 – 6 % of the oil and gas is used to produce plastics in Europe ((PEMRG) 2016). However, even with such a low percentage, coal, crude oil and gas are resources that will eventually deplete.

In addition when considering that a further 3 – 4 % of the existing oil production is used during the manufacturing process of plastics it is not wonder that they are consider a non-renewable resource (Hopewell, Dvorak et al. 2009). Depending on their specific characteristics and properties each plastic type shown in Figure 3 has the relevant suitable application. For example LDPE is the most common used plastic for carrier bags and packaging films (Industry 1988).

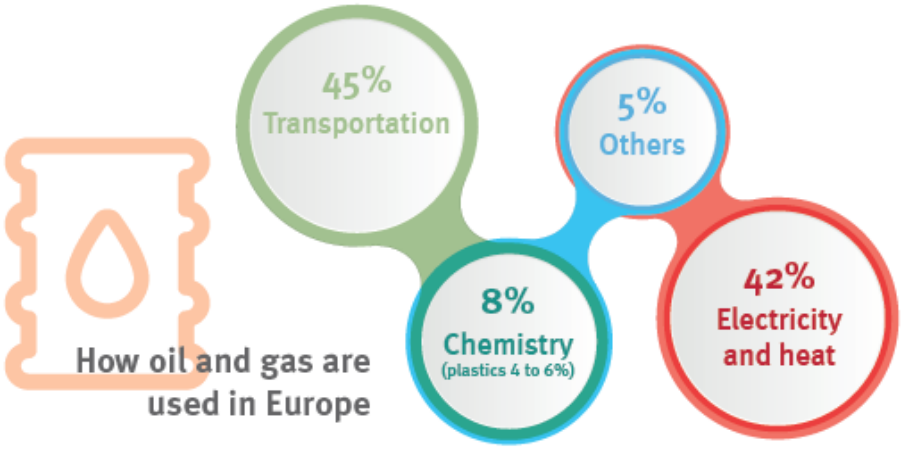

Figure 2: Percentage of oil and gas use for chemistry and plastic production in Europe ((PEMRG) 2016).

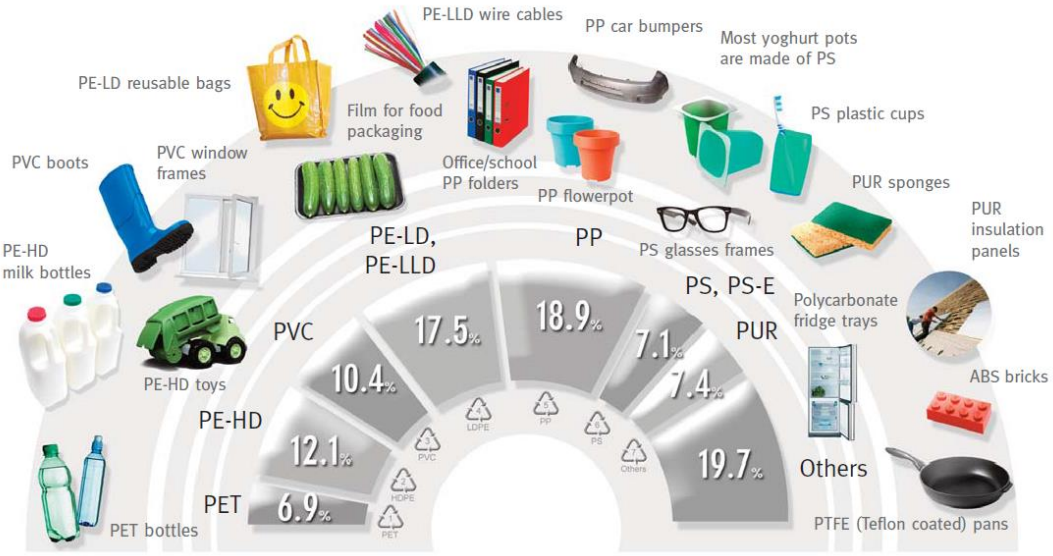

Figure 3: European plastic demand by polymer and indicative applications per polymer type ((PEMRG) 2016).

However the side effect of the excessive use in combination with inappropriate disposal patterns have created a huge issue in the world associated with the waste generated after its end of life use. Natural decomposition time of plastics range from 5 to 500 years and in some occasions up to several thousand years depending on the

material making the disposal after the end of use a challenge. In Figure 4 the tremendous growth in world plastic production since 1950 is illustrated and this number in 2015 rose to 322 million tonnes with UK being one of the five main countries contributing to the 65% of total plastic demand in Europe ((PEMRG) 2016).

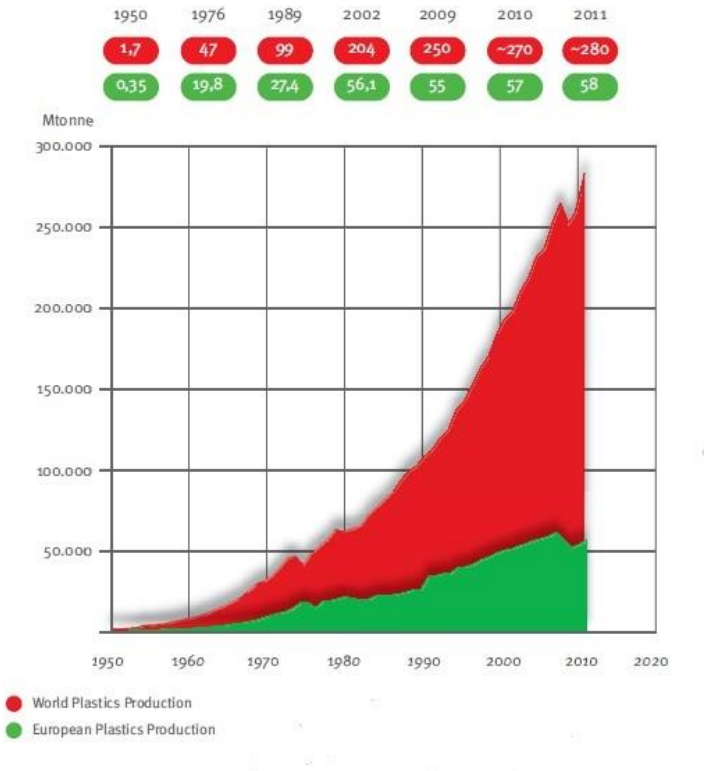

Figure 4: World plastic production 1950 – 2011 ((PEMRG) 2016).

After end of life use most of the consumer plastics are disposed with the packaging sector claiming up to 40% of the market share. In UK alone, plastic packaging waste arisings for 2014 came up to 2.2 million tonnes with an estimated overall UK waste plastic of 3.7 million tonnes ((WRAP) 2016). The breakdown for the plastic packaging arisings for UK in 2014 is shown in Table 1 (Foster 2008). Recycling has been employed to address and tackle the issue of plastic waste. Across the world different recycling schemes have been employed and in Europe specifically the Waste Framework Directive (WFD) has been the main driver to shape recycling and waste

policy. According to this directive increasing weight has been placed on recycling following the suggested waste hierarchy with energy recovery from waste being the last step to be considered before landfill disposal (Service 2011). In UK specifically, the landfill tax that has been implemented and currently stands at £86.10/tn for plastics in combination with the 5p carrier bag charge have contributed to diversion of specific waste streams ending in landfill (Customs 2017). Specifically the 5p carrier bag charge that was introduced in 2015 has reduced the number of used plastic carrier bags by 80% in England within a two year period and has proven to be successful (Affairs 2017).

Table 1: Plastic packaging waste for UK in 2014 in thousand tonnes (Foster 2008).

Consumer	LDPE/ LLDPE	HDPE	PET	PP	Other	Total
Bottles	1	188	397	5	2	594
Other rigid	7	27	278	114	98	525
Film	108	104	44	69	88	414
Total	**116**	**320**	**719**	**189**	**188**	**1,533**
Non-Consumer	**LDPE/ LLDEP**	**HDPE**	**PET**	**PP**	**Other**	**Total**
Bottles	0	203	18	5	5	231
Other rigid	0	15	21	42	30	108
Film	297	3	9	31	8	348
Total	**297**	**222**	**48**	**77**	**42**	**687**
Total	**LDPE/ LLDEP**	**HDPE**	**PET**	**PP**	**Other**	**Total**
Bottles	1	392	416	9	7	825
Other rigid	7	43	299	156	128	633
Film	406	108	53	100	96	762
Total	**414**	**542**	**767**	**266**	**231**	**2,220**

Sources: WRAP Plastic Flow 2014, WRAP Plastic Packaging Composition 2011

Local authority collection schemes vary depending on the area in UK however in 2013/2014 the total estimated collected plastic packaging waste was 500,000 tonnes nearly 60% higher compared to 2008/2009 volumes. Out of that 226,000 tonnes was PET bottles collected for recycling with LDPE, HDPE and PP being the main plastic

categories present in the waste stream and accounting for nearly 88% of the total generated plastic waste in UK. From the estimated 2.2 million tonnes, of generated waste plastic 891,000 plastic packaging was recycled in 2015 leaving approximately 1.31 million tonnes of non – recyclable waste to be directed towards landfill or energy from waste options((WRAP) 2016). Obviously with the priority being diversion and recycling of plastic waste there is still a huge amount of plastic waste to be tackled and treated.

1.2 Mixed Plastic Waste and related issues

The term mixed plastics incorporates all non – bottle plastic packaging from the domestic waste stream including rigid and flexible plastic items from various polymer types but excluding plastic bottles and non – packaging items. An estimated 1 million tonnes of domestic mixed plastic packaging waste in UK is collected at the kerbside per year and this number is increasing. This mixed waste stream will be directed in a materials recovery facility (MRF) and will be mixed with paper, card, cans and plastic bottlers prior to sorting. Post sorting the waste that has been left after all recyclable materials have been removed includes all the mixed leftover fractions which generally results in a much lower recycling rate of the mixed plastic waste stream (Foster 2008). This proportion still remains an issue due to unavailable sustainable waste management options relating to recycling technologies, financial implications and environmental issues. An example of a generic UK domestic mixed plastic feedstock in provided in Table 2. Further separation technologies such as flake and density

separation of such steams have been partially incorporated to specific waste management plants but are not fully deployed yet (Foster 2008).

Table 2: Generic composition of a UK mixed plastic waste stream (Foster 2008).

Polymer Type		Generic Composition (%)
Flexible	PE	25%
	PP	5%
Rigid	PP	17.2%
	PE	13.5%
	PET	15.3%
	PVC	3.5%
	PS	4%
Contamination		16.5%
Total		100%

Although technically all plastics can be recyclable either mechanically or as a feedstock there are limited benefits in doing so when considering all factors which leaves the window for alternative utilisation of such streams ((PEMRG) 2016).

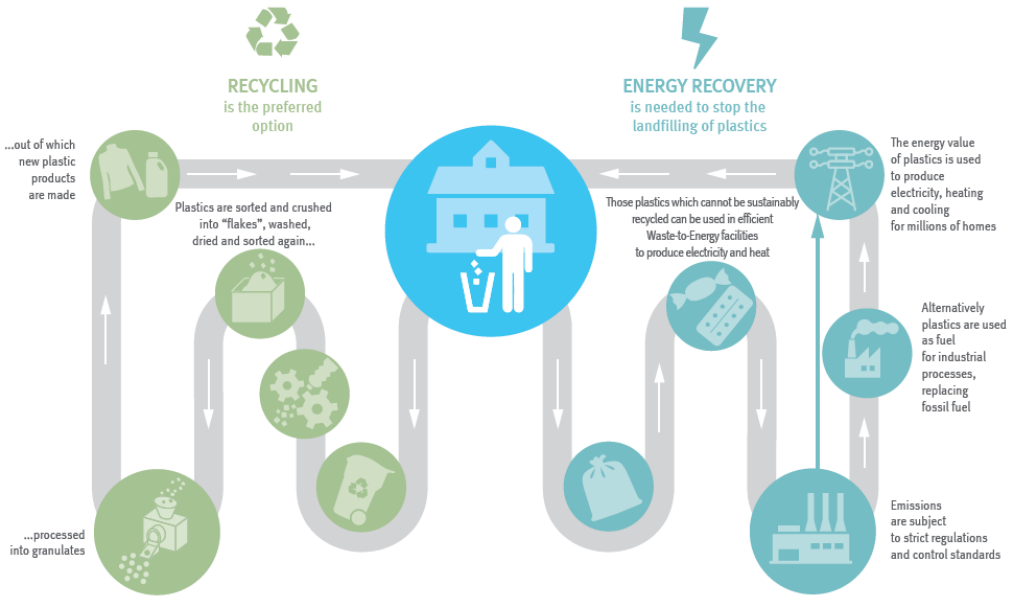

Figure 5: Suggested plastic resource circular economy ((PEMRG) 2016).

These mixed plastic streams that are not recycled generally end up in landfill or in energy from waste facilities that traditionally in UK have been associated with incineration facilities. An ideal closed loop circular approach excluding landfill is shown in Figure 5. In 2016, 8% of UKs municipal solid waste was incinerated through 15 existing incineration facilities, however the ratio of mixed plastic waste is limited normally up to 20% due to operational considerations (Foster 2008). The actual split in plastic waste treatment for Europe in 2014 is depicted in Figure 6.

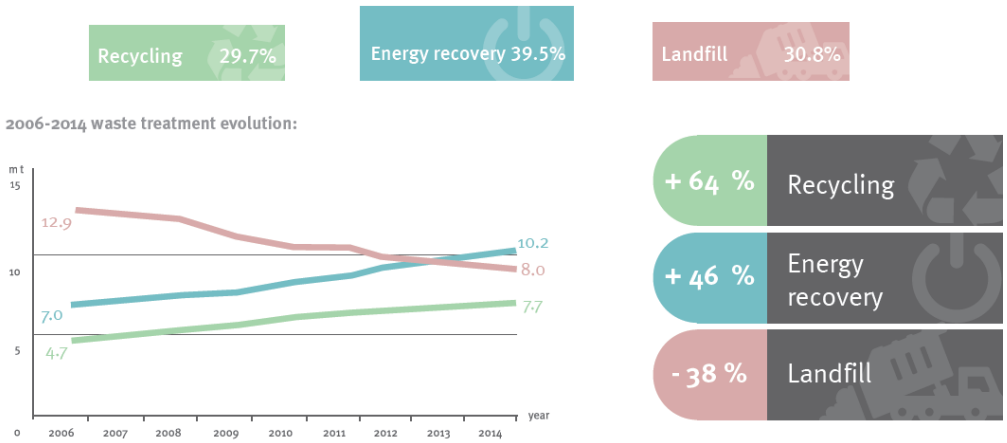

Figure 6: Plastics waste treatment in EU_{28+2} ((PEMRG) 2016).

According to this recycling rates and energy recovery have been on the increase with a corresponding decrease in landfill since 2007 ((PEMRG) 2016) and a similar trend is observed for UK with the total waste sent to landfill dropping to 23.1% in 2015 and 44.5% being recovered including recycling and energy recovery ((DEFRA) 2016). Energy from waste technologies, especially in UK have been focused on incineration installations with no or very limited applications in advanced thermal technologies such as gasification or pyrolysis that have minimised environmental impact in comparison to incineration (Foster 2008). The variation from one mixed plastic waste stream to another is increasingly variable therefore making it essential to identify the materials

and quantify the different fractions. The composition will have a direct impact on the environment and the relevant applications.

Landfill and marine disposal, have created a major issue with land and water contamination that is nearly impossible to reverse; making the need for immediate measures to be taken in the present across all levels of the waste management and disposal chain (Mr. Shailendra Mudgal 2011). Degraded plastic waste will end up accumulating either in water bodies and oceans or in underwater deposits through unregulated landfill sites and most recently from ingredients in the cosmetic industry creating issues with the microplastics (plastic fragments with size < 5mm) that have not been properly identified yet (DG Environment News Alert Service 2011).

Although we are aware of the problem the extent and size of it is still eluding us in its actual dimensions and full impact. Direct health implications affecting human and animal health and associated with chemicals present in plastics that are released during their degradation process have not yet been measured but flame retardants, phthalates and bisphenol are known substances to affect the endocrine system as well as specific toxic monomers (such as vinyl chloride, benzene, dioxins and plasticizers) that can affect the reproductive system and have been linked to cancer (Thompson, Moore et al. 2009, DG Environment News Alert Service 2011, North and Halden 2013, White 2013, Vipin Koushal 2014).

There is a major current issue with the waste and mixed plastic waste that has multiple implications on current available resources, land, waste management, environmental and health aspects of our everyday life. Although, significant measures have already been taken such as increasing recycling rates in several

countries, minimisation of disposed waste and reducing the average plastic product weight there is a huge area for further improvement specifically in energy from waste applications.

1.3 Background on fast pyrolysis and plastics

Recycling can be further divided into primary, secondary, tertiary and quaternary. Pyrolysis is considered alternatively as a tertiary recycling process where the original plastic can be converted into monomers or chemicals. It is the main conversion method for liquid hydrocarbon recovery from polymers. Pyrolysis is defined as the thermal decomposition of large molecular weight polymers under an inert environment towards the production of smaller molecular weight products (Williams and Williams 1997, Williams and Slaney 2007, (UNEP) 2009).

Policy and legislation have been the main drivers for energy from waste (EfW) applications. Following the waste hierarchy, energy recovery sits at the bottom of the pyramid. However, waste plastic can be considered as a resource rather than waste due to its abundancy and high heating value. That, in combination with a low retained moisture are favourable for most thermal conversion applications. Converting this resource that is currently wasted in a valuable fuel is a very interesting alternative and several technologies including pyrolysis, catalytic thermal degradation and gasification have been considered to achieve this (Demirbas 2004, Patni, Shah et al. 2013). Incineration of plastic waste releases hazardous substances such as dioxins, polychlorinated biphenyls, sulphur dioxide and furans (Yan, Liang et al. 2005, Hopewell, Dvorak et al. 2009). Appropriate selection of the conversion technology

greatly depends on the type of plastic to be converted as well as economic, environmental and technical aspects that need to be considered.

There is a direct link between the specific plastic types that can be considered for most conversion technologies. Plastics which may contain additives, flame retardants including bromine or antimony compounds and others containing nitrogen, halogens or sulphur all of which during the conversion process might release substances that pose a risk to human health are unsuitable. Preferable polymers that should be considered for conversion technology are PE, LDPE, HDPE, PP and PS and would lead to production of liquid fuels through pyrolysis, whereas PVC, PVA, PET, PUR , nylon and PTFE would be deemed unsuitable ((UNEP) 2009). It is for the above mentioned reasons, that the majority of research undertaken, has been focused on pure polymer feedstocks, in particular polyethylene, LDPE and HDPE, with known source of origin (Mastral, Esperanza et al. 2002, Cunliffe, Jones et al. 2003, Jung, Cho et al. 2010, Kumar and Singh 2011, Abbas-Abadi, Haghighi et al. 2014). Pure polymer materials in mixture combinations of known quantities and proportions have also been investigated, with less focus being put on real mixed plastic waste materials of unknown composition (Kiran, Ekinci et al. 2000, Bhaskar, Kaneko et al. 2004, Islam, Islam et al. 2004, Marcilla, García-Quesada et al. 2005, Lee and Shin 2007, Siddiqui and Redhwi 2009, López, de Marco et al. 2010).

Extensive research, has been undertaken in the past twenty years in order to better understand and optimise the pyrolysis of plastics specifically in relation to the suitability of different polymer materials for the process and the effect of the operating conditions (Kaminsky 1993, Williams and Williams 1999, Kaminsky, Predel et al. 2004, Kruse, Levine et al. 2005, Abbas-Abadi, Haghighi et al. 2014). Significant effort, has been

placed it the characterisation of the pyrolysis product and the effect that different feedstock composition might have as well as the variation of the process parameters (Kaminsky, Schlesselmann et al. 1996, Williams and Williams 1997, Kaminsky and Kim 1999, Pinto, Costa et al. 1999, Blazsó 2006, Arabiourrutia, Elordi et al. 2012, Sharma, Moser et al. 2014). A suggested range or reaction temperature has been provided in relation to the different polymers introduced in the process and further characterisation methods have been suggested based on the initial results from the conducted research using the PONA system (Paraffin, Olefin, Naphthene and aromatics) (Scheirs 2006). The wax/liquid product obtained from plastic pyrolysis has an average hydrocarbon chain length that can be comparative to various commercial fuels as shown in Table 3 (Lee 2006).

Table 3: Hydrocarbon range in commercial fuels (Lee 2006).

Fuels	*LPG*	*Petrol*	*Kerosene*	*Diesel*	*Heavy Fuel Oil (HVO)*
Hydrocarbons	$C_3 - C_4$	$C_4 - C_{12}$	$C_{12} - C_{15}$	$C_{12} - C_{24}$	$C_{12} - C_{70}$

According to, the majority of the reported results the wax/liquid product is situated towards the heavy fuel oil composition which is why a lot of sub sequent research utilising catalytic thermal degradation has been focused of further cracking the heavier components present with the aim of altering the average carbon length towards the diesel range (Akpanudoh, Gobin et al. 2005, Gulab, Jan et al. 2010, Artetxe, Lopez et al. 2013).

From all the previous conducted studies and research a satisfactory database of knowledge has been compiled with regards to:

- the fuel product composition from pyrolysis of single polymers or artificially prepared mixtures,
- suggested reaction kinetic models for the pyrolysis of plastic and plastic interaction in mixtures,
- characterisation polymer and polymer mixtures through analytical techniques,
- suggested reaction temperatures and residence time (or lapse time) and their respective effect on final product yields using different reactor and setups,
- effect of catalysts on further thermal decomposition of plastics pyrolysis and upgrading of the process

However, no specific studies have been identified, on pyrolysis of commercial mixed plastic waste with a bespoke fluidised bed reactor system able to cope with different mixed waste for the production of diesel range fuel which would be suitable to be used in an engine. Most identified systems either in batch or continuous operation were in small scale (100 g. up to 10kg/hr) or in micro scale (mg) and used only for feedstocks with a known composition. Any further work on actual MPW was done with analytical equipment and no comparative results have been found for the analysis of the produced fuel produced from a similar system and the selected feedstocks. Furthermore, although some work has been carried out in terms of the characterisation of artificially prepared plastic waste mixtures not sufficient work has been done in the characterisation of actual mixed waste streams with unknown components (Bhaskar, Kaneko et al. 2004, FakhrHoseini and Dastanian 2013). The proposed reactions and mechanisms that take place in pyrolysis of plastics are discussed in §2.3.2, with

different combinations of these reactions being adopted from researchers to develop models and explain the kinetics that take place in pyrolysis of plastics and plastic mixtures. Most of the suggested reactions and mechanisms however are based on pure polymers such as PE, PP, PS HDPE and lack the interaction between different polymers or the presence of oxygen and other contaminants in the plastic composition.

Finally, in terms of optimising specific fuel parameters like viscosity or density to achieve the desired goal; no previous work has been identified on this field nor utilising process parameters like residence time or reaction temperature to drive these parameters towards desired values to suit existing applications.

1.4 Aim and objectives of the study

The aim of the current study is to utilise and investigate existing mixed plastic waste feedstocks from UK commercial suppliers for the production of high quality fuel via fast pyrolysis process using a fluidised bed reactor. This end fuel product is intended for use in a high speed internal combustion engine. Initially, to achieve this the selected feedstocks have to be characterised as well as identify their main composition using literature data and comparing them with pure polymer materials in order to assess their potential for energy from waste applications particularly, with pyrolysis technology. The process developed is aimed to be a flexible process, able to accommodate a variety of mixed plastic waste feedstocks and to be scalable, therefore any conclusions derived will be incorporated in the scale up version. Any necessary

steps, identified to optimise the quality of the fuel in order to achieve the original aim have been incorporated in the current study. Specific objectives in this study were:

1. To identify specific plastic components from the commercial mixed waste feedstock and evaluate any material that could create issues in the process.
2. Through analytical techniques test small quantities of the samples under slow pyrolysis conditions and analyse the evolved gases and their composition to detect any possible harmful components.
3. Understand the kinetic models that apply to mixed plastics in order to interpret the results obtained in the quality of the fuel and adjust the process parameters accordingly to favour specific reactions.
4. Produce a diesel range fuel with the intention to utilise it in a high speed internal combustion engine and produce electricity on site to support the energy and heating demands of the plants where the pyrolysis equipment will be installed.
5. To understand and fully characterize the produced wax/liquid fuel from different mixed plastic feedstock streams.
6. To optimise the pyrolysis process in order to achieve objective in point 3 and should this not be achievable by optimising the process parameters, investigate suitable and relevant upgrading methods in situ or post process.

Building on, the previously completed research the current study aims to provide concrete information specific to the characterisation of mixed plastic waste, fuel product composition from the pyrolysis of this waste with a purpose built fluidised bed reactor system and also help understand how the key pyrolysis process parameters can be altered to optimise the relevant fuel properties. As a result, a commercial

solution could be provided to address the issue of treating non – recyclable mixed plastic waste and produce a useful product suitable for energy generation.

1.5 Thesis outline and overview

The structure of the thesis was based on the main objective set which was to produce a diesel range fuel with minimum contaminants in order to use it in a high speed internal combustion engine (3000 rpm ICE) for on - site energy and heat generation. To achieve this goal it was essential to address several of the issues traced from the problem of mixed plastic waste. These included the characterisation of the commercial mixed plastic waste feedstock followed by suggested design of experiments for the actual pyrolysis process. The experiments were based on the outcome of the feedstock characterisation. Characterisation of the liquid product and identification of the optimal process conditions that are specific for each feedstock was also considered an essential part of the study and needed fuel upgrading process. An analysis of the main influencing process parameters with regards to reducing the average fuel carbon number was a resulting part of the current study prior to suggesting further improvements with regards to catalytic upgrading methods.

Following, the introduction to the problem of mixed plastic waste, the all associated routes that are currently utilised to address this, a review on the current characterisation techniques and relevant progress in pyrolysis process, with connecting upgrading methods are all discussed in Chapter 2. The experimental setup, procedures and techniques used to characterise the feedstock and analyse the pyrolysis fuels are explained in Chapter 3.

Chapter 4 includes all the feedstock characterisation methods as well as analytical techniques to study the thermal degradation performance of the studied mixed plastic feedstocks. This chapter defined not only the expected composition of the mixed plastic steams but also helped define the operating process boundaries for the pilot scale pyrolysis experiments. Specific work that was carried out on actual unidentified mixed plastic waste feedstocks by combining TGA and DSC to verify the presence and quantity of specific polymers has not been found in previous work.

The core of all pyrolysis experiments and related discussion of results are summarised in Chapter 5 in combination with an evaluation of the outcome for each feedstock. Optimal conditions, in terms of the product wax/liquid fuel quality, have been analysed with the aim to reduce the melting point of the samples. A connection between, the melting point of the wax product fuel and the melting point has been established which was not identified in any previous work. A subsequent statistical analysis of the melting point of the samples to figure out which of the two investigated operating parameters, temperature and residence time, had the most significant impact on reducing the average melting point. Full analysis of key product samples was performed utilising viscosity, density, GC – MS, solubility and melting point. Finally, for further future upgrading from the samples produced under the optimum conditions further catalytic upgrading was considered for which a purpose built secondary downstream fixed catalytic bed was constructed in order to perform tests with selected catalysts. Details of the design for the catalytic bed and the selected catalyst characteristics are summarised in Chapter 6.

Chapter 2

Review of Plastics Pyrolysis and Upgrading Processes

2 Introduction

The composition of mixed plastic waste (MPW) originating from actual industrial sources varies significantly but, will inevitably contain one of the main polymers that comprise up to 73% of the total plastic waste generated in Europe. These include Low Density Polyethylene (LDPE), high density polyethylene (HDPE), polystyrene (PS), polypropylene (PP), polyvinyl chloride (PVC), polyethylene terephthalate (PET) with remaining being smaller percentages of a variety of materials ((PEMRG) 2016). Current actual demand per polymer in total volumes (million tonnes) is shown in Figure 7, for Europe for the years between 2013 and 2015.

Out of these the breakdown of the actual use per market segment and per polymer is shown in Figure 8, which corresponds to the general waste generation. Generated mixed waste contain the non-recyclable fractions and constitute up to 75% of the total generated waste that is either sent to landfill or used for energy recovery((PEMRG) 2016).

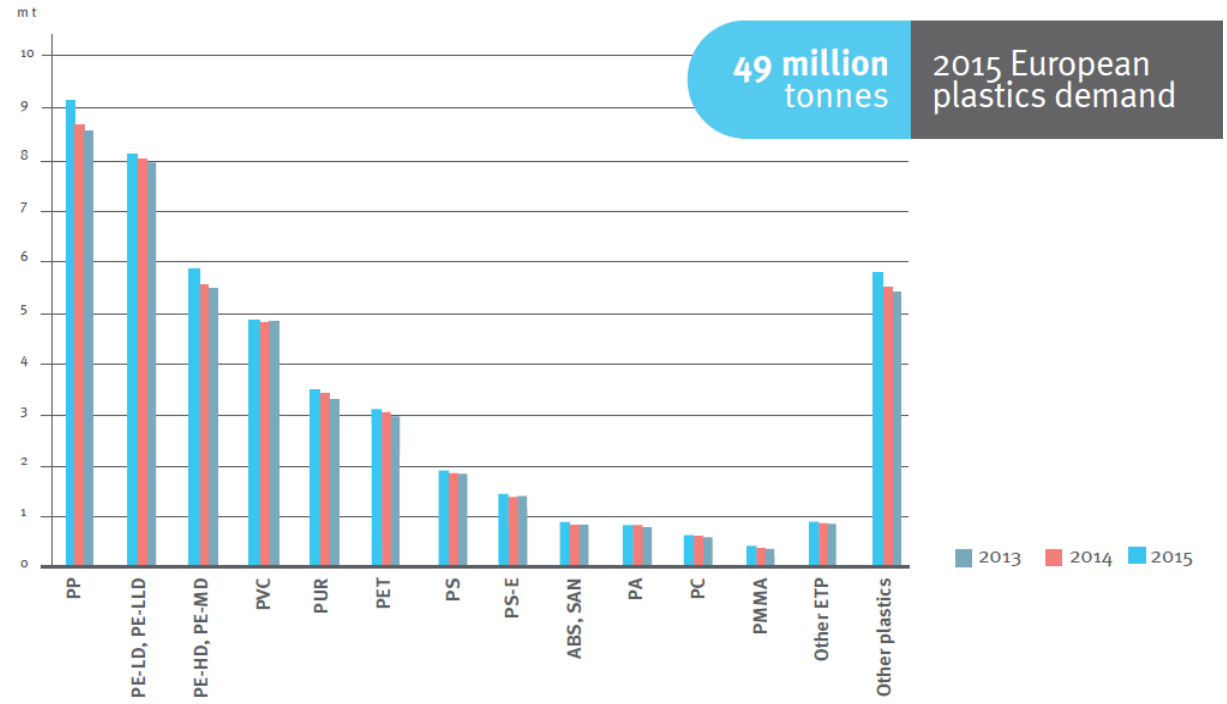

Figure 7: Plastic material demand in million tonnes per polymer in Europe for 2013 to 2015 ((PEMRG) 2016).

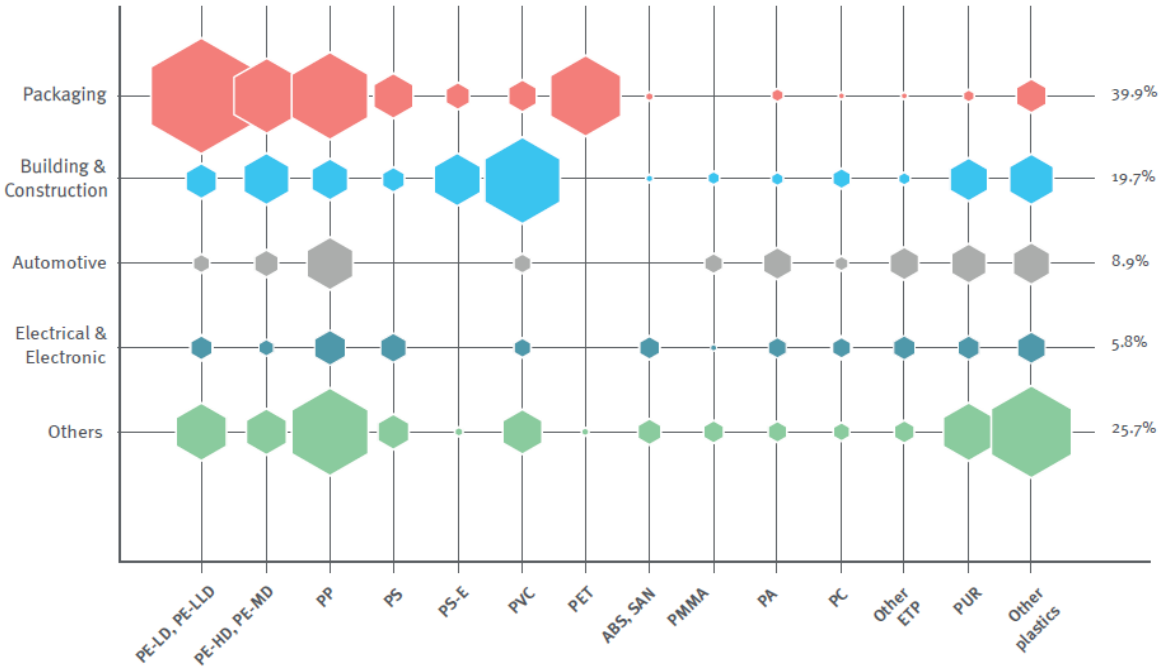

Figure 8: European plastics demand by polymer and market segment 2015 ((PEMRG) 2016).

Within the energy recovery technologies, specifically for plastics, pyrolysis has been gaining ground over the past few years (Bockhorn, Hornung et al. 1998, Dai, Yin et al. 2001, Blazsó 2006, Scheirs 2006, Buah, Cunliffe et al. 2007, Foster 2008, (UNEP) 2009, de Marco, Caballero et al. 2009, Adrados, de Marco et al. 2012, Patni, Shah et al. 2013). In comparison to, incineration and landfill or gasification, pyrolysis has the advantage of producing three end products; liquid, gas and solid, which are of higher value than the waste plastic itself and have significant potential for fuel applications and ability to mitigate environmental risks and decrease waste generation (Yan, Liang et al. 2005, Al-Salem, Lettieri et al. 2009, Shah, Jan et al. 2010). There are a number of factors influencing the pyrolysis of mixed plastic waste which have an effect on the final product quality and distribution (Scott, Czernik et al. 1990, Williams and Williams 1999, Sharma, Moser et al. 2014).

To consider the main product, from the pyrolysis process as a comparative fuel with diesel as a reference specific characteristics need to be analysed and improved such as viscosity and density for example, since the fuel product from pyrolysis of plastics have significantly different properties (Yang, Brammer et al. 2013, Frigo, Seggiani et al. 2014). In the current chapter an overview of the composition of mixed plastic waste is described as well as a review of the characterization methods used to define the major factors affecting the pyrolysis of such waste. All the other significant pyrolysis parameters affecting the process outputs are also discussed as well as the most effective analysis methods for the plastic waste derived fuel.

Finally tested upgrading methods for heavy fuel oils which are used to improve the pyrolysis fuel properties and qualities are reviewed.

2.1 Composition of Mixed Plastic Waste

A polymer by definition is a large molecule built by repeating a small chemical unit. This basic unit is different for each polymer (Brydson 1999). Most plastics are produced from oil and have varying properties such as density, average molecular weight, melting point depending on their composition, structure and production process. The degree of polymerisation is expressed with the number of monomer units (n) (Kissel 2002). For commercial plastic the length of the polymers can vary from 1000 to 10000 of such units.

The main elements that comprise the basis of most polymers are hydrogen and carbon with the exception of PVC which contains chlorine in the basic molecule and PET containing oxygen as shown in Figure 9. Several categories of polymers exist but these can be further separated into different classes such as polyalkenes/polyolefins (polyethylene, polyprolpylene), polystyrenes (polystyrene, styrofoam), polyhaloolefins (polyvinyl chloride) or polyesters (polyethylene terephthalate) ((CROW) 2015).

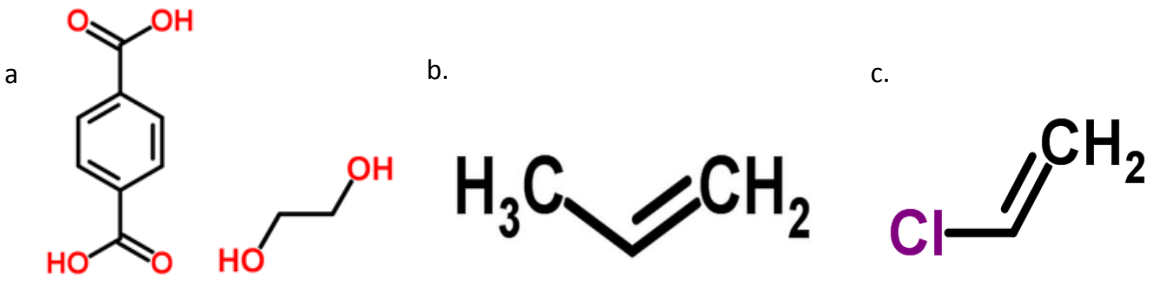

Figure 9: Basic mononer units for a) Poly(ethylene terephthalate), b) poly(propylene), c) poly(vinyl chloride) ((CROW) 2015).

Depending on the groups and units present in the plastic categories, different bonds will form between them with varying attraction strengths. Linear chain backbone structure between carbon atoms or carbon – oxygen bonds are quite flexible, while ring structures minimise the chain flexibility. Branched or linked structures, found in polypropylene affect the chain flexibility and stability. Another type of bond is a polar bond formed between a polar component such as chlorine and carbon which has a stronger effect in the chain dipole force formation. A similar effect is present in hydrogen secondary bonding due to increased forces of attraction that ultimately affect the chain mobility glass transition and melting temperatures (Brydson 1999). A subsequent effect of the different bonds formed is the related dissociation energy that is required to break such bonds with the highest being for a double carbon bond (146kcal/mole) and the lowest being between carbon and chloride (81kcal/mole) (Brydson 1999). Furthermore, when these plastic wastes are decomposed they result in various components depending on the original structure and composition. The crosslinking of the single units as well as the inter chain bond attraction and type of bonds formed will affect the respective glass transition, melting and thermal decomposition temperatures (Kissel 2002).

Two very important properties to be considered for any thermal treatment of waste plastics towards energy recovery are the density and heating value. These are depended both on the structure, composition and molecular weight. Indicative values are presented in Table 4, for the basic polymers and for natural gas and diesel as well.

Table 4: Heating values and densities for the major waste polymer categories (N.J. Themelis 2011, (CROW) 2015).

Material	Density ($kg.L^{-1}$)	Heating value ($MJ.kg^{-1}$)
PET	1.33	24
PE	0.85	46
PP	0.86	44
PVC	1.38	19
LDPE	0.93	28
HDPE	0.97	44
PS	1.05	41
Natural gas	0.712	47
Diesel	0.84	43

The high energy content of plastics and plastic waste comparable to that of diesel and natural gas makes them extremely attractive for energy from waste applications since high calorific value products can be obtained via pyrolysis. Different fractions of these materials will result in an average heating value with HDPE and PP contributing the most (Al-Salem, Lettieri et al. 2009). Polymers such as, polyvinyl chloride that contain larger atoms such as chlorine result in a higher density value as well as polymers that can crystallise (Brydson 1999).

These properties, affect significantly the behaviour and thermal degradation process of each of these materials. In the actual mixed plastic waste streams different contaminants have been reported from various researchers such as biomass, inorganics, tin foil (Singh, Wu et al. 2012, Çepelioğullar and Pütün 2013) as well as flame retardant modifiers, additives and rubbers that show thermal decomposition behaviour at significantly different temperatures and affect the evolved gases and products (Perret and Schartel 2009).

Presence of sulphur and nitrogen, has also been found in refuse plastic fuel (RPF) analysis resulting in distinguished thermal decomposition characteristics (Park, Seo et al. 2012). Even the different polymer blend contamination and variation of the proportions of polymers present have been reported to show important effects in the required activation energy for the thermal decomposition as well as the resulting products and emissions affected by material interaction (Chattopadhyay, Kim et al. 2009, Aboulkas, El harfi et al. 2010, Ahmad, Al-Sagheer et al. 2010).

Determining the composition of the plastic waste at the preliminary stages of the energy from waste utilisation, will have an important impact in terms of defining the process parameters (Sørum, Grønli et al. 2001), yields, end products and potentially hazardous emissions, hence making it important to characterise identify and quantify the actual polymers present in the waste mixture.

2.2 Mixed plastic waste characterisation

Thermal decomposition of mixed plastic waste can yield liquid useful products through pyrolysis but also hazardous substances depending on the composition of the mixed feedstock thus making the characterization of the feedstock one of the crucial elements of the process (Bockhorn, Donner et al. 2001, Meissner, Wróblewska et al. 2004). Accurate identification and characterization of plastic waste has been the aim of significant research in literature utilising a variety of different methods and analytical equipment to achieve a combined understanding of reaction kinetics, process conversion possibilities as well as emissions monitoring and useful product recovery. A more basic approach, in the analysis of the waste plastic feedstocks used includes the ultimate and proximate analysis of the samples that yields interesting results in

terms of the chlorine, sulphur wt.%, ash and moisture content and hydrogen/carbon ratio but would not provide sufficient information for the actual structure of the plastics relating to the polymer presence and identification (Jung, Cho et al. 2010, López, de Marco et al. 2011, Adrados, de Marco et al. 2012, Singh and Ruj 2016).

To obtain results that are more meaningful in terms of thermal degradation and decomposition relating to specific polymers and materials like cardboard, biomass or textiles, as well as products evolved under heated inert atmosphere, the following analytical methods have been used: thermogravimetric analysis under inert atmosphere coupled with either a Fourier transform infrared spectrometer (FT – IR), gas chromatography or mass spectrometry (Blazsó 1997, Arenillas, Pevida et al. 2004, Heikkinen, Hordijk et al. 2004, Brems, Baeyens et al. 2011). Pyrolysis – gas chromatography (Py – GC) or Py – MS techniques have been used to analyse the volatile pyrolysis products and detailed components in the evolved gases. Specifically, hazardous groups containing cyanides, chlorine and sulphur in their chains as well as other toxic compounds have been detected successfully, however there are some limitations to the amount of gases that can be analysed especially for heavier components (Blazsó 1997, Ahmad, Al-Sagheer et al. 2010, Hassan, Elsayed et al. 2016). Differential scanning calorimetry (DSC), has also been used coupled with a thermogravimetric analysis, although less extensively, to capture the enthalpy phase changes during the various temperature increase steps and help understand the kinetics associated with the reactions taking place and calculate reaction rates and constants (Al-Salem and Khan 2014). In addition, this method allows for calculation of the overall required energy for each phase change and to identify the thermal

decomposition stages under pyrolysis conditions (Camacho and Karlsson 2001, Cafiero, Fabbri et al. 2015, Salman (2015)).

A combination of the above mentioned analytical methods allows for a more detailed understanding of the kinetics and phase changes involved in the thermal decomposition of plastics and plastic mixtures through TGA coupled with DSC analysis as well as for the products resulting from the thermal decomposition of such waste plastics through Py – GC/MS analysis or TGA coupled with FTIR.

2.2.1 Thermogravimetric analysis

Thermal degradation behaviour has been observed for a variety of solid materials including polymers with the use thermal gravimetric analysis (TGA). Such a technique allows to calculate the overall mass loss associated with thermal decomposition (Basu 2013). Furthermore, the derivative thermo gravimetric (DTG %) can show the points where the rate of the mass loss peaks reaching a maximum and can be linked to each unique material.

Individual materials, have been tested previously such as polyethylene (PE), polyethylene terephthalate (PET), polyvinyl chloride (PVC) and high density polyethylene (HDPE) to identify specific reaction kinetics associated with the pyrolysis process and total mass loss as shown in Figure 10 (Conesa, Marcilla et al. 1996, Marongiu, Faravelli et al. 2003, Saha and Ghoshal 2005, Lee and Shin 2007, Al-Salem and Lettieri 2010).

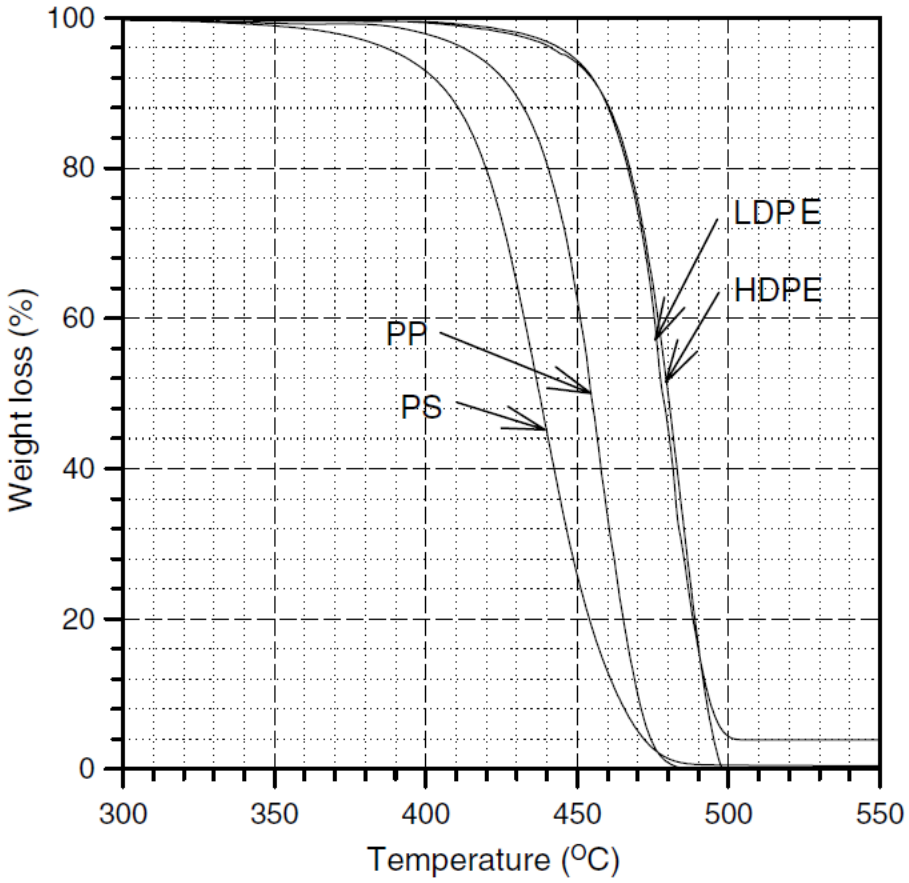

Figure 10: TGA curves of pure waste plastics with 10oC/min heating rate (Lee and Shin 2007).

Dynamic conditions, were tested with varying heating rates, exposed surface and altered initial sample mass as well as isothermal experiments with different masses. As a result, kinetic models for single components could be calculated from the dynamic runs, whereas polymer thermal degradation behaviour as well as kinetic rate constants with subsequent calculations of the overall activation energy were the result of the isothermal experiments (Conesa, Marcilla et al. 1996, Marongiu, Faravelli et al. 2003, Saha and Ghoshal 2005, Al-Salem and Lettieri 2010). Conesa et al. found for PE a relation between heating rate and TG curve displacement towards higher reaction temperature for the total sample mass loss consistent with the findings of Saha et al.

for PET and what Aboulkas et al. found for LDPE, HDPE and PP (Conesa, Font et al. 1994, Saha and Ghoshal 2005, Aboulkas, El harfi et al. 2010). Al - Salem et al. established inverse proportional relation between temperature and required reaction time and both identified complete conversion of the polymer at temperatures above 400ºC (Al-Salem and Lettieri 2010). TGA analysis has been conducted for HDPE, LDPE and PP under dynamic conditions with varying heating rates and it was reported that all polymers showed the same trend with a single step weight loss but at different degradation temperatures and required activation energy. A single proposed model, was indicated as a result for LDPE and HDPE (contracting sphere model) and for PP another one (contracting cylinder model) (Aboulkas, El harfi et al. 2010).

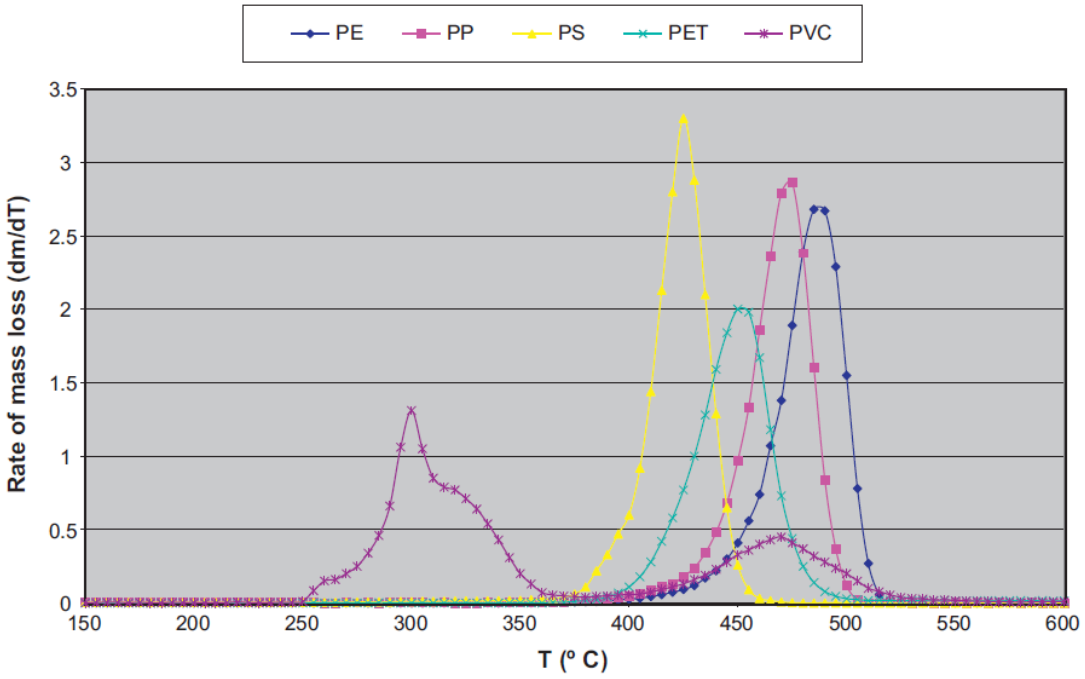

Figure 11: Derivative thermogravimetric plot (DTG) of individual plastics used in plastic mixture (López, de Marco et al. 2011).

Single polymer decomposition patterns and kinetic models associated with them are extremely useful but are not representative of the actual plastic waste composition which is why co – pyrolysis of different polymers and materials has been investigated

as well to establish reaction kinetics or resulting effect on products. Polymer blends namely: PET/PMMA (polymethyl methacrylate), PET/, PVC/PU (polyurethane), PP/PS and their interaction have also been investigated for their effect. It was found that there is a considerable interaction affecting the degradation steps and resulting gases and the combination of suggested kinetics has been proposed for such blends from a variety of studies (Aguado, Olazar et al. 2002, Kruse, Levine et al. 2005, Brems, Baeyens et al. 2011, Radhakrishnan Nair and Gopinathan Nair 2011, Al-Salem and Khan 2014).

Adding biomass and wood elements, in co – pyrolysis with plastics has been the objective of Çepelioğullar et al. that studied co – pyrolysis of biomass and PVC/PET blends under dynamic conditions and a stable heating rate (Çepelioğullar and Pütün 2013). The findings of this study, showed that material interaction affects the reaction kinetics and thermal degradation behaviour identifying different degradation steps for biomass and for each polymer. Chattopadhyay et al. also studied biomass co – pyrolysis with polymer components and arrived to the conclusion that addition of plastics favours the quality of the end product (Chattopadhyay, Kim et al. 2009, Hassan, Elsayed et al. 2016). Combined waste component identification has been attempted with TGA for a variety of mixed unidentified materials such as dried sewage sludge, PET/PVC/agricultural residues, real waste and wood residues in selected studies (Heikkinen, Hordijk et al. 2004, Çepelioğullar and Pütün 2013, Magdziarz and Werle 2014). Specifically, Heikkinen et al, observed the degradation characteristics of waste components and correlated to the observed DTG peak to identify them by (Heikkinen, Hordijk et al. 2004).

Finally, Municipal solid waste (MSW) and RDF have been investigated in several studies separating the presence of biomass with the use of the DTG curves observed. It could be derived, that the pyrolysis behaviour of plastic mixtures, can expressed with substantial accuracy, as the weighting sum of their components (Wu, Chang et al. 1993, Cozzani, Petarca et al. 1995, Sørum, Grønli et al. 2001, Grammelis, Basinas et al. 2009, Park, Seo et al. 2012, Singh, Wu et al. 2012). It was reported that biomass showed two degradation peaks at 200 – 400^{o}C and at 400 – 500^{o}C respectively whereas presence of plastics was identified at 300^{o}C and 470^{o}C (Singh, Wu et al. 2012). Building on, such observations Sørum et al. reported several distinguished peaks biomass originated wastes such as spruce, newspaper, cardboard, recycled paper, all within the region of 300 – 400^{o}C and for the plastic components the DTG peaks observed were more separated and distinguished with LDPE/HDPE in the region of 460 – 500^{o}C, PP at 450^{o}C, PS at 400^{o}C and PVC with a double reported peak at 300/450^{o}C (Sørum, Grønli et al. 2001). Based on, the mentioned studies it is feasible to identify components from mixed waste feedstocks using thermogravimetric analysis and relating the DTG peaks at the relevant decomposition temperatures to specific, previously identified components and understanding their decomposition kinetics.

2.2.2 Differential Scanning Calorimetry

Differential scanning calorimetry, is a technique complimentary to thermogravimetric analysis and most times used in combination. This method, allows for more detailed results in terms of the phase changes observed relating to heat capacity, glass

transition, crystallization, melting and thermal decomposition temperatures (Kong and Hay 2002). In contrast to,, thermogravimetric analysis DSC has the flexibility to show whether the phase changes occurring absorb or release heat therefore allowing for a better understanding of the reaction kinetics whether that is combustion (exothermic reaction) or pyrolysis (endothermic reactions) depending on the way the identified peaks are facing (upwards or downwards depending on the software) (Basu 2013).

This technique, has not been utilised as extensively as thermogravimetry, for feedstock characterization but mostly for reaction kinetics and calculation of required heat for the pyrolysis reaction. Specifically, TGA – DSC, was utilised in the pyrolysis of printing paper and cardboard aiding towards the identification of cellulose and hemicellulose or extractive components by identification and quantification of the observed reactions (Zhu, Jiang et al. 2008). Reyes et al. observed the transitions for polyethylene/ethylene – vinyl acetate (EVA) copolymer mixture and identified different decomposition temperatures changing with the respective and calculated the enthalpy change associated with these observed reactions. There was clear separation of decomposition phases between ethylene and ethylene – vinyl acetate peaking at 380^{o}C and 340^{o}C respectively with a sharp and broad observed peaks respectively (Reyes-Labarta, Olaya et al. 2006). The composition of binary blends (PP/HDPE and poly(acryl – butadiene – styrene)/PP) was studied with TGA – DSC and the melting temperatures observed were used to identify the components since PP and HDPE had nearly 40^{o}C difference between observed values (Camacho and Karlsson 2001). A variety of different polymers namely, PP, PE, PET, PS, ABS (acrylonitrile – butadiene –styrene), HIPS (high impact polystyrene), PBT (polybutylene terephthalate) was analysed with DSC to obtain the required heat for thermal decomposition for single

components and their mixtures by Cafiero et al. and TGA – DSC was utilised by Salman et al., as well to assess the catalytic hydrocracking of polypropylene (Cafiero, Fabbri et al. 2015, Salman, Nisar et al. 2015). In addition to, thermal decomposition that is observed with thermogravimetric analysis DSC has been used to identify the type of reactions taking place and the associated energy required for these. It has also been used as a characterisation tool, utilising the melting phase at the observed temperatures combined with the thermal decomposition phase changes.

2.2.3 Fourier Transform Infrared Spectroscopy

Infrared spectroscopy, is based on the principle or infrared radiation that causes vibration to the molecular framework of specific compounds or to the individual bonds or functional groups within the molecule. Identification of such functional groups in the acquired spectra helps in identifying the initial bonds and molecules vibrating (Colthup, Daly et al. 1990, Stuart 2005). FT – IR analysis is very flexible in the sense that it can be used with the appropriate accessory to analyse gas and solid samples with a quick response. Spectra of analysed substances, can be used on an individual mode to analyse solid samples and even liquid oils obtained from pyrolysis of many other feedstocks (Banar, Akyıldız et al. 2012). Analysis acquired at regular intervals allows this equipment to be coupled to TGA to analyse evolved gases from pyrolysis of coal, mixed waste and mixed plastics and various other components such as flame retardants, PTFE, PVC as well as comparative analysis of MSW/RDF/waste tyre rubber/biomass (Camacho and Karlsson 2001, Ma, Lu et al. 2002, Arenillas, Pevida et al. 2004, Zhu, Jiang et al. 2008, Perret and Schartel 2009, Odochian, Moldoveanu et al. 2011, Chen, Zhuo et al. 2012, Singh, Wu et al. 2012, Cafiero, Fabbri et al. 2015).

Although, FTIR is a very flexible analytical method that recovers quick results and can be coupled with other equipment or used on a stand-alone basis for analysis of liquids and solid samples the spectra that can be obtained do not provide conclusive results, thus making essential for complimentary analysis when accuracy is of essence.

2.3 Fast pyrolysis reaction kinetics

Pyrolysis, is the thermochemical decomposition of material in the absence of oxygen or with limited supply to produce a range of useful products. In pyrolysis, large hydrocarbon molecules thermally decompose and break down into smaller molecules with a simpler structure to produce gas, liquid and char (Basu 2013).

Specifically, for plastics and long complex polymer chains, pyrolysis is very complex with a variety of phenomena taking place, generally acknowledged as depolymerisation that will be covered in this section (Lee 2006). Depending on, the structure of the polymer and the basic carbon backbone different types of cracking take place that are affected from the physical properties of the polymer and ultimately affect the decomposition behaviour as well (Brydson 1999). Decomposition temperature is the final observed temperature following glass transition and melting temperatures that are specific for each plastic material (Brydson 1999). The required energy in order to break the bonds formed in the long polymer chains is called dissociation energy. This energy value is increasing from the single carbon bond to polar and hydrogen bonds with the highest value required to break a double carbon bond as mentioned in §2.1 (Brydson 1999). A combination of both physical and chemical interactions take place during the pyrolysis process and these are discussed with regards to literature findings.

2.3.1 Thermal degradation

There are several structural factors in the polymer composition that affect its thermal properties. Among these, chain flexibility, inter - chain bond attraction and how regular the polymer is ultimately affect its thermal behaviour (Brydson 1999). With the application of heat, polymer structure and properties change significantly and undergo three specific major phase changes prior to completely decomposing or what is also referred to as a polymer depolymerisation (Lee 2006, Marongiu, Faravelli et al. 2007). Initially, depending on the polymer, with temperature increase the material reaches the glass transition temperature (T_g), where it changes into a rubber like phase due to a freer movement of the molecular rotation of the chain bonds. Presence of hydrogen bonds or polar groups such as Cl, as well as the molecular weight of the polymer will greatly affect and differentiate the glass transition temperature and the overall thermal degradation points (Brydson 1999).

Table 5: Transition phases in selected polymers (Brydson 1999).

Polymer	T_g (°C)	T_m (°C)
Polyethylene	-20	120
Polypropylene	5	150
Polytetrafluoroethylene	115	327
Poly(vinyl chloride)	80	-
Polystyrene	100	230
Polyethylene terephthalate	67	256
Nylon 6	50	215

Following this, the second phase change is melting of the polymer at the melting temperature (T_m) changing its state into liquid and finally with increasing temperature the decomposition phase is reached at T_d (Kissel 2002). The glass transition, crystallisation and melting temperatures are shown in Figure 12, for PET with DSC analysis. During pyrolysis the polymers undergo all of the above mentioned phase changes very rapidly. The respective glass transition and melting temperatures are given in Table 5, for selected polymers. Depending on the structure and composition of the polymers both glass transition and melting temperatures are affected and this is mainly attributed to the different side chains (Brydson 1999).

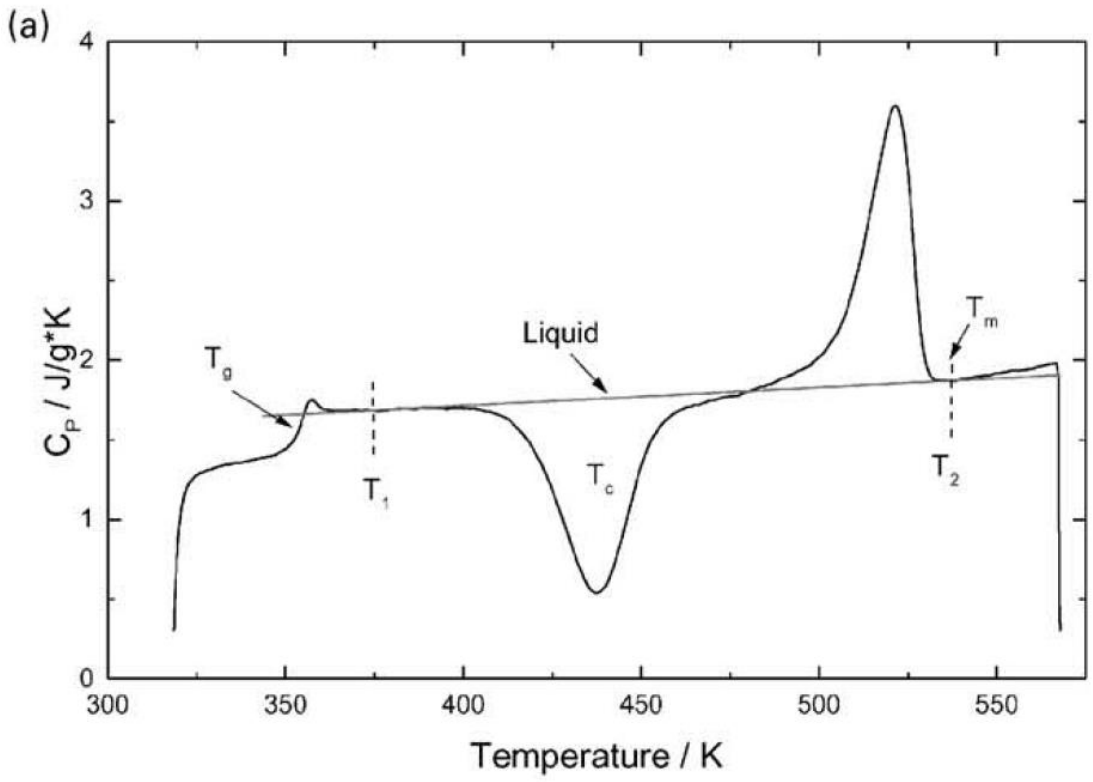

Figure 12: DSC analysis of amorphous PET with Tg (glass transition temperature), crystallization (Tc) and melting temperatures (Tm) (Kong and Hay 2002).

At temperatures above the initial phase transition stages all polymers start to decompose and thermally crack. This is occurring at a temperature range above 350^{o}C (Kissel 2002). Depending on, the feedstock introduced and the process selected the temperature for pyrolysis varies between 400 – 1000^{o}C. Within that limit several reaction take place including thermal cracking of the polymers, as well as additional secondary reactions between the primary vapour products. Indicatively such reactions include further thermal cracking, repolimerization and recondensation with resulting char formation (Martínez, Murillo et al. 2013). With increasing temperature the molecules in the polymer structure vibrate with greater intensity until they reach a sufficient level to overcome the van der Waals force and escape causing the evaporation effect (Brydson 1999). When even greater energy, via heat, is supplied the bond enthalpy between the molecules cracks and the chain is breaking into smaller molecules. Three basic types of cracking, that also occur during pyrolysis, are suggested (Reeves 1996):

1. Random cracking
2. Chain strip cracking
3. End chain cracking

Polymer cracking reactions and secondary composition of the primary products has been studied intensively and is relating to the type and intensity of bonds existing between the polymer chain molecules. Depending on the type of cracking and breaking of molecules a series of other reactions take place. The most important being: initiation reactions, propagation, hydrogen chain transfer and finally termination reactions that define the composition of the compounds in the final products. Details of the thermal cracking reactions are discussed in the following sections.

2.3.2 Polymer chain cracking and reactions

In polymers the bond between hydrogen and carbon, or covalent bond is the basic of the polymer chain as well as the single and double carbon bonds C – C, C =C. Depending on the formation of the bonds, the energy required to break them is different and is referred as bond dissociation (Brydson 1999). With the carbon single bond having the lowest required dissociation energy, it is the weakest point in the polymer chain and will crack first leading to random cracking reactions , which ultimately result in molecular weight reduction of the actual polymers. In Figure 13, this principle is illustrated in terms of carbon bond stability where R is a functional group.

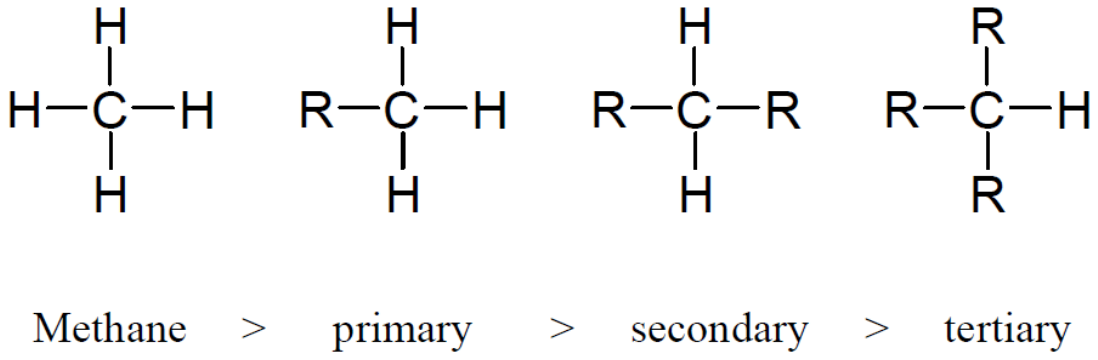

Figure 13: Stability of carbon bonds (Reeves 1996).

In PE and HDPE the effect of random carbon cracking is dominant and the same applies for the linked branches of LDPE which will tend to crack first (Ranzi, Dente et al. 1997, Saha and Ghoshal 2005, Levine and Broadbelt 2009). Polypropylene due to the tertiary bonds is a material more prone to thermally cracking, towards smaller molecules with the same amount of energy applied and the same principles are

applicable for the thermal cracking of PS with makes random cracking the driving force in thermal decomposition of these four major polymers.

Chain strip cracking refers to the side carbon groups, of the branched polymers, breaking off the main backbone chain during thermal decomposition. This process, leaves unsaturated ends on the polymer chain that are subject to further reactions such as further cracking, aromatisation or coke formation which is more applicable to polymers with reactive side groups, illustrated in Figure 14 (Murata, Sato et al. 2004). In this occasion, chain scission occurs as a two phase reaction (gas/liquid), as a result of temperature increase causing the end chain to break (Murata, Sato et al. 2004, Lee 2006, Marongiu, Faravelli et al. 2007). Increasing reactor temperature, has a positive correlation with the intensity of the movement resulting in shorter molecular weight hydrocarbon products.

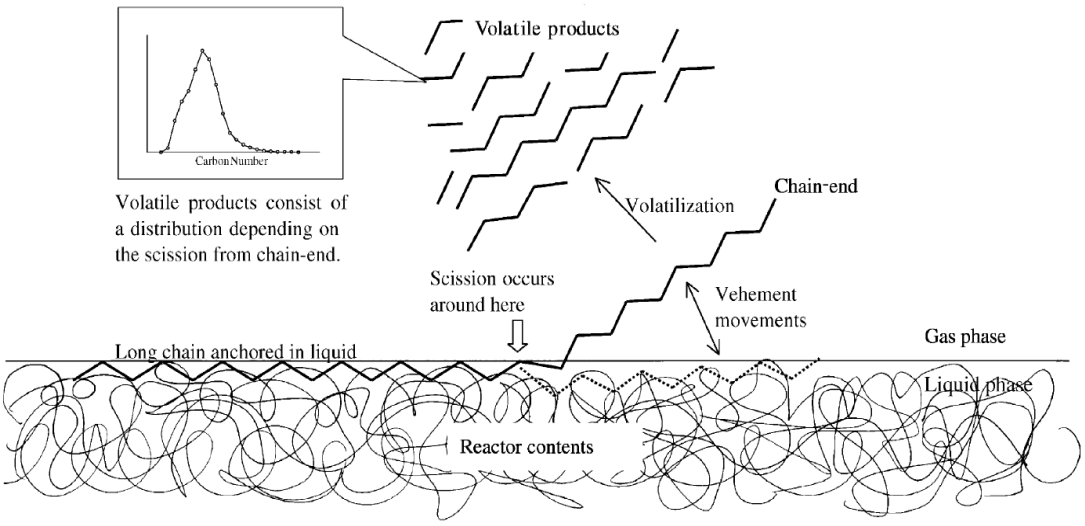

Figure 14: Suggested end - chain polymer scission in the gas - liquid phase breaking towards volatile products (Murata, Sato et al. 2004).

This effect explains why the lighter hydrocarbon components are promoted in process with higher reaction temperatures such as gasification and fast/flash pyrolysis (Murty, Rangarajan et al. 1996, Uemura, Azeura et al. 1999, Mehl, Marongiu et al. 2004, Gao 2010). Polymer cracking, with the mechanisms discussed previously, is the initial step in thermal degradation and pyrolysis specifically but several other reactions following them are involved and these result in the final products.

The combined reactions will be part of one of the following stages: 1.Initiation reactions, 2. Propagation, 3.Hydrogen chain transfer, 4. Termination reactions (Bains, Balke et al. 1994, Murata, Sato et al. 2004, Blazsó 2006).

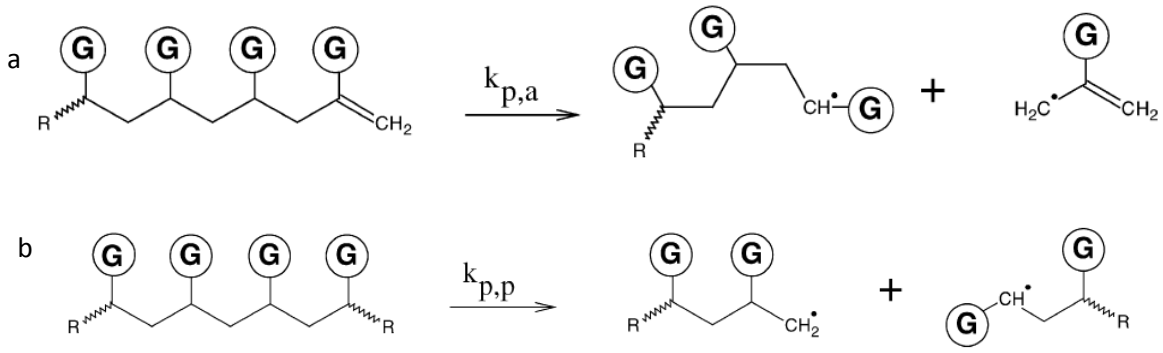

Figure 15: Random scission reaction (a) and end chain scission reaction (b) in pyrolysis of polymers (Marongiu, Faravelli et al. 2007).

The outcome products, are a result of a combination of these reactions could be molecules including alkane, alkene, alkynes and dialkenes as well as free radicals that contain electrons in the end or in the middle of free uncombined radicals. Initiation reactions, include mostly all the thermal cracking mechanisms mentioned previously.

The type of cracking can take either the form of random scission reactions or end chain scission reactions as shown in Figure 15, where G is a side group in the polymer chain that can be either hydrogen, CH_3 or phenyl for PE, PP or PS whereas the side groups

do not appear to react (Marongiu, Faravelli et al. 2007). After the initiation reactions have taken place a great number of new smaller hydrocarbon molecules and free radicals are generated. Propagation and termination reactions follow the initiation reactions and form the final components.

During propagation reactions, further scission reactions are taking place between the free radicals and β – scission has been reported as the main reaction that enhances further cracking of the generated radicals in combination with additional further end chain and random scission reactions that continue taking place (Marongiu, Faravelli et al. 2007).

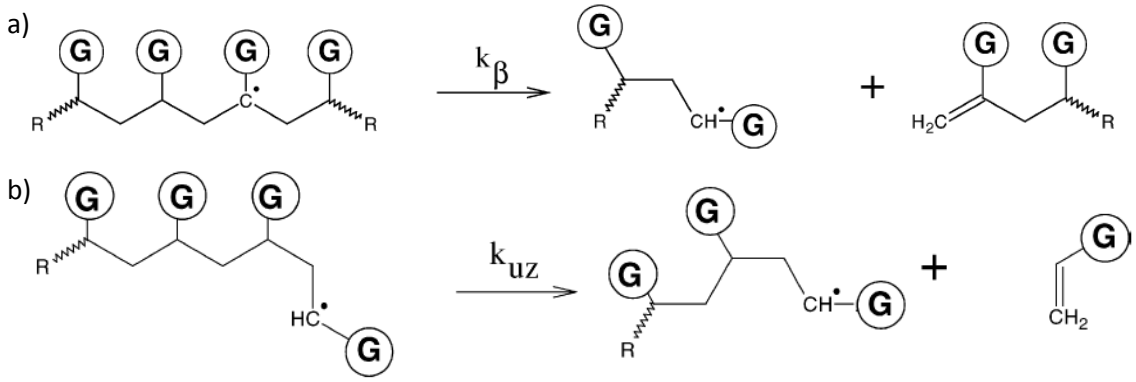

Figure 16: β - scission example reactions a) mid scission of a free radical chain, b) at the end chain of a free radical (Marongiu, Faravelli et al. 2007).

An illustration of two β – scission propagation reactions in the middle and at the end of the chain is provided in Figure 16. From the mid chain β – scission propagation reaction unsaturated molecules and smaller radicals are generated whereas from the end chain β – scission and unzipping reactions alkenes are generated. The initial long polymer chains are cracked with the initiation reactions and create a vapour – gas phase in the reactor during pyrolysis. In the vapour phase the free radicals and smaller hydrocarbon molecules are further cracked with the described propagation reactions. There is a

connection between residence time and the propagation reactions that take place in the vapour that can account for the molecular weight of the resulting products during pyrolysis.

Hydrogen atom abstraction (H – abstraction) or hydrogen chain transfer (metathesis) includes a proton transfer via hydrogen to specific locations and results in reducing the molecular weight of the generated radicals as well as creating saturated hydrocarbon molecules in the end product. Both intermolecular and intra – molecular transfer reactions can take place.

Finally, radical recombination, isomerization and termination reactions as shown in Figure 17, with two examples, one of alkyl radical isomerization reaction via hydrogen transfer (a) and the second being termination reaction via recombination of radicals (b), define the end product composition (Marongiu, Faravelli et al. 2007).

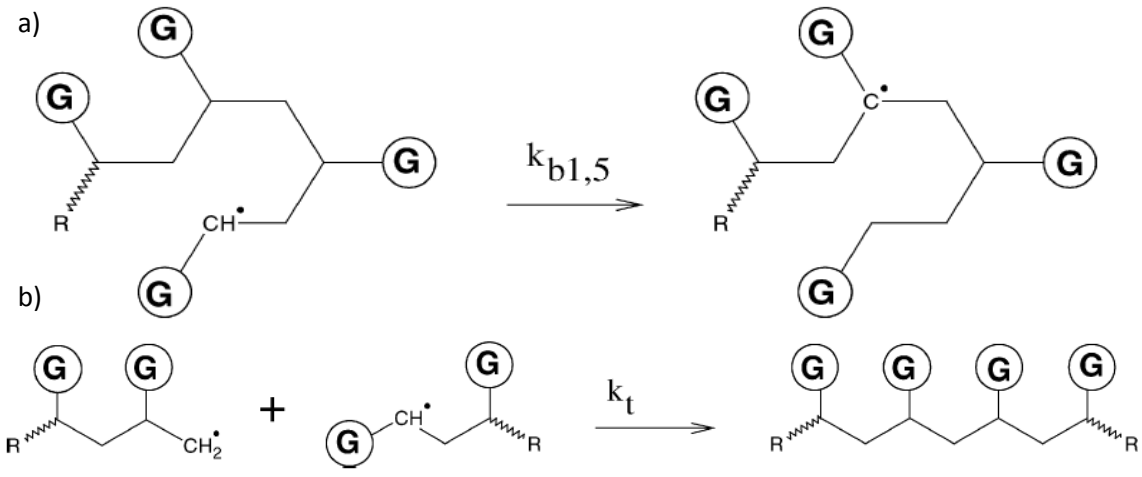

Figure 17: Radical isomerization by H abstraction reaction (a) and termination reaction (b) (Marongiu, Faravelli et al. 2007).

Initiation, β – scission, H – abstraction, radical recombination and termination reactions have been described. In the liquid state, during the degradation process the evolution of gases creates an increasing gas – liquid interface which allows further intramolecular attractions. Such intermediate reactions can account for increased amounts of C_6 or C_{10} present in the final products (Ranzi, Dente et al. 1997). Furthermore, the unsaturated molecules that are produced from end chain polymer cracking of PE, PP and PS are further cracked with β – scission and H – abstraction reactions in the vapour phase of the generated free radicals. During the backbiting process (intramolecular H-abstraction) the end polymer chain can also form products in the gas state through a series of isomerization and β – scission reactions as well as monomer units during the β – scission un zipping reactions of end chain radicals (Marongiu, Faravelli et al. 2007).

When the β – scission or a primary radicals occurs it can result in ethylene production which is one of the main components observed in the gas fraction of pyrolysis of plastics. Again, via β – scission mechanism of the secondary radicals primary radicals and alkenes or dialkenes are produced. The presence of dialkenes can be accounted from the secondary radical scission which creates unsaturated terminal positions (Mastral, Berrueco et al. 2007). The resulting products can be 1 – alkene, unsaturated backbone molecules, alkene backbones formed from alkyl radicals and a – ω dialkenes resulting from backbone species. Also termination reactions result in unsaturated bonds in the final product. The number of unsaturated bonds could be indicative of the initiation and termination reactions while the alkene presence is related to β – scission reactions of free radicals (Gao 2010). There is also a suggested connection between the occurrences of different reactions at different temperatures. At lower temperatures

between 400 – 450^{o}C, intramolecular H- abstraction reactions (backbiting) between primary radicals are favoured that end up generating stable secondary radicals through a variety of isomerization mechanisms shown in Figure 16 (b) with route 1,5 being the favoured reaction. At higher temperatures above 500^{o}C, β – scission reactions are more dominant resulting in smaller molecule generation and eventually increasing the gas fraction yield (Mastral, Berrueco et al. 2007).

2.3.3 Reaction kinetics of pyrolysis of plastics

Considering, the complexity of reactions taking place during pyrolysis (up to some hundred thousand) identifying the actual reaction kinetics has proven to be a challenge. Pyrolysis of polymers such as PE, PS and PP is better described by a radical chain mechanism in the liquid phase for temperatures higher than 200^{o}C (Marongiu, Faravelli et al. 2007). There are also several steps between the initiation reactions and formation of the final products including secondary scission reactions in the vapour phase. The theoretical expected products from literature would be either alkanes (paraffin), alkene (olefins), dialkenes (D) as well as free radicals both from end chain and mid chain scission products (Murata, Sato et al. 2004, Marongiu, Faravelli et al. 2007, Mastral, Berrueco et al. 2007). A general description of the reactions taking place in all stages is given by the following resulting reactants and products (Murata, Sato et al. 2004, Marongiu, Faravelli et al. 2007, Gao 2010):

Initiation

$P_n \rightarrow O_j + P_{n-j}$

β – scission reaction

$O_n \rightarrow c_1(P_j + D_{n-j}) + c_2(O_j + O_{n-j})$

Termination

$D_n \rightarrow D_j + O_{n-j}$

Where P_n is a paraffin with a total carbon chain length n, O is an alkene (olefin) generated from the initiation reactions with a carbon chain length j that can vary within the limits of the total carbon chain length n with c_1 and c_2 values depending on reactions taking place, processes and the presence of a strong position (Ranzi, Dente et al. 1997, Marongiu, Faravelli et al. 2007). In order to understand, and model the complex reactions taking place in pyrolysis of plastics a lot of suggested reaction models have been investigated in previous literature (Williams and Williams 1999, Bagri and Williams 2002, Murata, Sato et al. 2004, Aboulkas, El harfi et al. 2010, Çepelioğullar and Pütün 2013). An understanding of the relevant kinetic reaction models that apply in the pyrolysis of mixed plastic waste is the aim of the current study in order to interpret, control and optimise the outcome of the process. A single step reaction model for thermal degradation described using the Arrhenius equation has been used previously although it is a simplified version that cannot accommodate an extensive range of heating rates, temperatures and conversion levels the same kinetic parameters (Cozzani, Petarca et al. 1995, Conesa, Marcilla et al. 1996, Ranzi, Dente et al. 1997, Williams and Williams 1999, Murata, Sato et al. 2004):

$$\frac{da}{dt} = kg(a) = A_0 e^{\frac{Ea}{RT}} g(a) \qquad \text{(Equation 1)}$$

Where a is the fraction of the polymer decomposed, g(a) is a function of a, E_a (kJ/mol) is the activation energy and A_o is the Arrhenius pre – exponential constant. When taking into account the order of the reaction the kinetic law can be expressed with:

$$\frac{da}{dt} = A_0 exp\left(\frac{-E_a}{RT}\right)(1-a)^n \qquad \text{(Equation 2)}$$

Where a, is the polymer conversion ratio, R is the gas constant, T is the sample temperature and n is the reaction order (Conesa, Marcilla et al. 1996, Bagri and Williams 2002, Murata, Sato et al. 2004, Buekens 2006). Based on this first order reactions, individual kinetic constants have been obtained for a variety of single polymers such as HDPE, where various heating rates and temperatures were investigated and validated with thermogravimetric experimental data. From this study different kinetic constants and activation energies were obtained (Conesa, Marcilla et al. 1996). HDPE was investigated extensively with regards to conversion as a function of temperature and it was found that the reaction order changes but a reaction order of 1 can be assumed for temperatures above 400ºC to increase the conversion range as shown in Table 6.

Table 6: Reaction order values for different temperatures (Ceamanos, Mastral et al. 2002).

Temperature (ºC)	Order	Conversion range
390	0.90	0.08 – 0.96
410	0.88	0.13 – 0.96
430	0.86	0.10 – 0.99
450	1.00	0.43 – 0.97
470	0.99	0.37 – 0.97

Kinetic parameters E_a (around 365 kJ mol^{-1} at T ≥ 430°C) and A_o (with a suggested kinetic constant value of 2.53 *10^{24} e $^{-41718/T}$ (min^{-1})) for the different heating rates were also calculated for the dynamic conditions and comparatively for isothermal conditions (Ceamanos, Mastral et al. 2002). These kinetic factors for LDPE and HDPE at different heating rates and dynamic conditions were also studied by other researchers and LDPE exhibited a lower activation energy with lower reaction order numbers (Park, Oh et al. 2000). Based on the reaction kinetics for HDPE and PE pyrolysis different models have also been developed for the evolution and prediction of the evolved gas product distribution based on Flynn and Wall methods to obtain detailed component analysis (Ballice 2001) either grouped components such as paraffin, olefins naphthenes and aromatics (PONA) (Lee 2006) or even to establish a link between structure and reactivity (Levine and Broadbelt 2009, Al-Salem and Lettieri 2010). A summary of all the suitable suggested reaction mechanisms for HDPE, LDPE and PP was provided by Aboulkas et al. (Aboulkas, El harfi et al. 2010).

Pyrolysis reaction kinetics of PET was also investigated with TGA to predict the performance of this polymer in the reactor and to identify the product distribution under dynamic conditions using the n order number reaction model. The activation energy was between 322.3 and 338.98 kJ/mole at 500°C pyrolysis temperature (Saha and Ghoshal 2005).

The study on PVC however, that thermal degradation for this material is a two-step process, where the first step is mainly a dechlorination process accompanied by depolymerisation described with first order reaction kinetics (E_a = 130 kJ/mol) and the second step involves further cracking of the remaining residue resulting in low molecular hydrocarbons such as alkenes and aromatics (Ma, Lu et al. 2002).

A random chain dissociation (RCD) model was developed to interpret the entire conversion range of PE, PP and PS and their mixtures utilising kinetic parameters obtained from a simple first order model and taking into account polymer molecular weight and branching. Although, branching was found to have a significant effect the molecular weight was not found to be important (Westerhout, Waanders et al. 1997).

The effect of polymer interaction in plastic mixtures and blends has also been reported in existing literature of co pyrolysis studies (Chao-Hsiung, Ching-Yuan et al. 1993, Cozzani, Petarca et al. 1995, Sørum, Grønli et al. 2001, Faravelli, Bozzano et al. 2003, Kruse, Levine et al. 2005, Hujuri, Ghoshal et al. 2008, Kaminsky, Mennerich et al. 2009, Aboulkas, El harfi et al. 2010, Czégény, Jakab et al. 2012, Chin, Yusup et al. 2014).

Individual plastics (HDPE, LDPE, PP, PS, ABS and PVC) were analysed with TGA to find out the reaction order, activation energy (E_a) and exponential factor (A_0) and following that two different mixtures at different fractions of these polymers were also studied for the their kinetic behaviour as shown in Figure 18.

As a result, it was suggested that the pyrolysis behaviour of plastic mixtures can be expressed as the weighting sum of their individual components when this is a known parameter (Wu, Chang et al. 1993). Although this is a good approximation for research when the individual fraction of such components is given, in actual mixed plastic waste the fractions of the individual components are unknown.

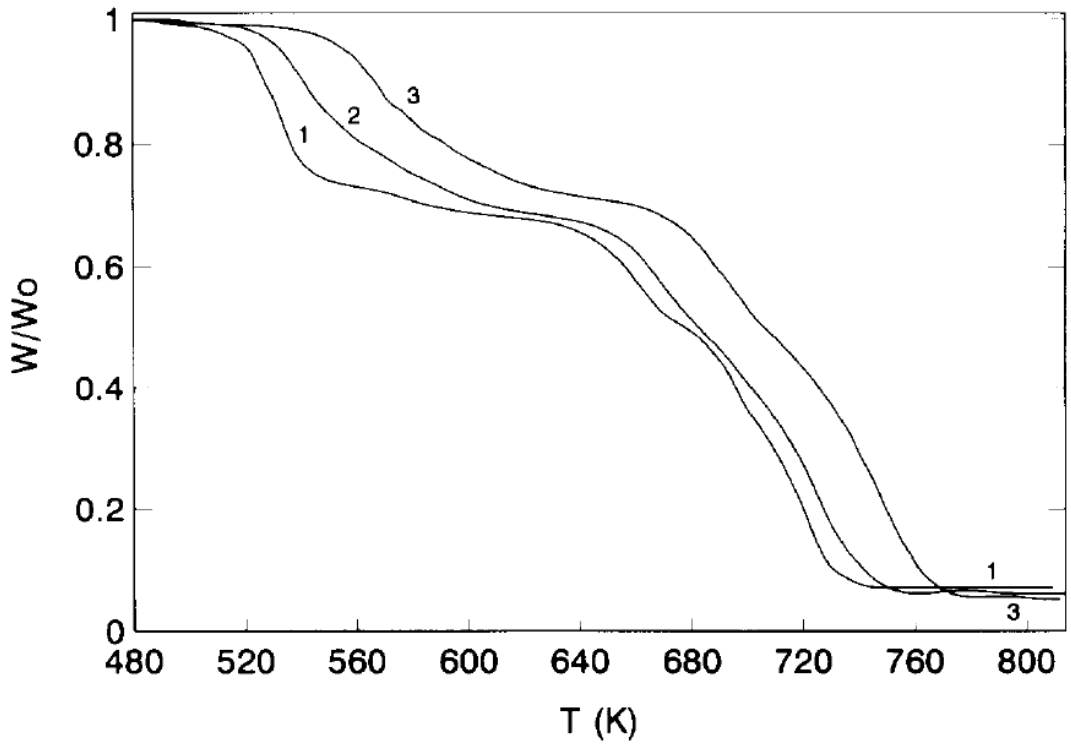

Figure 18: Residual weight fractions with reaction temperature with different heating rates for a plastic mixture including HDPE, LDPE, PP, PS, ABS, PVC (Wu, Chang et al. 1993).

A similar mixture including HDPE, LDPE, IPP, PS, ABS and PET in various percentages with PVC excluded was analysed to study catalytic degradation (HZSM-5 zeolite) in relation to the gas and liquid evolution and product distribution. The results illustrated higher density product with the use of catalyst but the quantity of aromatic hydrocarbons increased with the higher molecular weight hydrocarbon present in the products being hexatriacontane. Over 100 compounds, were identified in the non - catalytic decomposition products proving how complicated the kinetics and resulting products can be when considering pyrolysis of plastic mixtures (Vasile, Pakdel et al. 2001).

More developed kinetic models have attempted to explain the effect of temperature with regards to primary and secondary reactions. Specifically it was identified that two different setups, a pyroprobe and a fluidised bed reactor were more suitable to study the primary and secondary reactions of HDPE pyrolysis respectively. The reported resulting major product, from primary reactions was 1 –hexane whereas from secondary reactions propene at lower temperatures and ethane at higher temperatures. Branched hydrocarbons were reported to be also a result of secondary reactions which were destroyed with increasing temperature (Hernández, Gómez et al. 2007).

Finally, more complex ordinary differential equations based on a selection of the radical mechanisms was developed with a mechanistic model to predict the product distribution from PE pyrolysis. This mechanist model was able to predict the process formation of aromatics and polyaromatics on top of alkanes olefins and diolefins, that was previously reported in literature, incorporating different pyrolysis temperatures and residence times as well. Although, there are some overestimated mechanisms the results validated by experimental data as shown in Figure 19, proved an increase in cracking and production of aromatics when the residence time increases (Mastral, Berrueco et al. 2007). A similar approach, was studied for plastic mixtures utilising a continuous distribution theory in a batch reactor (Miskolczi and Nagy 2012).

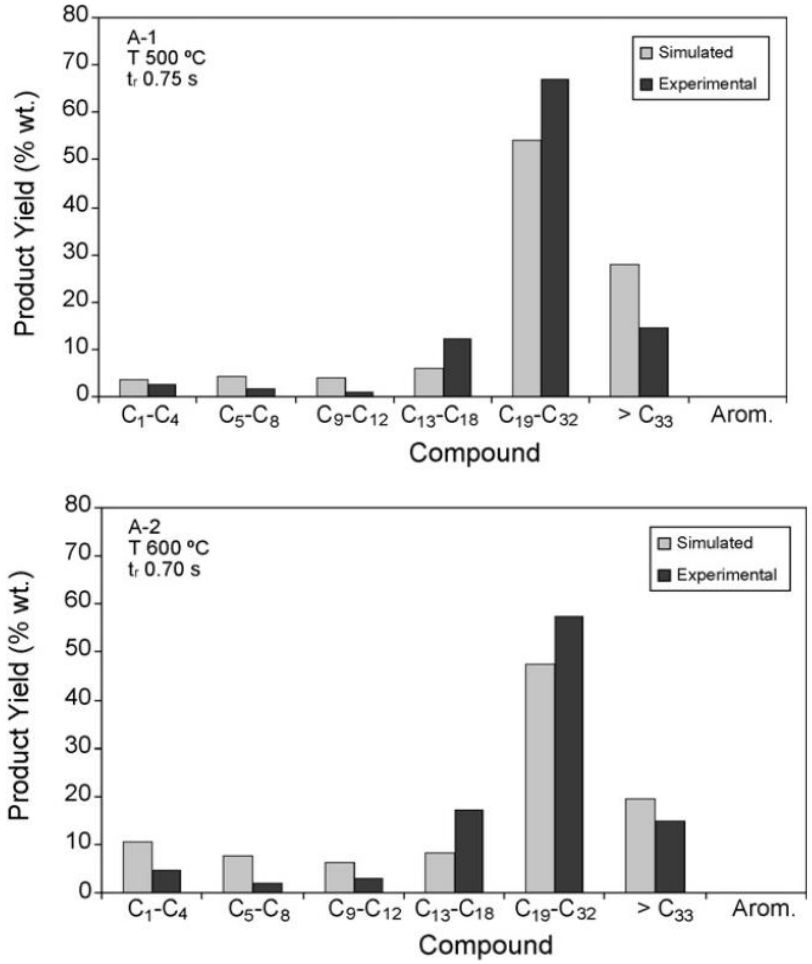

Figure 19: Comparison of product distribution between simulated and experimental results at different pyrolysis temperatures (Mastral, Berrueco et al. 2007).

2.4 Influencing factors for plastic pyrolysis

There are several significant parameters, that could affect or have previously been reported to affect the pyrolysis process and in specific pyrolysis of plastics. The most important will be discussed in this section and include the composition of the feedstock, reaction temperature, pyrolysis type, heating rate, reactor type, residence

time, pressure, carrier gas, selection of catalyst and particle size with an effect on surface area to name a few (Scott, Czernik et al. 1990, Li, Li et al. 1999, Williams and Williams 1999, Demirbas 2004, Gulab, Jan et al. 2010, López, de Marco et al. 2011, Abbas-Abadi, Haghighi et al. 2013, Abbas-Abadi, Haghighi et al. 2014, Efika, Onwudili et al. 2015, Kan, Strezov et al. 2016, Miandad, Nizami et al. 2016).

Out of these, specific parameters have proved to have a more significant effect on the actual product distribution, quality and yield which are the main areas of interest in pyrolysis of plastics and process optimisation. Process parameters such as feedstock composition, reaction temperature and residence time have previously been identified to significantly influence the reaction kinetics and are further discussed in detail in this section.

2.4.1 Composition of feedstock

The composition of the feedstock in one of the most crucial parameters that have a direct impact not only on the pyrolysis process parameters such as average reaction required temperature but on the resulting product composition as mentioned in §2.1 through to §2.2.2. To make things more complicated contamination of the plastic mixtures that come from actual waste streams and the unknown consistency of the mixed waste feedstocks poses a challenge during pyrolysis.

Generally, mixed plastic waste will include one of the main polymers present in the generated waste such as HDPE, LDPE, PP, PS, PVC and PET from which PET and PVC already contain oxygen and chlorine in their structure which causes issues with emissions and product quality.

The thermal decomposition behaviour of PET and PVC has been the target of several studies in order to understand the stages of potential release of hazardous vapours and address them (Collins, Fiveash et al. 1969, Marongiu, Faravelli et al. 2003, Bhaskar, Tanabe et al. 2005, Miskolczi, Prof. Bartha et al. 2009, López, de Marco et al. 2011, Yuan, Chen et al. 2014). The presence of PET results in increased amounts of oxygenated compounds in the final product analysis (Yoshioka, Grause et al. 2004) whereas pyrolysis of PVC results in production of hydrogen chloride creating toxic and corrosive conditions (López, de Marco et al. 2011).

In reality there will be inert material, organic food residues, metals contaminant elements such as sulphur, fillers, coating materials such as PTFE and several other materials in small quantities such as polyamides that might have a minor effect in the overall process and need to be accounted for (Lonfei, Jingling et al. 1986, Simon and Kaminsky 1998, Bockhorn, Donner et al. 2001, Meissner, Wróblewska et al. 2004, Yoshioka, Grause et al. 2004, Sáez, Font et al. 2005, Perret and Schartel 2009). Different approaches have been used to remove such contaminants from the waste streams pre or post pyrolysis in order to avoid contamination and related environmental issues. Desulfurization methods, have been applied to address high sulphur concentrations in pyrolysis oils (Aydın and İlkılıç 2012) and specific element removal such as nitrogen, bromine and chlorine with catalytic methods (Brebu, Bhaskar et al. 2005, Yuan, Chen et al. 2014).

Identification and if possible elimination of such materials from the plastic waste stream would be the ideal solution.

Each polymer has a unique structure, bonds that affect molecule interaction different molecular weight and densities that affect the melting and ultimately decomposition temperature. In addition to the different polymer structures that were mentioned in §2.1 there are also the branched and cross – linked polymers such as LDPE and PEX respectively. Both the functional side groups of the polymer and its structure will affect significantly the pyrolysis (Gao 2010).

Interaction of plastic materials, in plastic mixture feedstocks has been extensively studied both from actual municipal waste streams for the recovery of olefins (Kaminsky, Schlesselmann et al. 1996, López, de Marco et al. 2010) or from artificially composed mixtures representative of the actual waste streams (Williams and Williams 1997, Bockhorn, Hornung et al. 1998, Westerhout, Kuipers et al. 1998, Vasile, Pakdel et al. 2001, Bhaskar, Kaneko et al. 2004, Williams and Slaney 2007). Fundamental studies, on individual polymers such as polyethylene, HDPE, LDPE, polypropylene, polystyrene, PET and PVC (Pinto, Costa et al. 1999, Lee, Noh et al. 2002, Sáez, Font et al. 2005, Onwudili, Insura et al. 2009, Abbas-Abadi, Haghighi et al. 2014) and their mixtures have shaped the basic foundation of understanding the process parameters connected to the feedstock composition and the resulting effect on products (Williams and Williams 1999, Vasile, Pakdel et al. 2001, Kruse, Levine et al. 2005, Marcilla, García-Quesada et al. 2005).

Different reaction temperatures depending on feedstock composition have been suggested as a result of previous studies due to the different thermal decomposition

temperatures of the materials and the subsequent effect on product yields (Kaminsky, Schlesselmann et al. 1995, Westerhout, Kuipers et al. 1998).

In addition, the gas and oil fraction of the individual polymers has shown differences depending on the original feedstock with HDPE, LDPE, PP and PVC producing mainly aliphatic components whereas PS produces mainly aromatic components and PET yields oxygenated and aromatic compounds whiled the resulting product from the mixture has shown a reduced boiling point range in comparison to the products from the single polymers (Williams and Williams 1997, Williams and Williams 1999, Lee, Noh et al. 2002, Yoshioka, Grause et al. 2004).

Plastic interaction from the mixture of polymers directly affects the gas composition of the evolved gases in comparison to the gas fractions produced from individual polymers as shown in Figure 20.

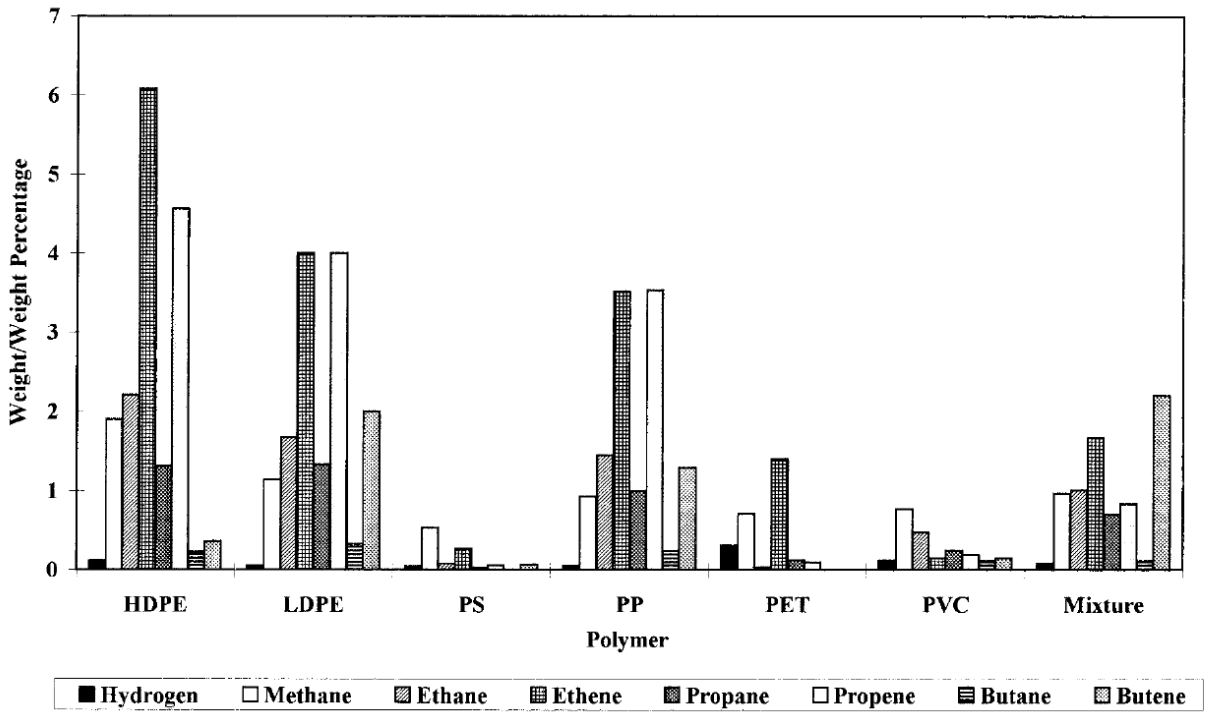

Figure 20: Comparison of gas yields from single polymer pyrolysis and a plastic mixture in a fixed bed reactor (Williams and Williams 1997).

2.4.2 Reaction temperature

Another of the most crucial and important parameters in pyrolysis is the selected reaction temperature that is directly related to the cracking temperature of the polymers that are pyrolysed. Reaction temperature, has multiple functions in pyrolysis affecting several outputs in the process on top of the cracking temperature. It also affects the overall product yields and the final compound distribution in the liquid and gas fractions.

In theory, the cracking temperature of the polymers is the point where the energy supplied with heat and van den Waals force to the polymer molecules is greater than the enthalpy of the C-C bonds in the chain (Patra and Yethiraj 2000, Sobko 2008, Gao 2010). Depending on the polymer type the thermal cracking temperature is specifically related to its structure.

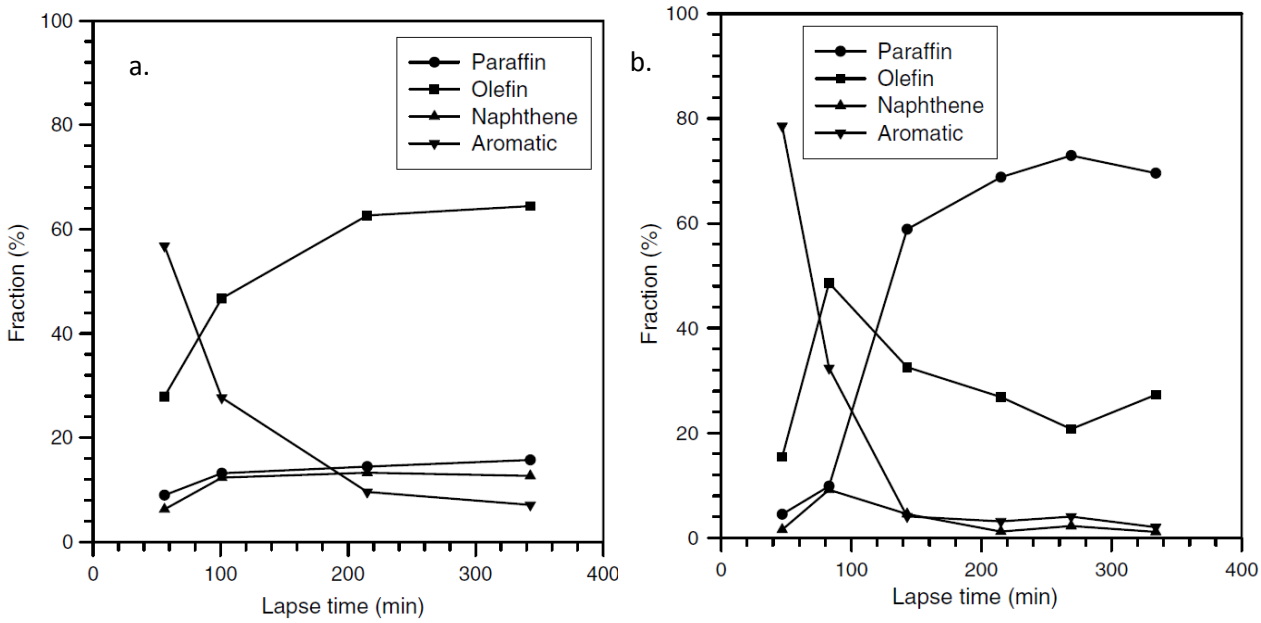

Figure 21: Paraffin, olefin, naphthene and aromatic distribution (PONA) of the liquid products in relation to lapse time of reaction for pyrolysis of a waste plastic mixture at 350oC (a) and 400oC (b) (Lee and Shin 2007).

Specifically, for PS reported values of cracking temperatures vary between different studies from 380^{o}C in Ciliz et al., whereas Demirbas et al. found it to be 650^{o}C and Miandad et al.,specified the optimum pyrolysis temperature at 450^{o}C, after comparing a different temperatures in relation to the product yields as well. The reactor for all three studies was a batch reactor (Demirbas 2004, Kiran Ciliz, Ekinci et al. 2004, Miandad, Nizami et al. 2016).

The differences in the reported results could be attributed to the location of the temperature sensors where that is in the vapour stream at the top of the reactor or in the bottom part where the temperature read could be lower. A variety of different polymers (HDPE, LDPE, PP, PS) were pyrolysed at two temperatures one low (350^{o}C) and a higher (400^{o}C) to test the effect of the degradation temperature on the characteristics of the liquid product using a stirred semi batch reactor with the results illustrated in Figure 21. At the lower temperature, the product distribution evolved from aromatics towards olefins whereas at 400^{o}C from aromatics to paraffins and olefins in the final product (Lee and Shin 2007).

By analysing, the molecular weight distribution of the liquid products it resulted that the paraffin and olefin products due to their wide distribution were produced from random scission reactions but at higher temperatures the lighter olefin products were a result of additional end chain scission taking place (Lee and Shin 2007). Higher reactions temperatures (700 – 850^{o}C) only were studied in the pyrolysis of MSW in a fluidised bed reactor to investigate the gas produced. As expected, the gas volume increased with increasing temperature and the composition changed towards increased methane and hydrogen production by simultaneous reduction of ethane, ethylene, propane and butylene moving towards the 850^{o}C end (Garcia, Font et al. 1995).

Similar studies were carried out with plastics obtained from municipal waste (HDPE, LDPE, PP, PS, and PET) at a reaction temperature range of 450 – 600^{o}C in a batch reactor. The temperature distribution in the reactor and the overall split of the yields with increasing temperature are given in Figure 22 and Figure 23. The gas product distribution, showed an increase in hydrogen production with increasing temperature with a subsequent decrease in low molecular weight hydrocarbons consistent with previous findings in literature (Singh and Ruj 2016).

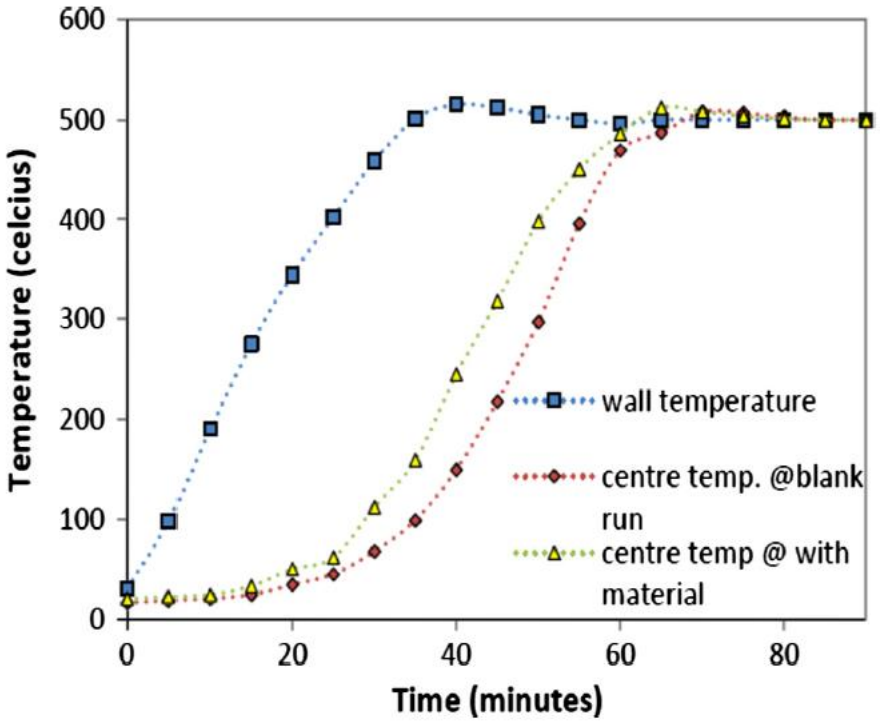

Figure 22: Temperature profile in the pyrolysis reactor with introduced feedstock and at a blank run (red curve) for 500oC (Singh and Ruj 2016).

On the composition of the products resulting from pyrolysis of LDPE and PS at reaction temperatures of 300^{o}C to 500^{o}C in a batch reactor, it was observed that LDPE and PS not only have different thermal degradation temperatures (425^{o}C for LDPE and 350^{o}C for PS) but the increase in reaction temperature has a different effect on the produced liquid fraction (Onwudili, Insura et al. 2009).

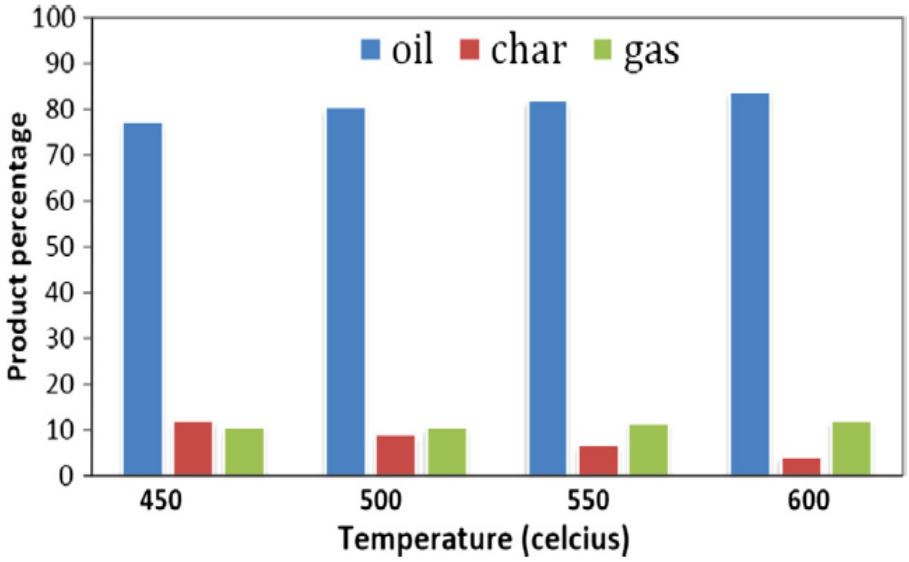

Figure 23: Yields of pyrolysis products with increasing reaction temperature (Singh and Ruj 2016).

HDPE, was pyrolysed in a fluidised bed reactor at temperatures ranging from 650°C to 850°C to study the effect on product distribution and gas composition. The gas composition with increasing temperature is shown in Table 7, and is in relevant agreement with findings from previously mentioned researchers and studies, resulting in further breakdown of pentane and butane components towards lighter components as hydrogen (Mastral, Esperanza et al. 2002). Using a semi batch reactor, for pyrolysis of a plastic mixture resembling municipal plastic wastes (the mixture included PE, PP,PS,PET and PVC) to study the effect of reaction temperature and find the optimum combination of reactor parameters was the objective of another study by López et al. This study however, focused more on the characteristics of the liquid product and less so in the gas and solids. It was found that at temperature of 460°C, a viscous liquid was produced with a high concentration of long hydrocarbon chains.

Table 7: HDPE pyrolysis gas composition with increasing temperature (wt% of feed) (Mastral, Esperanza et al. 2002)

Temperature (°C)	645	640	650	650	685	685	700	685	730	725	715	730	780	780	780	800	850	850	850	850
Res. time (s)	0.82	0.99	1.46	2.57	0.79	1.3	1.69	2.12	0.78	1	1.38	2.27	0.7	0.81	1.34	1.55	0.64	0.86	1.22	1.71
H_2	0	0	0	0	1	0.4	0.7	0.6	0.85	0.5	0.4	0.5	0.7	0.6	1.2	0.9	1	1.5	1.8	3.6
CH_4	1.1	0.8	2.2	1.6	4.7	4.8	4.8	5.1	6.2	5.9	6.2	6.6	8.8	9.7	14.2	13.7	11.8	15.3	16.7	22.2
C_2H_4	3.5	2.6	7.5	5.3	18.3	16.7	19.1	17.1	26.8	26.1	25.8	21.4	32.9	36.9	41.9	39.7	38.4	40.5	37.1	32.9
C_2H_6	1.2	0.9	2.1	1.6	4.6	3.4	3.5	3.5	3.5	3.9	3.7	4.1	3.3	3.8	4.12	4.4	2.9	2.5	2.7	3.2
C_2H_2	0	0	0	0	0	0	0	0	0	0	0	0	0.1	0.1	0.1	0.2	0.4	0.6	0.5	0.4
C_3	4.2	3.2	7.9	6.1	15.1	17.4	15.6	14.8	18.1	18.6	18.4	22.1	17.9	19.8	14.1	15.3	13.2	5.4	3.9	1.8
C_4	3.5	1.6	9.4	6.1	9.5	17.1	12.5	10.3	18.9	15.1	14.2	16	12.4	12.9	9.1	7.5	7	4.8	2.3	1.7
C_5	3.9	Na	2.16	1.4	6.7	Na	7.9	4.6	4.7	7.2	6.4	5.4	2.8	3.1	1.7	1.6	na	2.2	0.2	0

[a] na, not analysed.

At higher temperatures, a higher concentration of aromatics was obtained although the overall liquid yield was compromised. In Table 8, the composition of the produced liquids is presented and the lack of paraffin compounds was common across all temperatures (López, de Marco et al. 2011).

Table 8: Aromatics and non- aromatics detected in liquid products from pyrolysis at different reaction temperatures (López, de Marco et al. 2011).

	EXPERIMENT	460 °C	500 °C	600 °C
Aromatics	Mono-aromatics	68.0	69.7	70.8
	Indane derivatives	n.d.[a]	1.1	6.1
	Poly aromatics (PAH) and derivatives	3.7	3.1	22.4
	Total	71.7	73.9	99.3
Non-aromatics	Naphthenes	0.9	n.d.[a]	n.d.[a]
	Lineal olefins	14.4	15.1	0.4
	Branched olefins	7.0	7.2	n.d.[a]
	Total	22.3	22.3	0.4
Unidentified		6.0	3.8	0.3
C5–C9	Aromatics	68.0	69.2	70.6
	Non-aromatics	10.1	10.4	n.d.[a]
	Total	78.1	79.6	70.6
C10–C13	Aromatics	1.2	3.1	23.3
	Non-aromatics	6.3	6.3	0.4
	Total	7.4	9.4	23.8
>C13	Aromatics	2.5	1.7	5.3
	Non-aromatics	6.0	5.6	n.d.[a]
	Total	8.5	7.3	5.3

[a] Not detected.

These reported results, are slightly different with reported results from Li et al. who pyrolysed PE, wood and tyres at increasing pyrolysis temperature range and found aliphatic hydrocarbons to increase initially and finally decrease at even higher temperatures and the aromatic compounds having an adverse effect at different temperatures (Li, Li et al. 1999). The molecular weight distribution of the acquired oils from LDPE pyrolysis at increasing reaction temperatures was found to decrease from Williams et al. with combined increased aromatisation of the oils. The average carbon number distribution of the wax obtained products was from C_{11} to C_{57} and of the oils from C_8 to C_{44} but at higher pyrolysis temperature the concentration of aliphatic compounds above C_{30} was significantly reduced (Williams and Williams 1999). Hernandez et al. observed the presence of different hydrocarbons in the gas composition and related a high concentration of 1 - hexene with primary cracking and increased presence of ethane and propene when secondary cracking at increased temperature takes place (Hernández, Gómez et al. 2007) The importance of reaction temperature is directly related to the selected materials for pyrolysis and has a clear effect on the liquid, gas and solid products although not with the same weighing factor.

2.4.3 Pyrolysis type

Slow, intermediate fast and flash pyrolysis are dependent both on the reactor selection and configuration but ultimately have an effect on the resulting products and recovery of different fractions of products. The type of pyrolysis process depends on

the selected heating rate as well as shown in Table 9 and residence time that affect the final pyrolysis temperature (Basu 2010).

Slow pyrolysis process or conventional are related to higher residence times (min up or days) whereas, fast and flash have very short residence times (seconds), high temperatures and high heating rates that make this type of pyrolysis more suitable for applications with plastics.

Intermediate pyrolysis sits in between fast and slow pyrolysis and is a recent addition associated with the auger screw reactors with a residence time of a few minutes (Yang, Brammer et al. 2013, Yang, Brammer et al. 2014).

Table 9: Characteristics of some pyrolysis processes (Basu 2010).

Pyrolysis process	Residence time	Heating rate	Final temperature (ºC)	Products
Carbonisation	Days	Very low	400	Charcoal
Conventional	5 – 30 min	Low	600	Char, bio –oil, gas
Fast	< 2s	Very high	~500	Bio – oil
Flash gas	< 1s	High	<650	Bio-oil, chemicals,
Ultra – rapid	< 0.5 s	Very high	~1000	Chemicals, gas
Vacuum	2 – 30 s	Medium	400	Bio – oil
Hydropyrolysis	< 10 s	High	<500	Bio – oil
Methanolysis	< 10 s	High	>700	Chemicals

Recovery of products and related yields greatly depends upon the type of pyrolysis and respective reactor setup. As shown in Figure 24, slow pyrolysis or carbonisation produces equal amounts of solid, liquid and gas products whereas torrefaction favours char yields primarily and gas as a second product (Bridgwater 2012). The most favourable type of pyrolysis, for recovery of oil and liquid products

is fast or flash pyrolysis that has been used in several studies (Scott, Czernik et al. 1990, Bhadury, Singh et al. 2007, Xue, Zhou et al. 2015).

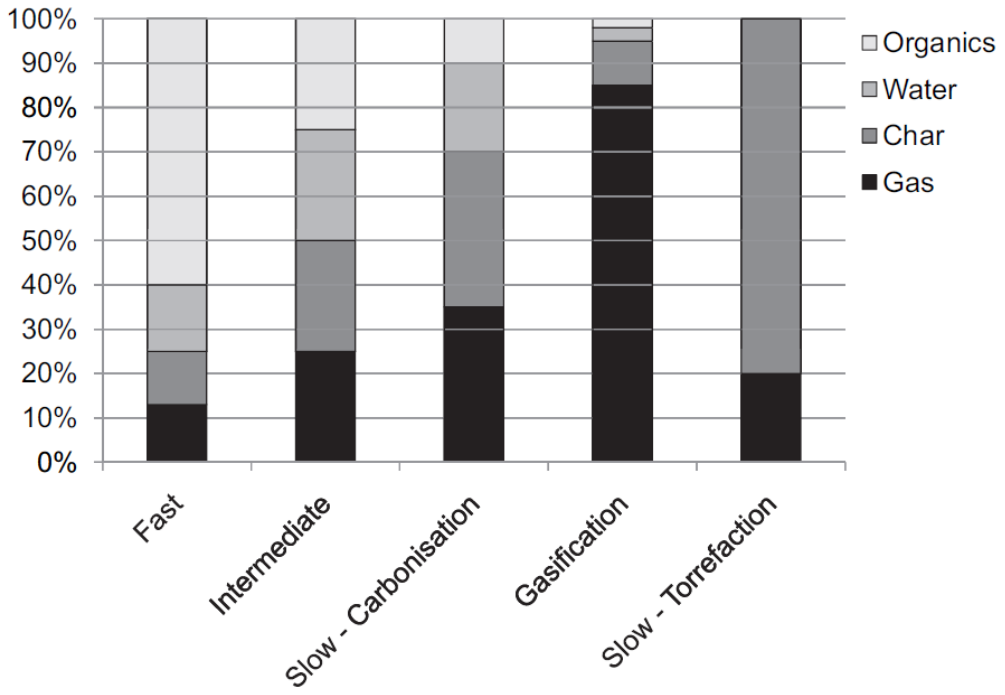

Figure 24: Product recovery for different pyrolysis type and gasification (Bridgwater 2012)

2.4.4 Heating rate

Most times heating rate is impossible to separate from the pyrolysis reactor, final temperature and operation conditions. Heating rate is defined as the increase of temperature per unit time (°C/min). Specifically, in fast of flash pyrolysis the heating rate can be as high 1000°C/min to 10,000°C/min since the contact time between the material upon entering the reactor is in seconds and it nearly instantly vaporises and decomposes (Basu 2010, Gao 2010, Bridgwater 2012).

Referring to, heating rate and its effect makes more sense in batch and slow pyrolysis processes where the sample is slowly heated from ambient to cracking temperature in several minutes and then it remains constant with values ranging from 10°C/min up to 100°C/min in several studies in literature (Williams and Williams 1997, Uemura, Azeura et al. 1999, Lee and Shin 2007, Marcilla, Hernández et al. 2007, Williams and Slaney 2007, Efika, Onwudili et al. 2015). Specifically, the effect of heating rate in pyrolysis of PET from waste soft drinking bottles with thermogravimetry, using three heating rate steps (10°C /min, 15°C /min and 25°C/min) showed that higher heating rates promoted the rate of the pyrolysis reactions (Saha and Ghoshal 2005).

Table 10: Effect of heating rates on RDF pyrolysis (Efika, Onwudili et al. 2015).

	Heating rate °C min^{-1}			
Products	5	20	90	350
	Yield (wt% of RDF)			
Gas	14.4	15.4	16.6	46.9
Solid	25.0	24.1	23.0	22.8
Oil	55.0	53.0	51.1	23.0
Balance	94.4	92.5	90.7	92.7
Char surface area m^2 g^{-1}	169.7	nd	nd	84.4
GCV of solids (MJ kg^{-1})	18.5	nd	nd	16.4
Gas composition	Yield (wt% of RDF)			
H_2	0.4	0.4	0.4	0.7
CO	4.4	4.5	4.7	18.7
CO_2	8.2	8.8	9.3	11.5
CH_4	0.6	0.7	0.8	4.9
C_2–C_4	0.8	0.9	1.4	11.0
GCV of gas (MJ/m^3)	12.5	12.8	14.0	24.8

nd: not determined.

Instead of, testing small incremental steps in heating rates values, two extreme heating rates were selected one for flash pyrolysis at 500°C – 800°C and one for slow pyrolysis at a heating rate of 5.0°C/min but no clear effect of the heating rate was identified in

terms of the evolved gases and catalytic effect on the plastic thermal degradation for both processes (Marcilla, Hernández et al. 2007). Finally, Efika et al. investigated the effect of slow to rapid heating rates at varying reaction temperatures (700^{o}C – 900^{o}C) and arrived to the conclusion that slower heating rates resulted in more oxygenated alkanes and alkenes in the final product while the higher heating rates produced more aromatics possibly due to the promotion of specific promotion reactions. The effect of tested heating rates on product yields and gas composition is shown in Table 10 (Efika, Onwudili et al. 2015). As a summary, the conclusions from the studies on heating rates are somehow contradicting without specific concluding remarks on a clear correlation and considerable effect on the final product especially in flash pyrolysis.

2.4.5 Residence time

Residence time, in pyrolysis is defined as the amount of time the vapour stays in the pyrolysis reaction zone and could be in the order of minutes or longer in slow pyrolysis or in the order of seconds and even milliseconds for fast/flash pyrolysis (Basu 2010). Calculation of residence time depends on the reactor used and the operating parameters. As such it is a straightforward calculation for batch processes and semi batch processes that the product is removed once the reaction is complete and it includes the duration from the heat up phase until the final removal of the products and residuals (Lee and Shin 2007, Onwudili, Insura et al. 2009, Gao 2010).

As shown in Figure 25, for a semi batch process at two different reaction temperatures the liquid yield is expressed as a function of reaction time and it can be seen that it has a positive effect especially at 400^{o}C increasing the liquid yield recovery. These findings, were in agreement with Miandad et al. that used a pilot scale batch

reactor for PS pyrolysis and found the liquid yield to increase up to 75min residence time at the highest reaction temperature but observed no significant effect past the 75min threshold. However there were observed variations in the quality of the liquids in terms of its viscosity measurements (Miandad, Nizami et al. 2016). Influence of residence time, in a semi – batch reactor was also studied at different reaction temperatures (460ºC - 600ºC) for the pyrolysis of plastic waste to find that residence time did not have as a significant effect as reaction temperature apart from very short reaction time (0 -15 min) (López, de Marco et al. 2011).

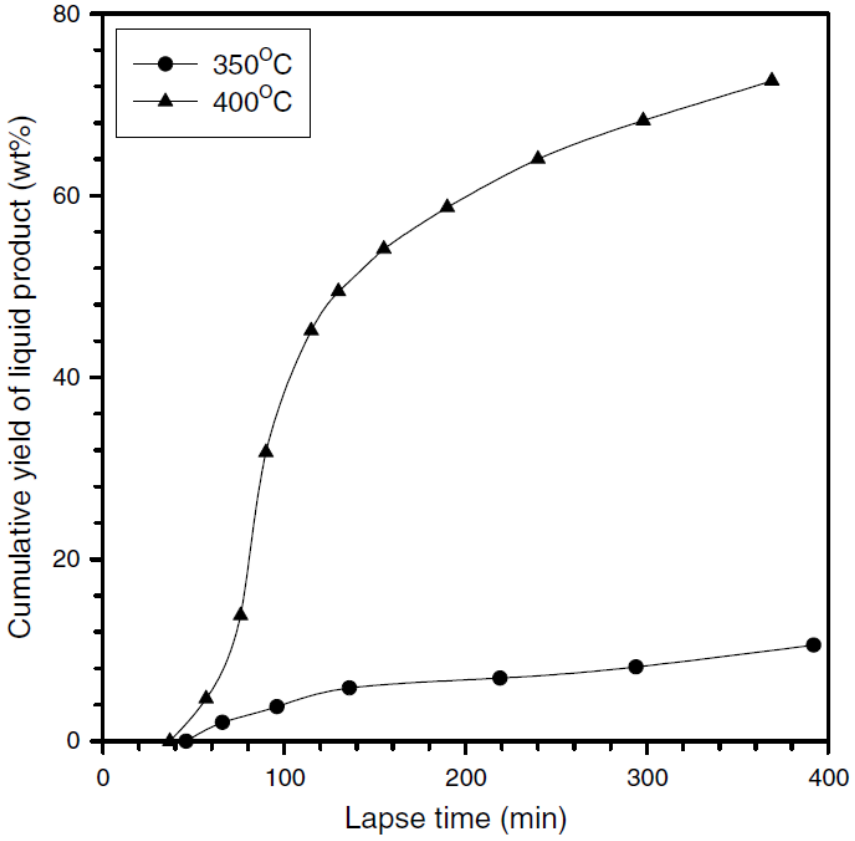

Figure 25: Cumulative yield of liquid product as a function of residence time for waste plastic mixture at 350oC and 400oC pyrolysis temperature in a stirred semi - batch reactor (Lee and Shin 2007).

Singh et al., however identified a relation between the studied residence time and the produced fuel quality where at higher reaction temperature increased residence time

resulted in heavier hydrocarbons in the gas stream as well as in the oil stream in the form of wax components (Singh and Ruj 2016) and this was also investigated by Onwudili et al. (Onwudili, Insura et al. 2009). The minor effect of residence time on a fixed bed tubular reactor was also confirmed by Westerhout et al. (Westerhout, Kuipers et al. 1998).

In fast and flash pyrolysis processes, residence time refers to the contact time between the plastic and the heated reactor area. Therefore, the calculation will greatly depend upon the volumetric feed rate ($\dot{m}$), carrier gas flowrate and reactor area (V) and will be unique to each reactor setup and in general is inversely proportional to the volumetric feed rate (Conesa, Font et al. 1994). Fewer studies have been conducted on the effect of residence times in fluidised bed reactors (Conesa, Font et al. 1994, Kaminsky and Kim 1999, Mastral, Esperanza et al. 2002, Kaminsky, Mennerich et al. 2009). Conesa et al. found that methane, benzene and toluene increase in the gas concentration with increased residence time and for the 500 – 800^{o}C reaction temperature range lower residence is required to achieve maximum yield (Conesa, Font et al. 1994). Mastral et al. investigate HDPE in a variety of pyrolysis temperatures (650 – 850^{o}C) and residence times (0.64 – 2.57 s) and found similar findings with batch processes, that is with increasing reaction temperature residence time had a great influence in the product distribution. Increased methane hydrogen yields were acquired at higher residence times with simultaneous decrease in C_3, C_4 and C_5 compounds as shown in Table 11 (Mastral, Esperanza et al. 2002).

Kaminski et al., found from the pyrolysis of a plastic mixture (containing polyolefins, PS, PVC, polyesters, paper and other plastics including fillers) in a fluidised bed reactor

that longer residence times produce higher amounts of tars and substituted aromatics with a decrease in benzene concentration (Kaminsky and Kim 1999).

Table 11: Effect of residence time at different reaction temperatures from HDPE pyrolysis (Mastral, Esperanza et al. 2002).

Pyrolysis gas composition (wt.% of feed)[a]

Temperature (°C)	645	640	650	650	685	685	700	685	730	725	715	730	780	780	780	800	850	850	850	850
Res. time (s)	0.82	0.99	1.46	2.57	0.79	1.3	1.69	2.12	0.78	1	1.38	2.27	0.7	0.81	1.34	1.55	0.64	0.86	1.22	1.71
H_2	0	0	0	0	1	0.4	0.7	0.6	0.85	0.5	0.4	0.5	0.7	0.6	1.2	0.9	1	1.5	1.8	3.6
CH_4	1.1	0.8	2.2	1.6	4.7	4.8	4.8	5.1	6.2	5.9	6.2	6.6	8.8	9.7	14.2	13.7	11.8	15.3	16.7	22.2
C_2H_4	3.5	2.6	7.5	5.3	18.3	16.7	19.1	17.1	26.8	26.1	25.8	21.4	32.9	36.9	41.9	39.7	38.4	40.5	37.1	32.9
C_2H_6	1.2	0.9	2.1	1.6	4.6	3.4	3.5	3.5	3.5	3.9	3.7	4.1	3.3	3.8	4.12	4.4	2.9	2.5	2.7	3.2
C_2H_2	0	0	0	0	0	0	0	0	0	0	0	0	0.1	0.1	0.1	0.2	0.4	0.6	0.5	0.4
C_3	4.2	3.2	7.9	6.1	15.1	17.4	15.6	14.8	18.1	18.6	18.4	22.1	17.9	19.8	14.1	15.3	13.2	5.4	3.9	1.8
C_4	3.5	1.6	9.4	6.1	9.5	17.1	12.5	10.3	18.9	15.1	14.2	16	12.4	12.9	9.1	7.5	7	4.8	2.3	1.7
C_5	3.9	Na	2.16	1.4	6.7	Na	7.9	4.6	4.7	7.2	6.4	5.4	2.8	3.1	1.7	1.6	na	2.2	0.2	0

[a] na, not analysed.

A synergistic effect between temperature and residence time was identified by Hernández et al. especially at higher temperatures where higher molecular weight hydrocarbons (propane, butane and pentane) decreased with increasing residence time due to secondary cracking reactions taking place (Hernández, Gómez et al. 2007). Using a fluidised bed reactor for pyrolysis of natural and synthetic rubber to study the effect of residence time on the gas composition only a weak influence was detected by increasing the residence time which resulted in slightly higher gas yields and carbon black recovery (Kaminsky, Mennerich et al. 2009).

Although, there has been substantial research in investigating the effect of residence time on product composition and overall yields the main focus of these studies is the gas stream and no straight correlation or clear influence have been identified although some significant observations have been made. Furthermore, for fluidised bed reactors the studies are not as extensive and there is a lack of focused results on the effect of the liquid product.

2.4.6 Pressure and other influencing factors

Pressure is a process parameter that has significant effect in pyrolysis and the resulting products however there have been few studies on it (López, Olazar et al. 2010). When pressure is applied in a pyrolysis environment the heavy molecular hydrocarbons are further cracked rather than vaporised as specific reaction temperatures (Murty, Rangarajan et al. 1996, Miranda, Yang et al. 2001, Murata, Sato et al. 2004).

Murata et al. studied the effect of temperature on PE thermal degradation and found that increased pressure favours the recovery of non - condensable gases at the expense on liquid product yields while decreasing the average molecular weight of the gas products. In Figure 26, it is illustrated that increased pressure in the pyrolysis decreases the average molecular weight distribution of the pyrolysed products (Murata, Sato et al. 2004). There is direct clear effect of pressures on the gas and liquid yield recovery from plastic pyrolysis and on the product distribution but also a number of other factors that are briefly mentioned affect the process. The composition, size, shape and physical structure of the feedstock influence the pyrolysis process by affecting heat transfer and subsequently affecting the heating rate, final temperature (Basu 2010).

Finally, reactive additives such as oxygen through minor oxygen ingress via the feeding mechanism or in small quantities in the feedstock (from PET) or hydrogen will react during the pyrolysis reaction and form specific compounds affecting the final product quality.

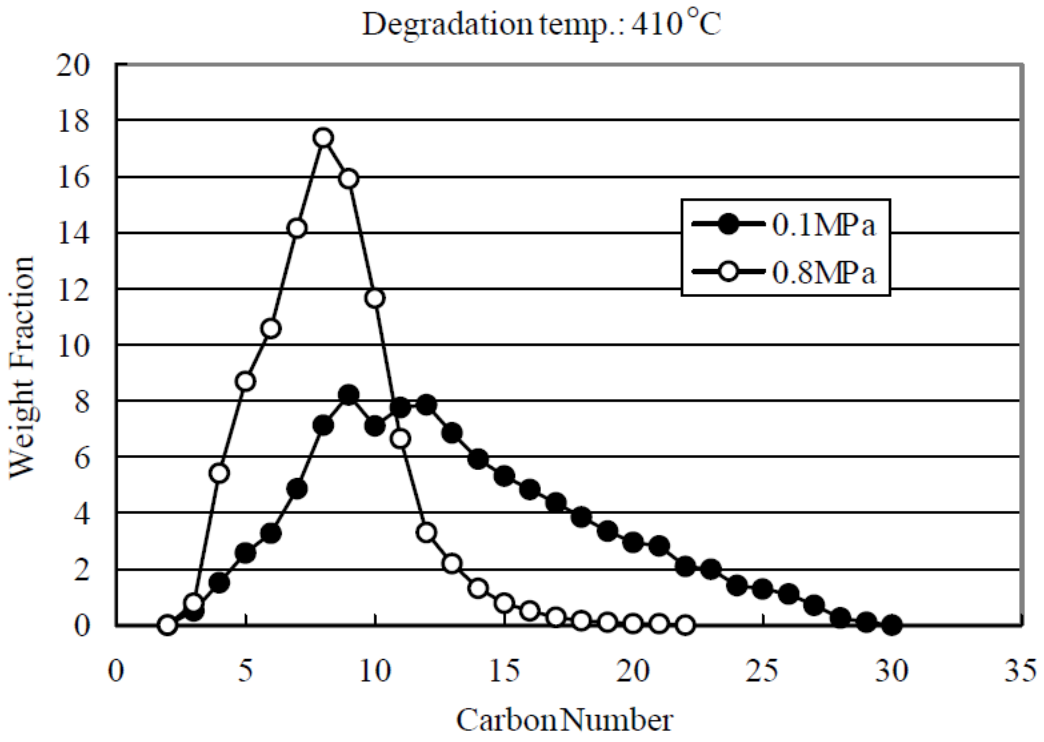

Figure 26: Carbon number distribution of the liquid product from PE pyrolysis (Murata, Sato et al. 2004).

2.4.7 Reactor configuration

A number of different reactors, have been used for pyrolysis over the years. The most important for pilot and commercial scale applications being: batch reactor, fixed bed, fluidised bed reactor, spouted conical reactor, bubbling bed, screw kiln or auger screw reactor and microwave pyrolysis reactor. Appropriate selection of the reactor will affect not only the mass and heat transfer rate properties but the mixing of the plastics, residence time, pyrolysis type, yields, product outcome quality and overall process efficiency. Therefore, reactor selection and configuration is one of the key elements in pyrolysis of plastics (Marcilla, García-Quesada et al. 2005, Aylón, Fernández-Colino et al. 2008, Bridgwater 2012, Al-Salem, Antelava et al. 2017).

The different reactors, have been used from micro scale, using thermogravimetry, to study the kinetics as discussed in §2.2.1 (Arenillas, Pevida et al. 2004, Al-Salem and Lettieri 2010, Park, Seo et al. 2012, Dimitrov, Kratofil Krehula et al. 2013, Acevedo, Fernández et al. 2015) up to pilot and semi industrial scale (Dai, Yin et al. 2001, Aylón, Fernández-Colino et al. 2008, Kaminsky, Mennerich et al. 2009, Martínez, Murillo et al. 2013, Kluska, Klein et al. 2014). Typically, the reactor setup will include either a pre – treatment, feeding system and liquid and gas product collection system after the reactor (Bridgwater 2012). Two of the most commonly used reactors, traditionally in pyrolysis of plastics are, the batch and semi batch reactors as well as the fluidised bed reactor. However, for continuous operation which is more suitable for commercial applications, the batch operation has the disadvantage of being an intermittent process.

Several researchers have used the batch or semi batch, setup for their studies (Williams and Williams 1997, Cunliffe, Jones et al. 2003, Kim and Kim 2004, Berrueco, Esperanza et al. 2005, López, de Marco et al. 2011, Kluska, Klein et al. 2014).

Another classification of the different reactors, is based on the heat transfer methods and flow both of the feedstock and the carrier gas. According to this, there are fixed bed reactors, fluidised bed reactors, conical spouted bed reactors and continuous auger reactors or screw kiln which have also been used in pyrolysis of plastics (Ballice 2001, Dai, Yin et al. 2001, Aguado, Olazar et al. 2002, Islam, Islam et al. 2004, Kaminsky, Predel et al. 2004, Lin and Yen 2005, Aylón, Fernández-Colino et al. 2008, Kaminsky, Mennerich et al. 2009, Martínez, Murillo et al. 2013). Fixed bed reactors are easier to design and operate however they might be problems encountered during

feeding and in heat transfer which is why they are normally used as a secondary reactor in such processes (Aylón, Fernández-Colino et al. 2008). In the fluidised bed, the reaction area consists normally of a silica bed that is in constant movement via means of a fluidising medium that allows for very good mass and heat transfer properties between the heat carrier and the feedstock (Garforth, Lin et al. 1998). A fluidised bed reactor setup is shown in Figure 27. Inside the fluidised bed reactor, there is even heat and temperature distribution, that allows for excellent heat and mass transfer rates. Key design consideration parameters, are the dimensions and material of the bed as well as the selection and calculation of the fluidisation velocity and selection of appropriate flows (Mastral, Esperanza et al. 2002, Kaminsky, Predel et al. 2004). For the latter reason, fluidised bed reactors are used in larger scale continuous operation commercial plants.

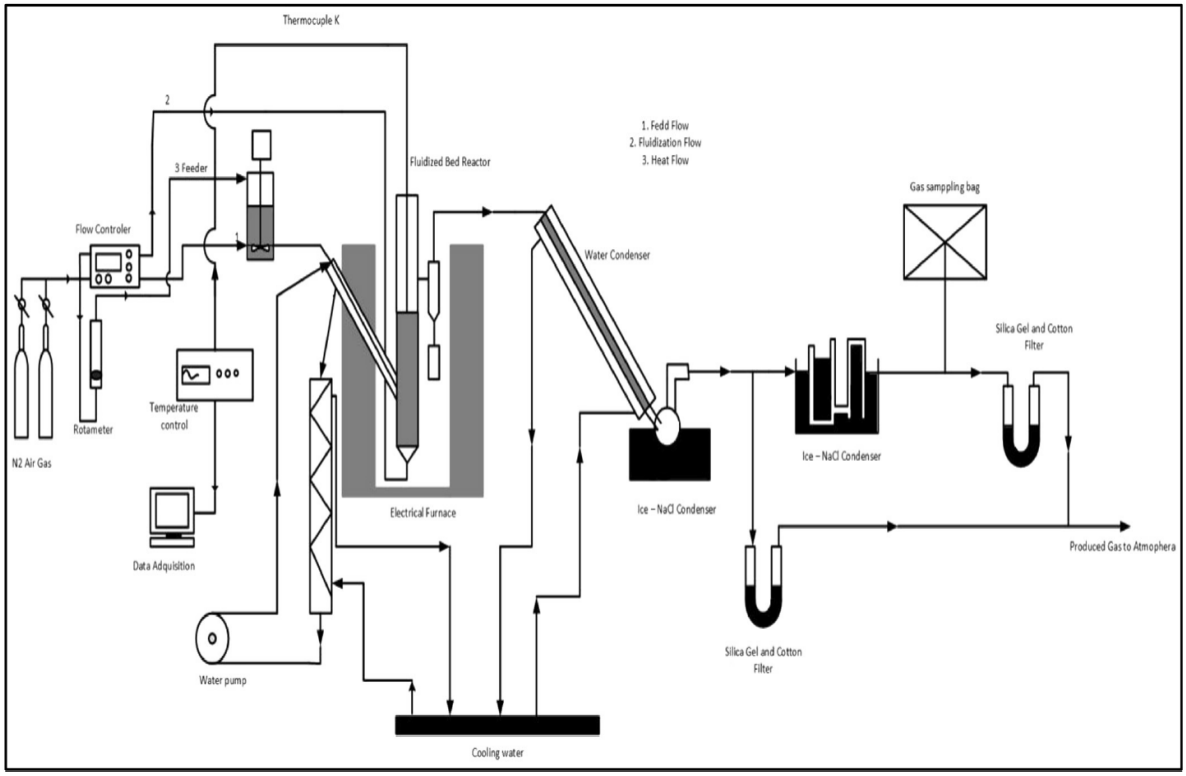

Figure 27: Fluidised bed reactor for pyrolysis of plastics setup (Mastral, Esperanza et al. 2002).

However, there are some issues associated with these reactors such as bed material loss and silica separation from the vapour stream and product. In recent years, a different reactor configuration has been used, for intermediate pyrolysis; this is known as screw kiln or auger reactor system and has been used in pyrolysis of tyres, biomass and waste materials. The main body of the reactor consists of an extruder screw (auger screw) that is used to transfer the feedstock across the internal heated surface of the reactor. The solid and liquid products are separated and collected at the end of the reactor. Since the main drive of the extruder screw is done via means of an external motor there appear to be fewer issues with blockages caused by the highly viscous nature of plastics (Bockhorn, Hornung et al. 1998, Williams and Williams 1999, Martínez, Murillo et al. 2013). Due to the movement of the screw there is a good mixing of the material and good heat transfer. The contact of the feedstock is done via convection and conduction with the heated surface area and the residence time is controlled by the rotation speed of the auger screw with the motor (Gao 2010, Yang, Brammer et al. 2014).

2.4.8 Catalysts

Catalytic cracking, has attracted significant interest in pyrolysis of plastics. Among the advantages of using a catalyst in the pyrolysis process are: increasing the rate of reaction and reducing reaction time, reducing the required pyrolysis temperature with a subsequent reduction in the energy demand, introduces in the liquid composition of the pyrolysis products diesel components that are more desirable, enhances selectivity to gasoline range and promotes isomerisation (Al-Salem, Antelava et al. 2017).

Traditional fuels such as diesel, petrol, kerosene and LPG are comprised of hydrocarbons ranging from C_1 to C_{24}. The liquid product obtained from pyrolysis of plastics and mixed plastic waste is a mixture of a variety of different heavier molecular weight components ranging from C_1 to C_{80} and can in some occasions include up to 100 different components (Aguado, Serrano et al. 2007).

One of the main components in mixed plastic waste, which is PE (or in the form of HDPE/LDPE) results in the heaviest fractions in the resulting liquid after pyrolysis whereas the products from PS and PP have been reported to be mostly lighter molecular weight hydrocarbons in comparison to PE which is why most of the catalytic studies focus on PE, HDPE or LDPE materials (Sharratt, Lin et al. 1997, Garforth, Lin et al. 1998, Luo, Suto et al. 2000, Manos, Garforth et al. 2000, Bagri and Williams 2002, Lin, Yang et al. 2004, Miskolczi, Bartha et al. 2004, Marcilla, García-Quesada et al. 2005, Mastral, Berrueco et al. 2006, Olazar, Lopez et al. 2009, Obeid, Zeaiter et al. 2014).

Catalysts, can be classified either as homogenous or heterogenous depending on the state they are. Heterogenous catalysts, are solid and generally preferred due to the ease of separation from the liquid product and their recovery allowing for regeneration and reuse. Nanocrystalline, zeolites are the most commonly used heterogenous catalyst for polyolefin pyrolysis. Conventional acid solid, mesostructrured catalyst, metal supported on carbon and basic oxides have also been considered (Aguado, Serrano et al. 2007, Shah, Jan et al. 2010, Al-Salem, Antelava et al. 2017).

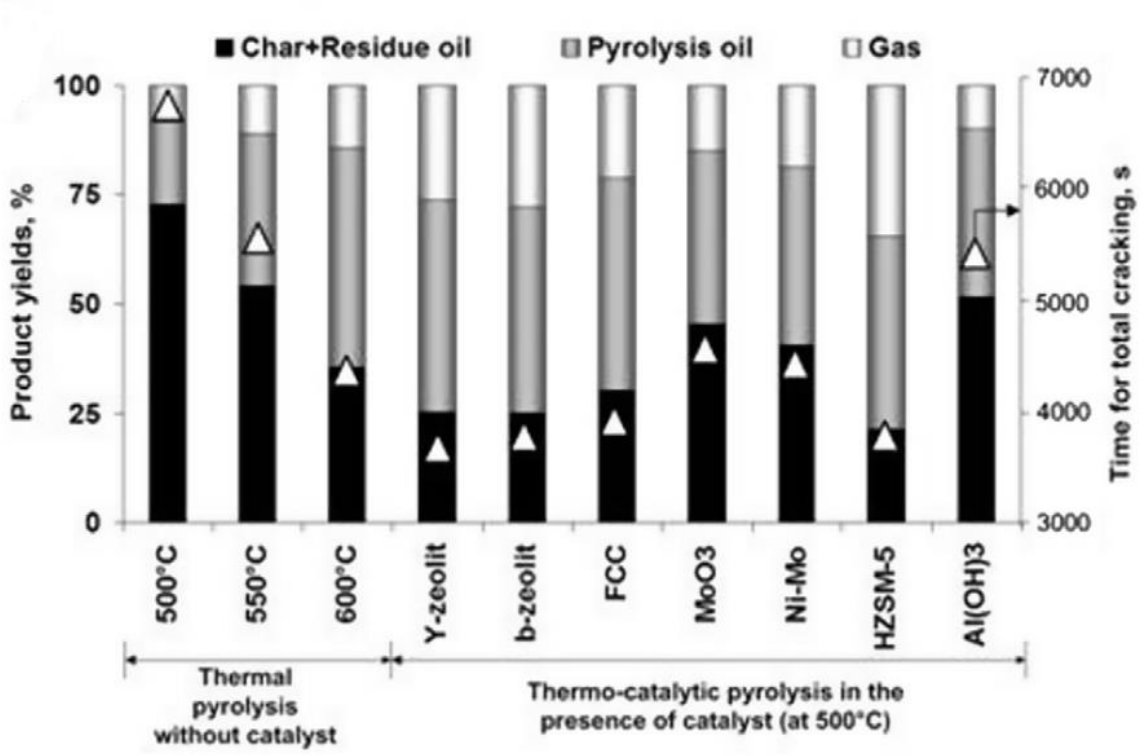

Figure 28: Comparative yields from thermal and catalytic pyrolysis of mixed plastic waste (MPW) using different catalysts with a residence time of 3000 s for full conversion in a batch reactor (Ateş, Miskolczi et al. 2013).

.

From the zeolite catalysts the acid based ones (HZSM -5 and H – ultrastable Y – zeolite) have been reported to be the most effective ones in plastics pyrolysis in comparison to the less acidic ones such as silica alumina and mesoporous when assessed based on their Si/Al ration (acidity) (Garforth, Lin et al. 1998, Gao 2010, Artetxe, Lopez et al. 2013, Al-Salem, Antelava et al. 2017).

In Figure 28, the effect of catalyst on thermal degradation of mixed plastic waste for a variety of different catalysts in comparison with simple thermal degradation is illustrated (Ateş, Miskolczi et al. 2013). It can be seen that the catalytic effect increased the liquid and gas production in comparison with simple thermal degradation with MoO_3 and $Al(OH)_3$ having the least significant shift and HZSME -5 contributing the most

towards gas production. The latter effect for n-HZSM – 5, ZSM – 5 and Y – zeolite catalysts has been reported by several researchers with different combination effects (Seo, Lee et al. 2003, Akpanudoh, Gobin et al. 2005, Lin and Yen 2005, Aguado, Serrano et al. 2007, Marcilla, Gómez-Siurana et al. 2007, Syamsiro, Saptoadi et al. 2014, Muhammad, Onwudili et al. 2015). Artetxe et al. also reported the increased selectivity of HZSM – 5 with the highest acidic ratio towards light olefin yield although the results were conducted in a two - step unit with the catalyst being in a downstream fixed catalytic bed rather than in situ.

The effect of acid ratio on olefin selectivity yields is shown in Figure 29. Compared to thermal degradation results the heavy fractions (C_{21}+) which were 67 wt.% with the two step catalytic process the heavy fractions were further cracked towards light olefins by parallel enhancing secondary hydrogen transfer and condensation reactions (Artetxe, Lopez et al. 2013).

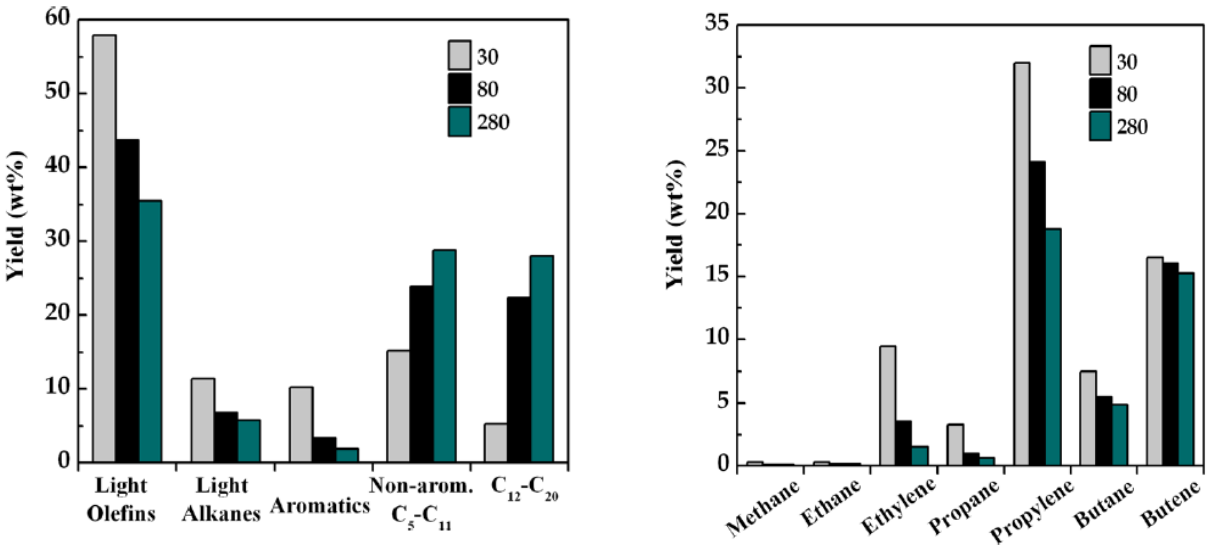

Figure 29: Effect of acidity ratio of the HZSM -5 zeolite on product fraction yields and individual yields of gaseous compounds from pyrolysis of plastics (Artetxe, Lopez et al. 2013).

Two different types of zeolite catalysts (HUSY and HBeta) were also investigated for their effect on selectivity on the liquid and gas sample but the result illustrated the same effect on increasing gas yields (from 17.8% on thermal degradation up to 96% in the presence of catalysts) in comparison to thermal degradation with a connecting increase in the measured paraffin content (Zeaiter 2014).

Table 12: Effect of individual catalyst on hydrocarbon range products of liquid fractions from HDPE pyrolysis (Ahmad, Ismail Khan et al. 2013).

Catalyst[a]	Distribution of hydrocarbon range products (%)				
	C_6–C_{12}	C_{13}–C_{16}	C_{17}–C_{20}	C_{20}–C_{30}	≥C_{30}
No catalyst	32.56	30.80	14.19	12.35	10.95
$BaTiO_3$	15.45	33.83	16.71	24.38	8.05
$Pb/BaTiO_3$	17.91	27.45	19.64	31.49	3.49
$Co/BaTiO_3$	24.34	35.45	22.42	13.05	4.4
$Pb–Co/BaTiO_3$	18.55	31.34	25.71	16.02	7.88

[a] Catalyst loading: 1%.

Ahmad et al. investigated the catalytic thermal degradation of HDPE using heterogenous mild acidic nano structured catalysts ($BaTiO_3$, $Pb/BaTiO_3$) to obtain high yield of liquid products with a favoured distribution towards naphtha range hydrocarbons but resulted in increased gas yields for the majority of the catalysts tested with a consequent effect in cracking heavier molecular weight hydrocarbons towards lighter fractions as shown in Table 12. Depending on, the aim of the catalytic upgrading process different options are available to consider for shifting the process yields and product component distribution.

Although, the acid based zeolite catalysts have been extensively studied and considered for the pyrolysis of plastics, all studies gravitate towards the same conclusion of promoted gas yield with a simultaneous dramatic decrease in the liquid

yield. If the aim of a project, is to improve the quality of the liquid yield as in the current study towards a diesel range distribution such an effect of breaking most of the liquid fraction into gas products is not desirable. Therefore, alternative options should be considered such as a two-step catalytic system of different types of catalyst with either depolimerization effect or visbreaking properties for heavy and super – heavy oils that have a close consistency with the oils produced from pyrolysis of plastics (Jing, Li et al. 2008, Chao, Chen et al. 2012, Bezergianni, Dimitriadis et al. 2014, Hart 2014). Some of the suggested alternative catalyst are homogenous or need to be in solution that makes the system more complicated and expensive.

2.5 Characterisation methods of pyrolysis products

From the pyrolysis of plastics three product streams can be recovered: liquid/wax, gases and solid char. The liquid and gas fractions contain mainly hydrocarbons of varying molecular weight and composition and char is normally produced in small quantities. For each respective product stream, different methods have been employed to analyse them. The main focus, on product analysis from pyrolysis has been for the liquid products and a number of different methods have been employed ranging from simple ultimate and proximate analysis including density and heating value up to detailed liquid hydrocarbon component separation and identification with GC – MS analysis (Kaminsky, Schlesselmann et al. 1995, Kaminsky and Kim 1999, Blazsó 2006, Buekens 2006, Williams and Slaney 2007, Strezov and Evans 2009, Jung, Cho et al. 2010, Szabo, Olah et al. 2011, Banar, Akyıldız et al. 2012, Donaj, Kaminsky et al. 2012, Abnisa, Daud et al. 2014). Following a GC – MS analysis, very interesting information can be recovered with regards to the carbon

number distribution of the product composition (Williams and Slaney 2007, Abbas-Abadi, Haghighi et al. 2013, Sharma, Moser et al. 2014).

Depending on the study and on the plastic material input for the pyrolysis process different qualities of the liquid recovered product have been reported. Some studies, report only liquid products and other identify heavier fractions with a solid waxy consistency (Arabiourrutia, Elordi et al. 2012, Artetxe, Lopez et al. 2013).

Table 13: Melting temperature ranges (°C) for the wax samples obtained from pyrolysis (Arabiourrutia, Elordi et al. 2012).

Material	450 °C	500 °C	600 °C
HDPE	70–83	70–80	85–95
LDPE	65–75	60–70	80–95
PP	55–70	50–60	70–85

For the waxy consistency, one additional product analysis can be performed to characterise its physical properties, its melting point as shown in Table 13 (Arabiourrutia, Elordi et al. 2012).The intended end use of the liquid product from pyrolysis in commercial applications is to be a substitute for commercial fuels namely diesel being one them. For this reason the focus on liquid analysis for several studies has been the analysis its physical and chemical properties that are relevant to an engine performance (Szabo, Olah et al. 2011, Abnisa, Daud et al. 2014, Ahmad, Khan et al. 2015).

These can be further separated into:

1. thermodynamic properties such as cetane number or cetane index which can be calculated from the fuel density and distillation range,
2. flowing properties that relate to the liquids viscosity, cloud point, pour point, cold filter plugging point and flash point values,

3. component distribution including carbon residues, sulphur content, water and ash content, and PAH content,
4. performance properties refer to colour, particulates, lubricity, acid value, oxidation stability and copper corrosion which relates to the sulphur content.

Sharma et al. analysed the liquid obtained from waste plastic grocery bags for its distillation range and the majority of the analysis mentioned above including GC – MS, FTIR and NMR to compare them against ULSD (ultra - low sulphur diesel) and test their blends. The results for the average carbon number of two different fractions from the distillation of the original liquid one lower temperature distillation range (PPEH-L) and the second from higher (PPEH –H) are shown in Figure 30 (Sharma, Moser et al. 2014).

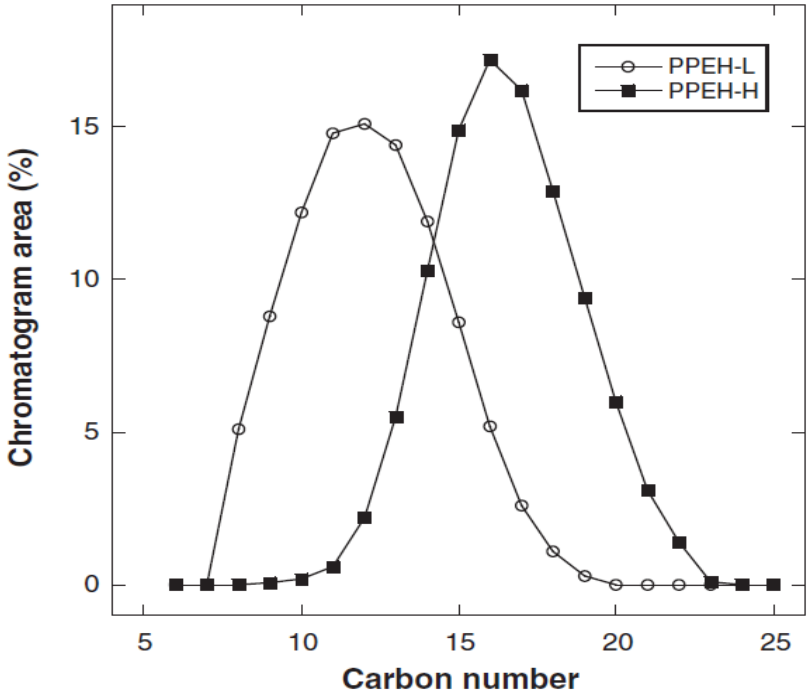

Figure 30: Composition of two different fractions from the pyrolysis liquid of waste plastic grocery bags (Sharma, Moser et al. 2014).

Qualitative and group quantitative methods such as FTIR SEC (size exclusion chromatography or gel permeation chromatography), SIM – DIS (simulated distillation)

and melting point have also been used on pyrolysis oils to assess the individual fractions and grouped components relating to properties such as boiling point or presence and intensity of specific functional groups for FTIR. All the previous depend on the quality and conditions under which the specific oils have been produced (Williams and Williams 1997, Miskolczi, Angyal et al. 2009, Kumar and Singh 2011, Banar, Akyıldız et al. 2012, Abnisa, Daud et al. 2014). In Figure 31, the comparative spectra of different liquids are shown and the differences in the presence of various functional groups can be seen; in the 2930 – 2830 cm^{-1} region the stretching vibrations of $–CH_2$ and $–CH_3$ groups whereas in the region of 1470 – 1365 cm^{-1} only the presence of $–CH_3$ was identified and the major difference was observed in the region of 800 – 1000 cm^{-1} where C-H vibrations cause infrared bands indicative of vinyl type double bonds (Miskolczi, Angyal et al. 2009).

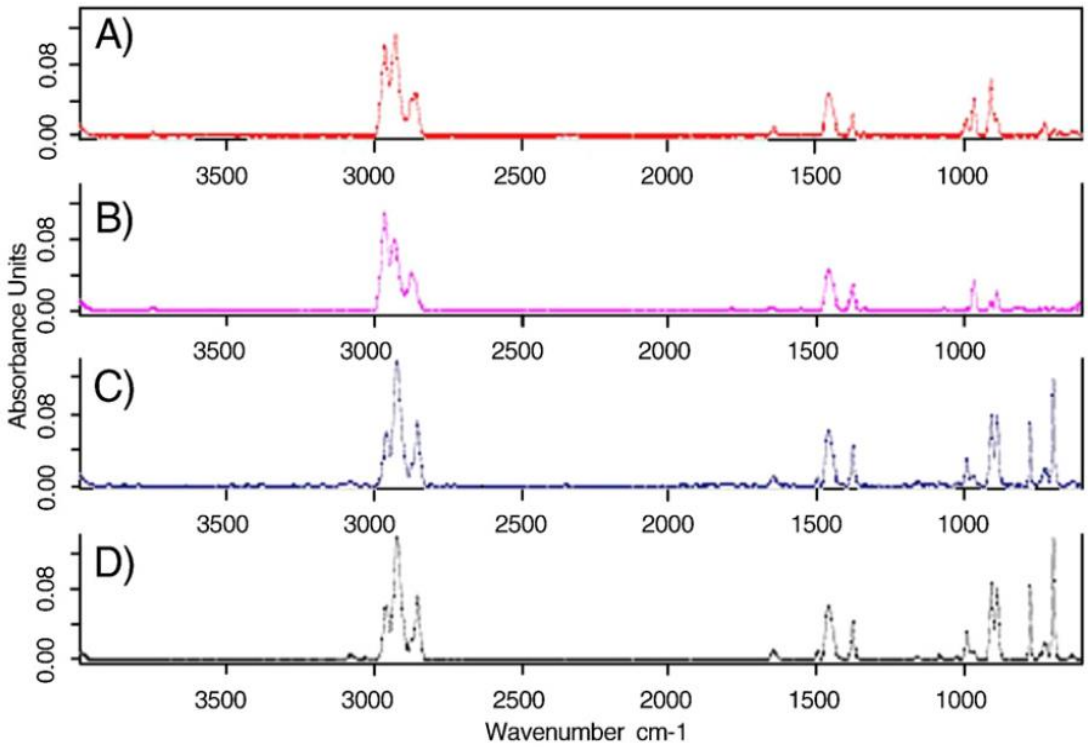

Figure 31: Infrared spectra of (A) HDPE, (B) HDPE and catalyst, (C) PP, (D) PP and catalyst (Miskolczi, Angyal et al. 2009).

These results, were afterwards analysed in relation to their molecular weight distribution in order to compare them against conventional fuels (Miskolczi, Angyal et al. 2009).

Following, the analysis of the products, from various studies and the targeted approach to compare oils obtained from pyrolysis of plastics as substitute for conventional fuels towards energy generation. Parts of the fractions, of the pyrolysis oils show promising potential to be considered for such applications due to the similarity in composition (mainly hydrocarbons, olefins, less aromatic and paraffin) however part of the pyrolysis oils heavier fractions need further upgrading due to their composition that renders them unsuitable (Miskolczi, Angyal et al. 2009, Strezov and Evans 2009, Arabiourrutia, Elordi et al. 2012, Ahmad, Khan et al. 2015).

2.6 Process optimisation and heavy crude oil (wax) upgrading processes

When considering the outcome, in terms of liquid product from the pyrolysis of plastic and plastic waste there have been a number of issues that need to be addressed. Some of these include, the quality of the produced oil and its corresponding suitability for applications in internal combustion engines that normally run on diesel fuel, the total product yield recovery that is directly linked with financial aspects of commercial, the variation in composition and components in the oil fraction derived from different raw feedstocks as well as the utilisation of different fractions of pyrolysis derived oil via further upgrading processes. Since the liquid product from pyrolysis of plastics consists of hydrocarbons ranging from C_6 – C_{80} the need to further break the average carbon number and produce a higher grade oil closer to the diesel or kerosene

range is of essence (Demirbas 2004, Miskolczi, Bartha et al. 2004, Abnisa, Daud et al. 2014). Miskolczi et al. attempted to shift the average carbon number distribution of the pyrolysis oils produced from simple thermal degradation with the use of catalytic upgrading as shown in Figure 32 (Miskolczi, Bartha et al. 2004).

Initially, the focus on literature was on designing the appropriate experiments and assessing the optimum process parameters (namely reaction temperature, residence time and carrier gas flowrate) with regards to the maximum obtained liquid yield and decomposition rates (Barbooti, Mohamed et al. 2004, Aydın and İlkılıç 2012, Miandad, Nizami et al. 2016). However, less focus has been placed on investigating the process parameters to actually improve specific characteristics of the oils and waxes towards a dedicated purpose, for example improving its viscosity characteristics for suitable applications.

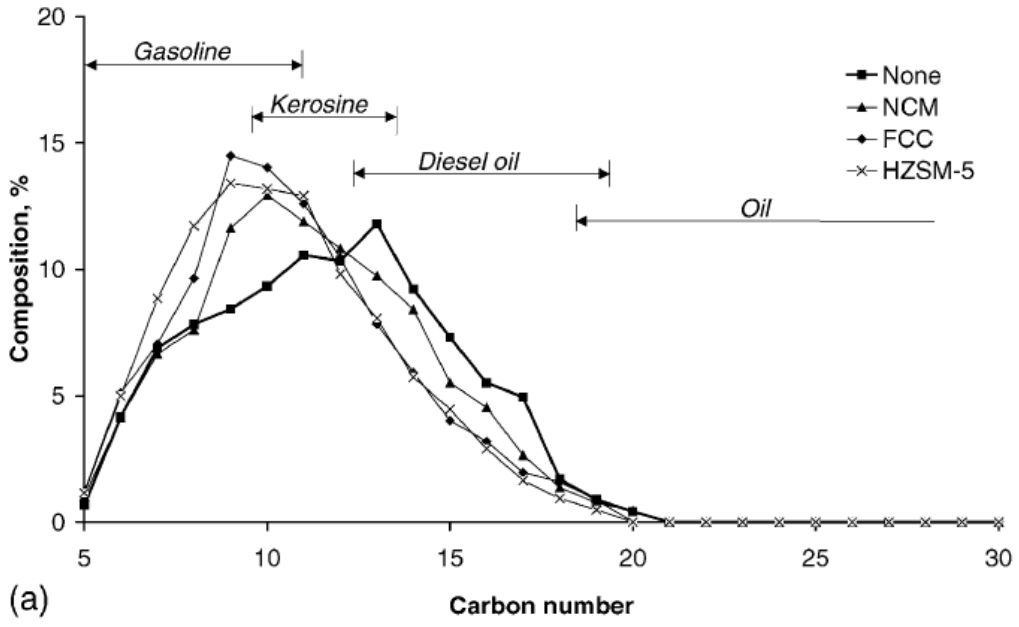

Figure 32: Composition as a function of carbon number (Miskolczi, Bartha et al. 2004).

Co – pyrolysis with biomass such as forestry waste (Martínez, Veses et al. 2014), palm shell (Abnisa, Daud et al. 2014) and jatropha oil (Biswas and Sharma 2013) has been investigated to improve the quality and stability of the produced oils from both sources with positive reported results in terms of reducing acidity, oxygen content and density while increasing the overall heating value of the produced liquid. Some post process considerations also have focused on the quality of the pyrolysis oils blends with diesel fuel (5% - 40% v/v) (Kumar, Prakash et al. 2013, Churkunti, Mattson et al. 2016) and tests in a compression ignition engine proved successful in reducing emissions and improving the brake thermal efficiency of the engine, whereas Mani et al. reported increased emissions and smoke levels (Mani, Nagarajan et al. 2011). Finally, specific catalytic upgrading methods can be applied in the vapour stream post – pyrolysis to break the viscosity of the evolved products which is an in – situ upgrading technology applied in heavy oil sector (Chao, Chen et al. 2012) or selective catalysts like FCC to control product yield and distribution (Lin and Yang 2007, Jing, Li et al. 2008). Also, processes like distillate and lube dewaxing via isomerisation and paraffin isomerisation should be given consideration (Degnan 2000).

Chapter 3

Materials and Methods

3.1 Introduction

There is a great diversity in the composition of actual Mixed plastic waste from industrial and commercial sources. Although, the majority of the waste is comprised from six main plastic types, the actual non-recyclable feedstocks may contain a combination of several different components including biomass and inorganic matter. To address the issue of plastic waste management both recycling and incineration have been employed with the remaining waste destined for landfill ((WRAP) 2016).

Within the area of energy production from waste, pyrolysis has been used extensively to derive different products. Pyrolysis is a fully developed technology that has been used previously for the degradation and cracking of polymers towards the production of economically viable hydrocarbon fuel. The pyrolysis process with the existing fluidised bed reactor (FBR) has a working temperature of 450 – 670^{o}C using nitrogen as the carrier gas to achieve thermal cracking in the absence of oxygen. Five actual feedstocks from industrial suppliers were selected for testing. The effects of feedstock variety, reaction residence time and reaction temperature were investigated

in terms of obtaining the optimal desired end product. Once the process optimal conditions have been established with the existing setup the design and use of an appropriate system to use catalysts for further cracking and potentially upgrade the existing samples was considered.

The sequence of the experimental method and analytical techniques used is outlined in Figure 33. The variety in the feedstock composition in connection with the complexity of the pyrolysis reactions drives and greatly affects the end product therefore making it crucial to initially identify and characterize feedstock key components. In the following paragraphs the feedstock characterisation analysis, experimental processes, sample fuel properties and analysis as well as catalyst characterisation and catalytic experimental setup are presented. The driving factor for the current research and objectives were:

- observe the shift in the average melting point of the produced fuel from mixed plastic waste, as well as the change in viscosity,
- attempt to decrease the average melting point and thus resulting in a lighter fuel,
- Establish optimal process conditions in terms of product quality, and identify the key weighing process parameters,
- Monitor product yields at optimal process conditions,
- Identify further upgrading routes.

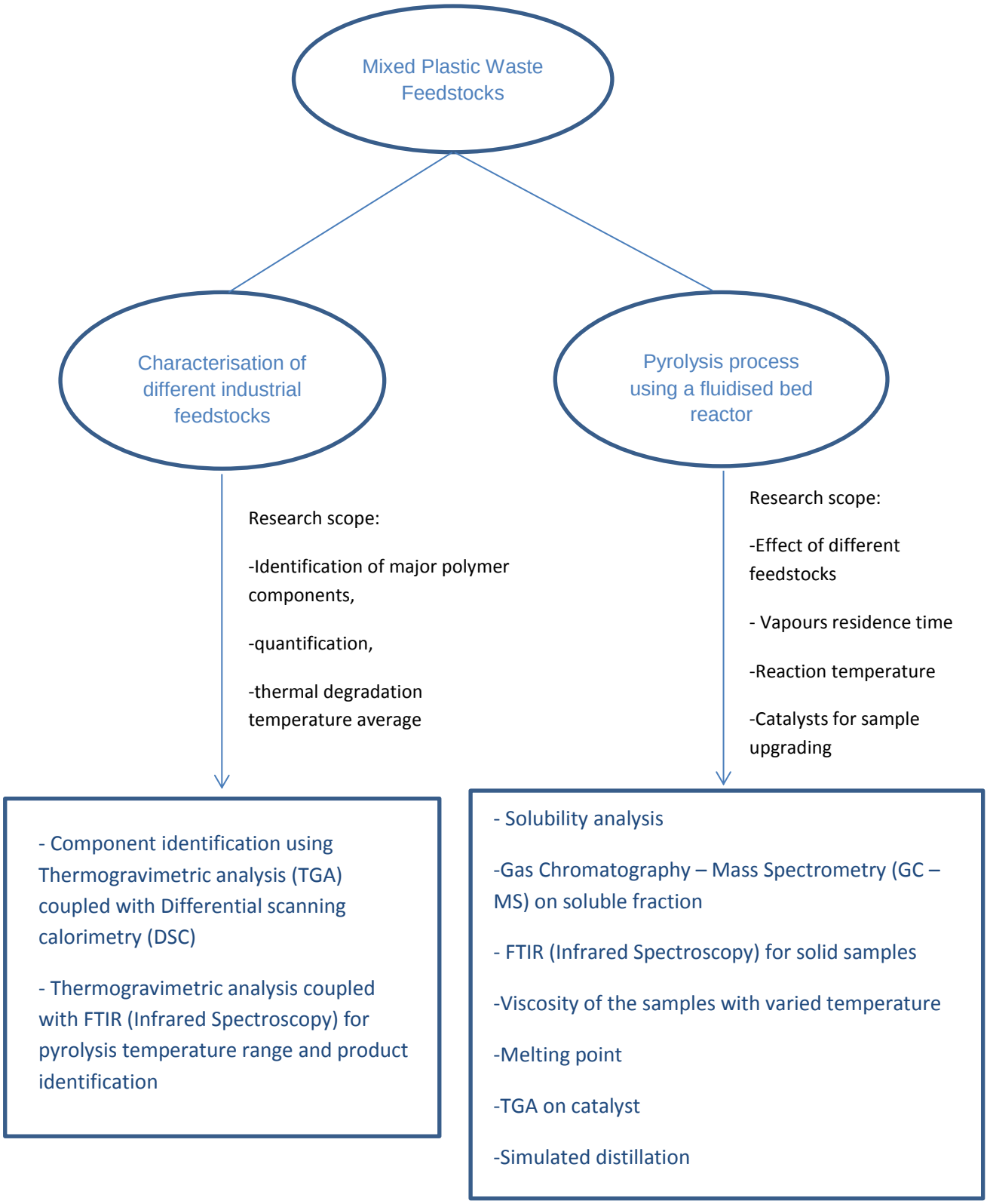

Figure 33: Experimental method and techniques used.

3.2 Feedstock Properties

A selection of different Mixed plastic waste feedstocks, as received by existing UK suppliers, were analysed and tested. Suppliers ranged from packaging consumer product companies, to supermarket chain, food packaging company and waste management services. For ease of identification, each supplier was given an abbreviation of their commercial name. Each different supplier followed their own waste separation process however the mixed plastic waste required pre-treatment and analysis prior to being pyrolysed. Initially, four feedstocks were analysed for ultimate and proximate analysis, moisture content and combustible matter as well as for their calorific value.

For the pyrolysis process, defining the moisture content is very crucial. All different feedstocks as these were received by the suppliers had a significant variation in the moisture content of up to 30 wt.% therefore making it essential to establish a suitable drying method to bring the moisture content close to zero. There was also a significant variation in the ash content and the actual combustible matter of the 12 wt.% range which is expected to have an effect in the mass balance and the final product yields in the pyrolysis process.

The analysis was carried out in external laboratories according to the following standards and testing methods:

- Carbon, Hydrogen, Nitrogen, Oxygen calculated according to EN14775 standard test method.
- Sulfur calculated according to EN15289 standard test method.
- Moisture content calculated according to EN14774-2 standard test method.
- Ash content calculated according to EN14775 standard test method.
- Gross Calorific value (dry basis) calculated according to EN14918 standard test method.
- Combustible matter (dry basis) calculated according to EN15440 standard test method.

3.2.1 Pre-treatment methods

The feedstocks were received in raw form, after the sorting process, still containing residual moisture and in intact pieces of varying sizes. To facilitate the heat transfer in the reactor bed as well as the feeding system a uniform particle size needed to be established in moisture free samples. Two pre-treatment methods for the feedstocks were drying the samples and shredding the material in particle size appropriate both for the feed screw system and heat transfer in the reactor bed.

3.2.2 Shredding

Material was shredded using a Retsch SM 300 cutting mill with 6 disc stainless steel rotor cutting knives suitable for a range of materials, specifically plastics and recycling material. The material entering the feeding hopper varied from 60 to 80 mm

dimensions and after grinding with the parallel cutting knives multiple sieves of different mesh sizes allowed for smaller particles of 0.20 – 0.25 mm particle size to pass through the trapezoid shape sieve holes resulting in even particle size distribution. Material was shredded to <0.25mm particle size to facilitate feeding process and heat transfer in the reactor bed.

3.2.3 Drying

To eliminate existing moisture in the received samples drying of all samples was required as a pre-treatment method. Residual moisture can affect the end product of the pyrolysis and needs to be removed to not affect the average pyrolysis temperature. Provided that the average melting temperature for the majority of polymers exceeds 100^{o}C the set temperature to drive moisture out was set at 80^{o}C. The samples were left at constant temperature for sufficient time until the weight loss stabilised. Moisture content was reduced to below 1 wt.% following a process of drying the shredded feed stocks for 6 hours at 80^{o}C combined with periodical agitation. Drying time was established based on the feed stock with the second highest moisture content which was Tk and the measured time for the weight loss to stabilise. All remaining samples were dried at the same temperature for the same amount of time. An additional drying process was performed for samples Tk, Sn and Gr following the initial drying step to establish the effect of further drying. After all samples were dried for 6 hours at 80^{o}C they were placed in an oven with a temperature of 85^{o}C and left to dry for an extended period of time of additional thirteen days. The samples were weighed every day for the first three days, following that, after five days and on the last day of the measurement. The recorded moisture loss, was expressed as a percentage on the sample weight and all curves were plotted on the same graph.

3.3 Experimental setup and process

For the fast pyrolysis experiments a purpose built fluidised bed reactor was used, in combination with a filtration and product collection system. All experiments were carried out at the facilities of the company developing the technology in Swindon. The Mixed plastic waste feedstock was inserted in the reactor via a moving screw feed system from the side of the reactor (Figure 34). All the pyrolysis reactions take place in the high temperature fluidisation area inside the reactor, on top of the reactor bed. Thermal cracking in the absence of oxygen is ensured by using an inert gas as the carrier gas specifically, for this setup Nitrogen, which is pre heated. Main parts of the system include, the fluidised bed reactor, nitrogen pre – heaters and manifold, alkaline injection system, hot gas filter, condensation and feeding systems. For the fluidised bed reactor, silica sand was used as the fluidisation and heat transfer medium with sand particle diameter of 0.3 mm for the reactor bed. Additional area above the reactor bed was added to ensure that there will be no transfer of the bed sand outside the reactor. Distribution of the fluidising gas was achieved via 8 perforated parallel pipes with 0.3mm diameter holes in equal distances. These pipes were welded on a flange internally at the base of the reactor bed. A nitrogen pre heater, is also used to heat the gas prior entering the reactor bed. This is achieved with the use of cartridge heaters inside the nitrogen pipeline. The heated gas is connected to a distribution manifold which is heated with the use of high temperature heater tapes and then evenly dispersed through the perforated pipes inside the reactor bed with a set flow rate to ensure appropriate fluidisation of the bed is established.

Heat is provided, to the reactor by using externally knuckle electric heaters in jackets along the length of the reactor with insulation on top and internally with the heated nitrogen passing through the bed. Temperature is monitored in several parts of the system using high temperature thermocouples and logging the values during the process. The heaters have additional thermocouples therefore the temperature is checked in two points: inside and outside the reactor for each different part of it. The shredded and dried feedstock is kept in a feed hopper and once the temperature has reached the expected value it is pushed to the lower hot fluidisation area with the use of a single extruded screw inside the fluidised bed reactor. After the feedstocks have been pyrolysed the vapours are carried through the area above the reactor bed (freeboard area) towards the filtration system.

Products of the process include the liquid products, char inside the reactor bed and remaining gaseous products. Vapours at this stage include liquid and gaseous products and are still kept in high temperature above their dew point until the pass through the filter and enter the condensation system. The Hot Vapour Filter (HVF) ensures that any solid particles including fine chars present in the vapours will be removed. The condensation system consists of three water cooled condenser and a water scrubber with the liquid product being collected at the bottom of each condenser. At the end of each experiment the reactor was dismantled, cleaned and all products were collected according to following described procedures. Collection of the char occurs at three points; inside the reactor (via subtracting the known amount of sand from the total weight), from the HVF after it has been cleaned and by adding the collected char at the bottom of the HVF filter from inside the fitted charpot.

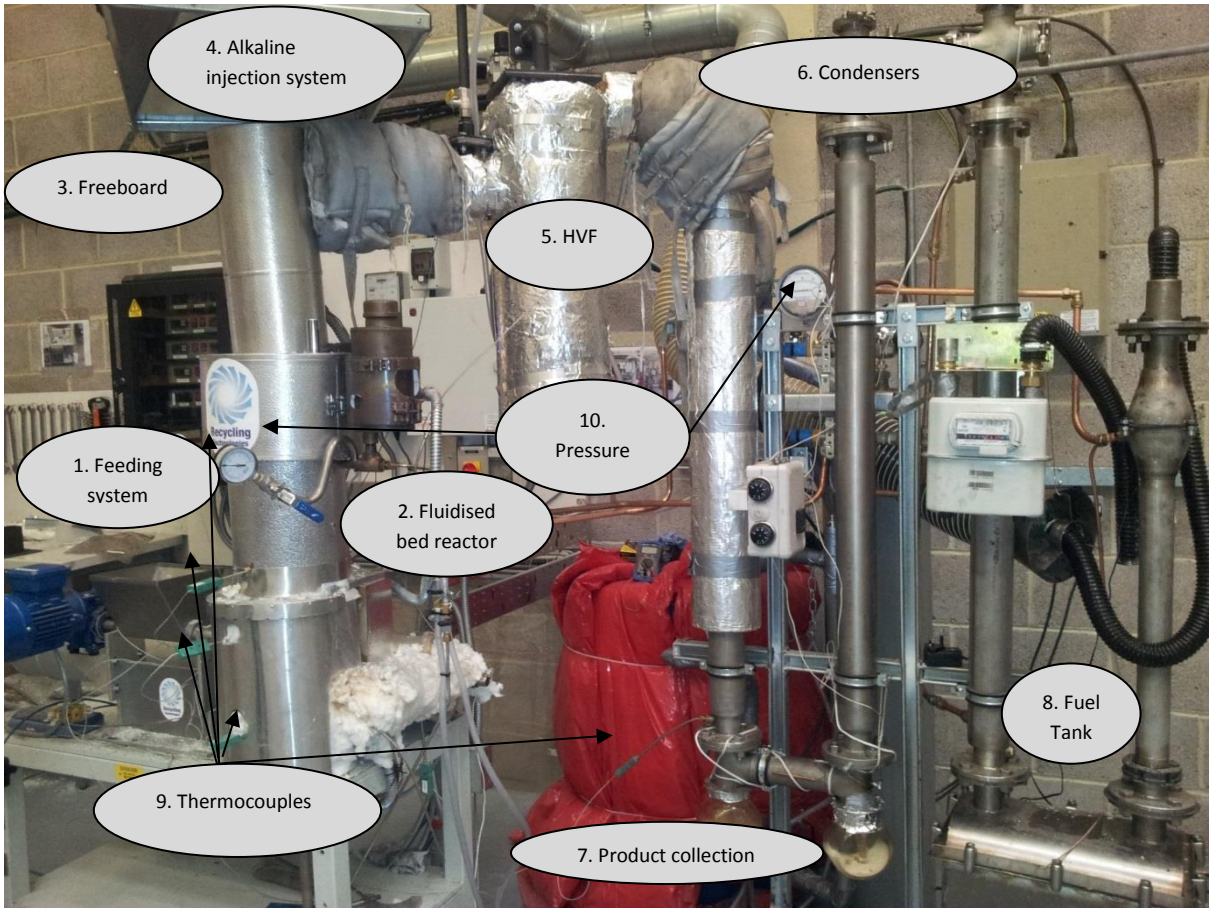

Figure 34: Pyrolysis apparatus with fluidised bed reactor.

The temperature of the cooling water for the first water condenser is 80^{o}C and for the second at 40^{o}C.Collection of the condensed product happens at the end of the condensers in a glass flask that is attached to them for the first two condensers. The third condenser is cooled at 20^{o}C and with the water scrubber they are connected to a larger collection metallic fuel tank (Figure 34). Similarly, collection of the fuel was conducted from the bottom of the three condensers and the metallic fuel tank as well as from scrapping any condensed fuel from the inside vertical walls of the condensers. All collected material was added and included in the mass balance.

An Alkaline Injection System, is also put in place before the HVF, and it consists of a hopper to store and when needed add the alkaline such as sodium bicarbonate and coat the filter. Connecting and isolating valves using nitrogen system as the transfer medium assist in the delivery of the powder through the transition pipe which connects the reactor freeboard with the HVF. Using the pyrolysis vapours and their existing velocity of the pyrolysis vapours to carry the alkaline towards the HVF and coat it. This process is used when there is certain contaminants present in plastics, including chlorine from PVC that need to be removed. High temperature thermocouples, were attached at different parts of the system (Figure 34). Although it is an open vent system, pressure is monitored in two different parts of the setup. One pressure gauge is reading the pressure inside the reactor and a differential pressure gauge is installed across the hot vapours filter to avoid any product or char over deposition and potential blockage (Figure 34).The experimental setup excluding the fluidised bed reactor was constructed, procured and commissioned in the premises of the developing company's workshop, in Swindon, UK. The fluidised bed reactor was built at Warwick University.

The sequence for the experiments started by purging the system with Nitrogen gas at minimum flow of 10L.min^{-1}. Following that, heating for the condensation system, water supply and pump for the condensers were switched on as well as the heater tape elements (Omega, UK) for the condensers. Heat controllers for the heating of the main reactor and the nitrogen pre heaters were switched after. All controllers, eight in total, were set to the desired temperatures for each experiment. To monitor the temperature in different points of the reactor the thermocouples were connected to a Pico TC – 08 Thermocouple Data Logger (USB) and to a computer with the appropriate software.

All temperatures were measured in real time and recorded 10 minutes before the experiment started. Temperature measurements were taken every 30 sec.

As soon as the operating conditions inside the reactor bed were reached and stabilised for at least 15 minutes the feeding of the plastics started. For different feedstocks, the speed of the motor for the feed screw mechanism was calibrated and adjusted and the flowrate of the nitrogen stream varied between 14 $L.min^{-1}$ and 20 $L.min^{-1}$ for different runs to achieve different residence times. The feedstock was weighed prior to being inserted and once the feed hopper was emptied additional feedstock was added.

To maintain stable operating conditions when there was a temperature drop inside the reactor bed, feeding of the plastics stopped and was resumed only after the reactor temperature recovered to the required levels. Minimum duration for each run was 60 minutes which was the time to obtain substantial amount of fuel for analysis and to acquire a measurable mass balance. Total duration of the experiments included heat up phase, experiment run, cooldown phase dismantling/clean-up and re setting the reactor was 2 days. The temperature range for the pyrolysis reactions was 500^{o}C - 670^{o}C. These limits were adhered to due to the nature of the feedstock that defined the value of the lower operating temperature and limitations on the heating elements of the equipment for the upper operating temperature.

Once the plastics went through the pyrolysis reactions the vapours passed through the freeboard area and the hot vapours filter that had an operating temperature of 490^{o}C downstream to the condensers where the liquid product was collected in a sequential condensation system whereas the remaining non – condensable gases

were vented externally. Gas samples were collected in Tedlar bags for analysis and liquid samples were retrieved for analysis at the University of Birmingham using techniques listed in the following sections. Depending on the feedstock and the char deposition inside the reactor bed each experiment was completed once it was not possible to maintain stable temperature inside the reactor any more. The range of operating conditions for the experiments are outlined in Table 14. Only the nitrogen flowrate and temperature varied for the experiments that were carried out.

Table 14: Experimental operating conditions.

Parameter	Value
Feedstock throughput (g/h plastic)	300 – 500
Reactor temperature range (20^{o}C at start – up)	500 – 565^{o}C
Nitrogen Flowrate (L.min^{-1})	14 – 28
Plastic particle size range (mm)	1 – 4
Maximum moisture content (wt% d.f.b.)	<5
Sand bed	2450g of 3.0 mm
Sand density (g/cm^{3})	2.648
Pressure (bar)	1.0 – 1.1

For the reactor bed the diameter to height ratio was set to one with a total reactor volume 823.28 cm^{3}. An added part, was attached beneath the reactor bed with a declining diameter shaped in a conical vessel connected to 0.635 cm in 90^{o} angle bended pipe with an isolating valve at the end to facilitate the sand removal and renewal from the reactor bed.

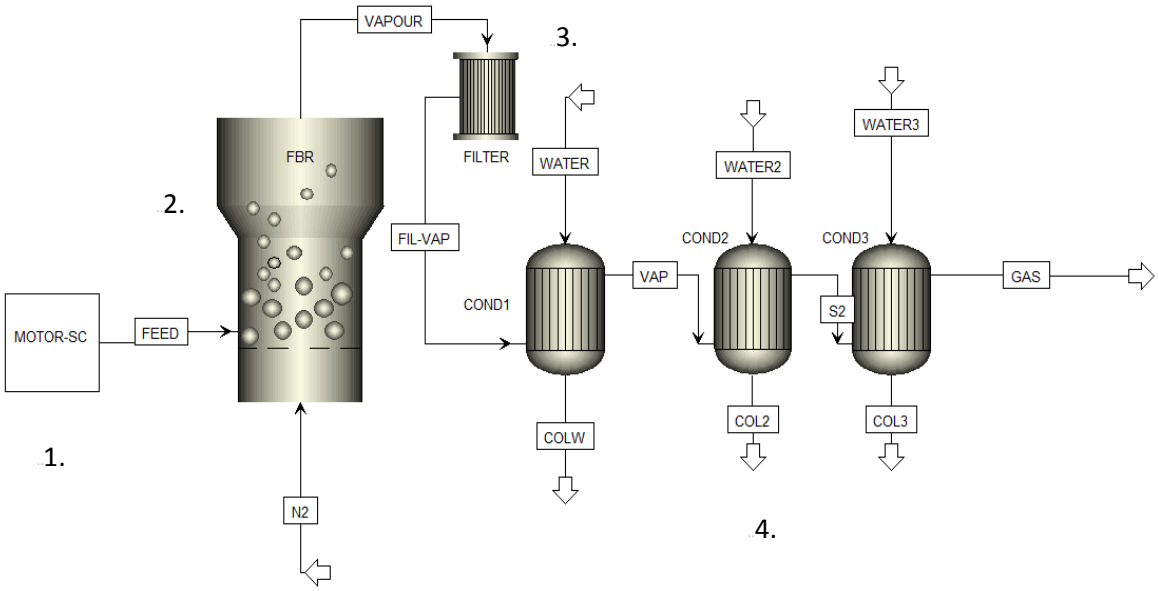

Figure 35: Reactor bed schematic with 1. Motor feed screw system, 2. Fluidised bed reactor, 3.Ceramic filter with reverse nitrogen clean-up system, 4. Condensation system.

Connected to the reactor bed with a flange a second stainless steel segment (freeboard 1 area) with identical dimensions was attached and served as an additional area to avoid sand transfer from the reactor bed.

The last part for the main body of the reactor (freeboard 3 area) connected also with a flange had a reduced diameter and a smaller height the leading to a bend and a reducer at the end of the bend and connected to a 1.905 cm diameter transfer pipe to accelerate the vapours before these will move downstream to the hot vapours filter.

3.3.1 Determination of operating parameters for the fluidised bed reactor

To establish appropriate fluidisation velocity and confirm the suitability of the dimensions of the pyrolysis reactor the following calculations were required, minimum

fluidisation velocity (u_{mf}) (Wen and Yu 1966), Reynolds (Re) and Archimedes numbers (Ar)(Wang, Chen et al. 2007), terminal velocity (u_t), transport disengagement height (TDH) and the required pressure to fluidise the bed (DP)(K. Smolders 1997). Equations 3.1 to 3.6 were employed for the above mentioned calculations and the parameters listed in Table 15, were taken as known parameters with regards to the bed dimensions, fluidisation gas characteristics and sand parameters. Initially the Archimedes number needs to be calculated according to equation 3.1.

$$Ar = \frac{\rho_g \times (\rho_S - \rho_g) g d_s^3}{\mu^2} \quad (3.1)$$

Where; $\rho_g$is the density of the fluidising gas at 500°C, ρ_s the density of the sand (kg.m^3), d_s is the diameter of the sand particle (mm) and μ the viscosity of the fluidising gas at 500°C (Pa.s).

$$Re_{mf} = \sqrt{C_1^2 + C_2 \times Ar} - C_1 \quad (3.2)$$

Where: C_1 =33.7

C_2=0.0408

$$u_{mf} = \frac{\mu}{\rho_g \times d_s} \times Re_{mf} \quad (3.3)$$

Since the particle is in the Allens regime the equation 3.4 can be used to calculate terminate velocity u_t.

$$u_t^{1.4} = 0.072 \times \frac{d_s^{1.6} \times (\rho_s - \rho_g) \times g}{\rho_g^{0.4} \times \mu^{0.6}} \quad (3.4)$$

$$\Delta P = (1 - \varepsilon) \times (\rho_s - \rho_g) \times g \times h \quad (3.5)$$

$$TDH = 6 \times \left[(u_f - u_{mf}) \times d_{bo} \right]^{0.6} \quad (3.6)$$

Where; ϵ is the voidage in the bed, u_f is the fluidisation velocity (m.s) and is equal to three times the minimum fluidisation velocity and d_{bo} is the maximum diameter of the bubble at the surface of the bed (mm).

Table 15: Fluidised bed characteristics and dimensions.

Parameter	Value
Reactor dimensions	
Material	Stainless steel
Inner diameter, ID (cm)	10.16
Bed Height, (cm)	10.16
Freeboard 1, ID (cm)	10.16
Freeboard 1 Height, (cm)	10.16
Freeboard 3, ID(cm)	5.08
Freeboard 1 Height, (cm)	40.00
Reactor bed characteristics	
Plastic feed (g./hr)	500.00
Average pyrolysis temperature (°C)	500.00
Sand particle diameter (mm)	0.30
Density of sand (ρ_s) (g/cm^3)	2.40
Density of Nitrogen (ρ_g) at 500 °C (kg/m^3)	0.4356
Viscosity of Nitrogen (μ) at 500 °C (Pa.s)	$3.51*10^{-5}$
Minimum fluidisation velocity u_{mf} (m.s)	0.03
Terminal velocity u_t (m.s)	1.26
Voidage in bed ε_{mf}	0.4179
Gas residence time τ_g (s)	1.74 – 2.58

3.3.2 Mass balance

Once the plastics inside the reactor bed are pyrolysed the released vapours are condensed as a liquid product in the condensers whereas the char and any ash remain in the reactor bed, transition pipes and partly deposited on the hot vapours filter. All added char resulted in the total char mass. The remaining non – condensable gases were therefore calculated by subtracting the mass of the collected liquid product and the mass of the char. The total feed rate (g.h) was calculated by weighed the total feedstock used and averaging with over the total experiment duration as indicated by the following equation:

$$Feed\ rate = \frac{W_F}{t_R} \times 60 \qquad (3.7)$$

Where w_F (g.) is the total weight of the feedstock used for each experiment and t_R (min) is the total run time of each run. For the calculation of the yield the mass for the fuel product and the char over the mass of the feedstock were expressed as a percentage as shown in equation 3.8. The gas yield was given by equation 3.9.

$$Y_i = \frac{W_i}{W_{Feed}} \times 100 \qquad (3.8)$$

$$Y_g = 100 - Fuel\ yield\ (wt\%) - Char\ yield\ (wt\%) \qquad (3.9)$$

Where Y_i is the yield for each product, w_i the weight of each component and w_{Feed} the weight of the plastic fed from the overall run.

3.4 Characterisation of feedstock and products

Different equipment and instruments were employed to characterise the feedstock properties and behaviour as well as to analyse the produced liquid and gas products from the pyrolysis process. Identification of the plastics present in the feedstock was achieved via a serious of different characterisation techniques. The quality of the produced fuel properties and the process parameters impact was assessed via Gas chromatography – mass spectrometry, changes in viscosity and density. True boiling distribution was used a reference to use it against the upgraded products.

3.4.1 Thermogravimetric analysis (TGA)

Two different thermogravimetric analysers (TGA) were used for the characterisation of the feedstocks. One of them was a TGA, Exstar 6000 analysis equipment from SciMED (Scientific and Medical Products Ltd 2017)with the option of connecting the evolved gases to a Fourier Transform Infrared Spectometer FT/IR. For the analysis aluminium, open sample pans, 5mm diameter, 3mm height were used for temperatures up to 600^{o}C. The second analyser used was an STA 449 Jupiter model from Netzsch used with open high temperature alumina sample pans 8mm diameter and 4mm height of 0.085 mL capacity for a working temperature of up to 1200^{o}C. The second was a simultaneous thermogravimetric and differential scanning calorimeter.

Nitrogen was used as a carrier gas was for the TGA (Exstar 6000, Scimed) with a flowrate of 200mL.min^{-1}. 5 – 8 mg of 3mm particle size samples were used for the

analysis and placed to the sample pan. Starting from ambient temperature 25^{o}C/min a 10 minute isothermal condition was maintained, followed by heating the sample up to 475^{o}C with a heating rate of 10^{o}C/min. The method ended by holding the sample at 475^{o}C for eight minutes.

3.4.2 Differential Scanning Calorimetry (DSC)

A simultaneous thermal analyser from Netzsch (STA 449 Jupiter model) performed thermogravimetric analysis and differential scanning calorimetry (DSC) measuring the mass change and the thermal effects connected with phase changes from the samples. The equipment had a temperature operating range from -150^{o}C up to 2400^{o}C by a Tungsten furnace using Argon as the inert purging gas with a 100mL.min^{-1} flow rate. Open end high temperature alumina sample pans with 8mm diameter and 4mm height of 0.085mL capacity for a working temperature of up to 1200^{o}C were used to place the samples for mass up to 18 mg but with a weighing range up to 3500 mg.

All endothermic reactions recorded have the peaks facing upwards while the exothermic reactions appear with the peaks facing downwards. A heating rate of 10^{o}C /min the sample was heated from 25^{o}C to 500^{o}C, and it was left to cool down afterwards. All the data and changes were recorded with Proteus software and the mass loss of the sample was measured simultaneously with the recording of the energy changes that were taking place inside the chamber of the

sample. The results were plotted in graphs with the DSC curve and the TGA curve in one graph with the temperature reference x – axis. Mass change is reported in w.t.% and the total mass loss was determined by subtracting the residual mass from the starting value. The second derivative of the mass change curve is depicted to identify the points of the most rapid mass change.

3.4.3 Fourier Transform Infrared Spectroscopy (FTIR)

Additional analysis was carried out with a TGA, Exstar 6000 analysis equipment from SciMED, coupled with a Fourier Transform Infrared Spectometer FT/IR -6300 from JASCO. The optical bench is equipped with 28 degree retro reflector (corner – tube) mirror Michelson interferometer (Jasco 2107). Once the spectra acquisition was completed the Spectra Manager II software was used for data analysis. For the analysis a resolution of 4 cm^{-1} and number of scans set to 32 were selected. The percentage of transmittance percentage was presented against wavenumber (cm^{-1}) in graphs with the peaks facing down.

All feed stocks that were analysed evolved from the TGA analyser mentioned in §3.4.1 with the detailed method. The evolved gases from the samples were carried through to the FT/IR with a flexible plastic tube and with a heated transfer line at a temperature of 140^{o}C. Heating was achieved with a heater tape around the transfer line controlled with an individual controller and a type K thermocouple. An illustration of the equipment set – up is provided in Appendix D. For the wave number range and the specific gases analysed selected for the gases analysis was from 700 to 4000 cm^{-1}.

3.4.4 Gas Chromatography – Mass Spectrometry (GC-MS)

A Gas Chomatography – Mass Spectrometry analyser was used to carry out the full characterisation analysis of the individual spectra for selected samples that were in solution of toluene and isopropanol. A GCT premier from Waters/Micromass Ltd, orthogonal acceleration time of flight mass spectrometer was used with a Gas Chomatographer 7890A from Agilent attached to it. The column used was an Agilent Q –plot 5MS column suitable for natural gas, refinery gas, C_1 – C_3 isomers, CO_2 methane air/CO and all sample results were run through a library search to identify the major components. Injection volume is 1µL with injector temperature of 300^{o}C and a split of 50:1.

The method used for the GC – MS analysis is the following:

1. Hold at 60^{o}C for 10 minutes to allow all Hydrocarbons from hexane and below to come out.
2. With a heating rate of 10^{o}C/min heat from 60^{o}C to 320^{o}C.
3. Hold at 320^{o}C for 30 minutes to allow all the heavier molecular weight hydrocarbons to be released.

Total run time was 68.5 min.

All spectra and results were analysed with the MassLynx software control and the online library was used for identification of the individual peaks with a match of 80% probability and above.

3.4.5 Gas Chromatography (GC)

Several gas samples were collected with a micro pump at the exit of the third condenser from the reactor set- up. They were analysed initially with a gas chromatographer from Agilent technologies with a splitless injector with injection temperature of 250^{o}C and a packed column in Chemical Engineering laboratory at University of Birmingham. The detector was a thermal conductivity detector which is more suitable for identification of volatile components. The sample (2ml) was kept at the initial temperature of 40^{o}C for 8 min and was heated with a heating rate of 50^{o}C/min up to 250^{o}C. At 250^{o}C the sample was held for another 20 min. However no components were identified with this system apart from one peak at the retention time of carbon dioxide. A second gas chromatographer from Agilent in Chemistry department was used with a different method and a different detector. The method started by holding the sample at 60^{o}C for 10 minutes, raising the temperature at a heating rate of 40^{o}C/min until 300^{o}C and retaining the sample at that temperature for another 40 minutes until no more peaks were coming out.

The detector used in the GC was and FID (Flame Ionisation Detector) detector, which does not take into account all the components such as CO_2 and since a significant number of peaks appeared, it was considered better to run the same sample with the GC –MS equipment that was also used for the fuel samples so there could be a library identification at the same time using the method established with the FID detector.

A secondary method to avoid the column bleed effect was tried complimentary at a lower constant temperature of 50^{o}C for 45 minutes. These results are reported as well.

3.4.6 Viscosity Measurement

Measured viscosity of the samples was used as a value to test the efficiency of the process and validate the upgraded samples. The equipment used was a controlled stress/controlled strain/ controlled rate rheometer with a 40mm 2^{o} steel cone aluminium plate of parallel geometry. The model was from TA Instruments the Rheology Advantage AR -2000. A shear stress against shear rate mode was used with the temperature parameter on the x – axis to include all the sample behaviour with plate gap size of 1000μm.

The standard method for calculation of kinematic viscosity of diesel, transparent is ASTM D445/ISO 3104 which determines the reference temperature to measure kinematic viscosity at 40°C since this is used as the basis for the ISO viscosity grading system (ISO 3448). For the oils that do not have proper fluid characteristics at 40°C the option of 60°C can be used and for petroleum wax 100°C is used. The method developed for these specific samples included a step temperature increase of 5^{o}C from 60°C up to 80°C and one final measurement at 100°C. This method was developed due to the nature of the sample and its property to change viscosity with temperature increase. Specifically the onset value was the starting measured melting point and the final value to test the maximum value where viscosity change was observed before release of light hydrocarbon vapours.

3.4.7 Simulated Distillation (SIM –DIS)

According to method ASTM-D2887 a True Boiling Point distribution range for carbon numbers of petroleum and its distillates can be obtained. Following this standard the true boiling point range is achieved by simulated distillation (SIMDIS) using an Agilent 6850N gas chromatography (GC) and calibrated in accordance with the ASTMD2887 in order to analyse and characterize the soluble fraction of the samples. The Agilent 6850N GC (Agilent Technologies, Inc., Germany) was fitted with a J&W DB-HT 5 m length, 0.53 mm internal diameter and 0.15 μm film thickness capillary column, combined with a Programmed Temperature Vaporisation (PTV) injector in order to heat the sample fast up to 355^{o}C so it will be vaporised before being inserted to GC. The method was adjusted to ASTM-2887-08 to allow for higher temperature in combination with the PTV injector in order to analyse fractions with boiling point up to 343^{o}C.

A Flame Ionization Detector (FID) was used and maintained at 260^{o}C. With a syringe, 1 μL of the sample in solution was injected into the GC. The flowrates of the gases were: 450 mL.min-1 air, hydrogen flow 40mL.min-1 and nitrogen as make up gas with a flow of 32.3 mL.min-1, respectively. Helium with a flow of 20 mL.min-1 was used to elute the column. With a heating rate of 20 ^{o}C.min-1 the samples were heated from 40 to 260^{o}C. Calibration of the GC was done with a hydrocarbon mixture of the range C5 – C40 standards. The conversion of high-boiling-point (or high molecular weight) fractions to lighter fractions (BP < 343^{o}C) was defined as the conversion of the 343^{o}C +hydrocarbons (HCs) that are found in the feed oil to the produced upgraded oils.

3.4.8 Density

To measure the density of selected samples a gas pycnometer was used AccuPyc II 1340 by Micromeritics, using the gas displacement method to measure volume and automatically calculate density for a known mass of the sample (Micromeritics 2017). Helium was the carrier gas for the purges required for the measurement. For a known volume of the sample holder a weighed sample was introduced and the sample container was pressurised at 0.020 psig. For the analysis the number of purges was set to three for five repetitive cycles and the sample density was calculated as the average of the repetitions. The basic principle of the equipment was the measured volume change inside a known volume for the given gas and calculating the density for the known mass. Density was reported in $g.cm^{-3}$ through the connected software AccuPyc 1340 including the standard deviation.

3.5 Experimental characterisation methods

In addition to the analytical equipment some experimental methods were employed for further analysis of the produced fuel product. The produced fuel sample was in a solid state and therefore for the GC – MS analysis it was required to be in liquid phase. Hexane and heptane were reported as the more efficient solvents however when these were tested they were not efficient and the soluble fraction was insignificant (Gao 2010, Arabiourrutia, Elordi et al. 2012) .

Therefore there was a need to test different solvents and their combinations. Two more methods were employed to assess the process efficiency and the changes in the fuel quality.

A melting point test of the fuel samples was undertaken and these results were compared against a melting point curve of hydrocarbons that was comprised of Octadecane up to Tetrapenacontane. The hydrocarbon range was selected from initial GC – MS results of the samples that gave an indicative range of the hydrocarbon consistency present in them. Finally a minor study on fuel blends with commercial diesel was carried out and combined with identification of the crucial hydrocarbons that influenced the miscibility and subsequently the fluid properties of the blends.

3.5.1 Solvent Analysis

Product fractions were obtained as solid after condensation, (see Figure 36) it was essential appropriate solvents were identified and the solubility of different samples served as indication of Tetrahydrofuran, Dichloromethane, Acetone, Dimethyl Sulfoxide, Hexane, Cyclohexane, N- Heptane, Octane, Decane, Toluene, Isopropanol, Mesitylene, Xylene, Diethyl ether, Acetonitrile, Heptanol, Ethanol. Both polar and non - polar solvents were tested in different ratios, individually and in combinations. The following ratios were tested 1:10 / 1:100 and 1:1000 with the second proving to be the most efficient. However, none of the above individually or combined diluted the sample completely.

Figure 36: Photographs of example solid fuel products from two experimental runs with different conditions.

The soluble fraction was calculated for the most effective solvents that were tested (Toluene and iso- propanol). Sample weight was 1.000 g ±0.050 g and the solvent quantity used was 75 mL Toluene and 25 mL iso – propanol. Filter paper contained the sample and was used to pass the solvent through. Once Toluene was used iso propanol was in sequence to dissolve the polar components. The remaining sample in the filter was dried and weighed afterwards to calculate the non – soluble fraction.

3.5.2 Melting point curve

A melting point curve was compiled from measurements of single hydrocarbons starting from Octadecane ($C_{18}H_{38}$) being the first solid hydrocarbon in ambient temperature up to Tetrapentacontane ($C_{54}H_{110}$) which is the highest molecular weight hydrocarbon of the components present in GC- MS analysis. This enabled comparative reference for the sample melting point measurements. Present in the sample analysis were also alcohols. These, starting from dodecanol ($C_{12}H_{26}OH$) and above are in the solid phase as well. Therefore the selected hydrocarbon range was selected from

octadecane until tetrapentacontane ($C_{54}H_{110}$) and one individual alcohol was included in the study. A selection of hydrocarbons available in the School of Chemical Engineering at UoB were tested to determine their melting points:

- pentadecanol ($C_{15}H_{32}O$),
- octadecane ($C_{18}H_{38}$) – nonadecane ($C_{19}H_{40}$) – eicosane ($C_{20}H_{42}$) - heneicosane ($C_{21}H_{44}$) - docosane ($C_{22}H_{46}$) - tricosane ($C_{23}H_{48}$) - tetracosane ($C_{24}H_{50}$) - pentacosane ($C_{25}H_{52}$) - hexacosane ($C_{26}H_{54}$) - heptacosane ($C_{28}H_{58}$) - octacosane ($C_{28}H_{58}$) - nonacosane ($C_{29}H_{60}$),
- triacontane ($C_{30}H_{62}$) - hentriacontane ($C_{28}H_{58}$) - dotriacontane ($C_{32}H_{66}$) - tritriacontane ($C_{33}H_{68}$) - tetratriacontane ($C_{34}H_{70}$).

The remaining hydrocarbons values were completed from existing available online data (Aldrich 2015) and the acquired values were compared with existing available databases. A block heater SBH200D/3 from Stuart instruments was used to heat up the individual hydrocarbons. Temperature was controlled via a digital setting display and it was gradually increased by a step of 1^{o}C. A digital thermometer was used to double check the actual block temperature and the hydrocarbons were placed in glass tubes so the phase change was visible.

For each measurement 2.00 ± 0.30 g. of hydrocarbons were used. The starting and end point of the melting point were noted. The melting point curve was plotted for each individual hydrocarbon on the x – axis against the end melting temperature in y – axis

in Celsius degrees. Relating the melting point of different wax samples to the chain length and melting points of this melting point curve could serve as an indicator of the approximate average chain length of the wax samples.

3.5.3 Melting point

The equipment used for the melting point measurements of the wax product, was a digital Stuart SMP10 melting point apparatus with a digital display and selection of temperature set at 1^{o}C resolution (Equipment 2017). Two samples were tested simultaneously in one open end capillaries of ø 1.5mm. Observation was undertaken via means of a magnifying lens and built in light. The possibility to stop the heating when a change was observed in the sample improved the accuracy of the measurements. Three measurements per sample were taken to minimise observation error. Both starting and end point of the melting point were measured.

3.5.4 Fuel blends characterisation for engine test suitability

A study on the fuel and how miscible it is with conventional diesel for potential use in engines was completed. Two different blends were prepared by mixing at ambient temperature 5% and 10% w/w Plaxx with Ultra Low Sulphur Diesel (Oils 2008) with the following specifications:

- Density at 15^{o}C, kg/m^{3} - 835,

- Viscosity, Kinematic at 40°C, mm /s (cSt) - 3.4,
- Flash Point, (Closed Cup, PM) - 80°C,
- Cetane Number - 52,
- Strong acid number Zero.

The mixed sample was subsequently heated to 75^{o}C with simultaneous agitation by hand to create a homogenous mixture. The created blends are shown in photos in Appendix D. They formed a thick emulsion which at ambient room temperature had limited flow characteristics. Viscosity change in the blends of 5% and 10% were compared with the pure sample viscosity analysis. Lubricity analysis should be performed to compliment the viscosity results for engine runs suitability. These could not be performed under the current state of the samples since the emulsion could not flow into the equipment.

3.5.4.1 Hydrocarbon blends analysis

To explain and understand the effect of the wax sample when blended with diesel a secondary more detailed study was carried out. The wax samples consist of a combination of hydrocarbons within the range of C_8H_{16} - $C_{54}H_{110}$ including alcohols, alkanes, alkenes and carboxylic acids, resulting in an average melting point that can be associated with the melting point and chain length of a single respective alkane or alkene of specific molecular weight. Therefore, considering that only hydrocarbons in solid phase would affect the blends with diesel, a series of them were tested following

two directions. Investigating the quantity of sample that could be blended and how that affected the blends and their consistency. For that reason 10% and 20% w/w were prepared to assess the diluting limits and secondary the defining crucial chain length that had altered the consistency of the blends and connecting both parameters.

Starting from Octadecane ($C_{18}H_{38}$) the alkane in solid phase at ambient temperature (>21^{o}C) several alkanes with increasing molecular weight were tested up to Tetratriacontane ($C_{34}H_{70}$). The study was completed in three steps. Initially, from the performed GC – MS analysis the peaks with the higher relative percentages were identified and the corresponding chemicals tested in 10% w/w blends with ULSD to identify any obvious effects. These alkanes were: Nonadecane ($C_{19}H_{40}$) – Eicosane ($C_{20}H_{42}$) – Heneicosane ($C_{21}H_{44}$) – Docosane ($C_{22}H_{46}$) – Tricosane ($C_{23}H_{48}$). The first initial blends were attempted by adding the plaxx samples (0.500 g ± 0.060 g) in diesel (5.000 g ± 0.660 g) at ambient temperature with simultaneous agitation of the mixture. The blend was left overnight to observe any potential changes in the consistency. One major observation within the first tests was that from Docosane ($C_{22}H_{46}$) and above all hydrocarbons would not dissolve into diesel with simple agitation in ambient temperature. To verify the initial observations a 20% w/w blend was prepared with plaxx (0.700 g ± 0.050 g) added in diesel (3.700 g ± 0.050 g) for the same samples. The same effect was noted for Docosane ($C_{22}H_{46}$) again.

Therefore, in the second step of the study, for Docosane ($C_{22}H_{46}$) and the alkanes above, addition of heat was employed in the process. The samples were heated gradually, after being mixed with ULSD with the use of a block heater SBH200D/3 from Stuart instruments and simultaneous agitation. Temperature was monitored with two

thermometers in different point of the block heater and raised up to the limits of each hydrocarbons melting point range. Using the above described method all remaining alkanes were prepared up to tetratriacontane ($C_{34}H_{70}$) in 10% w/w blend following the same quantities mentioned before. Additionally, one alcohol pentadecanol ($C_{15}H_{32}OH$) was tested both in 10% and 20% w/w. Alcohols from dodecanol ($C_{12}H_{26}OH$) and above are in solid state in ambient temperature 24^{o}C and above and could potentially affect significantly the consistency of the wax samples. After all blends were prepared they were left overnight and any changes in their consistency are reported.

3.6 Characteristics of catalysts

For the catalytic process two different hydrotreating catalysts were selected both in quadra – lobe shapes from AkzoNobel. The first was Co–Mo/ Al_2O_3 (Cobalt – Molybdenum oxides on alumina silica support) and the other Ni–Mo/ Al_2O_3 (Nickel – Molybdenum oxides on alumina silica support). To assess the catalyst their surface area, pore volume and pore width were calculated using the (BET) Brunauer – Emmett – Teller method via nitrogen operated absorption – desorption analysis. To reduce and activate the catalyst a Thermogravimetric analyser was employed using a 5.7% Hydrogen/ Nitrogen flow using a method up to high temperatures to detect the mass change and temperature where reduction was occurring.

3.6.2 BET surface area analysis

To measure the surface area, pore size, pore volume and diameter the Brunauer – Emmet – Tellet method of adsorption - desorption using nitrogen as the

adsorbate gas was used. A Micromeritics ASAP2020 surface area and porosity analyser was employed to perform the adsorption and desorption of the catalyst at 77.425 K and obtain the adsorption isotherm. Preparation of the catalyst samples included grinding them into fine powder form prior to weighing after. The sample mass for NiMo and CoMo was 0.0476 g and 0.0856 g respectively. Following that both samples were heated at high temperature for degassing and to remove any absorbed substances. The results of the process are given in Table 16. All calculations for specific surface area, pore size and volume were based on the BET method following ASTM C1274 standard of physical adsorption. The method followed the principle of the BET equation (3.10).

$$\frac{P}{V(P_O-P)} = \frac{1}{V_m C} + \frac{(C-1)P}{V_m C P_O} \qquad (3.10)$$

Where:

P = nitrogen partial pressure,

P_o = saturation pressure for the set temperature of the experiment,

V = volume of gas adsorbed at pressure P

V_m= the volume adsorbed and

C= a given constant

The equivalent BET surface area was calculated from the following equation (3.11)

$$S_{BET} = \frac{V_m n_a a_m}{m_v} \qquad (3.11)$$

Where:

n_a = Avogadro number,

a_m = cross sectional area of the molecules at 77.425 K,

m_v= the volume of gram molecule equal to 22.414 mL

V_m= the volume adsorbed

Table 16: Characteristics and properties of NiMo and CoMo.

	NiMo	CoMo
Cobalt (II) oxide, (wt. %) CoO	-	1-10
Nickel (II) oxide, (wt. %) NiO	1-10	-
Molybdenum (VI) trioxide, (wt. %) MoO_3	10-20	10-20
Aluminium oxide, (wt. %) Al_2O_3, support	20 -70	> 50
Silicon dioxide, (wt. %) SiO_2 , support	20-70	-
Boron oxide, (wt. %) B_2O_3	-	10-20
Diameter a (mm)	1.5 ± 0.03	1.40 ±0.03
Diameter b (mm)	1.3 ± 0.02	1.21 ±0.03
Length, (mm)	6.0 ± 3.0	5.0 ± 2.0
BET surface area ($m^2.g^{-1}$)	261.90	243.65
External surface area ($m^2.g^{-1}$)	229.34	248.18
Micropore area ($m^2.g^{-1}$)	32.56	-
Micropore volume ($cm^3.g^{-1}$)	0.014	0.0018
Maximum pore volume, ($cm^3.g^{-1}$)	0.68	0.43
Median pore width (Å)	141.38	86.37

3.6.3 Thermogravimetric Analysis for activation temperature

During activation the catalyst is reduced in high temperature by using a hydrogen enriched carrier gas to drive oxygen out of the catalyst structure and replace it with hydrogen. For the catalyst reduction a Thermogravimetric analyser with a mix carrier gas of hydrogen nitrogen was employed. To identify the activation temperature and reduction the catalyst was exposed to high temperature with a fast heating rate. A Thermogravimetric analyser from NETZSCH Proteus Thermal Analysis (TG 209 F1) was used with open end high temperature alumina sample pans (8mm diameter and 4mm height of 0.085mL capacity for a working temperature of up to 1200^{o}C). The carrier gas was 5.7% H_2/N_2 with a flow rate of 40 mL.min^{-1} was used for the reduction. Temperature was raised from 25^{o}C to 950^{o}C with a heating rate of 10^{o}C/min and at 950^{o}C the temperature was retained stable for 5 minutes. The mass change was recorded and reported via the TG and DTG curves and plotted against temperatures. All results are reported in Chapter 6.

Chapter 4

Characterization of Mixed Plastic Waste Feedstocks

4.1 Introduction

Thermogravimetric analysis has been used significantly for the identification of thermal decomposition behaviour and studies on the reaction kinetics of natural polymer components such as lignin, cellulose, hemi cellulose and plastics, waste components or combinations of these. All of the above mentioned studies predominantly were used as the first step for pyrolysis, gasification or combustion behaviours employing different carrier mediums. The variety in composition of mixed plastic waste (MPW) relating to significantly different thermal degradation behaviour and reaction kinetics creates serious challenges in the operation and design of the thermal system. Determining the key components of 5 selected samples, from existing commercial suppliers, as well as the main derived components from their thermal degradation is the main objective of this chapter prior to the scaled up pyrolysis experiments of a smaller number of selected samples.

Characterisation via ultimate and proximate results and pre – treatment applications are discussed in Sections 4.4 and 4.3 respectively. Two different

thermogravimetric analysers were used for the purpose of this study. One was coupled with a Fourier Transform Infrared Spectroscopy for online gas sampling (Section 4.6) and the other was coupled with a Differential Scanning Calorimetry (DSC) to detect the exact phase changes when the same thermal degradation method was applied as described in Section 4.5. The pyrolysis behaviour and characteristics of six added components representative of the main groups present in the mixed plastic waste have also been investigated and related with the observed peaks in the mixed plastic waste samples.

4.2 Mixed Plastic Waste industrial feedstocks

The actual Mixed plastic waste feedstocks that were received for the current study were from a variety of commercial UK companies including: packaging consumer product company, big supermarket chain, food packaging company, paper industry residues factory and waste management services. In comparison to previous studies that investigated artificially prepared mixed plastic feedstocks or specific research on Municipal solid waste (MSW), no studies dedicated to actual existing commercial mixed plastic waste feedstocks, from the UK market have been identified (Adrados, de Marco et al. 2012, Abbas-Abadi, Haghighi et al. 2013, Ateş, Miskolczi et al. 2013, Ahmad, Khan et al. 2015, Chandrasekaran, Kunwar et al. 2015) . Initially, the feedstocks tested for proximate and ultimate analysis were four but for the thermogravimetric analysis five samples of interest were identified. Each different supplier, follows their own waste separation process and information was provided for the expected materials in the mixed feedstocks in Table 17. However, due to the nature of mixed plastic waste and depending

on the level of contamination the results will vary. For the Tk sample a significant amount of the composition was accounted for aluminium that was known proportion of the waste component.

Table 17: Main plastic components of all selected samples.

Samples	Tk	Tc	Sn	Gr	Cr
Main components					
LDPE	√	√	√	√	√
HDPE	√	√		√	√
PP	√	√	√	√	√
PS			√	√	
PET		√			
PVC		√			
Cardboard			√	√	

Identifying the major components as well as the thermal behaviour of the pure materials with the thermogravimetric analyser is essential to define the operating conditions for the actual experiments such as the reaction temperature in addition to the expected quality of the produced fuel. Furthermore, characterisation of the feedstock is crucial in terms of isolating any hazardous material that could lead to operating problems such as chlorine or fluorine in polytetrafluorethylene traces.

From the five commercial feedstocks, supplying their waste, the Cr sample had an expected consistency similar to LDPE material, so it was not considered for a complete set of experiments. The commercial companies Sn, Cr and Tc, providing feedstocks withdrew their interest and feedstock supply during the course of the project

therefore limiting the possibility for further in depth studies. Therefore, the samples selected for the complete pyrolysis experiments were only Gr, Tk as well as pure LDPE to serve as a reference. The selection process and sequence of analysis carried out with all samples considered at different levels is illustrated in Figure 37.

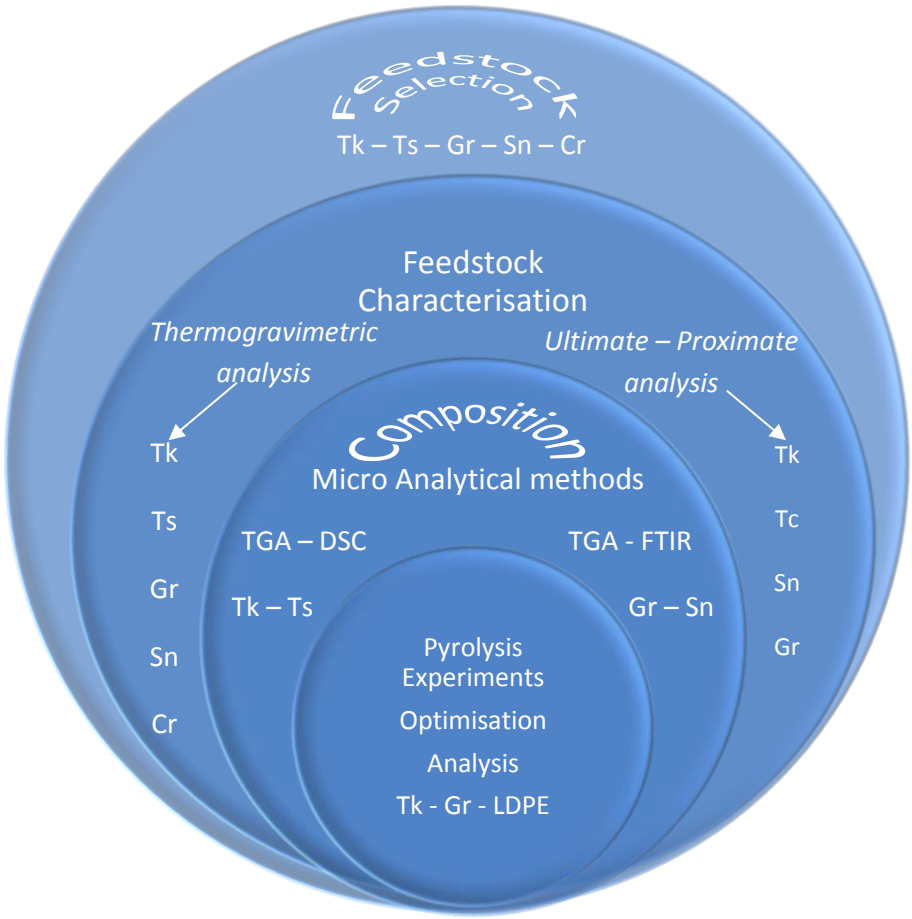

Figure 37: Sequence of analysis for different feedstocks.

In terms of mixed plastic waste characterisation the variety of the initial selected samples served a very useful purpose for comparisons. However for the design of experiments and optimisation, narrowing down the samples to study was essential to focus on deeper analysis.

4.3 Pre – treatment methods

Two different treatment methods were chosen to prepare the samples for analysis. Drying and reducing the particle size via shredding. For the TGA and DSC analysis the required particle size was in the scale of microns. A cryomill by Retsch with liquid nitrogen was used to achieve these values. All results are described in Sections 4.3.1 and 4.3.2.

4.3.1 Drying

The moisture content varied from obtained feedstocks between 0.30% and 35% on as received basis. It has to be noted that due to the variation of mixed plastic waste moisture measurements vary significantly and these should be considered as indicative values. Due to the fact that Tk feedstock was the first sample obtained for experiments and analysis the initial drying curve and method was established on this feedstock with an indicative moisture content of 26.90 w.t.%.

As shown in Figure 38, for oven temperature of 80^{o}C and with an initial moisture percentage over 40% for the Tk sample the moisture content dropped to below 5% after two hours and thirty minutes of drying and agitation. The moisture loss appeared to stabilise after the initial two hours. Based on, the results obtained from this drying curve the method applied to all ground samples prior to pyrolysis experiments was:

Oven drying of grinded samples at 80°C for four hours minimum with simultaneous agitation.

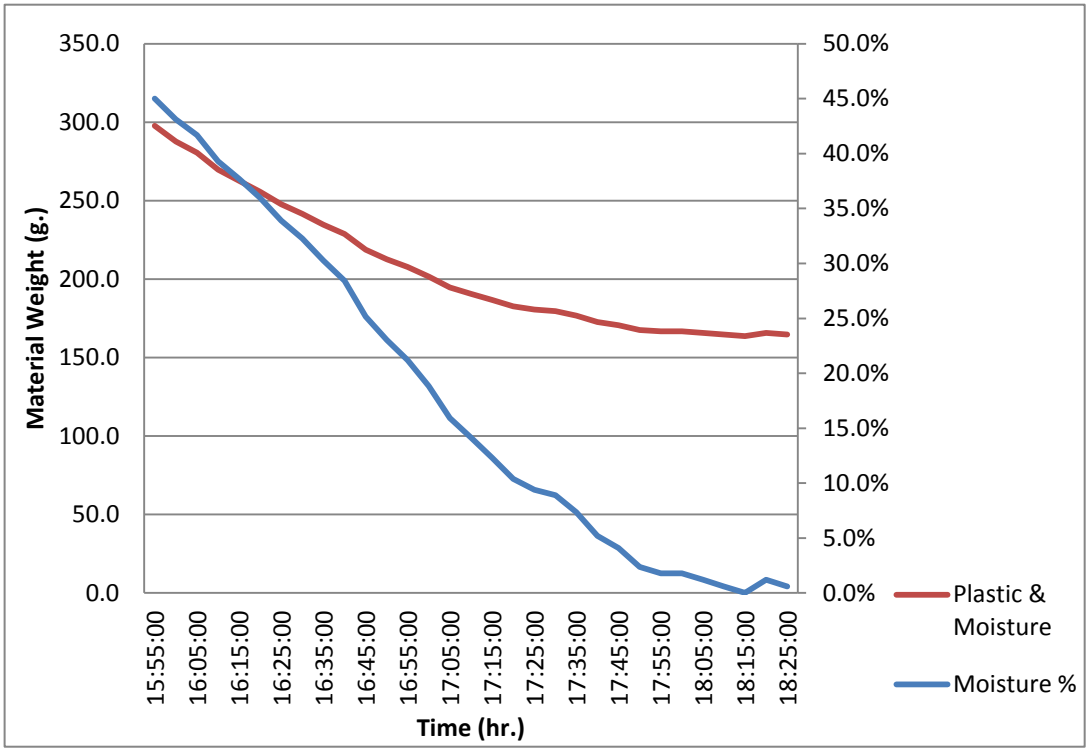

Figure 38: Drying curve for Tk sample with moisture content as received with time on x- axis.

An achieved moisture content of below 5% w.t. is acceptable for the pyrolysis experiments however following the applied initial drying method of 4 hours an additional drying study was completed. Randomly selected samples for three different feedstocks were selected after they had been initially dried.

These were placed in an oven with 75°C and left to dry for several days. In between the drying period the samples were taken out and weighed. All weights were recorded and the results for the additional weight loss as a net value from the initial weight are shown in Figure 39.

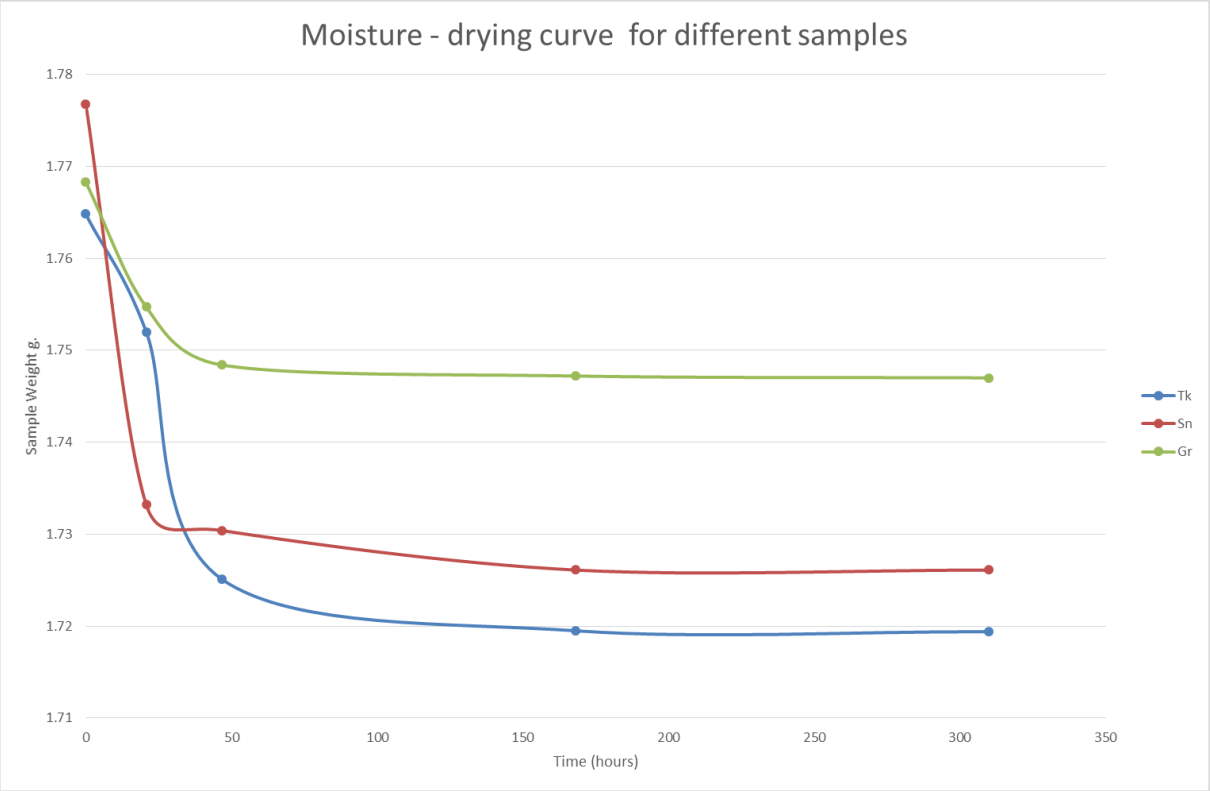

Figure 39: Drying curves for three different samples following the initial drying process.

The weight loss expressed as a moisture percentage of the initial weight are shown in Figure 40. From both graphs it can be derived that the residual moisture in the samples does not exceed 3 w.t.% and although there is some additional drying effect taking place with prolonged exposure to an elevated temperature this effect is not significant to consider altering the existing method. Therefore, it can be considered that with the existing method the remaining moisture in the samples is generally < 3 w.t.% even though it can be even lower.

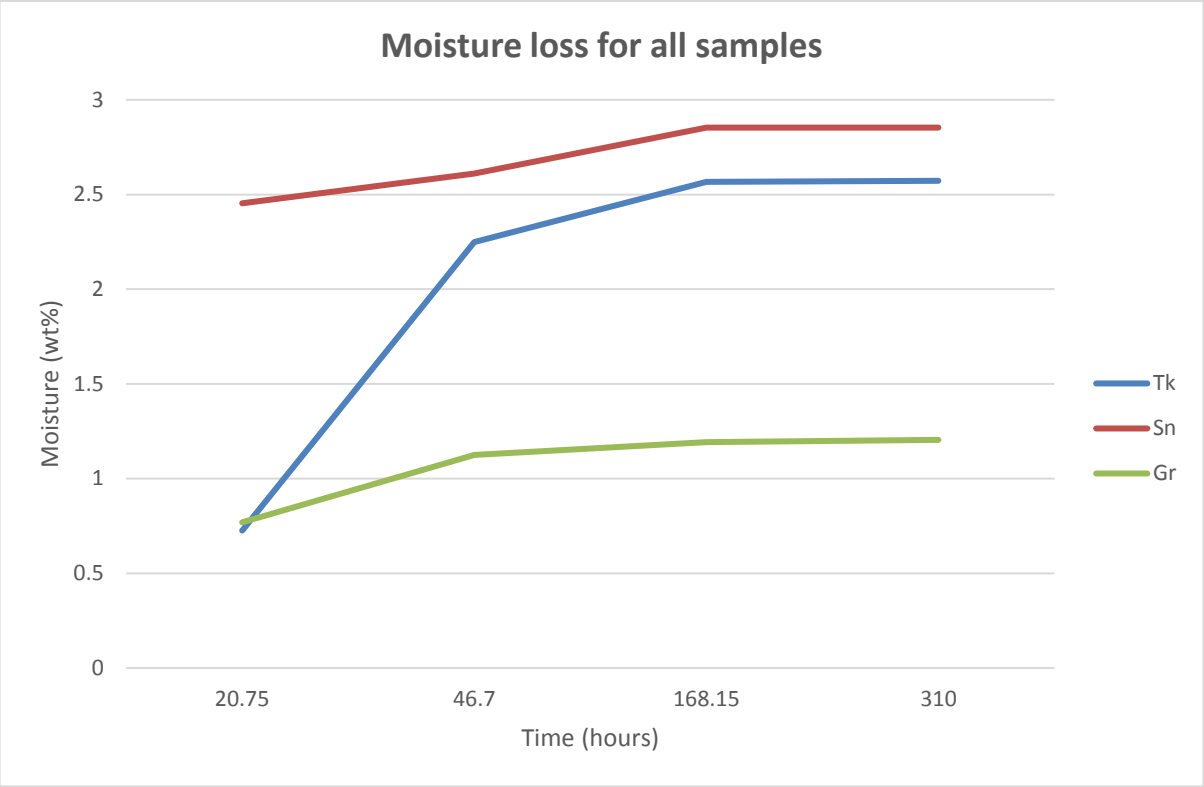

Figure 40: Total recorded moisture loss for all three samples.

4.4 Ultimate, Proximate analysis, Calorific value

For the initial analysis and evaluation of the feedstocks ultimate and proximate analysis were outsourced to an external laboratory (Environmental Scientific Group) to assess the moisture and ash content as well as the feedstock composition and heating value in terms of technical and financial viability for the pyrolysis process. The moisture content defined the requirements for a pre – treatment drying method that has been described in Section 4.3.1.

The total ash content had significant variation with feedstocks Tk and Tc having the highest percentages. This value has been taken into account for the recovery of

products and for any process and equipment modifications to accommodate for ash removal in a continuous pyrolysis process.

There was also, a significant variation in the actual combustible matter in the range of 12% which will affect the mass balance and final product yields in the pyrolysis process. Sulphur content, is within acceptable low limits for all feedstocks. One significant noteworthy difference is the oxygen content that is considerably high for Sn feedstock directly affecting and lowering its heating value. Oxygen, in the actual structure can, not only, affect the pyrolysis process, providing for oxidation in the reactions occurring but could also result in oxygenated compounds in the liquid or gas products.

Table 18: Analysis of four different industrial feedstocks from ESG laboratories.

Parameter	Feedstock Tk	Feedstock Tc	Feedstock Sn	Feedstock Gd
		Ultimate analysis, wt.% (d.b)		
C	70.96	74.63	64.43	85.26
H	11.80	12.66	9.62	14.56
N	0.12	0.10	0.15	0.20
S	0.02	0.02	0.08	0.02
O*	4.00	5.29	21.52	0.00
		Proximate analysis, wt.%		
Moisture(a.r.)	26.90	0.30	34.30	0.30
Combustible matter(d.b)	86.90	92.70	95.80	98.30
Ash(d.b)	13.10	7.30	4.20	1.70
a.r. as received - d.b. dry basis	* by difference		b.b.a.f dry basis ash free	
Heating value,MJkg^{-1}(d.b.a.f.) HHV	**43.80**	**48.14**	**31.29**	**44.62**

With regards to, the variation in the heating value all values were high with relation to other conventional biomass feedstocks used in similar processes and other comparable waste feedstocks used in other studies found in literature (Sørum, Grønli et al. 2001, López, de Marco et al. 2010, Sharma, Moser et al. 2014). In terms of, energy and mass balance the initial analysis provided sufficient information to select the feedstocks to move forward and issues that might need addressing in the process.

4.5 Thermogravimetric and Differential Scanning Calorimetry analysis

Thermogravimetric analysis was used on a stand-alone mode to study the thermal decomposition of all selected industrial feedstocks as well as the thermal behaviour of pure polymers for identification of total mass loss and temperature points where this was occurring. For selected feedstocks it was coupled with a differential scanning calorimeter to identify the different decomposition phase changes and the type of reactions taking places in respective temperature ranges. Identifying those phases in combination with literature data and information provided from the suppliers helped assemble an understanding of all individual or dominant materials presents and their behaviour in the pyrolysis process. Finally, the same feedstocks were used in a thermogravimetric analyser coupled with a Fourier Transform Infrared Spectrometer to analyse the spectra of the evolved gases and identify the changes of potentially hazardous gas products via library identification of the observed spectra.

4.5.1 Thermal decomposition of pure polymer materials with TGA

The materials analysed for their thermal decomposition were High density polyethylene (HDPE), Polypropylene (PP), Polystyrene (PS), Polyvinyl Chloride (PVC), Polyethylene terephthalate (PET), Cardboard. Low Density polyethylene (LDPE) has a similar consistency with high density polyethylene and the same cracking temperature as reported. Their only difference is in the melting temperature therefore all data were used from existing literature. According to the reported demand for plastics ((PEMRG) 2016) all the above mentioned polymers account for 72.6% of total consumption and disposal. In addition, cardboard was also tested due to its dominant reported presence in one of the feedstock samples. Cardboard can account, also for the small biomass percentage present in mixed plastic waste feedstocks.

Following the method described in Section 3.4.1, all samples were analysed and the results for the weight loss and first derivative of weight loss were plotted in the same graphs. The comparative results are presented from graphs 41 through to 47. Additionally the temperature for the peak loss was identified for all materials the total weight loss was recorded and the summarised results are presented in the end in Table 19, for reference when analysed the actual mixed plastic waste feedstocks.

From Figure 41, there is a clear distinction in the DTA curves for polystyrene and polypropylene with the first one in the temperature range of 425^{o}C and peaking at 433.59^{o}C and a maximum mass loss of 97.7% compared to polypropylene that starts decomposing at a higher temperature and peaks at 460.84^{o}C with a maximum mass loss of 95.2%.

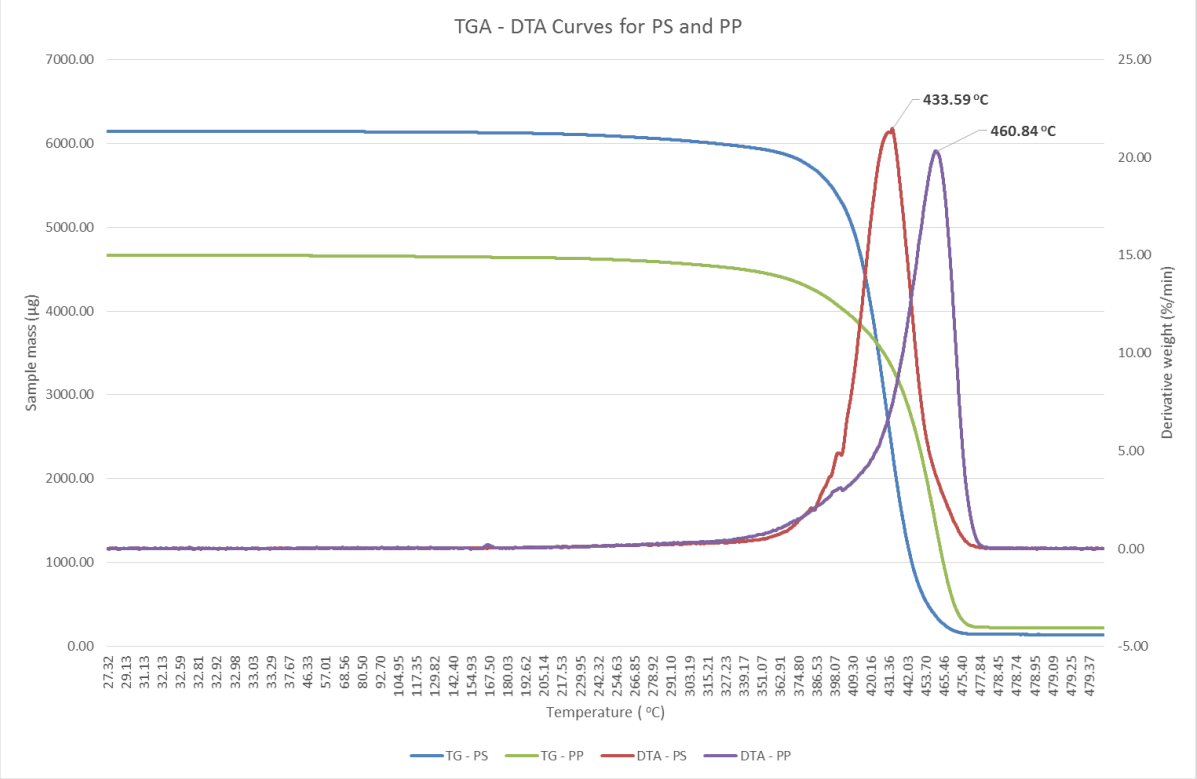

Figure 41: Comparison of TGA and DTA curves for Polystyrene and Polypropylene polymers.

When these materials are present in mixed plastic waste, they can be separated and identified by the different DTA curves. Similarly in Figure 42, a clear separation can be observed between the peak point in the DTA curve for cardboard at 357.27°C and a maximum mass loss of 82.6% compared to PVC that had double peak points one at ~ 284°C and a secondary at ~ 450°C. Therefore polystyrene, polypropylene, cardboard and polyvinyl chloride are materials relatively easily distinguished through by analysing and comparing the DTA curves. The same applies to high density polyethylene that is analysed further down in Figure 43. From there it can be observed that even though there are overlapping sections for the overall mass loss there is a distinct difference in the peak loss temperature that is consistent with literature findings.

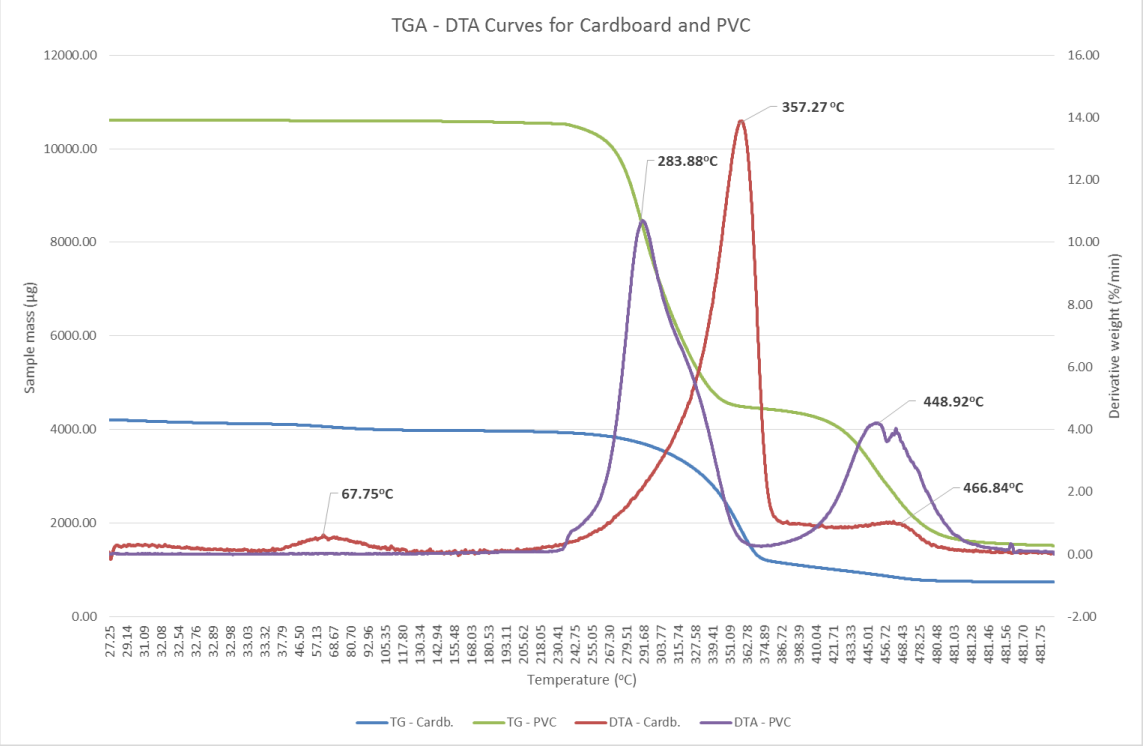

Figure 42: TGA and DTA curves for cardboard and Polyvinyl Chloride.

For polyvinyl chloride, there is one major mass loss and a secondary which again is consistent with findings in previous studies (Heikkinen, Hordijk et al. 2004).

A similar pattern is observed for Polyethylene terephthalate (PET) in Figure 43. In the occasion of PVC and PET identifying the materials presents some challenges due to the overlapping section and nearly identical DTA peak points in the sense that both present a similar curve pattern with double peak that are matching closely. However, in the occasion of PVC the first peak point is ~287.00^{o}C and the second at 450.00^{o}C whereas for PET the two peaks are closer set at 295.08^{o}C and ~ 443.00^{o}C.

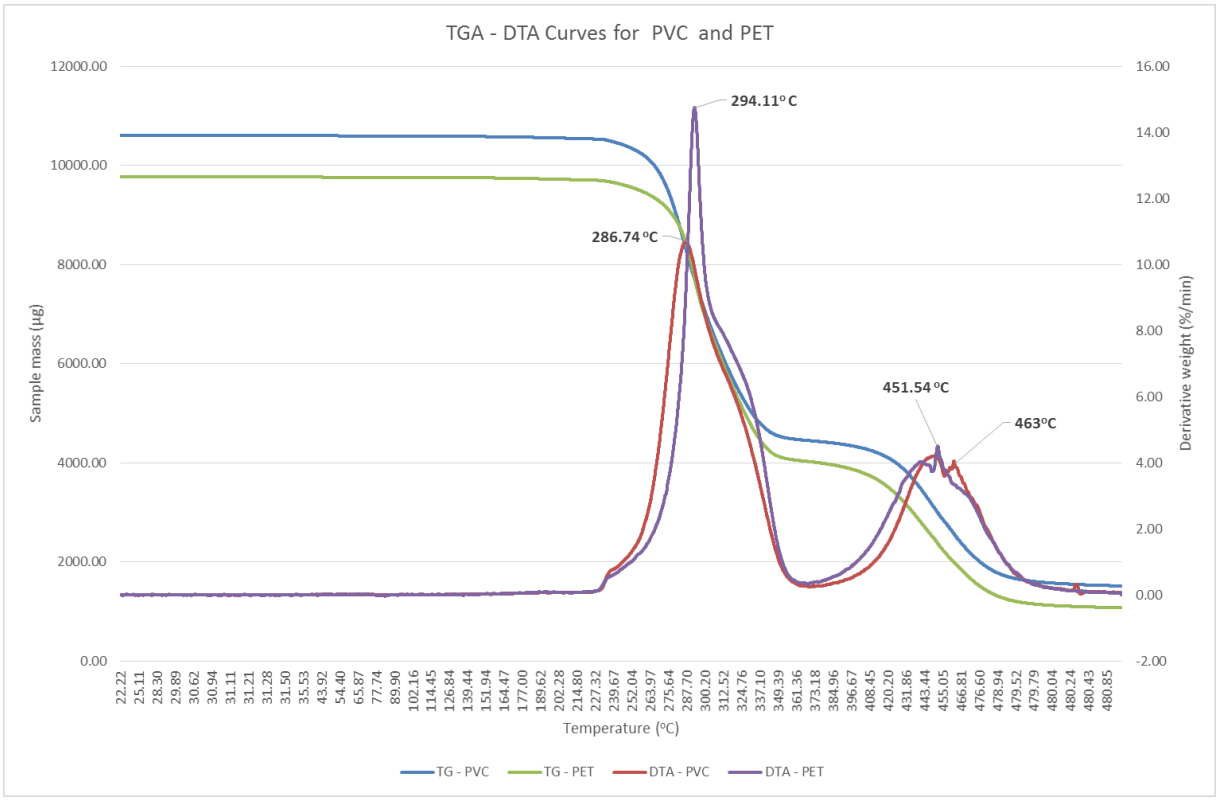

Figure 44: Comparative TGA and DTA curves for PET and PVC.

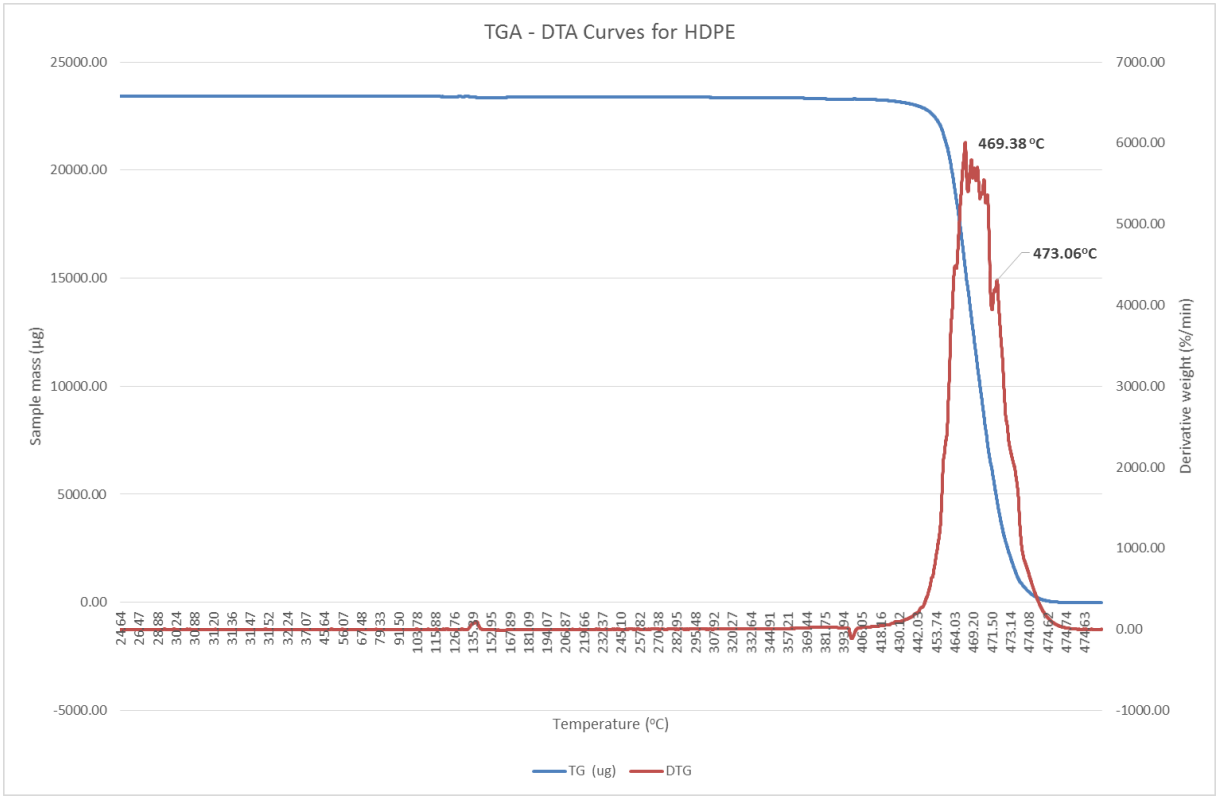

Figure 43: TGA and DTA curves for HDPE.

Still the task of separating such closely positioned peaks can be tricky only facilitated from the higher melting point of PET at 260^{o}C comparable with the melting point of PVC set at above 100^{o}C (Table 19). To validate the exact peak points the PVC sample analysis was repeated twice producing the exact same peak points. The total mass loss per material including primary and secondary peak loss temperature points are summarised in Table 19. These findings are also compared with other results found in previous studies (Marongiu, Faravelli et al. 2003). Results for PET, were in agreement with finding from Brems et al., who reported a thermal cracking temperature of 450^{o}C at a heating rate of 10^{o}C/min (Brems, Baeyens et al. 2011). Establishing the different thermal decomposition temperatures for each individual material for the main polymers lays the foundation for the identification of these materials in the mixed feedstocks by repeating the same process. Furthermore, in the occasion of overlapping sections the phase changes relating with melting temperature provides and alternative means of separation and is further analysed in §4.5.4.

For HDPE as shown in Figure 43, there are multiple peaks in the range of 469^{o}C up to 473^{o}C. This is the only material illustrating such a behaviour and it also exhibited the maximum mass loss. Conesa et al. reported a similar thermal degradation temperature of 475^{o}C at a heating rate of 5^{o}C/min (Conesa, Marcilla et al. 1996). Although there are some identifiable challenges in verifying the exact components especially in the occasion of PVC and PET there are ways to overcome and address this by close monitoring the onset and peak temperatures of the DTA curves as well as additional verification via melting point values of each material described in § 4.5.4 and summarised in Table 19. All values and data presented in column 5 on Table 19 have been taken from literature studies (Sørum, Grønli et al. 2001) (Gao 2010)

(Chattopadhyay, Kim et al. 2009) (Jung, Cho et al. 2010) (Marongiu, Faravelli et al. 2003) (Zhu, Jiang et al. 2008) both with analytical equipment as well as with actual pyrolysis experiments. The differences in the solid carbon and ash residue can be seen in photos taken (Appendix D). The results for the mixed plastic waste feedstocks are discussed in §4.5.2 but the structural difference in the solid residue composition can be observed between polystyrene and polyethylene terephthalate (PET) where PET results in a more crystallised structure that adheres to the sides of the crucible and could potentially create issues inside the pyrolysis reactor with agglomeration.

Table 19: Summary of pure polymer materials: melting and thermal decomposition temperature and maximum mass loss.

Material	Melting Temperature (ºC)	Thermal cracking temperature (ºC)	Mass loss (%wt)	Literature (Marongiou et al.(Ranzi, Dente et al. 1997)) (ºC)
HDPE	130 – 137	470	100	450/500
PP	130 – 167	455	95.2	450
PS	>132.2	425	97.7	320
PET	260	310/450	89.0	420
PVC	>100	332/420	85.7	320/450
Cardboard	-	352	82.6	350

4.5.2 Thermal decomposition of industrial mixed plastic waste feedstocks

The thermal cracking and decomposition profile of the following mixed plastic waste feedstocks were studied: Tk, Tc, Sn, Gr, Cr in conjunction with the analysis carried out for the pure polymer materials described in §4.5.1. For the Gr feedstock

two different runs were completed one for the initial batch received and a secondary run with a reported increased biomass percentage. All results, are reported in the following paragraphs and are compared with the results in §4.5.1 and §4.5.4 to evaluate and assess the complete thermal decomposition behaviour of these samples.

The Cr feedstock as previously mentioned in §4.2, was expected to contain materials such as LDPE, HDPE and small quantities of PP. The sample analysed and shown in Figure 45, provides one clear peak at 473^{o}C with a maximum mass loss of 99.29% both indicative of high density polyethylene material. Therefore, in terms of quantification all mass could be attributed to HDPE.

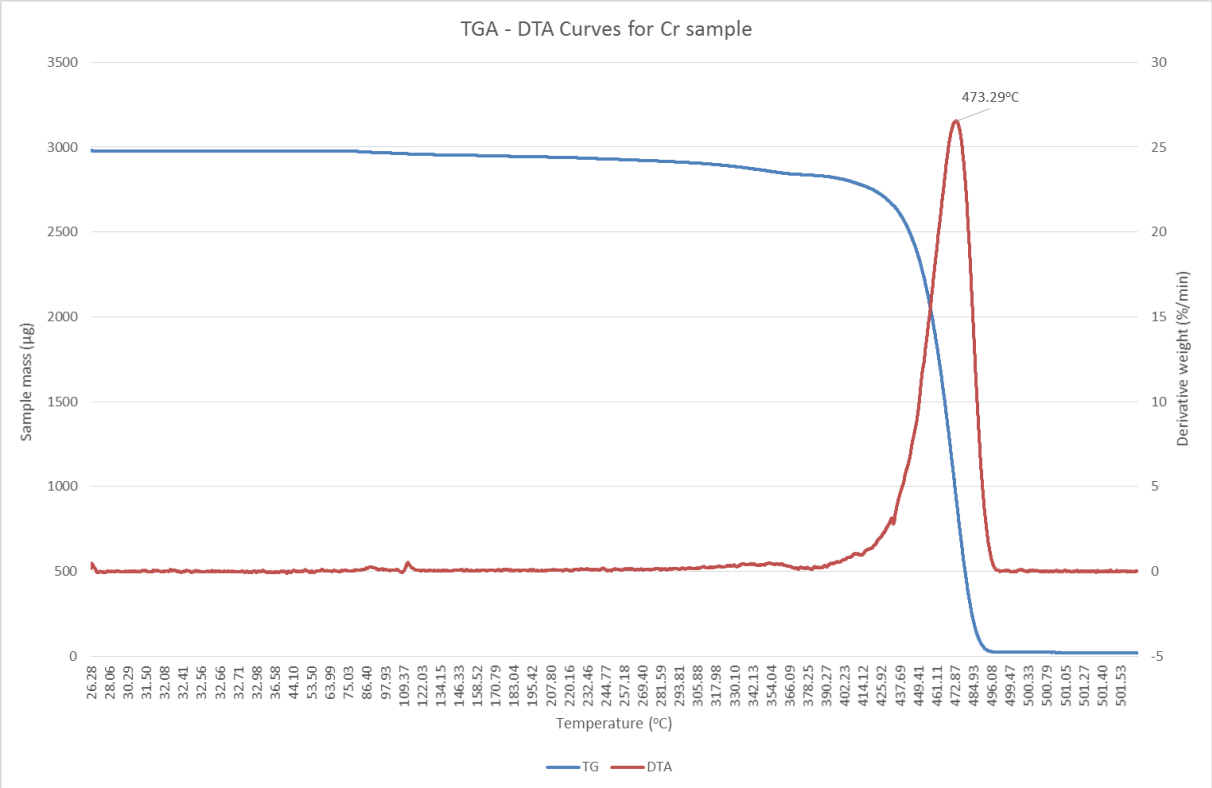

Figure 45: TGA and DTA curves for Cr sample including the maximum peak loss temperature.

For the Sn sample, according to the expected composition the materials were: LDPE, PP, PS and cardboard. However according to the findings shown in Figure 46, there were two clear peaks one at 359.68^{o}C indicative of cardboard or biomass material and

the second at 468.03ºC indicative or LDPE. Both The mass loss related to the cardboard accounted for 16.85% of the total mass loss whereas 75.15% accounted for LDPE. Total recorded mass loss was 92.01%.The Gr feedstock, in Figure 47, had a spread variety of materials including HDPE, LDPE, PP, PS and cardboard for the two different batches there were different identified peaks.

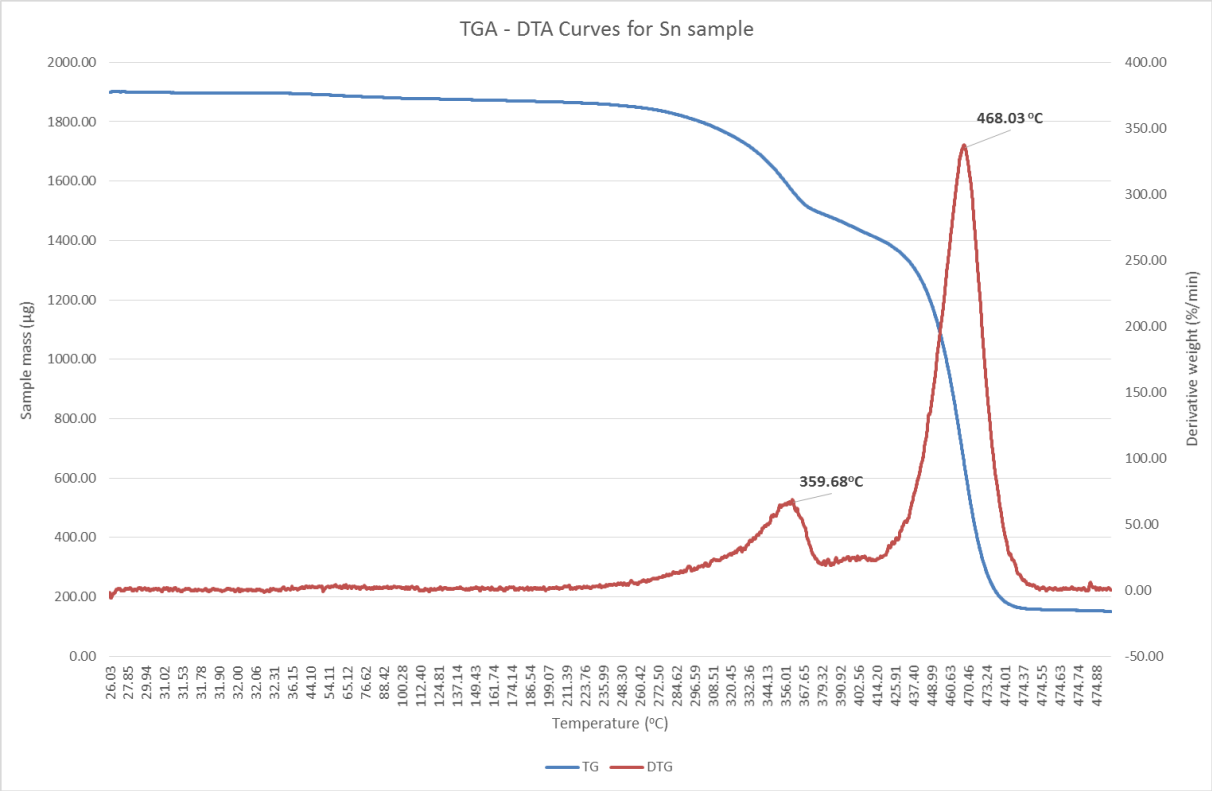

Figure 46: TGA and DTA curves for Sn sample with the maximum peak loss temperatures.

For the first batch one clear single peak at 472.21ºC on the top left corner was apparent indicative of HDPE material with a total mass loss of 99.9%. However, for the second sample of the new batch there were two clearly identified peaks as can be observed from the graph on the top right corner. The first one at 359ºC indicative of cardboard/biomass with a mass loss of 19.20% and the second at 469.98ºC relating to HDPE material with a 63.72% mass.

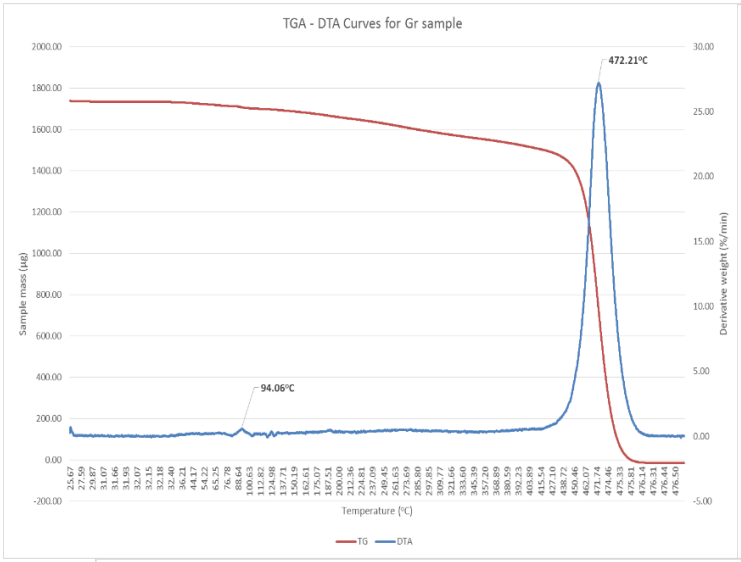

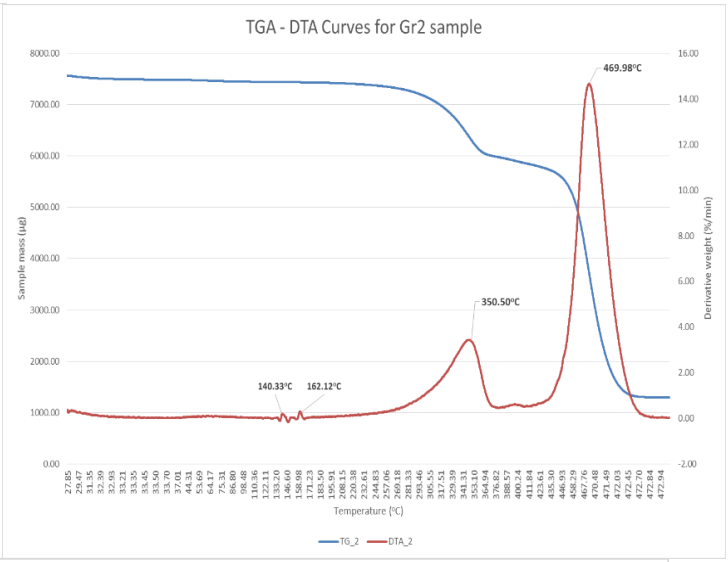

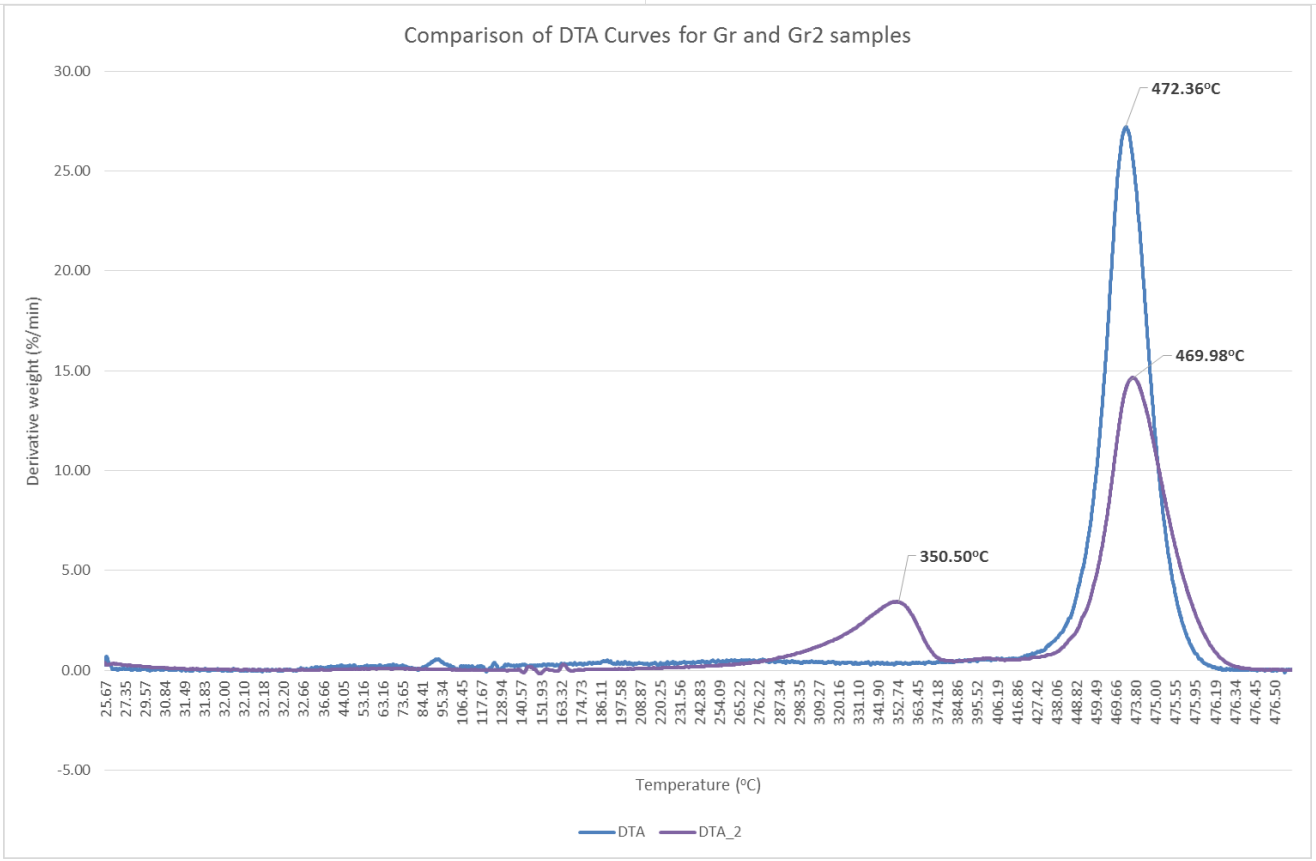

Figure 47: TGA and DTA curves for Gr and Gr2 feedstocks and the comparative DTA graph of both samples.

The total mass loss for the second sample is 82.92% in Figure 47, are accounting for the ash content potentially due to the biomass. The identified materials were consistent with the expected initial composition. There is also a slight shift in the curves as is can be seen from the figure above in the onset and end set temperatures.

For the Tc feedstock, the expected consistency included LDPE, HDPE, PP, PET and occasionally some PVC. Comparing the expected consistency with the findings shown in Figure 49, there are multiple peaks in the DTA curve within the temperature range of 430^{o}C to 472^{o}C. The clear peaks are in the following temperatures 447.25^{o}C that is relatable with the expected PET at 450^{o}C, 456.80^{o}C that is in the range of polypropylene at 455^{o}C from Table 19, 464.45^{o}C which correlates with the LDPE range, and 471.63^{o}C that can be identified as the HDPE cracking temperature resulting in total mass loss of 93.00%.

For the Tk material, in Figure 48, there is one clear peak at 470.27^{o}C attributed to HDPE whereas the total mass loss equals to 83.58%. It has to be noted that part of the ash or inert material for the Tk feedstock includes the aluminium element as well that is not apparent in the DTA and TG curves. Heikkinen et al., analysed and characterised a variety of mixed waste materials, utilising the assumption that devolitalisation characteristics of waste mixture including a variety of materials could be calculated as a sum of the contributions of the corresponding individual components(Heikkinen, Hordijk et al. 2004).

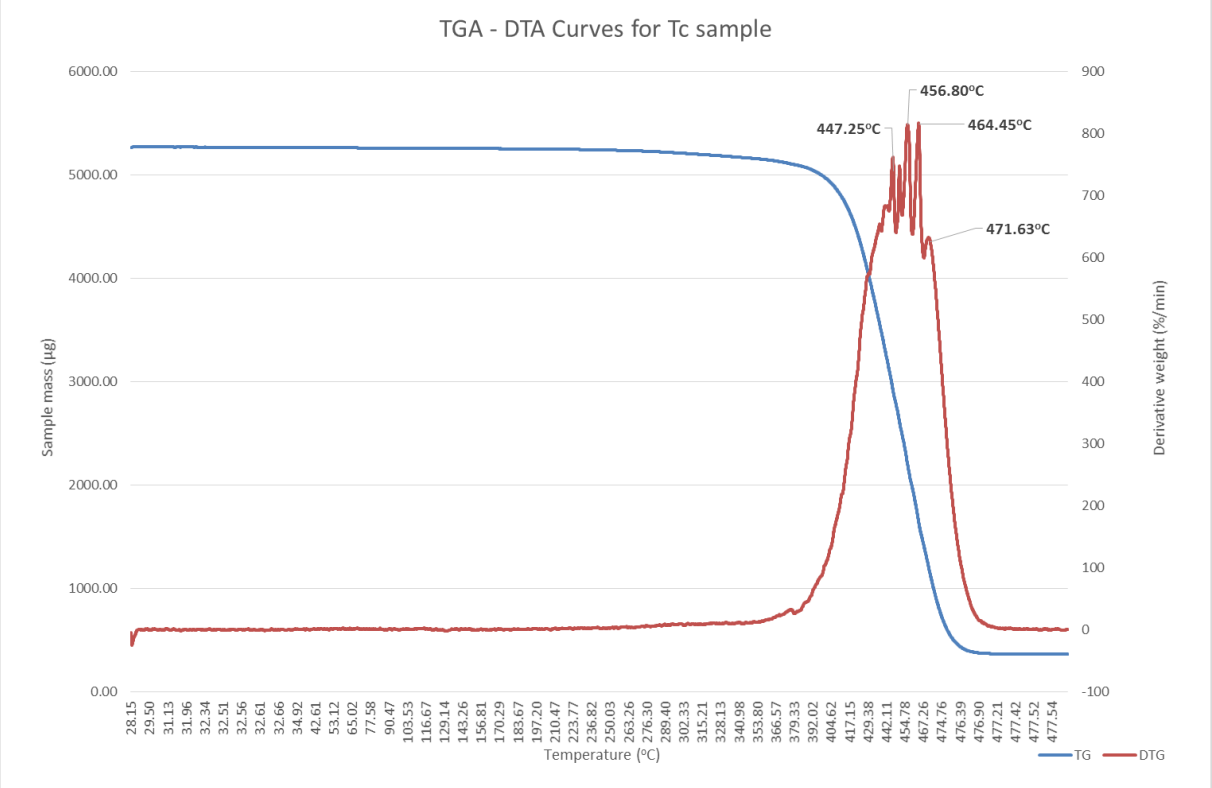

Figure 49: TGA and DTA curves for Tc feedstock including the maximum peak loss temperature.

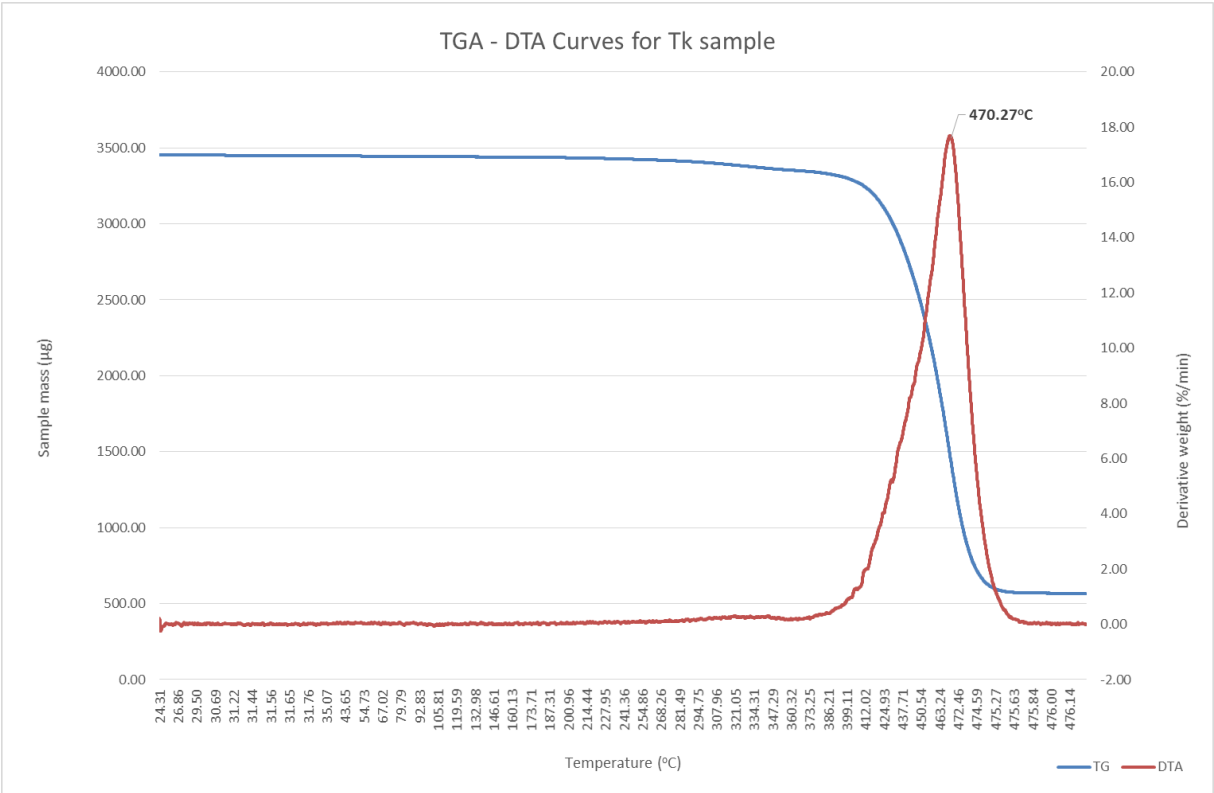

Figure 48: TGA and DTA curves for Tk feedstock including the maximum peak loss temperature.

A significant variety, and different patterns can be identified and verified within the complexity of these studied mixed plastic waste feedstocks. The first step, in the identification is studying their thermal decomposition behaviour and comparing it with the thermogravimetric analysis of the pure material. Further analysis and verification, are required due to the variety of components that can be found and the relatively small range in their respective cracking temperature range. All additional data is explained and added to the current observations in §4.5.4.

4.5.3 Differential Scanning Calorimetry (DSC)

With the method described in §3.4.2 four industrial feedstocks were analysed. These were Tk, Tc, Sn and Gr. Due to the unexpected exothermic curves, observed for Tc sample two additional analysis were completed on polyethylene terephthalate (PET). This material was reported to be part of the mixed feedstock and it is the only one containing oxygen in its structure that could justify an exothermic reaction with the present inherent oxygen considering that all experiments were carried out in an inert Argon atmosphere. Due to the similarity, with other feedstocks, the relative less complex composition and limited availability, Cr sample was not analysed with the DSC – TGA equipment and was not considered for further analysis. All results, were plotted in graphs with the heat flow curve for the DSC results on the secondary vertical axis, the TGA values in the primary vertical axis and the temperature in the x – axis. Endothermic peaks, are facing upwards and exothermic phase changes are observed in downward curves. All observed peaks, were integrated using a polynomial curve fitting, implemented through the existing equipment software and the amount of energy required for each observed phase was calculated and taken into account.

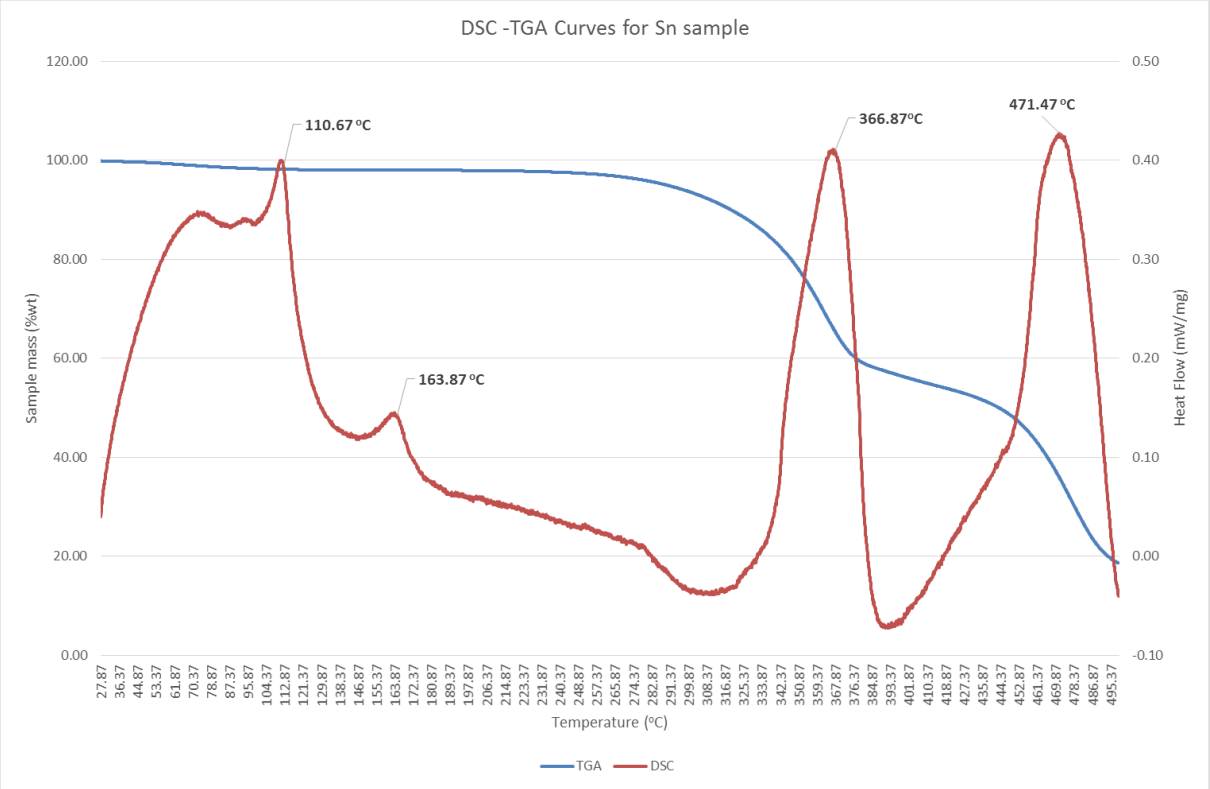

Figure 50: Thermal decomposition phases for Sn material with DSC – TGA heat flow/mass loss curves.

The results for Sn sample, are illustrated in Figure 50, where four distinguishable peaks can be observed. Two of them, are in the lower temperature range and can be identified as melting phase changes. The first one being at 110.67^{o}C relating to LDPE which agrees with the second peak observed in the cracking temperature range at 471.47^{o}C (Cafiero, Fabbri et al. 2015). For the second observed peak at 163.87^{o}C in the melting phase change it could be indicative both for polypropylene and polystyrene as both are reported to melt in overlapping temperature range. Due to the fact that, the thermal cracking endothermic curve appeared to peak at a much lower temperature at 366.87^{o}C than the one reported for polypropylene (450^{o}C) and closer to the one reported for polystyrene (320^{o}C) it was easier to derive that the second material was polystyrene by combining both findings (Camacho and Karlsson 2001). Comparing the total mass loss with the one analysed in §4.5.3 which was 92.01% with this

thermogravimetric analyser and Argon as the carrier gas the total mass loss was 81.36% which could be accounted due to feedstock variability of the 10%.

For the Gr feedstock, only the material from the first batch was analysed the one that was reported in §4.5.3 to include HDPE, LDPE, PP, PS and some cardboard. The results reported here are consistent with the findings in the previous part where only HDPE appeared to be present. Therefore as it can be seen in Figure 51, there is one clear peak in the melting phase change range at 124.56^{o}C within the range for HDPE material and consistent with the measured second cracking peak at 481.86^{o}C again indicative of HDPE. Finally the reported results for the mass loss are 85.27% whereas the findings in §4.5.3 provided a 99.9% mass loss calculation resulting in a 14.63% difference.

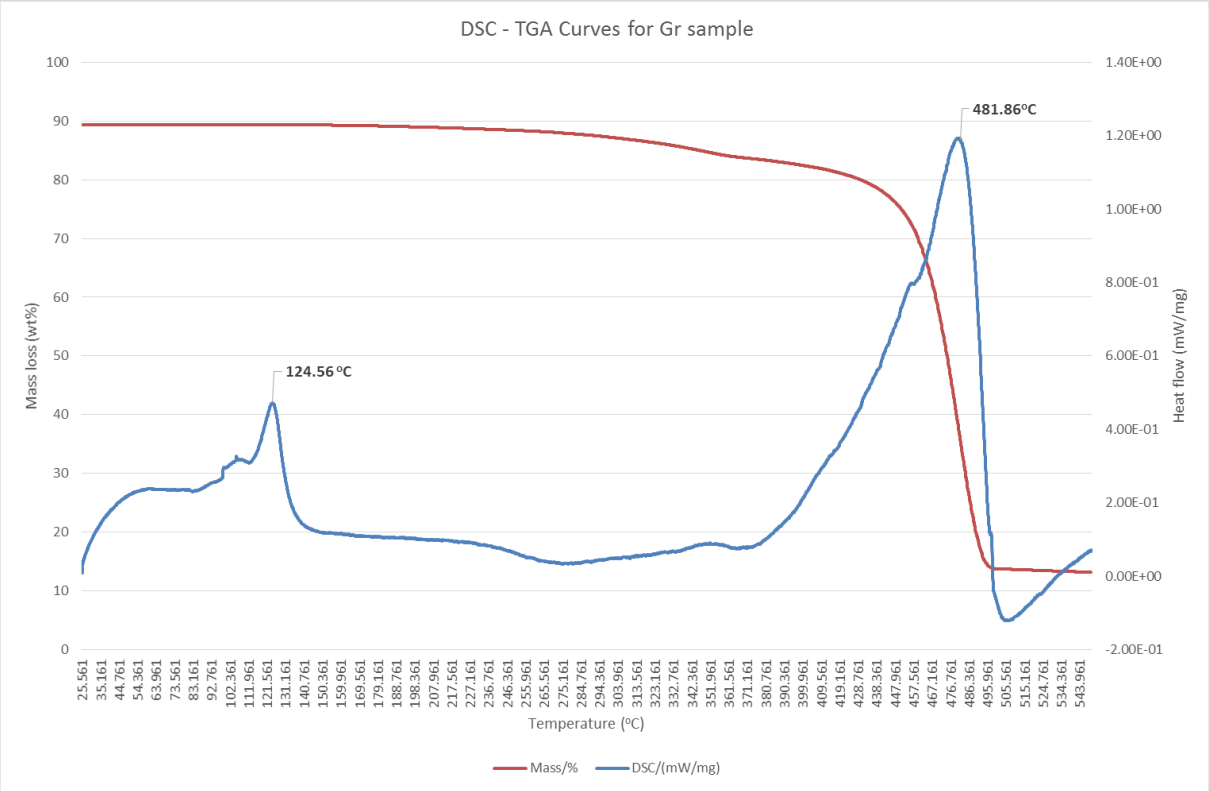

Figure 51: Thermal decomposition phases for Gr material with DSC – TGA heat flow/mass loss curves.

Even though according to the previous reported results in §4.5.3 there was only one peak for the Tk sample the DSC – TGA results indicate otherwise with regards to the melting phase change range shown in Figure 52. Instead of, only one peak as one might expect there are three different peaks at separate temperatures 110.22ºC, 130.07ºC and 164.97ºC. Combining both melting phase and cracking temperature the peaks identified could relate to the following materials with increasing temperature values: LDPE, HDPE and Polypropylene.

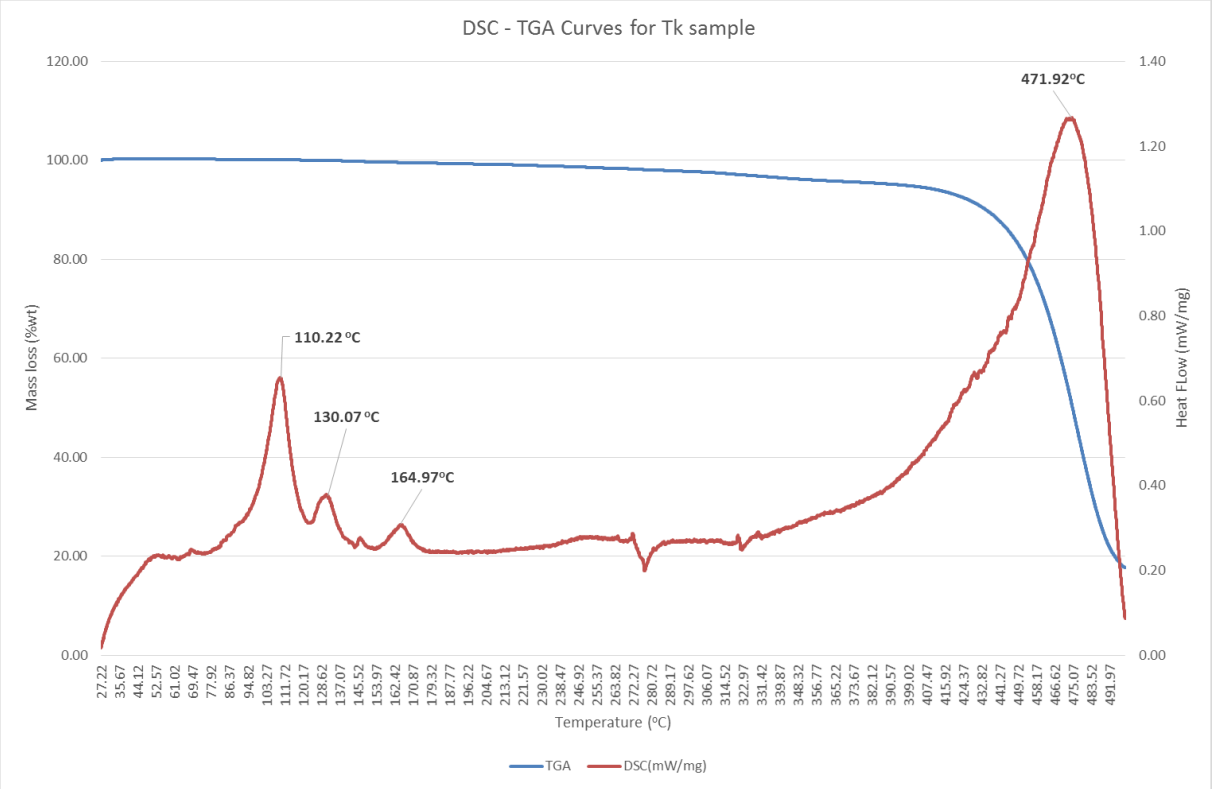

Figure 52: Thermal decomposition phases for Tk material with DSC – TGA heat flow/mass loss curves.

Similar results, have been reported from other studies (Reyes-Labarta, Olaya et al. 2006). The reason that polystyrene was not included, has to do with the fact that the onset of the cracking curve is above the temperature reported for thermal decomposition of polystyrene (320ºC). However, the results on the thermal decomposition side, are consistent providing a peak at 471.92ºC consistent with the

previous finding of 470.27ºC with a deviation of ± 1.5ºC. One potential explanation for this could be that because the thermal decomposition curve is quite wide incorporating from onset to end temperature of nearly 100ºC (407ºC – 500ºC). The individual peaks, relating to clear material identification are all included in this wide peak partly due to the overlapping reaction temperatures (Salman (2015)). The reported results, for the mass loss are 83.34% which are nearly the same with the previous value of 83.58%. The polymers in the Tc sample, feedstock were expected to be HDPE, LDPE, PP, PVC, PET and potentially other unidentified components.

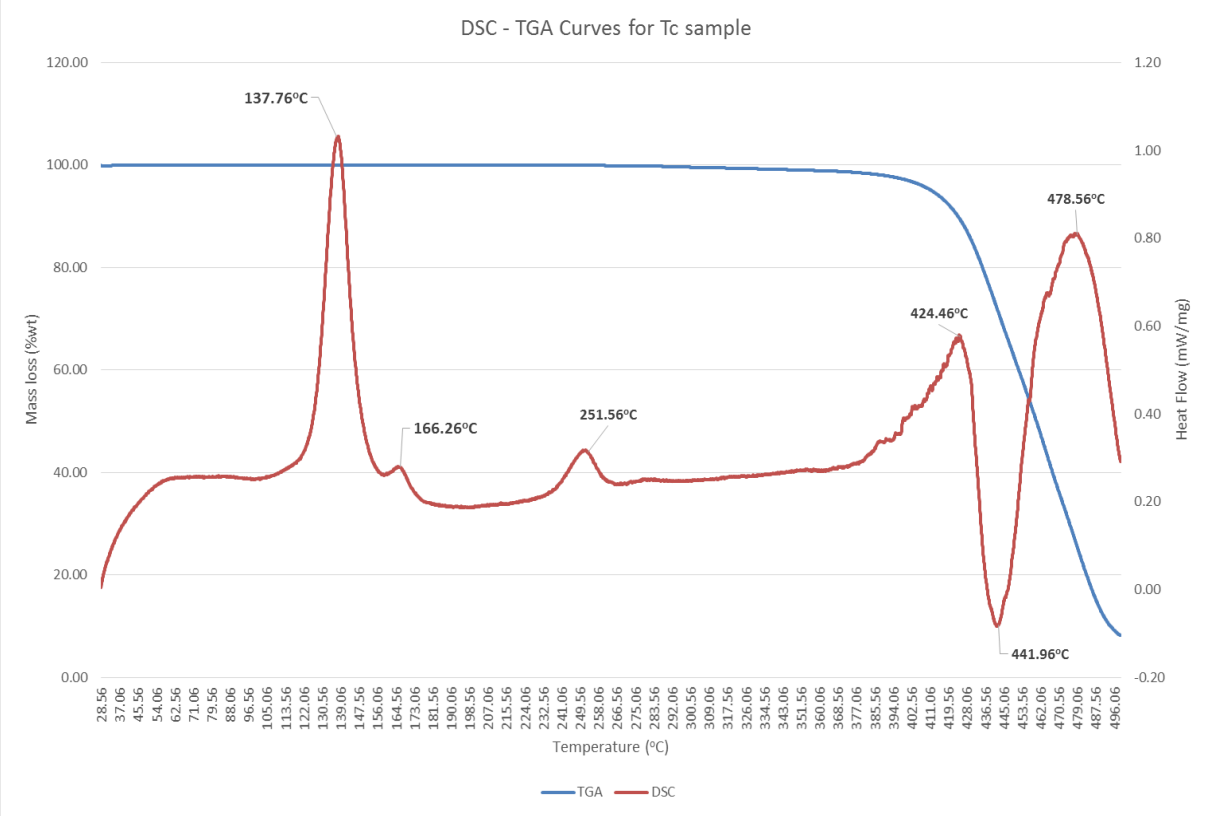

Figure 53: Thermal decomposition phases for Tc material with DSC – TGA heat flow/mass loss curves.

From the results in Figure 53, three apparent peaks can be observed corresponding to the respective relevant materials:

- A significant peak at 137.76^{o}C → HDPE
- A smaller one at 166.26^{o}C →PP
- The last at 251.56^{o}C → PET

However, towards the thermal degradation side of the graph in the higher temperature range instead of endothermic peaks appearing at the expected temperature there is initially a slight peak at 424.46^{o}C moving into a downward facing exothermic reaction peaking at 441.96^{o}C. This indicates, either the presence oxygen or oxidation reaction with a resulting release of energy. Following, the exothermic phase there is one last temperature peak at 478.56^{o}C. Therefore, due to the complexity of material thermal decomposition temperatures overlapping, in mixed plastic waste feedstock when combining the melting phase changes with the thermal degradation observations the initial peak at 424.46^{o}C could be correlated to polystyrene (PS) with a reported thermal degradation temperature of 425^{o}C or with the onset of polypropylene which thermally degrades at 455.00^{o}C. For the last observed endothermic peak at 478.56^{o}C, it is consistent with the previous observations for HDPE material. The mass starts decreasing at 382^{o}C and concludes at 500^{o}C with a total mass loss percentage of 91.78% of the initial mass (Figure 53). The reported results for the mass loss are consistent with the findings of 93.00% in §4.5.2.

In order to verify the existence and thermal behaviour of PET in the Tc sample, a pure PET sample was run replicated the same method and conditions the observed results are presented in Figure 54. Although the results between Figure 53 and Figure 54, are not identical as it can be seen from the graph the pattern of an endothermic peak at 301.98^{o}C followed by an exothermic peak 359.18^{o}C and a subsequent peak upward facing peak at 472.58^{o}C indicate that the exothermic behaviour can be attributed to

PET although, a secondary explanation for the shift in the peak temperatures could be due to the different material interaction. Another difference, is that in the phase change range there are not observed distinguished peaks. Total mass loss is 84.67%, 4.31% less than the results of 88.98% reported in §4.5.2.

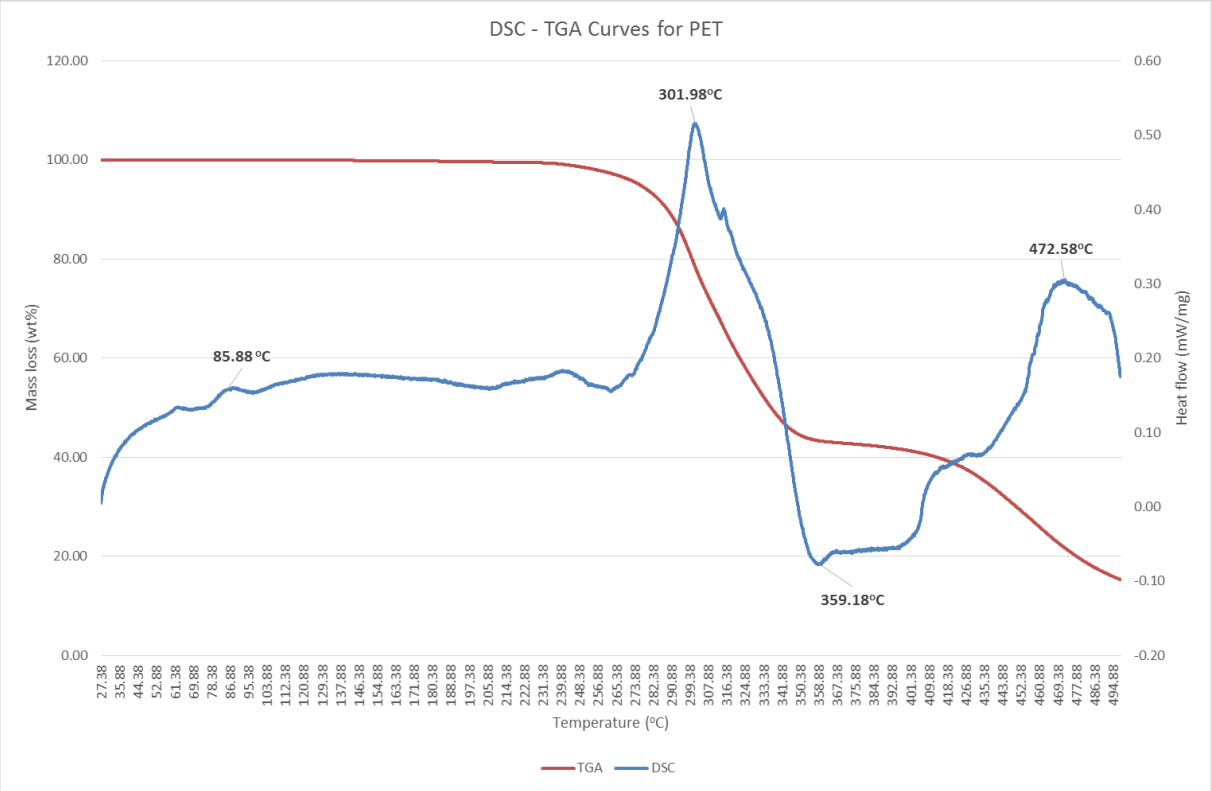

Figure 54: Thermal decomposition phases for PET material with DSC – TGA heat flow/mass loss curves.

4.5.4 Identification and comparison of components

Combining the results from §4.5.2 and §4.5.3 a summary Table listing the major components according to literature and the findings in this study has been compiled. Variations and adjustments, to the initial observations from the thermogravimetric analysis were added from the differential scanning calorimeter results that gave a more detailed view of the actual phase changes and separations.

Table 19: Summary of the thermogravimetric analysis results and identification of major components.

Feedstock	Melting Temperature (°C) DSC	Thermal cracking temperature (°C) TGA	Thermal cracking temperature (°C) DSC	Mass loss (%wt)	Materials
Cr	130 – 137	470	465	99.29	HDPE
Sn	110/163	360/468	366/471	92.0	LDPE/PS/Cardboard
Gr	124	360/470	480	83.0 – 99.9	HDPE/Cardboard
Tk	110/130/164	470	470	83.58	LDPE/HDPE/PP
Tc	137/166/251	430 – 470	350 – 470	93.0	LDPE/HDPE/PP/PET

Although, most of the polymers and plastics observed have overlapping cracking temperatures there are patterns with the illustrated analytical techniques to identify, quantify and verify with relative certainty the actual components and mass percentage of these. In the occasion of inconclusive results or broad curves covering a breadth of actual temperatures when using TGA the DSC technique can be used as a supplementary method to identify and check the actual components with the additional melting temperature phase change in combination with the cracking temperatures.

4.6 Fourier Transform Infrared Spectroscopy (FTIR)

In this section, the results for the Fourier Infrared Transform Spectroscope spectra that were obtained in connection with the thermogravimetric analysis described in §4.5.1 for different samples are presented and discussed. The evolved gases, were connected with a heater transfer line to the spectrometer and all spectra was obtained

and analysed at regular intervals of 1 sec, for the duration of the thermogravimetric process. The main objective of this analysis was to attempt and analyse the evolved gases from the thermal decomposition of the different feedstocks and relate their identified material composition differences with any potential observed variations in the evolved gases that could serve as a pre – cursor for the pyrolysis experiments.

Three of the industrial feedstock, spectra are presented in Figure 54 to Figure 56 for Sn, Tk and Tc samples. Once the spectra acquisition was completed the Spectra Manager II software was used for data analysis. For the analysis, a resolution of 4 cm^{-1} and number of scans set to 32 were selected. Spectra acquisition was obtained every second. Transmittance percentage, was presented against wavenumber (cm^{-1}) in graphs with the peaks facing down indicating the presence of specific functional groups. These identified functional groups, were run through a library search and compared against previous literature results. Expected functional groups, were in alkane, alkane and alkane deformation stretch range due to the nature of the decomposed material analysed which consisted primarily of polymers and biomass fractions. The wave number range for the evolved gases analysed was selected 700 to 4000 cm^{-1}. Because thermal degradation, occurred above 300^{o}C, no peaks were observed at the spectra acquired for the initial duration of the thermogravimetric analysis. Also, due to the fact that all feedstocks had different composition therefore varying thermal decomposition profiles the release of the gases occurred at different points. Therefore, from the series of saved spectra the one selected, was at the point of maximum release of the gases identified from the intensity of the observed significant peaks at the wave numbers of interest. These points, differ for all samples due to the variety in the feedstock composition and the changes in actual thermal

decomposition temperature resulting in the release of majority of the gases. The intensity, of the observed spectra was such that resulted in final accumulated results that validate the individual observations for the spectra. Therefore the most representative spectra are show here. In Figure 55, the results for the first sample Tk are shown.

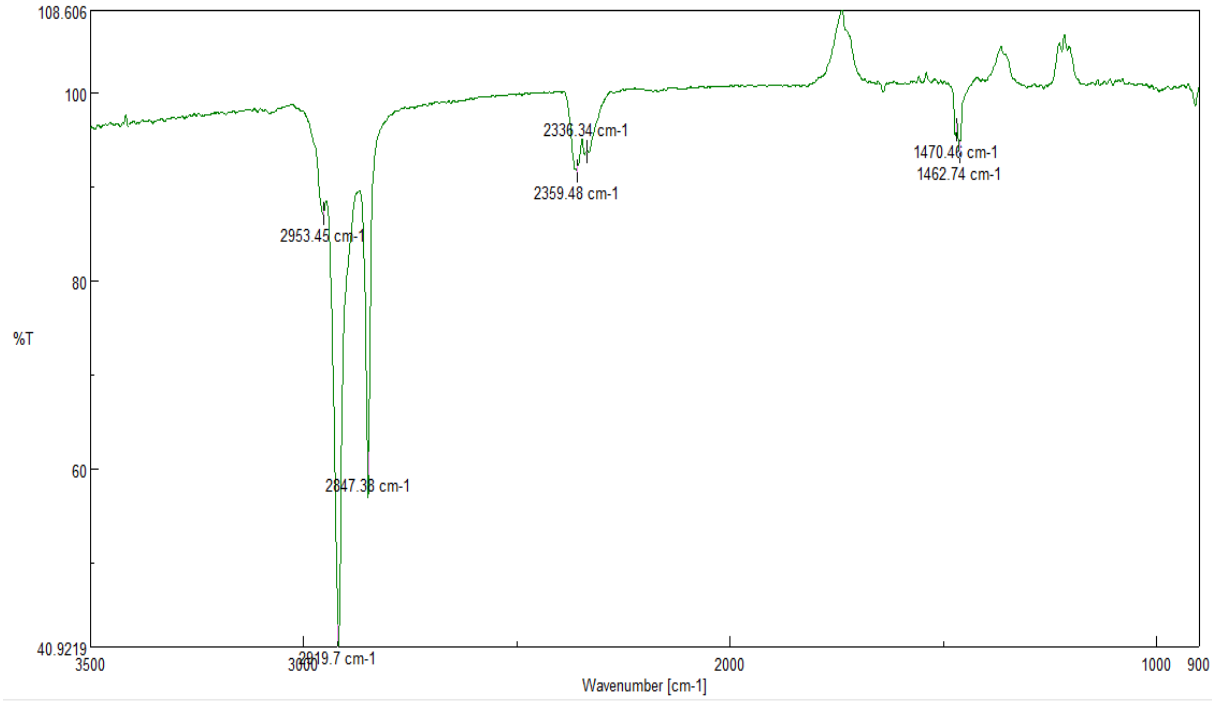

Figure 55: FTIR spectra for Tk material for the evolved gases from TGA equipment.

The strong identified peaks were in the region of 2953.45 cm^{-1}, 2919.7 cm^{-1} and 2847.38 cm^{-1} wavenumber length are identified with the C-H alkane stretch group (Colthup, Daly et al. 1990, Colthup, Daly et al. 1990) and are consistent with findings from other studies (Odochian, Moldoveanu et al. 2011, Singh, Wu et al. 2012) .

Furthermore, smaller peaks at the range of 1470.46 cm^{-1} and 1462.74 cm^{-1} wavenumber are reported to belong to alkane C-H deformation group (Colthup, Daly et al. 1990, Camacho and Karlsson 2001, Banar, Akyıldız et al. 2012, Cafiero, Fabbri et al. 2015) providing an overview of the produced gases that were transferred from

the TGA. Two smaller yet significant peaks appeared at the 2340 -2360 wavenumber lengths relating to CO_2 presence (Colthup, Daly et al. 1990, Singh, Wu et al. 2012).

In Figure 56, similar results have been recorded for the Sn sample with variations in the actual peak values and intensity. In detail strong identified peaks were observed at 2953.45 cm^{-1}, 2915.84 cm^{-1}, 2916.81 cm^{-1}, and 2849.31 cm^{-1} wavenumber length all under the C-H alkane stretch group (Robert M. Silverstein 2005). In the 2342 - 2362 wavenumber length range several smaller peaks are present relating to CO_2 (Camposo, Margem et al. 2013).

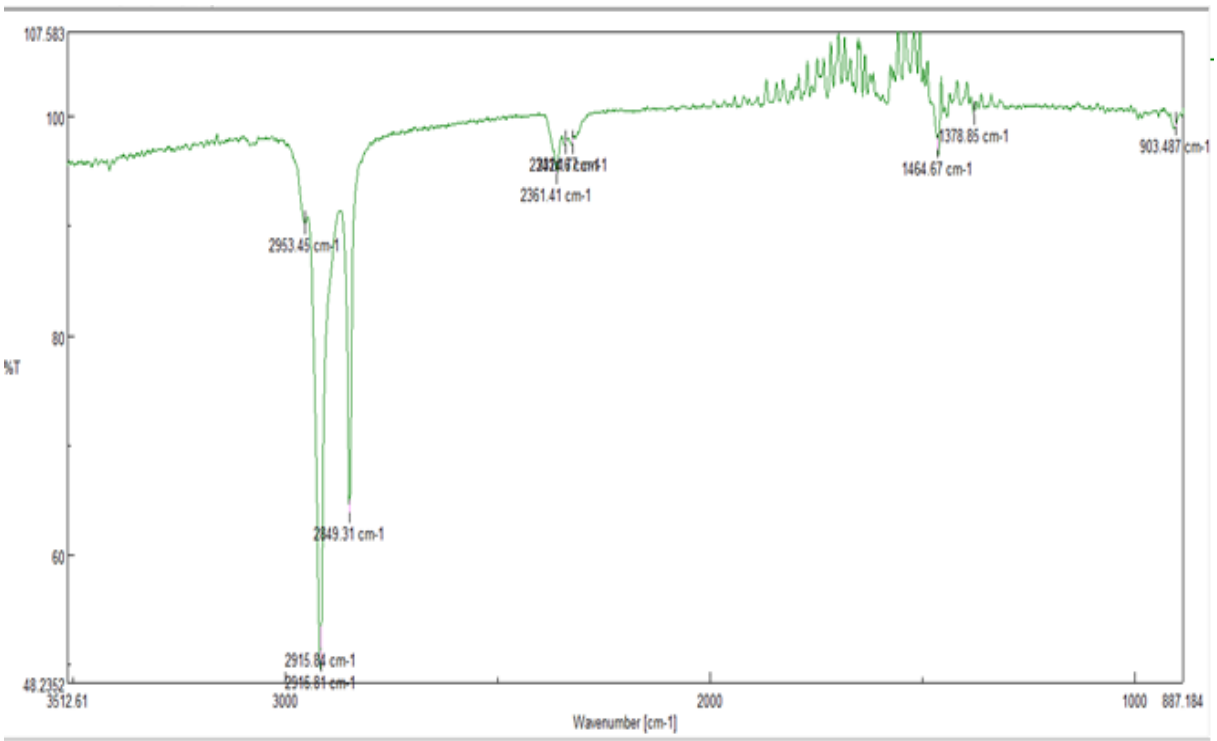

Figure 56: FTIR spectra for Sn material for the evolved gases from TGA equipment.

Compared to the results for Tk, the observed peaks in the 1464.67 cm^{-1} - 378.85 cm^{-1} wavenumber range for alkane C-H deformation group were less prominent indicating that there are fewer lighter alkane components produced. Both Tk and Sn samples had HDPE in significant quantities which explains the common peaks in the strong C – H

alkane stretch group. The variation in the smaller wavenumber lengths, relating to the C – H deformation could be related to the difference in HDPE percentage in the two feedstocks and the presence of biomass in the Sn sample.

In contrast, the Tc sample, had two additional strong peaks as shown in Figure 57, in the 1761 – 1730 region indicative of C=O stretch (Colthup, Daly et al. 1990) (Camposo, Margem et al. 2013) (Colthup, Daly et al. 1990) relating to carboxylic acids. The C-H alkane stretch group in the 3000 cm^{-1} wavenumber region was present in all three samples. Additionally, some smaller peaks in the region of 1462 – 1268 cm^{-1} wavenumber also belonged to alkane C-H deformation group (Robert M. Silverstein 2005)providing an overview of the produced gases that were transferred from the TGA.

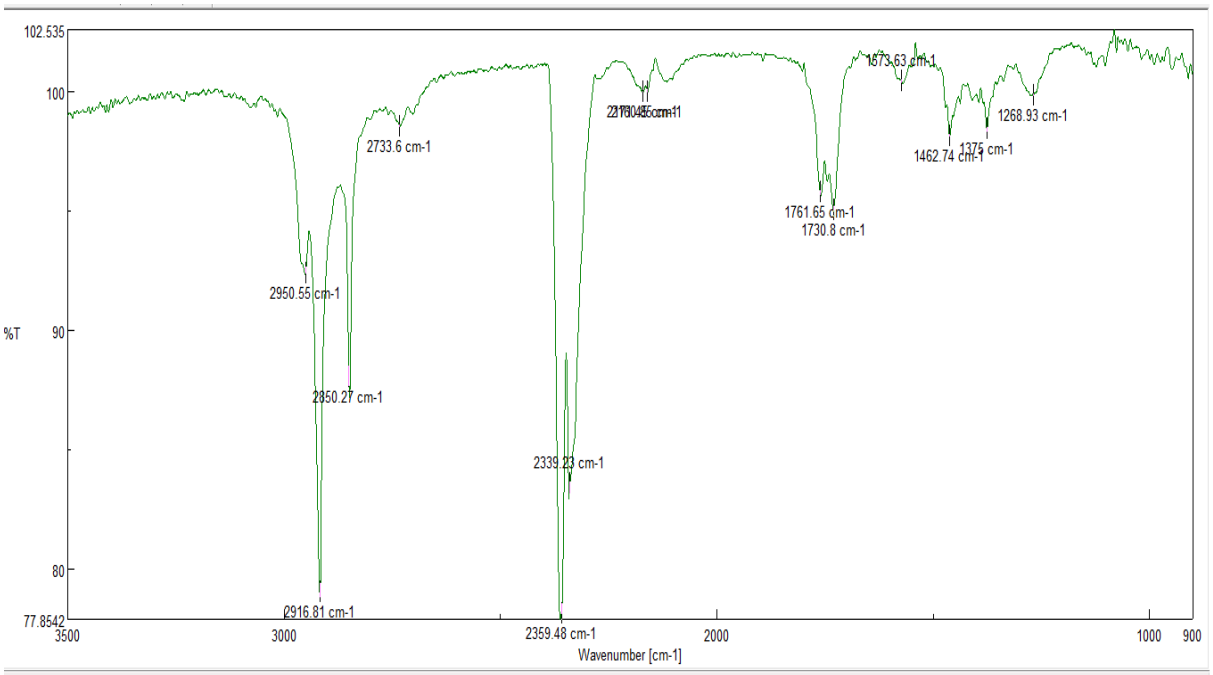

Figure 57: FTIR spectra for Tc material for the evolved gases from TGA equipment.

A significant peak also appeared at the 2340 – 2360 cm^{-1} wavenumber, that can is related to CO_2 presence. For the Tc sample, the CO_2 peak had a higher intensity. Both, the stronger CO_2 peak in combination with the presence of C=O stretch group, are indicative of the presence of oxygen in the structure of the sample.

Taking into consideration, the results from the TGA – DSC analysis that were indicating that PET was a component of the Tc sample and combining them with the current produced results it is safe to assume that the presence of oxygen as part of the feedstock composition would result in the product vapours and gas stream and in larger scale pyrolysis experiments could end – up in the liquid collected sample. Presence of acids in the vapour stream would significantly affect the quality of the end product and could create issues in future applications. To be in the position to identify the functional groups a small library for the relevant wavenumber range has been compiled from existing relevant literature.

4.7 Conclusions

Characterisation of the Mixed Plastic waste feedstock is crucial as the variation between different produced samples in not only significant but could have an effect on the plastic interaction in the pyrolysis process and the resulting gas and vapour stream. In addition identifying and excluding unsuitable plastic materials such as polyvinyl chloride that could produce dangerous chemicals or monitoring polymers with oxygen in their structure that can affect product quality is another significant factor that can be addressed and utilised by their characterisation and quantification. With the combination on analytical techniques described there has been a comprehensive understanding of how individual polymers can be identified by using both their cracking temperature and when necessary their melting temperature. Such identification, has been verified with the use of several actual industrial feedstocks. Finally, identification of the evolved vapour streams from different feedstocks has provided the additional proof that the variation in the feedstock results in a varied gas stream which will affect the condensed liquid product. Materials that contain polymers with oxygen in their

structure could results in a vapour stream with carboxylic acids affecting the acidity of the product. All these factors need to be taken into consideration when conducting the pyrolysis experiments and fuel analysis. Based on the work carried so far there has been a method to identify with a good approximation the polymers in the mixed waste samples and monitor the evolved gases of the different samples potentially with some additional work.

Chapter 5

Effects of reactor parameters and feedstock on product quality

5.1 Introduction

The aim of this work is first to characterize the produced fuel quality and secondly to improve its properties in order to use it as a fuel in high speed internal combustion engine. Several characteristics were analysed for this purpose the main being: product yield, distribution of main components with gas chromatography – mass spectrometry (GC-MS), viscosity, melting point, solubility, density and the blending option with diesel was investigated as well. Improving the fuel properties in terms of its consistency and average carbon chain length was the objective by using the pyrolysis process. To achieve this, two process parameters, reaction temperature and residence time, were selected and modified. A specific design of experiments was chosen to identify and quantify the effect of these parameters on product yield and quality. Also, the effect of feedstock variation and composition was assessed in terms of yield and product quality. The results of the experiments were correlated using the sample melting point as indicator in terms of the average chain length and respective molecular weight. In

addition, the outcome of the design of experiments was assessed statistically to identify the weighing parameter with the highest impact in terms of achieving the lowest melting point. Finally, the optimum conditions were established for each feedstock and further work to improve the product quality will be based on this as a starting point.

5.2 Effect of process parameters on the pyrolysis of plastics performed with the fluidised bed reactor

Although, there are several reported factors affecting both the product yield and the quality of the fuel notably (Kaminsky and Kim 1999, de Marco, Caballero et al. 2009, Gao 2010): pressure, heating rate, temperature, reactor type, carrier gas, residence time, for the current work two of them were chosen to study their effect. Using the existing fluidised bed reactor with a capacity of 0.5 – 1 kg/h and nitrogen as the carrier gas under near atmospheric pressure condition some of the defining parameters were already fixed. Two significant factors in the pyrolysis process were selected to test their effect on the composition of the produced fuel:

1. Reactor temperature,
2. Vapours residence time.

These parameters were chosen due to, their previous reported importance on the effect of the product composition and quality and because of the system configuration which was not designed to alter pressure (open end system) or heating rate (fast pyrolysis system)(Mastral, Esperanza et al. 2002, Hernández, Gómez et al. 2007, Lee and Shin 2007). All other influencing parameters were fixed such as particle size due to selection of reactor and reactor bed sand particle size, or moisture which was kept below 5 wt.% as previously described in Chapter 3.0. Feedstock composition is

another parameter affecting the outcome. According to the investigations described in Chapter 4, the lower limit for the plastics pyrolysis temperature was established at 450^{o}C and the upper limit was 650^{o}C due to electric heater capacity limitations of the equipment therefore the working temperature reaction range had a span of 200^{o}C. Feed rate, was calibrated for each feedstock and was kept stable with a fixed speed of the motor feed. The nitrogen flowrate was increased at set incremental steps and was the only parameter directly affecting residence time.

All graphs, are presented with relation to flowrate as a result. With this setup the feedstock was only inserted in the reactor once the desired temperature was reached. In a fast pyrolysis system like this, the heating rate was kept stable, to maintain a stable reaction temperature and did not change in the process.

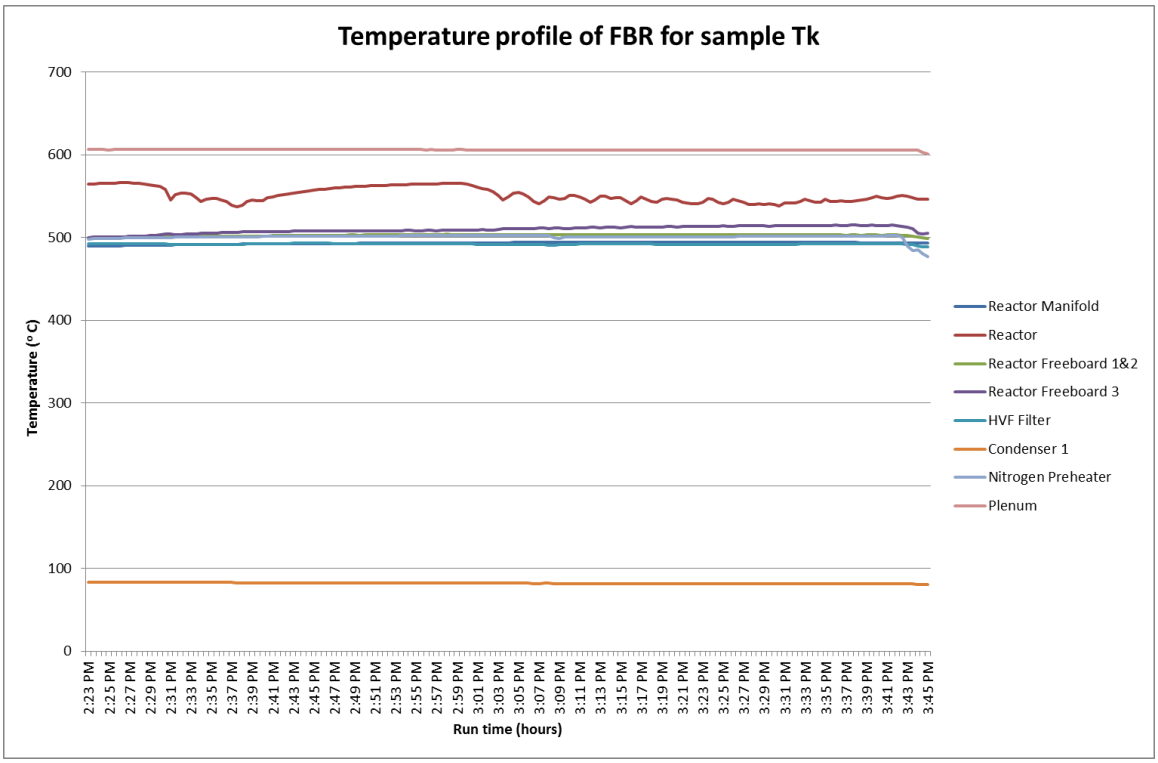

Figure 58: Logged temperatures for the duration of experiments at different reactor points.

In Figure 58, all logged temperatures at different points of the reactor are shown for the duration of one experiment. These measurements were connected to a laptop and constantly monitored. The reactor temperature shown in red (Figure 58), is the one that was monitored closely and showed significant variations throughout the experiments. Heat – up and cool –down time are not depicted, as the relevant experimental time started from when the material was fed in the reactor. Due to the long duration of the experiments only a representative section of the experiment is shown. If any variations or drops in the reactor temperature were observed the experiment was interrupted by stopping the feeding motor and it was resumed once the reactor temperature recovered to the desired level. The average temperature was calculated for the duration of the experiment. Any variation above 15^{o}C, from the chosen reaction temperature would call for a run interruption. Heating of the reactor was constant via the electrical heaters and heated gas. All drops were associated with the reactions taking place in the bed. Controlling the process by not feeding any more material was the available option. With the described system the pressure, heating rate, reactor type and carrier gas were fixed and the available parameters to vary were the temperature (with the limitations described above) and residence time. The breakdown of the design of experiments is outlined in §5.3.

5.3 Design of experiments

A three by three, orthogonal array set of tests was conducted for three different feedstock based on the above factors. In total, 9 experiments were run for each feedstock as shown in Table 20. For the assessment of the response single

experiments were conducted. Once the optimal conditions, were established for the industrial waste feedstocks three repetitions of the same conditions were repeated and the variation between the same runs is reported. The response and effect of the varying conditions was initially screened via the melting point measurement of the fuel samples. To narrow down the feedstocks, that would be analysed and investigated through the process variation, three feedstocks were selected. This selection was based on, commercial availability of feedstock and relevant quantities as well as having sufficient variation in the feedstock composition to establish any identified changes and validate the results. As an example Cr feedstock was very similar in composition and experimental results with LDPE therefore the added scientific value of the mixed waste was insignificant. From the initial five feedstocks that were investigating in Chapter 4.2 the ones for the focused specific study were:

1. LDPE which would be the pure plastic reference feedstock
2. Gr
3. Tk

With the existing reactor and making use from the literature (Williams and Williams 1997, Kaminsky and Kim 1999, Gao 2010) and the TGA analysis that was completed previously the starting pyrolysis temperature was selected as 500^{o}C. Due to equipment heating limitations the maximum pyrolysis temperature that could be reached was 580^{o}C which drove the temperature limits of the process. For the three selected feedstocks three temperature steps were tested with a variation of ± 10^{o}C. Temperature variation was dependent on the reactions taking place in the bed and heat transfer issues that occur in similar pilot scale systems. The isothermal temperature experimental steps were:

- 500°C as the initial step
- 530°C as the intermediate step
- 550°C as the higher temperature run.

Table 20: Design of experiments with temperature and residence time factors.

Temperature / **Flowrate**	**500 ± 10 (°C)**	**530 ± 10 (°C)**	**550 ± 10 (°C)**
14 L.min^{-1}			**Tk** **Gr**
16 L.min^{-1}	LDPE Tk Gr	LDPE Tk Gr	LDPE **Tk** **Gr**
18 L.min^{-1}	LDPE Tk Gr	LDPE Tk Gr	LDPE Tk Gr
20 L.min^{-1}	LDPE Tk Gr	LDPE Tk Gr	LDPE Tk Gr

Three point tests, are sufficient to indicate the process tendencies. Nitrogen flowrate served two purposes. First, it had a heated stream and it helped in the overall heating of the pyrolysis system and secondly, it was the fluidisation medium for the reactor bed.

In terms of, the flowrate range selection for the lower limit it had to be taken into consideration with regards to the minimum fluidisation velocity. Below 14 $L.min^{-1}$ there were issues encountered with fluidisation. A value of 16 $L.min^{-1}$ was set as the lowest possible value which still allowed fluidisation to occur.

A few complimentary experiments were run at even lower flowrates (14 $L.min^{-1}$) to investigate if this change would have a considerable impact in lowering the melting point of the sample. At that flowrate value however, the reactor was operating as a bubbling bed rather than a fluidised bed with reduced heat transfer properties. For the maximum flowrate values up to 28 $L.min^{-1}$ were tested however this had the side effect of vapour loss in the gas stream since such high values did not allow for optimum condenser performance. A value of 20 $L.min^{-1}$ was selected as the higher end of the flowrate. For each the low and high limits of flowrate were investigated to determine the effects of the window of operation. Therefore the limits of the process on the higher residence time (lower flowrate – 16 $L.min^{-1}$) against temperature and lower residence time (higher flowrate – 20 $L.min^{-1}$) could be established and the most effective conditions could be verified.

The aim was to improve the wax and heavy liquid product and lower the overall melting point of the fuel via thermal cracking. For this reason, the heavier fractions collected from the first condenser were selected to focus on for this study since they would be the ones affecting the fuel quality. In reality the final sample consists of a mix from products collected from all condensers. For each sample at least three measurements were obtained and the values presented in §5.3.1 to §5.3.3 are the average of the measurements including the standard deviation.

5.3.1 Effect of temperature

For the pyrolysis reactions the reactor temperature has been reported by many researchers to have the most significant effect on the overall yields, liquid and gas composition. Specifically, with increasing temperatures the gas yield increases (Kaminsky and Kim 1999, Liu, Qian et al. 2000, Jung, Cho et al. 2010) compared with decrease of the liquid yield. Within the 500 – 700^{o}C pyrolysis temperature range, the optimum reaction temperature and yields have been reported at different points depending on the reactor, process conditions and different compositions. Scott et al., reported the maximum yield for LDPE (89.8 wt.%) with a fluidised bed reactor at 515^{o}C (Scott, Czernik et al. 1990, Williams and Williams 1997, López, de Marco et al. 2011). Above 700^{o}C all findings agree on the wax/liquid yield decreasing (Conesa, Font et al. 1994, Mastral, Esperanza et al. 2002, Mastral, Berrueco et al. 2007, Jung, Cho et al. 2010) in favour of gas production although the plastic interaction can affect the outcome significantly. For example when polystyrene is present in the feedstock the

liquid product will have significant quantities of styrene in its composition (Kaminsky, Predel et al. 2004). Depending on the feedstock, different colour are produced; polystyrene results in a red – brown colour oil, HDPE/LDPE and PP produce a light coloured waxy product whereas presence of PET results in a dark coloured viscous oil (Blazsó 2006, Gao 2010). However, the focus of the current study is the thermal cracking of the waxes towards oil production which mainly occurs at temperatures above 500^{o}C (Williams and Williams 1999) thus temperatures in the range 500 – 565^{o}C were studied. For the current study, the effect of temperature upon the product composition and quality, product yield and overall mass balance are presented in §5.3.1.1 to §5.3.1.2.

All results, are presented as a function of the average melting point. Evaluation of the optimum conditions has also been determined by means of the melting point. Specifically quantifying the change between the higher melting point and lower melting wax products is the scope of optimising the process. For the wax products of the different conditions further analysis and verification has been completed in terms of change in viscosity density and with analytic GC –MS analysis for the points of boundary observed conditions.

5.3.1.1 Influence of temperature on fuel quality

The results on the effect of temperature are reported in this paragraph in terms of increasing the temperature without altering the residence time. Any changes are reported in terms of average melting point against reaction temperature. Any changes, between different reaction temperatures, detected in melting point values would

indicate a change in average hydrocarbon chain length of the samples. Reportedly samples with a lower melting point would have a composition of lower average hydrocarbon molecular weight as explained in §5.4.2. A full sample composition GC – MS, viscosity, density and solubility analysis was completed at the points of significant variation in §5.4.3 to §5.4.9 sections.

In Figure 59 to Figure 62, the effect of temperature on melting point is plotted and presented for the three selected feedstocks for the lowest flowrate. Only for Tk feedstock, comparative results are presented for the highest flowrate as well to counterpart the influence of temperature at different conditions. A comparative graph for all feedstocks summarises the overall effect of temperature.

The objective for the current study is to achieve the conditions that result in a sample with the lowest melting point therefore leading to a lighter fuel composition. Any impact of the optimal conditions in terms of mass balance and oil/wax recovery are reported in §5.3.1.2. Finally, quantifying the actual impact of temperature in comparison with the residence time effect is analysed via a Taguchi statistical analysis method.

In it is illustrated that the minimum melting point of the wax was 58^{o}C which occurred for the sample at a pyrolysis reaction temperature of 500^{o}C. This finding is in accordance with what has been previously reported in literature since at this temperature the oil and wax content is higher compared to products from higher temperatures that favours gas production leaving the heavier molecular weight components in the liquid – wax fraction (Williams and Williams 1999). Ruj et al., also found 500^{o}C to be the optimum reactor temperature for the recovery of maximum liquid and wax yield from mixed plastic waste using a batch reactor(Singh and Ruj 2016).

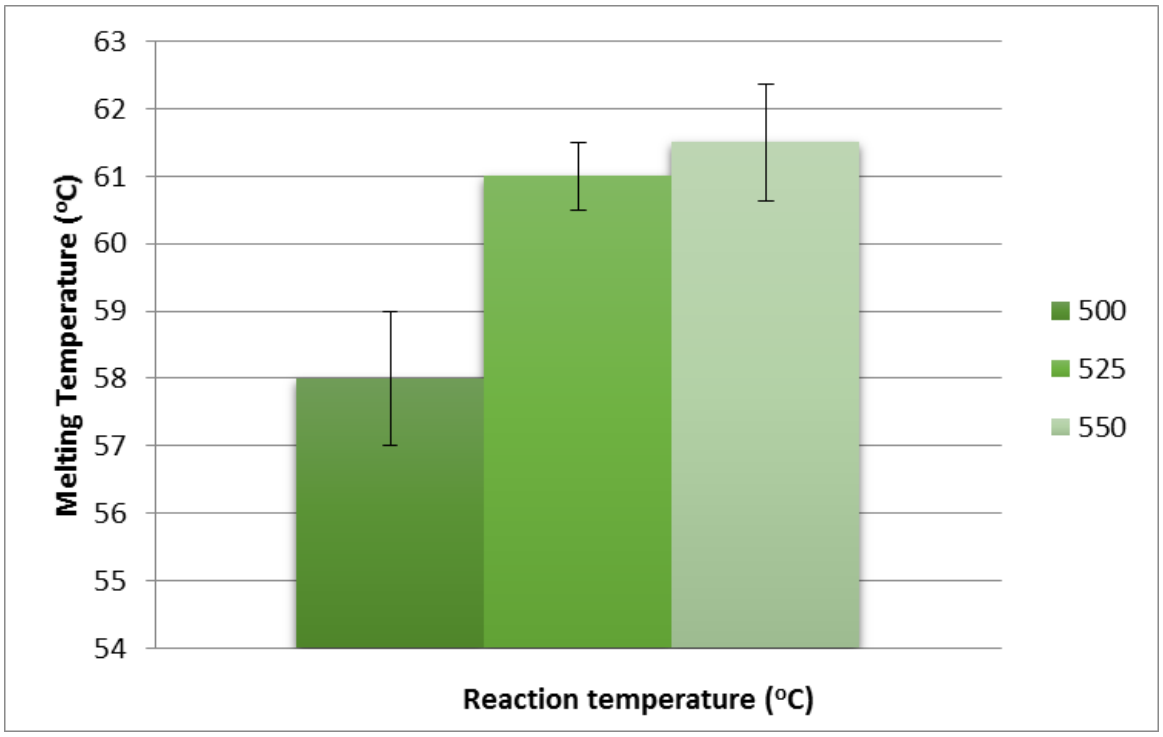

Figure 59: Effect of pyrolysis temperature for product waxes produced from LDPE feedstock with fixed carrier gas nitrogen flow rate of 16 L.min-1.

The increase in the average melting temperature is 3.5°C between reactor temperatures 500 – 550°C and out of that the 3.0°C the step change is observed between 500°C and 523°C indicating that further temperature increase beyond 523°C has little effect upon fuel composition. In contrary to, what would be expected for the LDPE feedstock to have a lower melting point after pyrolysis at 550°C range (564°C) which is the highest experimental pyrolysis temperature as seen in Figure 59, it presents the highest melting point.

At higher temperatures it has been reported that less viscous waxes (de Marco, Caballero et al. 2009) are produced and even liquid products at reaction temperature of 600°C (Williams and Williams 1999). However, with the increase in temperature the gas production is favoured thus affecting the liquid product which includes components

with heavier molecular weight and it greatly affects methane and benzene production; benzene in particular increases with increasing reaction temperature(Kaminsky and Kim 1999, Gao 2010). Kaminsky et al., however, reported a higher distillation residue for reaction temperatures above 710^{o}C as well as an increased content in condensed aromatics for longer residence time which count also account for the increase in melting point (Kaminsky and Kim 1999).Singh et al., also identified the presence of heavier hydrocarbons present in the oil and gas pyrolysis products as a result of increasing reaction temperature that could explain the higher melting point (Singh and Ruj 2016).This result could further be accounted for when taking into consideration that secondary re – combination reactions could be taking place resulting in formation of heavier components.

In Figure 60, the experimental results for the Tk feedstock are presented for the same fixed flowrate to study the thermal cracking effect. As reported previously in §4.5.3, the Tk feedstock consists mainly of LDPE, HDPE and smaller quantities of polypropylene with a significant aluminium content.

From Figure 60, the optimal results do not adhere to a linear appearance observed for the LDPE material and the lowest melting point is observed at the higher temperature of 552.8^{o}C, although the difference between the highest and lowest average melting points is less than 1.5^{o}C and part of these results may well be under statistical error. However, it has previously been reported in literature that although the oil yield increases with temperature ramp between 550^{o}C and 600^{o}C the density of the oil will increase as well due to the presence of aromatic components that results in a denser liquid product; change of density from 0.73kg/m^{3} to 0.79kg/m^{3} when increasing reactor temperature from 500^{o}C to 600^{o}C (Singh and Ruj 2016).

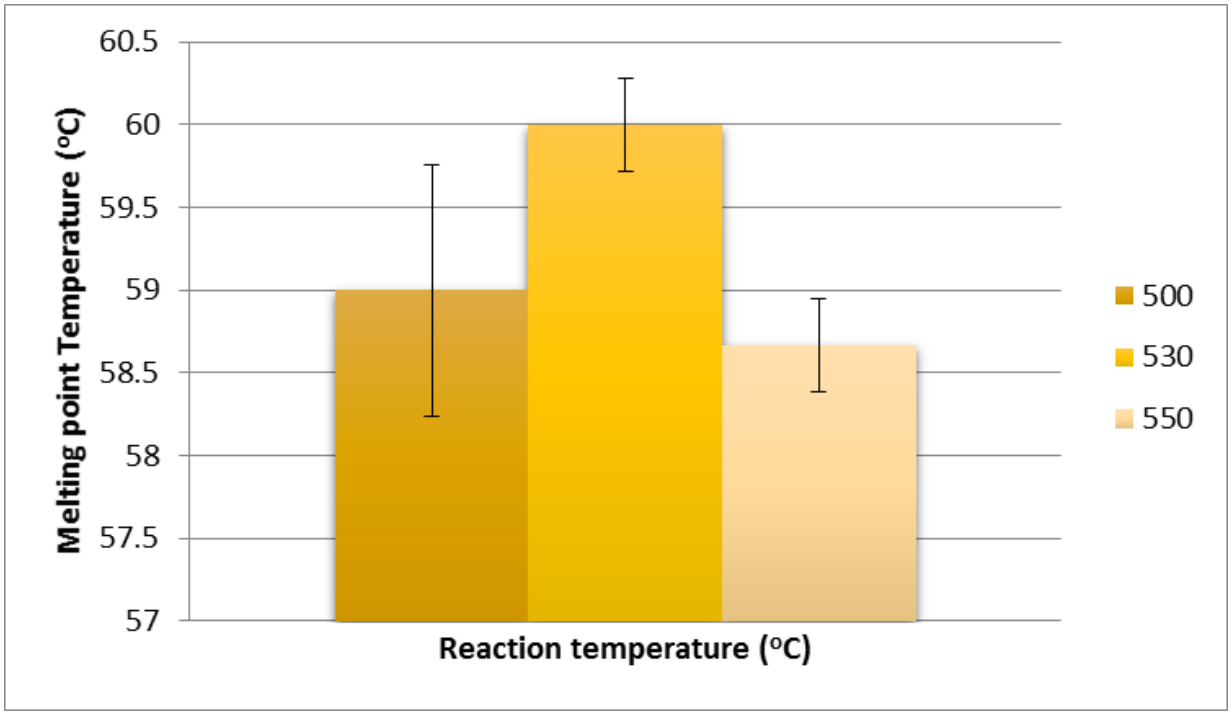

Figure 60: Effect of pyrolysis temperature for Tk feedstock with fixed carrier gas nitrogen flow rate of 16 L.min-1.

.

At the highest flowrate and the same Tk feedstock as shown in Figure 61, the same pattern in the melting point is apparent as with the LDPE material and with a significant difference between the highest and lowest measured melting point values of nearly 6°C. Therefore the thermal cracking effect is more prominent for lower residence time. As before, and in contrast with the results presented in Figure 59, the lowest melting value is at 500°C indicative of the optimum temperature conditions. It needs to be considered that this effect might and will vary when altering the flow rate as shown in Figure 60, following the same pattern observed for the LDPE although the melting temperature range is wider by nearly at 5.3°C in comparison with 3.5°C for LDPE. Similarly, the most significant step change is observed between 515°C and 528°C leaving only 1.3°C for an added thermal cracking effect at the higher temperatures.

At different flowrates and subsequently residence times, different thermal cracking effects and reaction interactions are taking place especially with relation to secondary cracking. Lower flowrate (inversely proportional to residence time) results in more secondary cracking taking place altering the effect or actual reaction temperature which can result in the different melting point patterns observed. However, there is also the option that longer residence time can lead to secondary backbiting/ re – combination reactions taking place, which allow the formation of other heavier components(Martínez, Murillo et al. 2013). At the lower flowrate the thermal cracking effect does not appear to have a linear correlation with temperature increase.

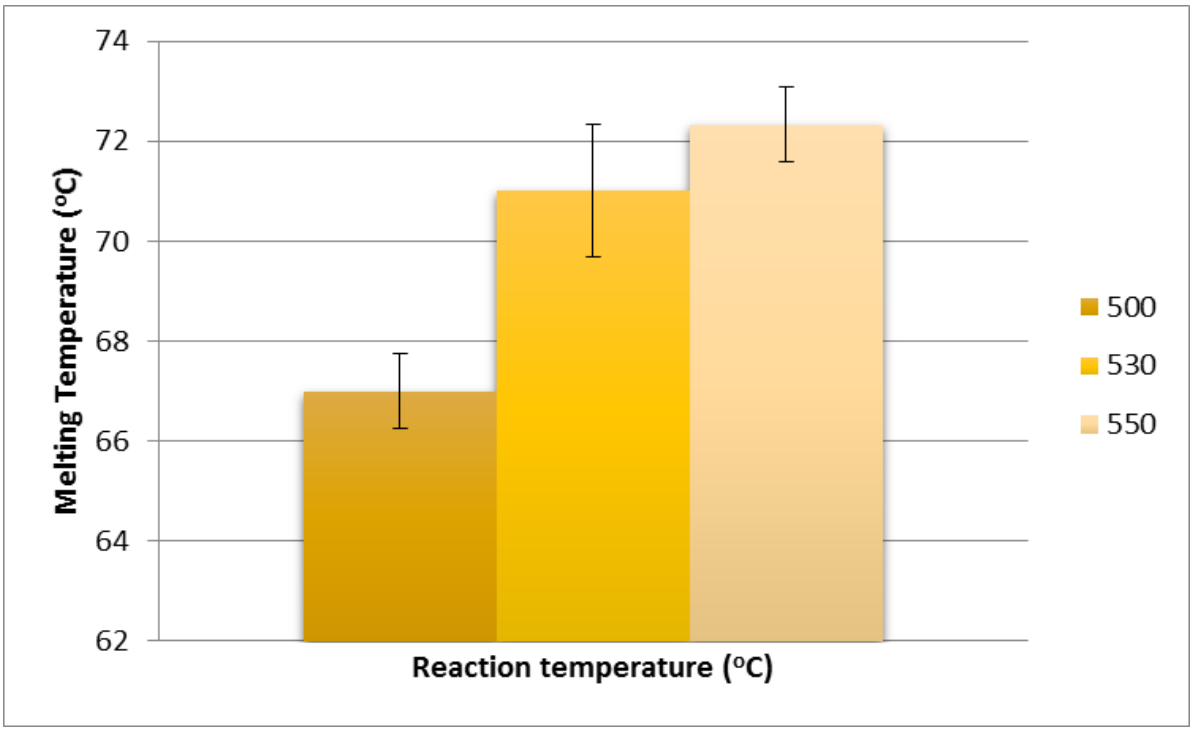

Figure 61: Effect of pyrolysis temperature for Tk feedstock with fixed carrier gas nitrogen flow rate of 20 L.min-1.

In terms of process parameter optimisation, between the lowest melting temperature of the wax which was 58.25°C at pyrolysis conditions of 550°C, 14Lmin^{-1} and the highest of 72.33°C melting temperature produced at 550°C and 20Lmin^{-1} the overall decrease was 14°C.

The results for the Gr feedstock are presented in Figure 62, for which the main two components as identified in chapter four, were HDPE and cardboard. The same behaviour can be observed for the Gr feedstock as shown in Figure 62, where the minimum melting point occurs at 517^{o}C peaking at the medium temperature point and the lowest measured melting point is observed for the highest experimental temperature.

These results, are consistent with the observations made for the Tk feedstock for the same flow rate. Therefore for both mixed waste feedstocks the optimum reaction temperature in terms of lowest melting point was at the highest end. However, with regards to the results of Gr, the range between the highest and lowest measured melting points are more prominent in comparison to the Tk feedstock indicating the composition of the feedstock affects significantly the effect of thermal cracking.

Both, Gr and Tk have HDPE material from the characterisation analysis that has been carried out in the previous chapter but both results vary from the reference LDPE samples. This could be attributed to potential polymer and other material interaction.

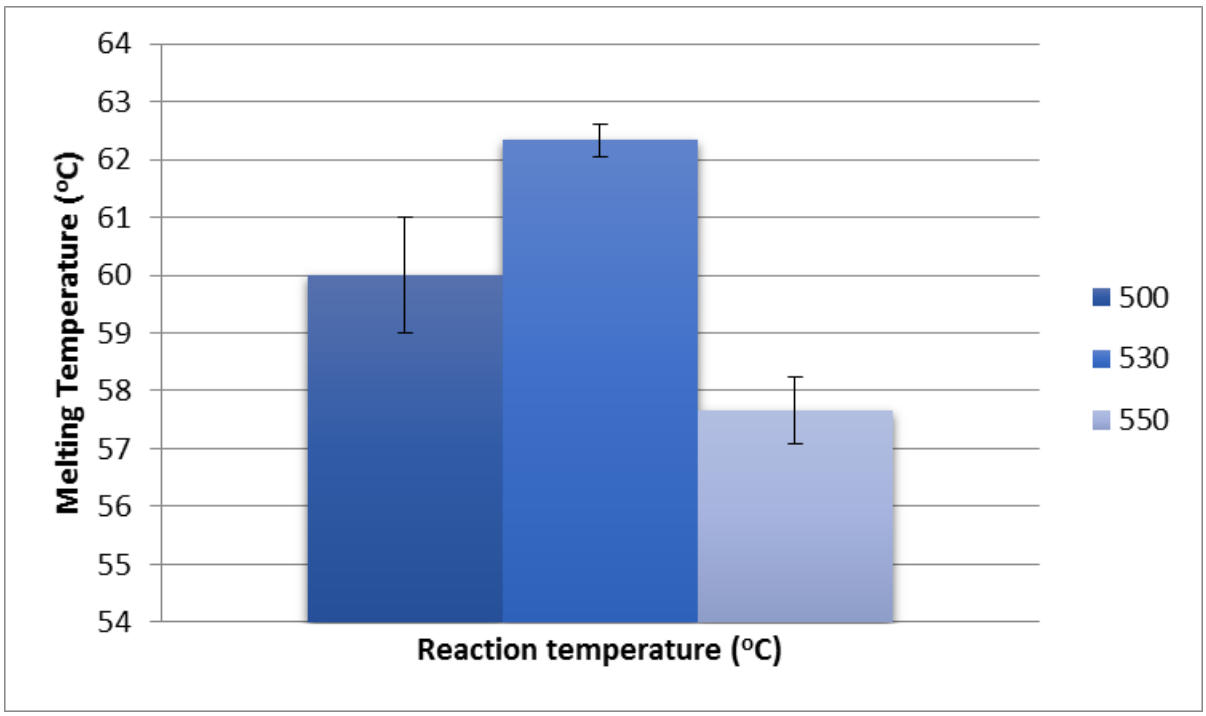

Figure 62: Effect of pyrolysis temperature for Gr feedstock with fixed carrier gas nitrogen flow rate of 16 L.min-1.

Summarising the results, for all studied materials with regards to the thermal cracking effect both industrial mixed waste feedstocks have shown a different behaviour than the pure polymer material. Instead of showing the optimum melting point for the lowest experimental pyrolysis temperature wax products from both feedstocks have the lowest melting point following processing at the highest pyrolysis temperature. This could be attributed to feedstock composition, as the extent of the thermal cracking effect is more intense for the Gr feedstock. Particularly, the range for LDPE is 3.5°C between the highest and lowest melting point, 1.4°C for the Tk at the same flowrate and 5.33°C for the highest flowrate and 4.67°C for the Gr material. The latter observations can be indicative of thermal cracking being dominant of mixed plastic waste at higher reaction temperatures.

5.3.1.2 Influence of temperature on product distribution

The primary goal of upgrading was to obtain a high fuel quality and the secondary was to maximise the total recovery of liquid or wax product. Figure 63 and Figure 64, show the overall mass balance of wax product, char and gas as a function of temperature. Reaction temperature has been reported by various researchers previously to have a significant effect on the product distribution of the gas and liquid products (Kaminsky and Kim 1999, Williams and Williams 1999, Miskolczi and Nagy 2012) and different liquid yields have been identified based on different materials and temperatures (Kaminsky 1993, Pinto, Costa et al. 1999). Generally, the liquid yield is dropping in favour of gas production for the majority of the studies with the effect of increasing temperature up to 800°C.

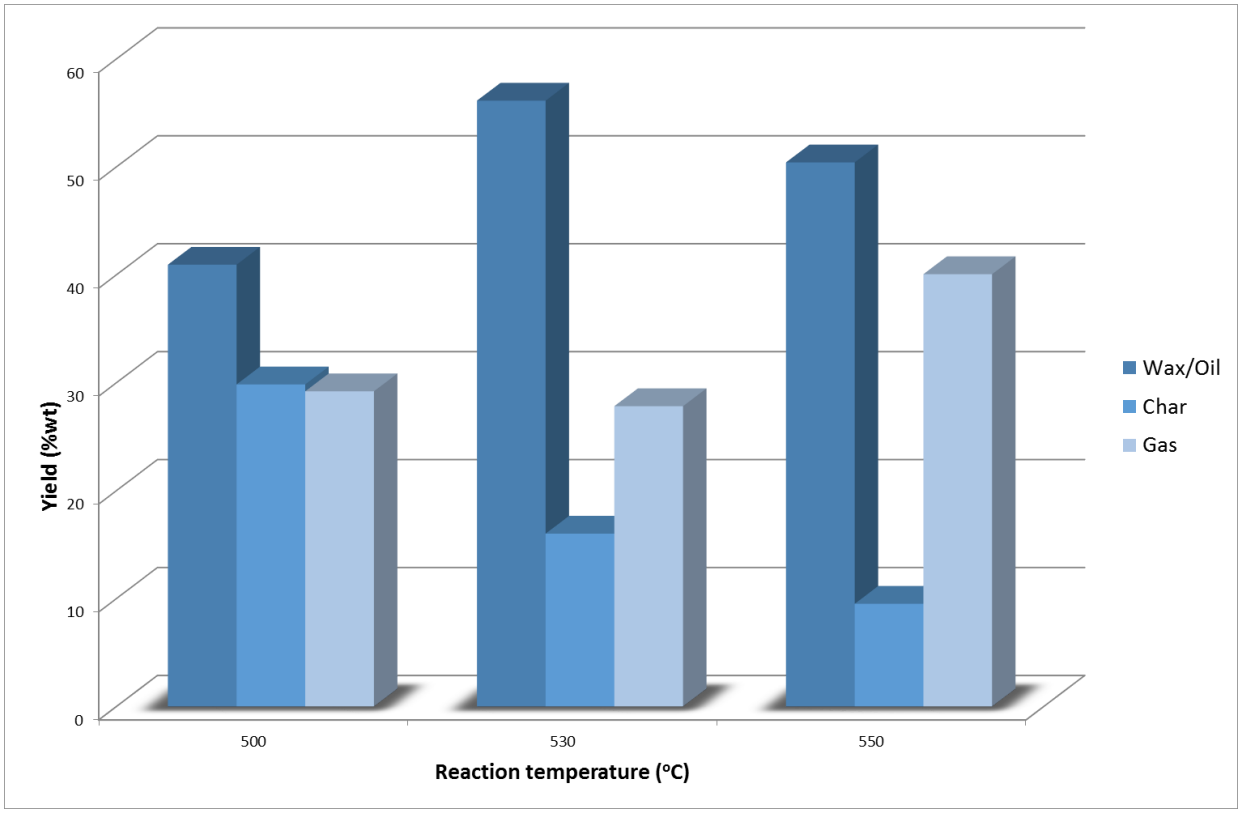

Figure 63: Effect of temperature on mass balance for Tk feedstock and a nitrogen flowrate of 16 L.min-1

In Figure 63, the total yields in correlation with temperature are shown for the Tk feedstock and the maximum liquid yield is obtained at 531.78^{o}C, which is combined lower char yield and is thus a desirable operating point to increase the liquid yield at the expense of char. There is a considerable difference between the lowest and highest wax/liquid yield in the order of 15 wt%. However, this could be explained from possibly unconverted material at the lower reaction temperature (500^{o}C), expressed as solid or char product which cracks further at higher temperatures in favour of wax product. A reaction temperature of 500^{o}C is quite low, when taking into consideration that from the TGA studies in Chapter 4, the cracking temperature was peaking at 470^{o}C and at larger scale (1kg/hr) heat transfer properties will tend to shift this temperature higher. Optimum conditions, for the wax product quality are different than the ones for maximum product recovery. As an example, for Tk feedstock the best quality wax product is obtained at pyrolysis conditions of 550^{o}C, 16Lmin^{-1} (Figure 60) whereas maximum wax yield occurs at 530^{o}C, 16 Lmin^{-1} (Figure 63). This would reflect in lower wax yield but of superior quality and needs to be taken into account when designing the optimum process conditions.

It has been reported previously, that at higher temperatures secondary reactions are more likely to occur therefore breaking the heavier molecules further (Williams and Williams 1997). There is slight drop in both the liquid and char yield for the highest experimental reactor temperature in favour of the gas production which is a consistent with similar findings reported previously from literature(Scott, Czernik et al. 1990, Conesa, Font et al. 1997, Williams and Williams 1999, Kaminsky, Predel et al. 2004).

For the Gr feedstock (composition included HDPE and cardboard material) the results are somewhat similar as illustrated in Figure 64, with the higher yield obtained for the mid experimental temperature and the lowest yield obtained for the lowest experimental temperature with a reported difference between them of 11 w.t.%. With the increase in temperature above 528.20°C towards the higher end both the wax/liquid yield and the char drop in favour of the gas production. The drop in liquid yield is significant 8.63 w.t% which could affect the overall efficiency of the process, however when taking into account the quality of the fuel the lowest melting point is at the highest experimental temperature (550°C).

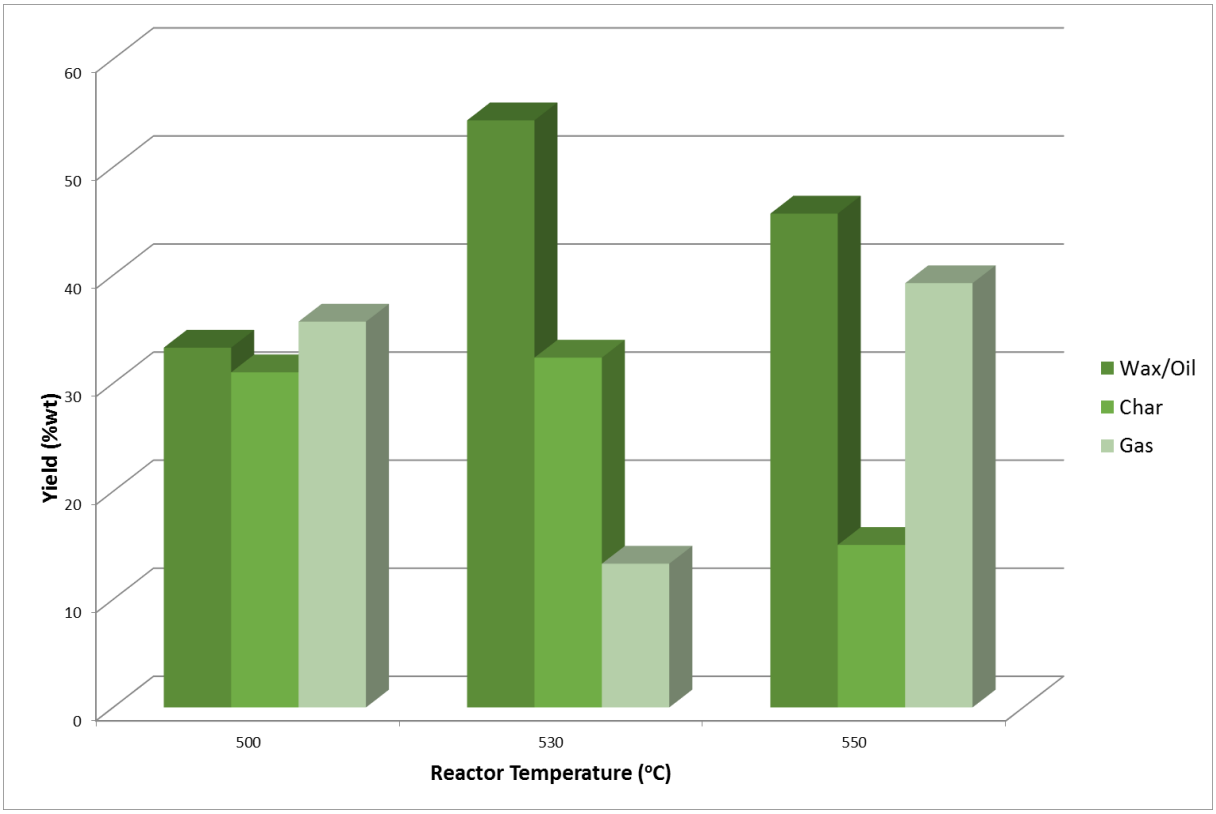

Figure 64: Effect of temperature on mass balance for Gr feedstock and a nitrogen flowrate of 16 L.min-1.

The results for LDPE, which is present in both mixed industrial feedstocks, in terms of product yield recovery for pyrolysis conditions of 500.13^{o}C and 16 16 Lmin^{-1} are: 53.52 w.t.% wax yield, char 25.26 w.t.% and gas 20.93 w.t.%. For 16 L.min^{-1} flowrate and pyrolysis temperature of 550^{o}C, wax recovery amounted to 95.08 w.t.% with char 1.36 w.t.% and gas 3.53 w.t.% which is the result of enhanced thermal cracking resulting from higher reaction temperature. Williams et al. reported from the pyrolysis of LDPE a wax yield of 89.wt.% at 500^{o}C using a fixed bed reactor therefore the results obtained are comparable with his findings (Williams and Williams 1999).Some complimentary experiments were run with HDPE at varying flowrates and with Cr feedstock the summary of these results are presented in Table 21.

As identified in §4.5.2 the main component in Cr feedstock was HDPE and for the feedstocks analysis reported in §4.5.3 the minimum mass loss was identified for the Tc feedstock at 85.7 w.t.% with the next being Tk at 89 w.t.% and Cr at 100 w.t.%. The mass loss for Cr, was identical with that of HDPE 100 w.t.%. The above mentioned results were relating to a scale of mg and it was mentioned that they could be indicative of the potential combined yield capacity of wax and gas products. When moving to a scale of few hundred g/h up to kg/h the results vary significantly however.

When the feedstock is either containing LDPE or HDPE or mainly consists of them such as Cr feedstock, the wax yield generally varied from 53.52 w.t.% up to 95.08 w.t.%. In Table 21, char can also include the ash, unconverted material and in the case of Tk, aluminium content as well.

Table 21: Summary of liquid, char and gas yields in w.t. %, for different feedstocks and varying experimental conditions where, L – Liquid yield, C – Char yield and G – Gas yield.

Experimental Conditions	16 L.min^{-1}		18 L.min^{-1}			26 L.min^{-1}
Material	***500.13°C***	***564.00°C***	***525.84°C***	***533.00°C***	***550.00°C***	***518.00°C***
LDPE	**L: 53.52%** **C: 25.26%** **G:20.93%**	**L: 95.08%** **C: 1.36%** **G:3.53%**				
HDPE			**L: 64.04%** **C: 12.61%** **G:23.35%**			**L: 61.68%** **C: 27.41%** **G:10.91%**
Cr				**L: 62.87%** **C: 11.68%** **G:25.45%**	**L: 66.90%** **C: 12.82%** **G:20.29%**	

Specifically, for the Cr feedstock at 530°C, 18 L.min^{-1} the experiment was repeated three times and the results were quite consistent with an experimental error of 7.2 w.t.% in terms of liquid yields. When feedstocks with a mixed consistency and higher ash are used the yields vary and drop. This could be due to plastic interaction or other factors that need to be taken into account. Different effects, take place at the lower temperature range (500 and 518°C) that affects the total yields of the wax product. At that reaction temperature, thermal cracking has not taken full effect, resulting in unconverted material potentially, remaining in the char and thus increasing the char yields shown in, the first and last column for LDPE and HDPE materials respectively. This effect, is enhanced in the last column with the synergistic effect of lower residence time.

5.3.2 Effect of residence time

Residence time of the vapours has also been identified to be one of the major factors affecting the pyrolysis process outcome and specifically the pyrolysis of plastics. The total carrier gas flow for the different reactor temperatures was taken into account for the total residence time calculation. The results are expressed in the selected flowrate values at the different temperatures but these were converted to total residence time based on the reactor volume divided by volumetric flowrate. An example calculation for reactor temperature 500^{o}C is provided in Appendice A.

These different residence time values varied from 1.78 s minimum up to 2.54 s for the maximum value. The range for the residence time variation with the existing setup due to fluidisation issue, feeding and temperature maintenance limitations thus excluding the 14 L.min^{-1} flowrate allowed only for 0.5 s extension. Even with these limitations the optimum conditions could be verified. For the calculations the reactor volume and the freeboard volume were added as total reactor volume area. In Table 22 all corresponding residence times (s) are in column 3 for different flowrates at different reaction temperatures.

Table 22: Experimental runs with varying flowrates at different reaction temperatures and related residence.

Experiment	Flowrate ($L.min^{-1}$)	Residence time (s)	Temperature (°C)
1	14	2.58	500
2	16	2.27	500
3	18	2.01	500
4	20	1.81	500
5	16	2.23	530
6	18	1.98	530
7	20	1.78	530
8	16	2.18	550
9	18	1.94	550
10	**20**	1.74	550

To establish, an understanding of the influence of the process parameters influence the flowrate of 16 $L.min^{-1}$ was selected to investigate all feedstocks across entire temperature range: 500°C - 550°C. LDPE was also tested for the 18 $L.min^{-1}$ for the entire temperature range and Tk was also tested for 20 $L.min^{-1}$. Individual runs were completed in the 18 $L.min^{-1}$ for Tk and Gr. The purpose behind the initial selection of experiments was to test the limiting conditions and establish any correlations between process parameters and the end fuel quality. Afterwards in order to have the complete set of experiments the outstanding experiments were completed. The 14 $L.min^{-1}$ flowrate was added to investigate the effect on the residence time since it appeared to have a significant influence on the melting point. However, it needs to be noted that 14 $L.min^{-1}$ was interfering with the minimum fluidisation velocity of the reaction as it was in the operational boundaries. Therefore the 14 $L.min^{-1}$ flow rate experiments were not pursued at other temperature range apart from 550°C. Only the industrial waste

feedstocks were tested. The observed effect, on the melting point was minor in the scale of 0.3^{o}C. Quantifying the effect of the variation in vapours residence time on the actual wax quality is illustrated in Figure 65 through to Figure 67.

5.3.2.1 Influence of residence time on fuel quality

In Figure 65, the variation in the average melting point is shown at 500^{o}C for LDPE and all tested flowrates. It can be seen that the lowest melting point is measured for the lowest flowrate 16 L.min^{-1} with a difference of 7.25^{o}C from the higher value which is nearly two times the difference observed for the respective study on the temperature effect. Similarly, in the 550^{o}C temperature end the melting point difference is a reported 5.5^{o}C between the lower and higher flowrates. Again the lowest melting point is observed for the longer residence time (16 L.min^{-1}). Both samples had a yellow colour waxy consistency although with slight changes. The analytical composition of selected samples included these with the lowest melting point is discussed in §5.4.5.

Although, there were irregular observations for the temperature variation in the previous section, it can be seen that for all different reactor temperatures and for all feedstocks the effect of the residence time is very strong with a clear correlation. Increase in residence time by controlling the gas and vapour stream results in a lower melting point sample for all temperatures and feedstocks.

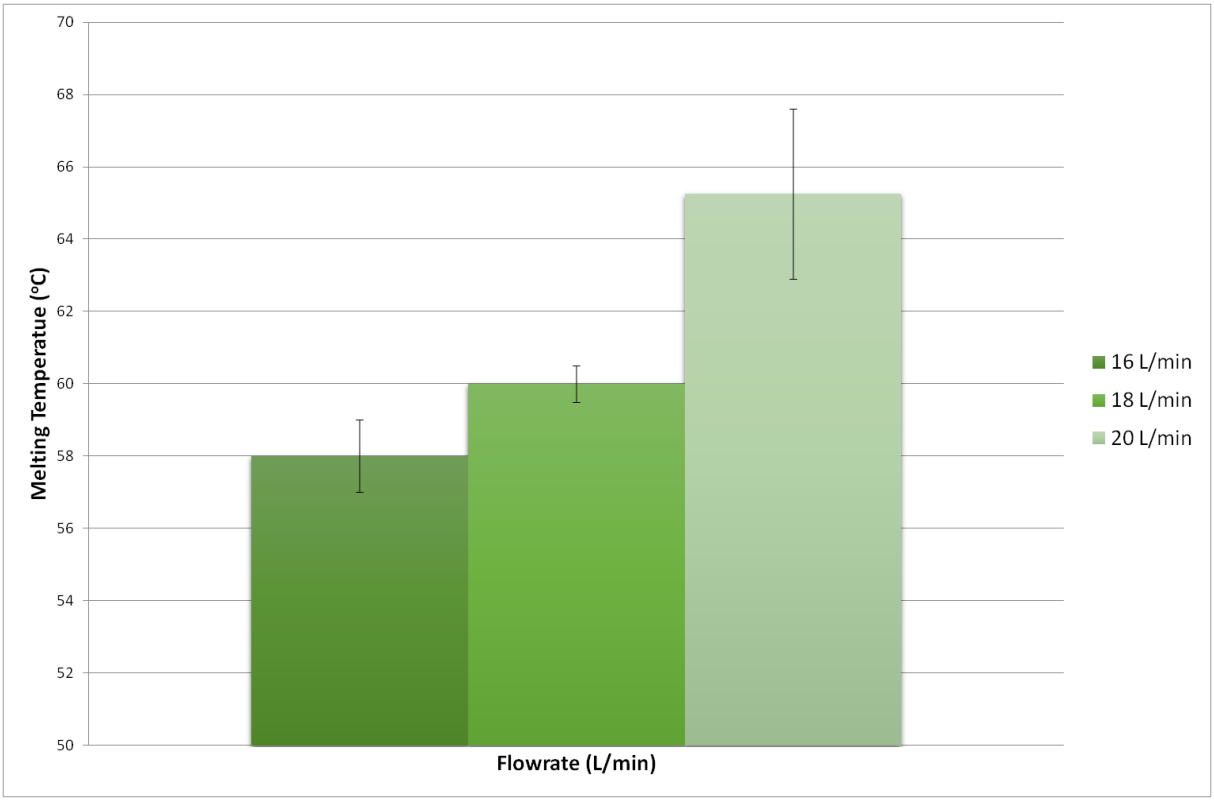

Figure 65: Effect of different carrier gas flowrate values on average melting point for LDPE feedstock at pyrolysis temperature of 500°C.

The tendency for a strong correlation between residence time and product quality is confirmed for the Gr feedstock as well although the difference here is smaller in the range of 1.75°C for the higher reaction temperature (550°C), shown in Figure 66. This effect, is repeated also for the lower reactor temperature with the recorded difference between the longer and shorter residence time being 12.3°C. The lowest melting point is observed for 16 $L.min^{-1}$. There is repeatability in the results both for Gr and LDPE at least for the residence time observations meaning that the effect of residence time appears to be stronger for the lower reaction temperature. Mastral et al. studied the effect of residence time on product yield and it has also been studied from Conesa et al. (Mastral, Esperanza et al. 2002, López, de Marco et al. 2011). Williams et al. reported that higher residence time result in more secondary reactions and further cracking which is consistent with the current findings (Williams and Williams 1997).

However as it is shown here, the extent of the residence time effect on product yield highly depends upon the feedstock composition as well as the flowrate.

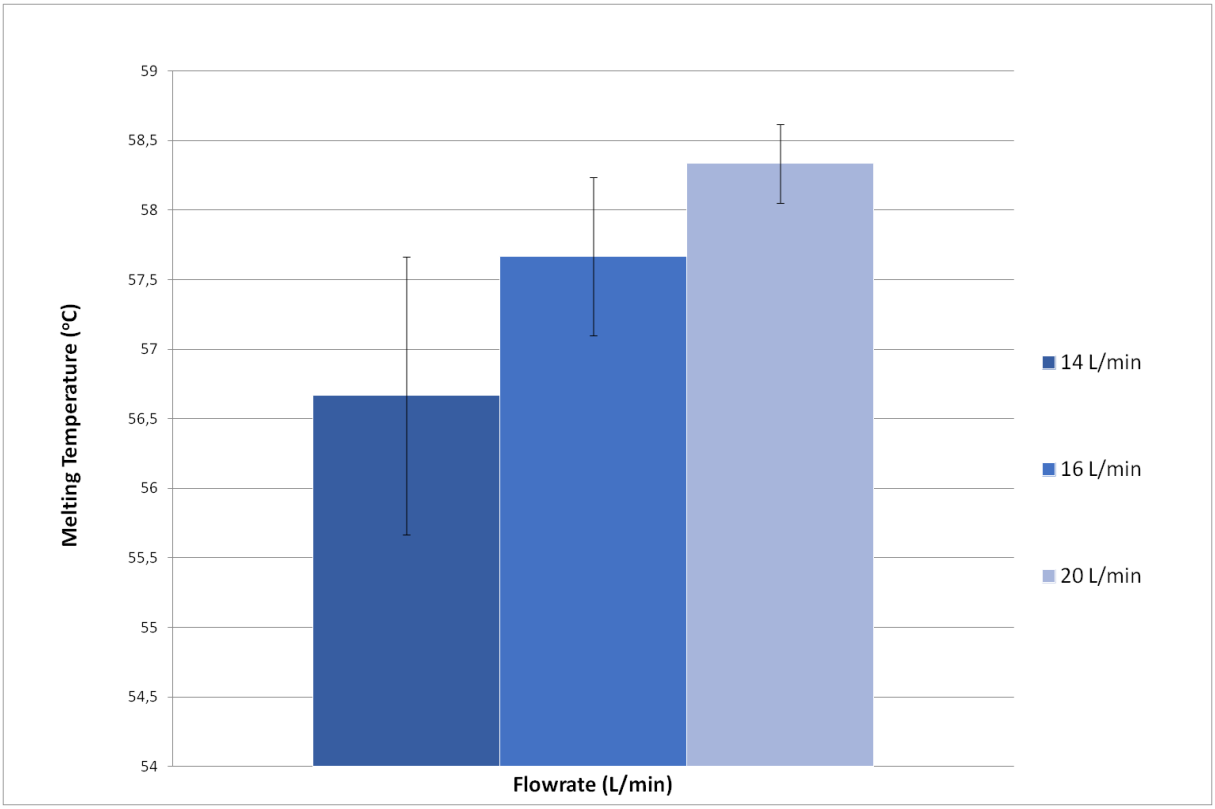

Figure 66: Effect of flowrate on average wax product melting point produced from Gr feedstock for pyrolysis temperature of 550°C.

From Figure 67, it can be seen that Tk feedstock results in the lower melting point wax sample, (60°C) for the lower flowrate of 16 L.min^{-1} at 530°C pyrolysis temperature. The difference between the two extreme melting measurements sits at an impressive 11.33°C difference which is a significant improvement in terms of lowering the average melting point. The same effect, is consistent for the 500°C but with a melting point difference of 8.0°C between the lower and higher residence time. Again both, for LDPE and Tk which contains LDPE the optimum flowrate is 16 L.min^{-1} or 2.23 s residence time compared to 1.74 s for the 20 L.min^{-1}. Consistent with, the pattern identified for the other two feedstocks, longer residence time results in samples with lower melting

This effect is enhanced when combined with the reaction temperature.

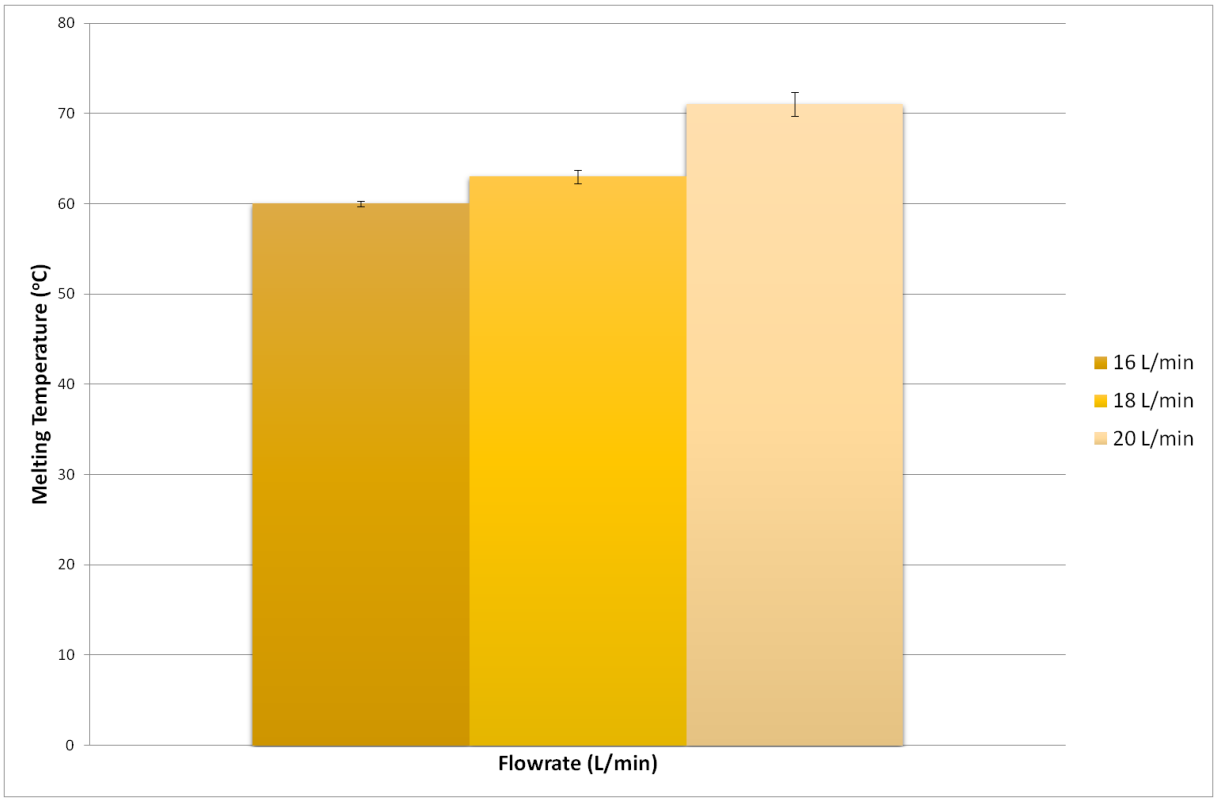

Figure 67: Effect of varying flowrates on average wax product melting point produced from Tk feedstock at pyrolysis temperature of 530°C.

For Tk at 500°C pyrolysis temperature the change between the lowest and highest melting point of the wax product when varying the flowrate is 8.0°C, at 530°C the same difference between the two extreme values increased at 11.33°C and for the 550°C reaction temperature the difference between the highest and lowest wax product melting points was 13.60°C. The change in variation of the lowest and highest melting points produced at different experimental temperature is enhanced with increasing temperature. Although, the effect of temperature in combination with residence time does not necessarily have a straight correlation for all feedstock the effect of longer residence has been identified for all reaction temperatures and feedstocks with the

optimum value being at 16 L.min^{-1} flowrate and further increase on residence time having little effect at least in terms of lowering the average melting point for the two feedstocks that was investigated. Theoretically, according to Mastral et al., increasing residence time can enhance further thermal cracking of HDPE via secondary cracking reactions including further β – scission of the free radicals. This would be obvious in the liquid/wax product as the expected percentage of hydrocarbons with an average carbon length of >C_{33} would be decreasing in favour of aromatic and benzene production across all reaction temperatures that were studied >600^{o}C (Mastral, Berrueco et al. 2007). Previous studies, focused more on the gas product distribution which changed with increasing residence time resulting in further cracking of C_3 – C_5 hydrocarbons towards lighter components for a wide spectrum of temperatures (500 – 850^{o}C) (Scott, Czernik et al. 1990, Williams and Williams 1999, Mastral, Esperanza et al. 2002).

5.3.2.2 Influence of residence time on product distribution

In this section the effect of residence time is discussed in terms of its effect on overall product yields. Specifically, in Figure 68, the outcome comparison for Gr feedstock is shown and it can be observed that with increasing residence time (lower flowrate) there is a decrease in the wax/liquid yield in the order of 7% w.t. The maximum gas production was reached for 18 L.min^{-1} flowrate and char yield showed a dramatic drop between 20 L.min^{-1} and 18 L.min^{-1} (for 1.74s and 1.93s residence time respectively) and stabilised afterwards.

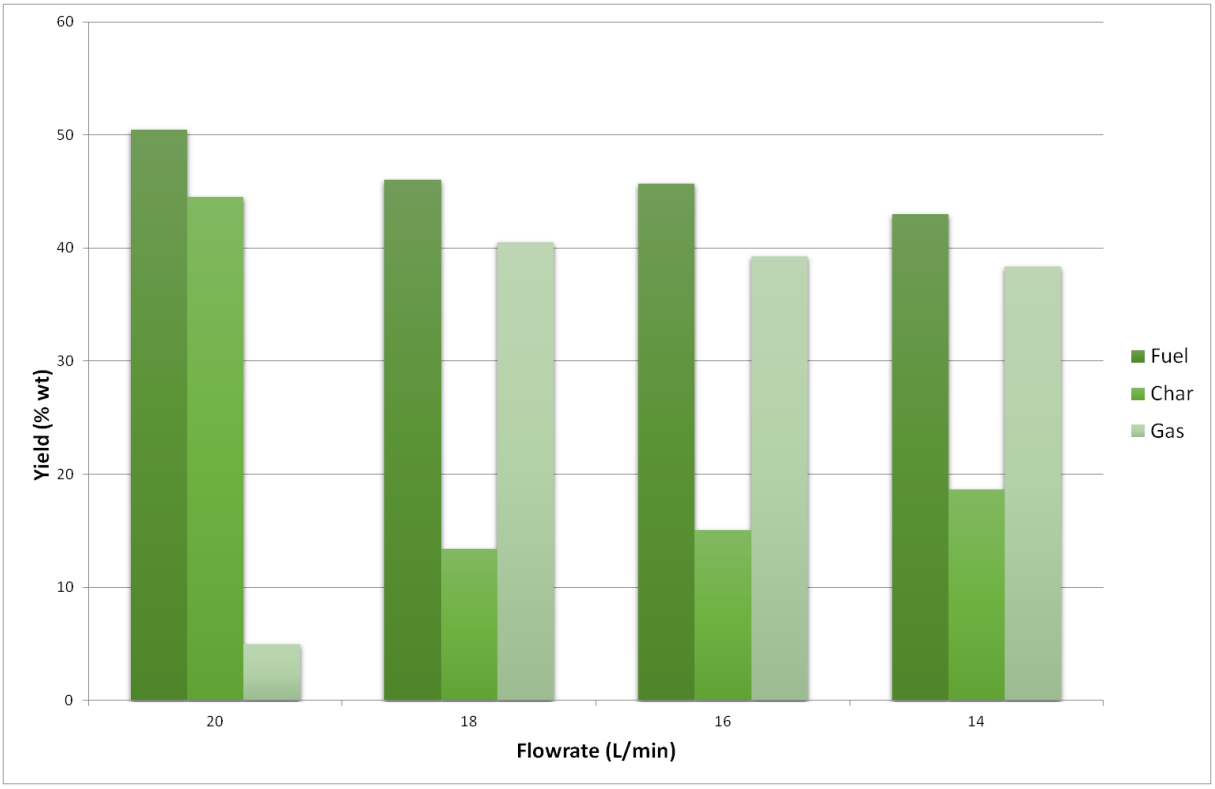

Figure 68: Effect of varying flowrates on product yield produced from Gr feedstock at pyrolysis temperature of 550°C.

Similar results, have been reported by Mastral (Mastral, Esperanza et al. 2002) before, although for higher reaction temperatures, whereas Conesa et al. (López, de Marco et al. 2011) has found that gas yield tends to increase with higher temperature and has not included correlations for the yield in connection to residence time. Although, in terms of wax/oil yield the maximum result is obtained for the 530°C range at nearly 60 %w.t. (59.69%) there is no obvious correlation in the remaining temperature ranges indicative of a residence time effect.

For the higher temperature (550°C), lower residence time (Gr feedstock), results in higher wax yield attributed to more intense thermal cracking whereas, for the mid-range the shift in wax yield is in the range of 8%w.t. change in yield between the highest and lowest flowrate values with little change between 18 $L.min^{-1}$ (59.69%) and 16

L.min^{-1} (59.19%). The change is gas production however, is significant with an increase in gas production of up to 30 % w.t. when decreasing the gas residence time that is a result of secondary cracking reactions producing lighter components. These separate observations do not allow for a clear trend to be noticed but for individual observations and interpretations to be made based on the results outcome. Only one clear trend is apparent that the wax yield increases with lower residence time.

In Figure 69, the comparative results at 530^{o}C are shown and again apart from a slight decrease in the product reflected in the subsequent increase in char yield and leaving the wax/liquid yield relatively intact no other straightforward effect is observed at least in relation to the total yields. This could be interpreted in a positive way since a better quality fuel could be produced at this reaction temperature with the higher residence time and leaving unaffected the liquid yield. At 500^{o}C, the difference between 18 L.min^{-1} (61.80%wt) and 20 L.min^{-1} (37.21%wt) that are the lower and greater wax yields is nearly 25% which is considerable. This could be further explained from the combined effect of thermal cracking which is not significant at the lower temperature (500^{o}C) and at higher flowrate (20L.min^{-1}) there is not sufficient time for secondary thermal cracking to take place.

Comparatively, the difference for the two extreme yields at 550^{o}C range is only 10% with the highest yield obtained for the highest residence time (16 L.min^{-1}) with an accompanying decrease in char yield, equal to 20%w.t. drop and subsequent increase in gas production 10w.t%. It is remarkable that for all different temperatures the optimum yield is observed for different residence times.

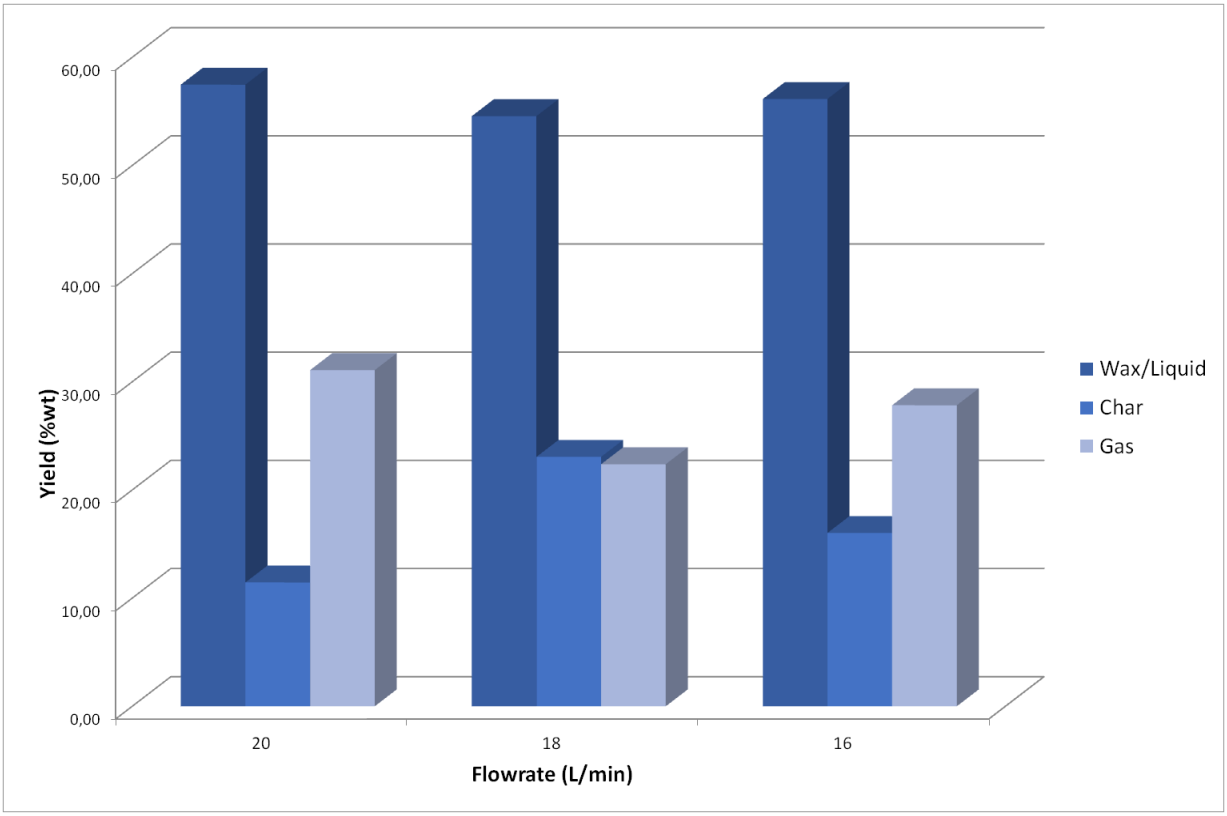

Figure 69: Effect of varying flowrates on product yield produced from Tk feedstock at pyrolysis temperature of 530°C.

The summary of the optimum conditions both in terms of fuel quality and mass balance is given in §5.6.2.

5.3.3 Effect of feedstock on fuel quality

Finally, the effect of feedstock has been studied both in terms of fuel quality and with regards to the mass balance. Pinto et al. has identified the effect of materials on the final mass balance (Pinto, Costa et al. 1999) and Park et al. has studied the different kinetics relating with various compositions of feedstocks (Park, Seo et al. 2012) and previously Scott et al. has acknowledged the importance of feedstock

composition on the final quality (Hartulistiyoso, Sigiro et al. 2015). Bockhorn et al. (Bockhorn, Hornung et al. 1998), Buah et al. (Buah, Cunliffe et al. 2007) and Gao (Gao 2010) have identified the importance of polymer interaction in the mixed feedstock on the final product composition.

5.3.3.1 Influence of feedstock on fuel quality

In Figure 70, the different melting points response for all different feedstocks and temperatures are plotted for a single flowrate (16 L.min^{-1}). It is apparent that no clear trend exists. Although LDPE, is contained in both mixed feedstocks the material interaction and contamination when these mixed samples are pyrolysed is reflected in the results and the relative different patterns they produce. Both, Gr and Tk have the same curve style although for Gr the gradient in the end is much steeper. The lowest melting point is at opposite ends for LDPE and the other two samples whereas the highest value is at the mid-range of the reaction temperatures. Although Gr, appears to have the highest melting point values it is apparent that it results in the lowest melting point of all three samples. This is evidently one of the key factors to be considered when taking into account the feedstock effect with regards to wax/liquid quality.

When comparing these results with the outcome for the other flowrates (18 L.min^{-1} and 20 L.min^{-1}) different patterns appear. A graph, for 18 L.min^{-1} and 20 L.min^{-1} both for products derived from LDPE and Tk is provided in Appendice A. The optimum results, are obtained for all of these feedstocks at varied pyrolysis conditions. For example, at 20 L.min^{-1} for Tk the same pattern with a peak at 530^{o}C appears but the lowest melting point value is for 500^{o}C rather than at 550^{o}C. LDPE maintains a

transferable pattern with the one shown in Figure 70, across all studied flowrates but the average melting point values are increasing. Although, this is not the case for Tk the same shift towards higher average melting point values is observed with increasing flowrates.

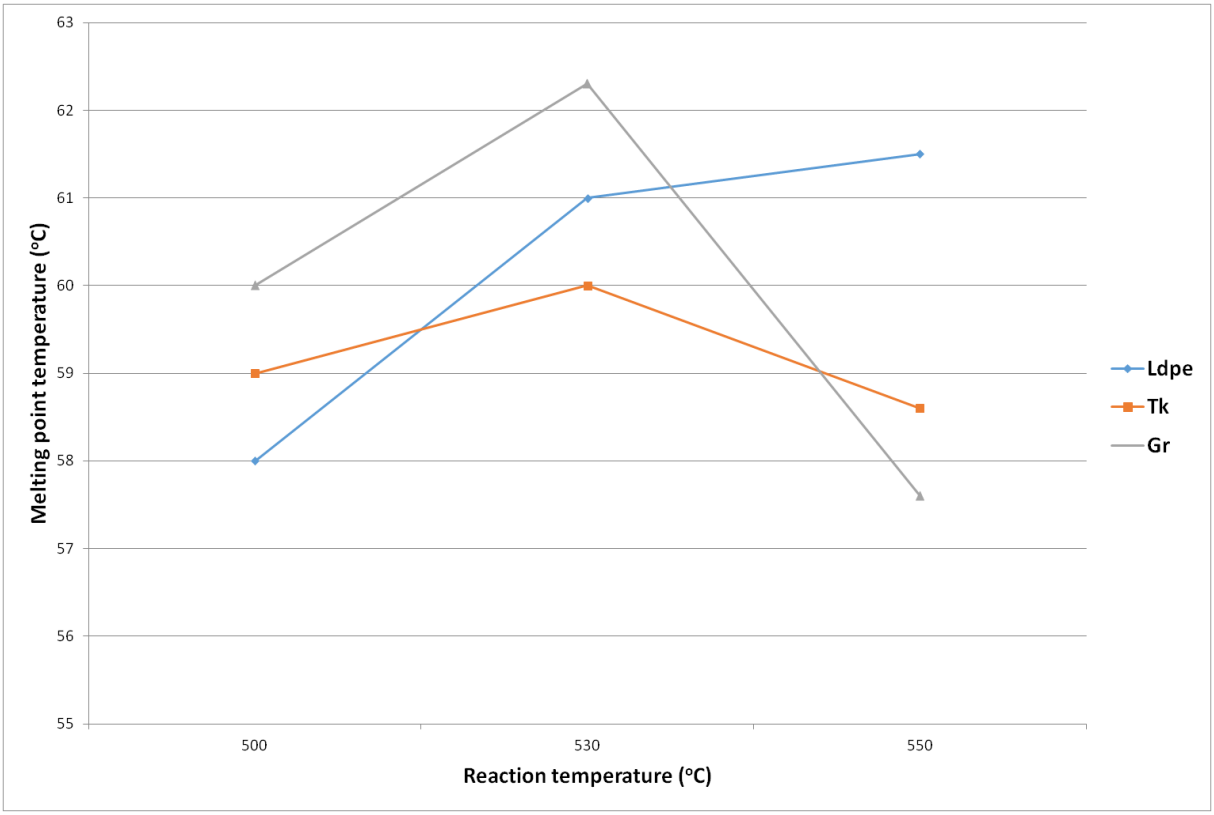

Figure 70: Average melting points at different reaction temperatures for wax products derived from LDPE, Tk and Gr feedstocks. Nitrogen flowrate at 16 L/min-1.

For Gr, the same pattern does not apply across all temperatures and flowrates. Indicatively, for Gr the second lowest melting point is for 20 L.min^{-1} at 550^{o}C. A summary of the optimum melting point values is provided in details at §5.6.2.

5.3.3.2 Influence of feedstock on product yields

With mixed plastic waste there are two different factors to be taken into account when considering overall yields. The first being the inherent variation of waste materials included that will result in different wax/liquid, char and gas yields and the second being the difference between compositions of varying feedstocks. In Figure 71 to Figure 73, the comparative results both for inherent feedstock variation as well as for different feedstocks are presented when maintaining the same process parameters. The results, presented are indicative of the experimental runs that resulted in the wax with the lowest melting point. Three runs are shown, in order to study the repeatability and consistency of the produced results in terms of product yield and product quality. The run conditions presented in the following Figures are:

- Tk at pyrolysis temperature 550^{o}C and 16 L.min^{-1} flowrate,
- Gr at pyrolysis temperature 550^{o}C and 16 L.min^{-1} flowrate,
- All feedstocks at 500^{o}C reaction temperature and flowrate of 16 L.min^{-1}.

Maintaining the conditions stable helps to isolate only the effect of feedstock on the final output. All remaining conditions have also been plotted. However, there are conditions under which the feedstock, does not affect significantly the outcome of the overall yields. These conditions are, flowrate of 20 L.min^{-1} at 500^{o}C and 550^{o}C reaction temperature, with a recorded wax yield difference of up to 10 w.t %. As seen in Figure 71, wax, char and gas comparative yields are presented against number or repeated experiments (1,2,3). From the graph, it can be seen that Tk, presents a significant variation on the wax yield as well as the char yield. This could be explained, when taking into consideration the feedstock composition as a mixture of LDPE/HDPE/PP

and aluminium identified previously in §4.5.4. These specific changes could be linked to the variation in the aluminium content of the feedstock depending on the received batches. A batch containing material with more aluminium results in higher char yield.

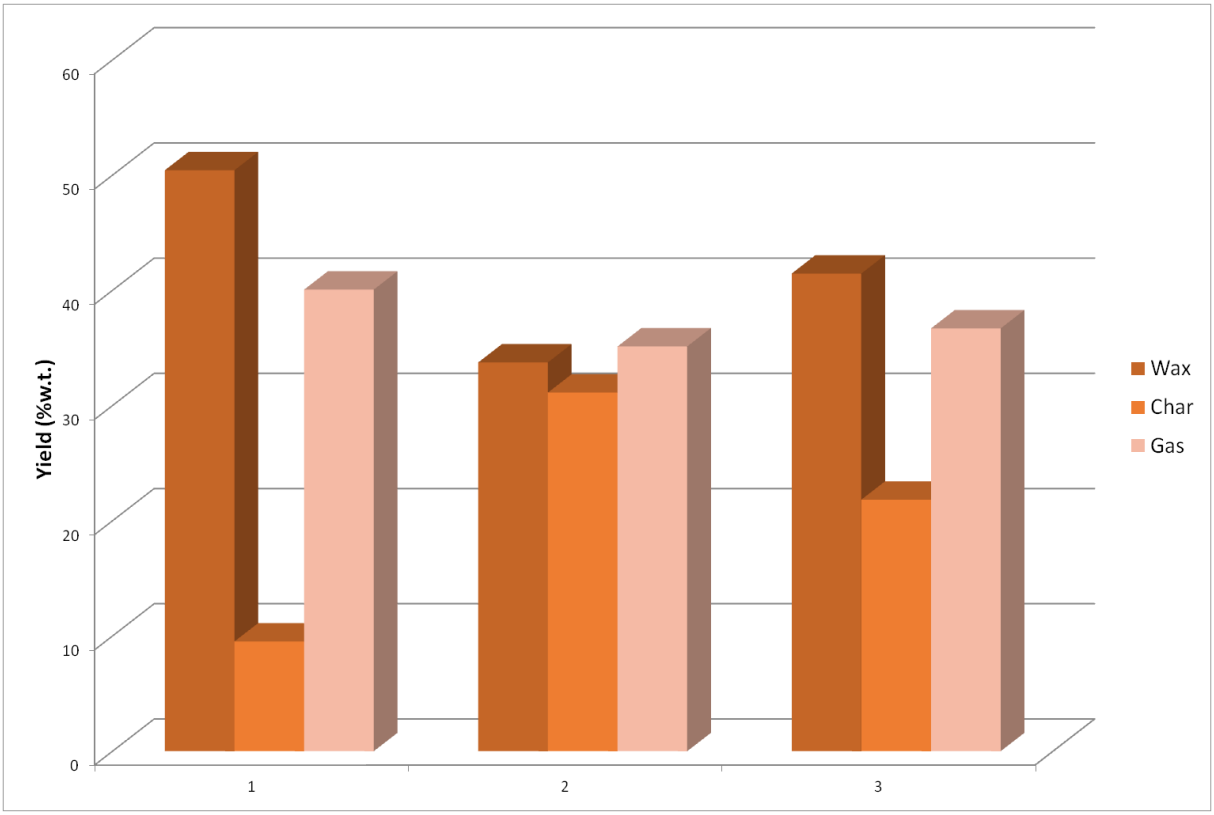

Figure 71: Wax, char and gas yields comparison for repeated runs (1,2,3) under the same experimental conditions - 550°C pyrolysis temperature and nitrogen flowrate of 16 L.min-1for Tk feedstock.

The difference in wax yield amounts up to 17% whereas for the char yield the difference in the yield reaches 20% and for the gas is limited to 5%. From Figure 72, it can be seen that for the Gr feedstock the variation in the results is much lower, varying from 4%w.t. in the wax yield, 3%w.t. for the char yield and 6%w.t. for gas production.

In Figure 72, the overall yields for LDPE, Tk and Gr are plotted in a single graph. The difference in wax yield between LDPE with the highest and Tk with the lowest is 12.58

%w.t. Tk has the highest char yield due to the fact that it includes the aluminium content as well and Gr has the highest gas yield. It is obvious, that the breakdown of different product streams is very varied depending on the actual feedstock. This could be due to material interaction affecting the pyrolysis reactions and process and the final output.

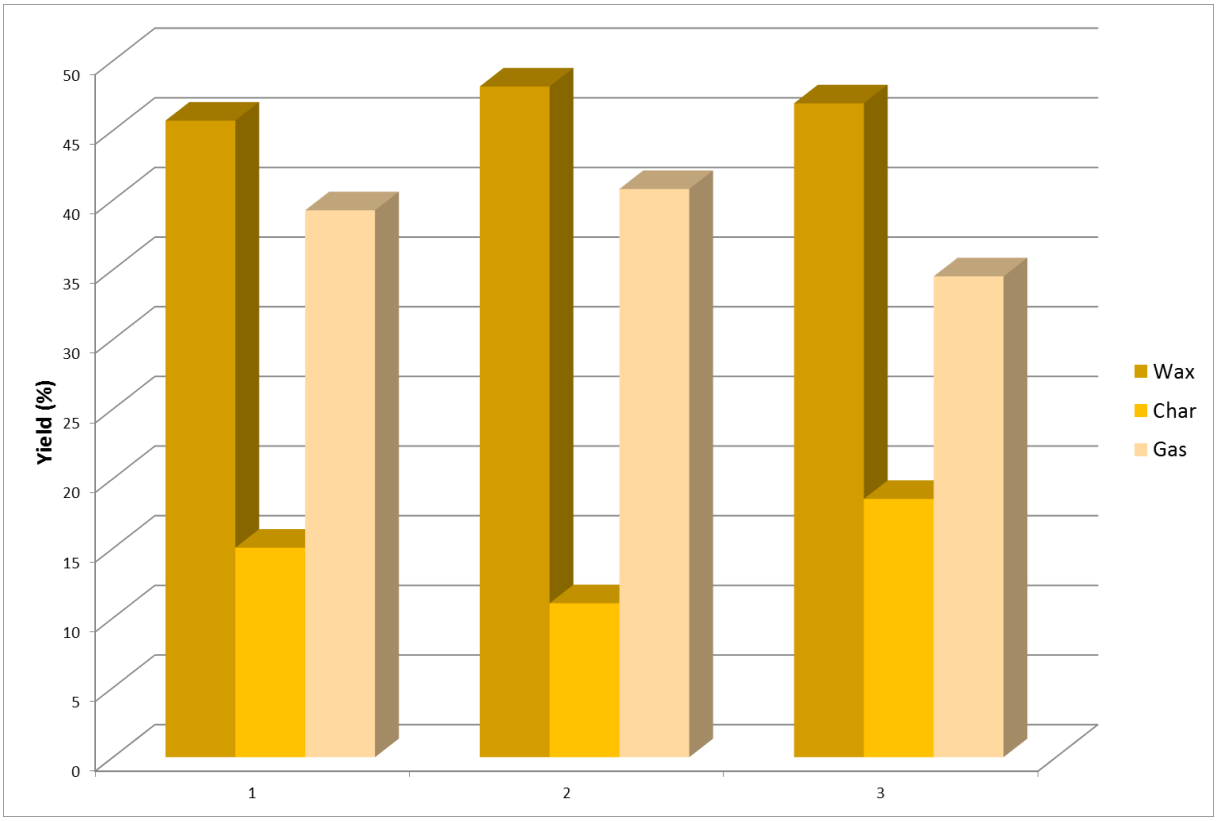

Figure 72: Wax, char and gas yields for comparative experiments the same run conditions of 550°C pyrolysis temperature and nitrogen flowrate of 16 L.min-1 for Gr feedstock.

From Figures 71 and 72, and from the entire set of experiment the limits for the variation of wax and char yields both for Gr and Tk feedstocks have been calculated to take into account both the minimum and maximum variation. Both, residence time and temperature combination of values have been taken into account. The yield variation limits are the following:

1. Wax yield: 3.05%w.t. – 12.58 %w.t

2. Char yield: 5.52%w.t. – 19.21 %w.t.

3. Gas yield: 0.80%w.t. – 24.68 %w.t.

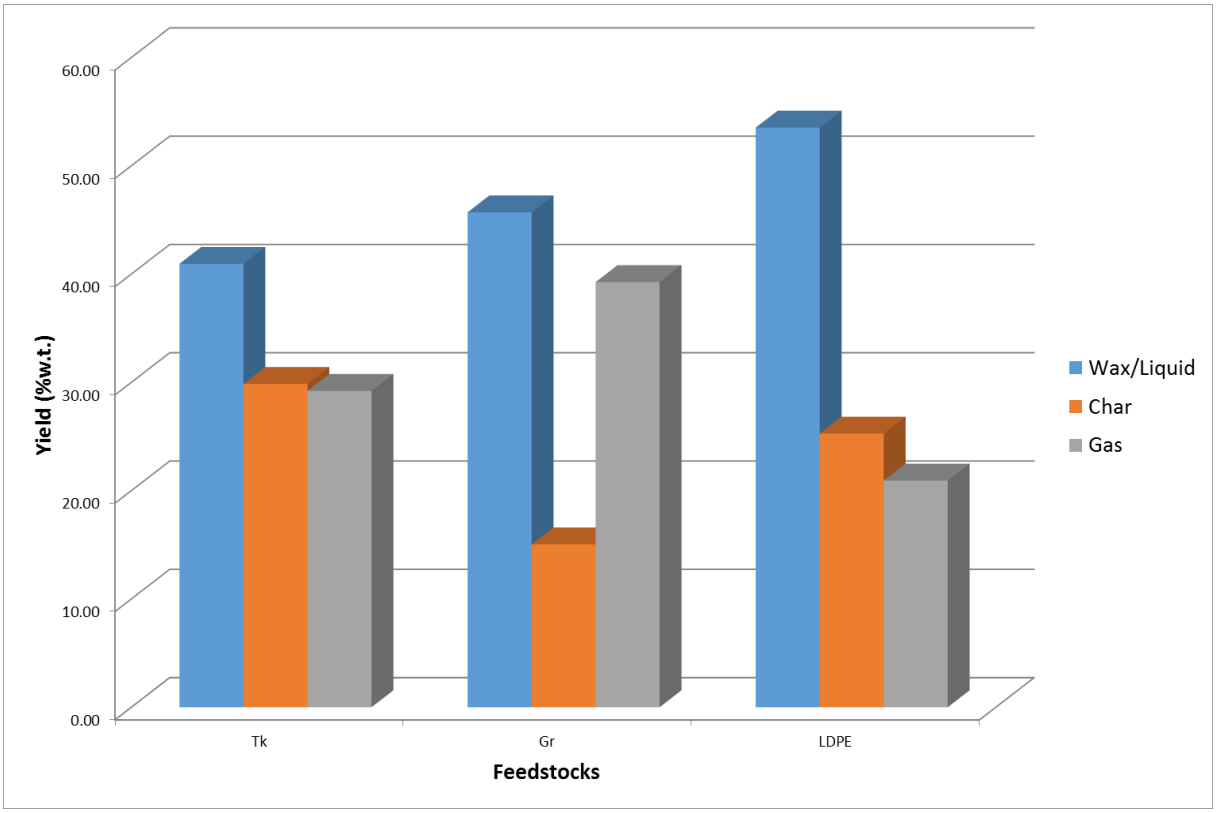

Figure 73: Comparative yields for all feedstocks at pyrolysis conditions of: 550°C reaction temperature and nitrogen flowrate of 16 L.min^{-1}.

Experiment number 8, from Table 22, was completed for all feedstocks and the comparative results are provided in Figure 73.The inherent variation in terms of wax yield that is attributed only to feedstock composition variation can reach up to 17 %w.t. for Tk feedstock for example, as seen in Figure 73, and adds to the complexity when taking into account the range of different feedstocks, which can ultimately result in a combination of different outcomes and in varying percentages as discussed previously. When adding the effect of residence time and reaction temperature in the final output it results in a very complex process. However, quantifying the weight of these factors

is crucial to controlling and monitoring such processes. The summary, of the completed runs, is discussed in §5.5 where the results are processed through the orthogonal array design of experiments and statistically analysed to evaluate the weight of the factors and in §5.6.

5.4 Product fuel analysis and characterization

In the previous section the melting point value was utilised as a means to assess the overall quality and performance of the process. Selected samples that were indicative of the extreme end values of the set of experiments were analysed further to validate and correlate the actual fuel quality and composition. Some of these selected samples were representative of the lowest and highest acquired melting point values for both samples. Initial samples were also analysed for comparison with a different reactor setup. They are only mentioned as a means for comparison. In addition to the Gas chromatography – Mass spectrometry analysis that provides the exact fuel composition and identification a series of complimentary analysis that are listed further down were added to better understand the wax consistency and future performance if to be utilised as a fuel for an internal combustion engine (ICE). Among these analysis viscosity and density are considered the most crucial for oil characterisation(Banar, Akyıldız et al. 2012).

5.4.1 Solvent analysis

With the method described in §3.5.1 the soluble fractions of selected samples were measured and recorded for toluene and isopropanol combined solvents that were

tested as the most efficient. It is remarkable that no sample was completely soluble therefore the results reported in Table 23 are ranging from 70 – 88 % solubility. This greatly affects subsequent analysis such as GC – MS, SIM - DIS and TAN number since only a fraction of the sample is analysed. The heavier components are expected to have remained in the solid fraction.

Table 23: Soluble fractions of different wax samples produced from Cr, Tk and Gr feedstocks after pyrolysis and their melting temperatures (onset and final). Column one refers includes the pyrolysis reaction conditions under which the wax samples were produced.

Wax sample (Average Reaction Temperature)	Onset Melting temperature (°C)	Melting T (°C)	Soluble fraction % (Toluene & 2 propanol)
Cr (530°C)	72.0±1.0	76.0±1.0	72.50
Tk (550°C)	69.0±1.0	72.3±1.6	80.67
Gr (530°C)	64.0±0.5	67.5±0.5	80.89
Tk (500°C)	59.0±1.0	61.3±0.5	82.95
Tk (530°C)	68.5±1.5	71.0±3.0	86.49
Tk (530°C)	64.0±0.5	63.0±0.5	86.95
Tk (550°C)	54.0±1.0	58.6±0.5	86.96
Gr (550°C)	54.0±1.0	58.3±1.0	87.40
Tk (531°C)	59.0±0.5	60.0±0.5	88.31

In columns two and three, and onset temperature and final melting points are also added as a comparative value. Next to, the feedstock the respective pyrolysis temperature from which the wax product wax produced is added. All samples, have been arranged in order of increasing solubility. The solubility of different samples,

produced under diverse reactor conditions varies as shown in Table 23. The wax samples with highest solubility generally have a corresponding relation with the lower melting points observed with the exception of Tk (produced from pyrolysis temperature of 500^{o}C). This is a supporting observation in terms of improved wax sample composition. Samples that contain lighter fractions, and have a lower melting point will be more soluble. It is expected that highest solubility in toluene and isopropanol includes all the compounds up to a certain molecular weight and the remaining fraction would include all the heavier compounds. Even though, the wax samples were in a solid state the results for solubility are all above 80% for the selected samples that were considered for this study with the exception of Cr that has been included for reference purposes.

5.4.2 Hydrocarbon melting point curve

The melting point was chosen as a parameter to measure the effectiveness of the process. This method was utilised only in one previous study as a complimentary analysis due to the nature of the end product which was also a wax (Arabiourrutia, Elordi et al. 2012) . A reference hydrocarbon melting point curve, was compiled in order to serve as the base of the process effectiveness by correlating the results with an average hydrocarbon compound. Utilising the results from an initial gas chromatography – mass spectrometry analysis, from a wax sample, array of different hydrocarbon components identified were included in the range comparing similar findings with literature for correlations (Williams and Williams 1999, Azinfar, Zirrahi et al. 2015).

Following the method explained in §3.5.2 the selected hydrocarbon range was selected from octadecane until tetrapentacontane ($C_{54}H_{110}$) which was the higher molecular weight hydrocarbon in the components present in GC- MS analysis (Wright, Court et al. 2015). Data from literature as well as testing a selection of hydrocarbons in the School of Chemical Engineering at University of Birmingham (Aldrich 2015). All melting point values plotted in Figure 74, include the range of the onset melting point as well as the final value. That range, depending on the hydrocarbon, was from 2 – 4ºC.

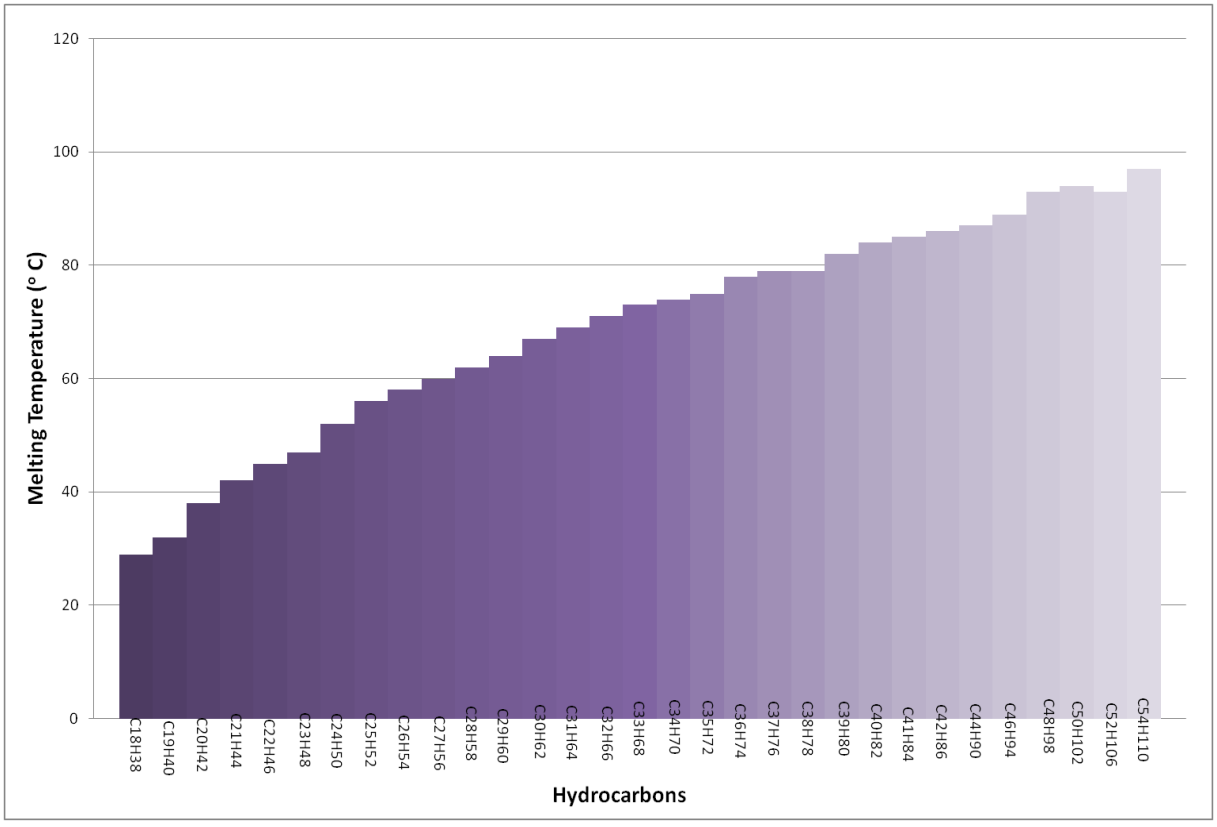

Figure 74: Hydrocarbon range melting point curve.

From Figure 74, it can be observed that with increasing molecular weight the melting point increases.

The scope of, the current study is to identify and quantify the optimal process parameters for different feedstocks. Within the operational limits, of the process in terms of melting point decrease the goal is to try and move towards the left end of this curve. Although, the actual wax samples are comprised of a variation and combination of alkenes, alkanes, alkynes and other compounds such as alcohols and carboxylic acids the average melting point will be appointed to that of a single hydrocarbon for the ease of comparison. In that way the sample from the first line in Table 23 has the same melting point with that of dotriacontane ($C_{32}H_{66}$). To keep things simple only alkanes were included in this curve. Any shift, in the melting point measurements can be related to the single hydrocarbon and changes in the consistency can be detected more easily.

5.4.3 Melting point comparative measurements – Gauge r&r analysis

To test the melting point, of the samples two different techniques could be used either a melting point apparatus or alternatively DSC equipment. Initially, due to the fact that the starting volatilisation temperature of the lighter fractions was unknown, the melting point apparatus was selected. The basic principle for this equipment is based on observation. Adding to, the fact that the melting point has a starting and ending point temperature it was considered essential to perform a gauge repeatability and reproducibility analysis by two different operators to assess the range of error.

From the same pyrolysis conditions (use of Tk feedstock produced at reaction temperature of 500^{o}C, 20 L.min^{-1} nitrogen flowrate) 6 different samples (each sample is entered as part number) were taken. Per sample, three melting point measurements

(trials) were recorded. All measurements, were repeated by a second person to check the reproducibility of the results. Measurements by the author are stated as operator A and a second operator, part of the technical research team, completed the second set of measurements (Operator B). For each operator the range of each measurement was calculated (R value) and the average range of all 6 samples. Also the sample average per sample (X value) and for all samples was completed.

In Figure 75, the results for the range chart by both operators, the average value chart (Xbar graph) as well as the sample interaction graph (part interaction) are shown. The average melting point for all samples by both operators was 60.36^{o}C with a range of 7.8^{o}C. Operator A has resulted in an average of 59.44^{o}C with a variation of 3.5^{o}C whereas operator B in an average melting point of 61.27^{o}C with a variation of 3.66^{o}C. There is a good distribution of the average values of all six samples from both operators around the overall average value as shown in Figure 75 (a). When looking into the range distribution per sample and per operator in Figure 75 (b) there are wide deviation for individual sample observed. This effect, evens out when the sample size increases bringing the range of a single sample from 9^{o}C down to 3.5^{o}C. This could affect however the validity of individual measurements when these are considered for experimental appraisal of wax samples.

In terms of repeatability, the equipment variation (EV) has been calculated by taking into account the variation from both operators to 2.11^{o}C. To calculate reproducibility or appraiser variation (AV) the difference between the overall average values of both operators has been used as well as the equipment variation, the total number of samples and measurements per sample. Reproducibility, was 1.19^{o}C which was lower

than the repeatability value. The total repeatability and reproducibility is 2.43^{o}C. The variation per part is 2.9^{o}C and the total variation is 3.80^{o}C.

Interpreting the calculated values the results can be accurately reproduced but repeated with a higher variation in their repeatability. Specifically, taking into account range of the melting point of hydrocarbons. The effect is minimised when the number of samples and measurements increases.

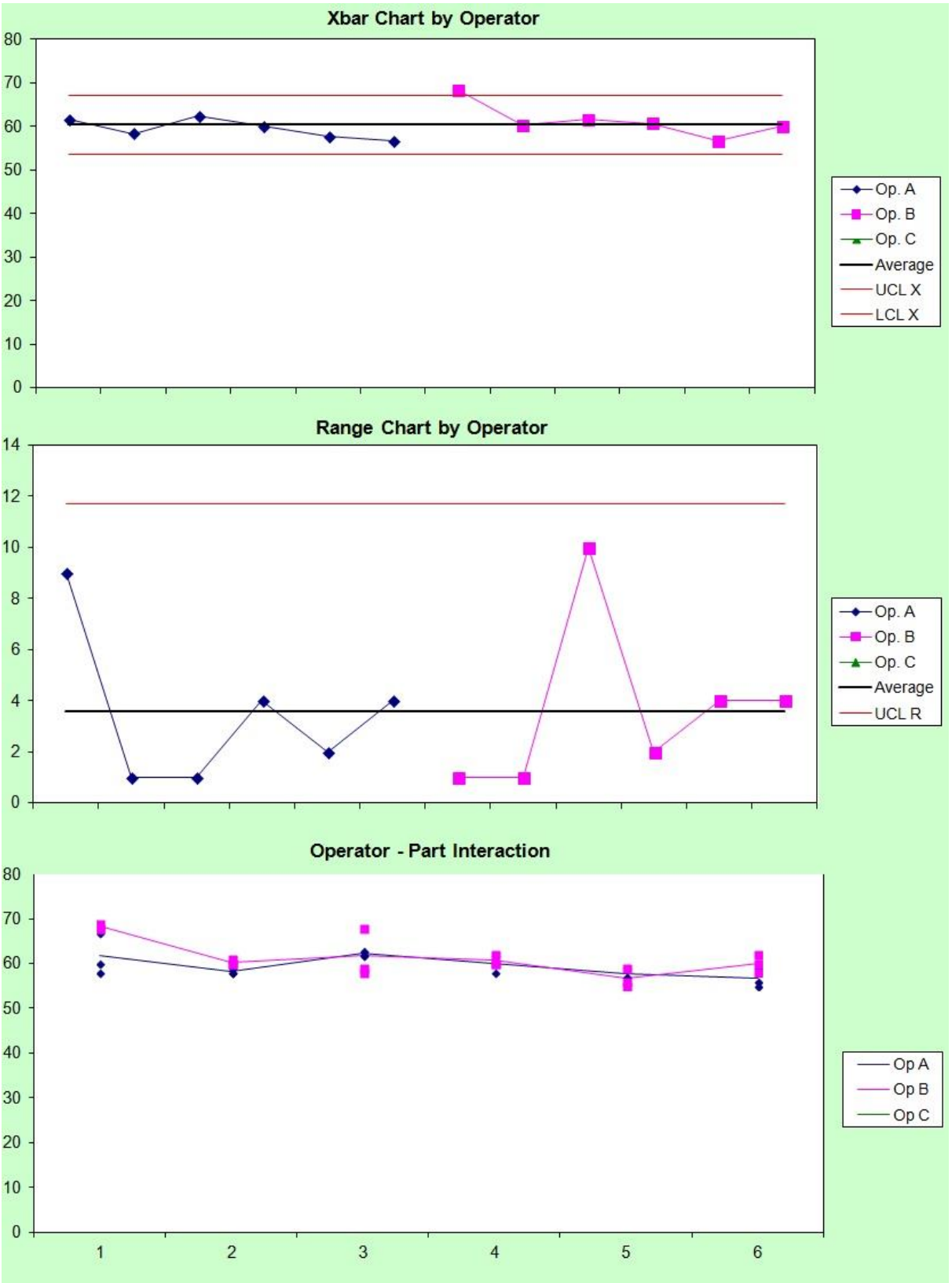

Figure 75: Results from repeatability and reproducibility analysis for melting point equipment. The wax samples analysed were produced from Tk feedstock under the following conditions: 500°C reaction temperature and 20 L.min-1 nitrogen flowrate. Average melting point is plotted on they-axis for a. average values of all samples and both operators and b. range variation of sample measurements c. part interaction from both operators.

5.4.3.1 Comparison of melting point with DSC analysis

Following the melting point measurements three samples were analysed additionally with differential scanning calorimetry to validate the results. These wax samples were all produced from Tk feedstock with process conditions shown in Table 24. The DSC equipment used, was from Perkin Elmer (Pyris 1) in Argon atmosphere. The samples were heated from ambient temperature with a heating rate of 10^{o}C/min, after trials of various heating rates, up to a maximum temperature of 80^{o}C. All endothermic peaks, were facing downwards and melting point can be considered as the onset of the DSC curve bending down. All results compared with the measured melting point are shown in Table 24.

Table 24: Comparative results for melting point with DSC of three Tk samples.

Feedstock	Melting point (^{o}C)	DSC onset temperature (^{o}C)
Tk(550^{o}C, 20 L.min^{-1}))	72.33	73.00
Tk (500^{o}C, 20 L.min^{-1})	61.33	56.50/58.50
Tk (550^{o}C, 16 L.min^{-1})	58.66	60.00/69.00

For the last two measurements, the graphs from the differential scanning calorimeter produced results with double peaks and since the hydrocarbons have an onset and a final melting point temperature this is reflected is these results. There are some deviations between the measurements from the melting point apparatus and the DSC however the limits are between 2.5^{o}C. The repeatability and reproducibility analysis as well as the comparative analysis with the DSC have shown that the melting point is a parameter quite variable with overlapping areas of the measurements.

By increasing, the number of sample measurements and averaging the values this effect can be minimised. For samples, with significantly different consistency and composition, this change is clearly reflected in the sample melting point and the results from Table 24 support this when changing from a sample with a melting point of 60^{o}C to one with a melting point of 70^{o}C different equipment provide the same range of results. A variation of 1 – 2.0^{o}C cannot be avoided.

5.4.4 Fuel blends with diesel

The initial end use for the wax was to test it as a fuel in the internal combustion engine at University of Birmingham, in the Mechanical Engineering department at a variable speed engine (800 -3000 rpm) with a non - heated speed and load fixed injection system. For this reason, a mini study on blending the fuel with diesel at different percentages was completed. The selected wax sample was blended with diesel in mixed ratios: 5% - 10% -20 wt.%. Prior to, running the blends in the engine a series of analysis had to be completed to verify the suitability and performance of the blends for the specific engine. These were:

1. Lubricity analysis for the respective blends of 5% and 10% that will be used in the engine and in different temperatures 40^{o}C and 60^{o}C.
2. LCD Viscosity analysis in the same two different temperatures 40^{o}C and 60^{o}C.
3. Define acid number (TAN) of the fuel to be used,
4. Density of the pure wax sample to calculate the average density of the blends.
5. Flash point, cetane number, TAN number, limited O_2 index.
6. Melting point with DSC – TGA.

From the above mentioned tests, viscosity, melting point and density were completed. Due to, both the texture and solid state of the sample, the lubricity analysis, TAN number and cetane number (due to lack of volume) could not be performed. In addition, limited O_2 index and flash point were analysis relevant to the engine performance, but since the wax fuel could not be injected these analysis were redundant at this stage, until a liquid state was established for the product fuel at room temperature. Focusing the study and experiments on, improving the melting point, density and viscosity was the new aim since these values were more relevant to the fluid characteristics of the wax fuel. Two different blends, were prepared by mixing wax sample at 5% and 10% w/w with Ultra Low Sulphur Diesel (Net 1998-1999) (Oils 2008) in ambient temperature. The wax sample selected, was from Cr feedstock produced from run conditions of 530^{o}C reaction temperature and 18 L.min^{-1} flowrate. This feedstock, was selected due to its composition consistency that allowed to run continuously, enabling to produce the available quantity that was required for an engine run (at least 1 litre). The created blends are shown in Appendix D. The blends formed a thick emulsion which at ambient room temperature did not have very good flow characteristics. The viscosity analysis focused on the 5% and 10% blends, which are presented and discussed. With the existing emulsions the lubricity analysis could not be completed since the blends were not in pure liquid state.

The viscosity analysis of the 5% and 10% blends is presented, and discussed in §5.4.6.To detect the hydrocarbon components within the wax samples that had the most significant effect on the solid consistency of the samples as well as the emulsion effect of the blends individual hydrocarbons were tested in diesel blends in similar percentages (5% and 10% wt).

Wax samples are comprised from a mixture of Hydrocarbons within the range of C_8H_{16} - $C_{54}H_{110}$ including alcohols, alkanes, alkenes and carboxylic acids. Specifically with regards to the molecular weight the transition chain length for alcohols and alkanes is*:*

1. ≥C_{12} H_{26} , alcohols with a molecular formula from Dodecanol and above are in solid form at ambient temperature

2. ≥C_{18} H_{38} , Alkanes with a molecular formula of Octadecane and above are in solid state at ambient temperature

From the existing GC- MS analysis the highest peaks that appeared on the results nonadecane ($C_{19}H_{40}$), heneicosane ($C_{21}H_{44}$) and tricosane ($C_{23}H_{48}$) were the prevalent peaks. An initial test, with a 10% w/w blend in diesel therefore was performed as well as for the lighter and mid-range hydrocarbons. A blend of 20% w/w was also completed for most of the samples. Additionally, heavier components ($C_{26}H_{54}$ – $C_{28}H_{58}$ – $C_{32}H_{66}$ – $C_{34}H_{68}$) were also screened for 10% and 20% to test their effect. Only one alcohol was tested $C_{15}H_{32}OH$. The results and observations are in this section. Four major points of change were identified:

1. Blending at ambient temperature at 10% and 20 % w/w and forming a homogenous mixture. This effect was observed for alkane blends up $C_{21}H_{44}$.

2. Blending at 10% and 20 % w/w with the addition of heat and forming a homogenous mixture. This effect was observed for alkane blends up until $C_{26}H_{54}$.

3. Not blending at 10% w/w with the addition of heat and forming a solid mixture once the blend was cooled. This effect was observed for alkane blends from $C_{27}H_{56}$ and above. The gradual cooling and solidification was more intense for dotriacontane ($C_{32}H_{66}$) both at 10% and 20% w.t. blends.

4. Not blending at all even at 10% w/w with the addition of heat and forming a solid mixture once the blend was cooled. This effect was observed for the one studied alcohol 1-pentadecanol ($C_{15}H_{32}OH$). Solid individual particles were observed at the bottom of the glass throughout the heating phase and did not blend during the process.

Especially, the components from $C_{28}H_{58}$ even in the 5% blend with diesel had a major effect in the consistency of the blend forming a solid phase as soon as the blend cooled down. Alcohols and carboxylic acids even more due to the extra hydrogen in their structure can form hydrogen bonds with each other and dipole – dipole interactions affecting their solubility and formation of new molecules. Diesel is composed of 75% alkanes or paraffins and the remaining 25% of aromatic hydrocarbons with an average molecular weight of $C_{12}H_{23}$, including a range from $C_{10}H_{20}$ to $C_{15}H_{28}$ ((ATSDR) 2017).

Summarising, the results of this study hydrocarbons up to heneicosane create no issue with diesel blends up to 20%wt. Hydrocarbons from docosane up to hexacosane can be blended only with the addition of heat up to 20%wt. Alcohols and hydrocarbons from heptacosane and above are components that even in 5%wt blend will create in issue when blend driving the mixture towards solid state. The latter were decided as an aim

to minimize or attempt to eliminate from the wax samples either by varying the process parameters or by catalytic upgrading of the wax.

5.4.5 GC – MS analysis

The wax samples, selected to analyse with GC – MS analysis were from specific pyrolysis runs with run conditions that produced waxes with the lower melting point temperature values as well as two samples that were from pyrolysis runs with higher melting point values to screen for changes in composition. Samples 1 to 5, of the waxes produced from the pyrolysis conditions outlined below were analysed included the relative area of the spectra from Tk and Gr feedstocks taking into account that for the LDPE similar analysis has been completed. Their melting point values, are provided as well to relate it with the components identified.

1. Tk (500^{o}C – 20 L.min^{-1}) → Wax melting point = 61.33^{o}C
2. Tk (530^{o}C – 18 L.min^{-1}) → Wax melting point = 63.0^{o}C
3. Tk (531^{o}C – 16 L.min^{-1}) → Wax melting point = 60.0^{o}C
4. Gr (550^{o}C – 16 L.min^{-1}) → Wax melting point = 57.6^{o}C
5. Tk (550^{o}C – 16 L.min^{-1}) → Wax melting point = 58.6^{o}C

Additionally, for Tk feedstock (pyrolysis conditions: 550^{o}C, 20 L.min^{-1}) with a product melting point of 72.33^{o}C and for Gr (pyrolysis conditions: 530^{o}C, 18 L.min^{-1}) with a product melting point of 63.00^{o}C, GC – MS analysis was carried out only with spectra identification not including the relative area percentages.

In Figure 76 to Figure 78, the main components that corresponded to the most significant peaks of the GC – MS results are shown. Most of the identified peaks, across all samples such as, octene and cyclodecane, were components that existed in all samples. Also the presence of oxygenated aromatic compounds was detected in previous research as well(Williams and Williams 1999). These common peaks, following their identification and respective retention time for each sample are summarised in Table 25.

The main objective, was to observe the changes in the fuel composition after varying the operating conditions. All samples, were prepared using Toluene and isopropanol as solvents. Variation of sample solubility is interpreted with relation to the analysed sample composition and discussed. For each analysis, the solubility of the samples is given below as well as the total relative percentage of the hydrocarbons < C_{23}. Moreover, the total alcohol and carboxylic content was estimated and the average Paraffin (Alkane/Alkene) to Olefin ratio which is indicative of the reaction kinetics taking place is also included. Increase in the paraffin to olefin ratio is indicating saturation of olefins due to hydrogen transfer reactions, whereas the opposite (decrease of P/O ration) suggests increased β – scission and termination reactions (López, de Marco et al. 2011, Zeaiter 2014). Propagation reactions and both initiation/ termination reactions favor the production of alkenes and unsaturated hydrocarbons whereas hydrogen transfer reaction result in saturated (alkane) components in the wax. Aromatics as a result, are produced during termination reactions in the pyrolysis process when previously released hydrogen is combined with free radicals while, napthenes occur from the combination of free radicals. Higher P/O ratio, is indicative of hydrogen presence and predominant hydrogen transfer reactions leading to the saturation of

alkenes. Lower P/O ratio is indicative of secondary reactions taking place, combined with lower molecular weight components in the results.

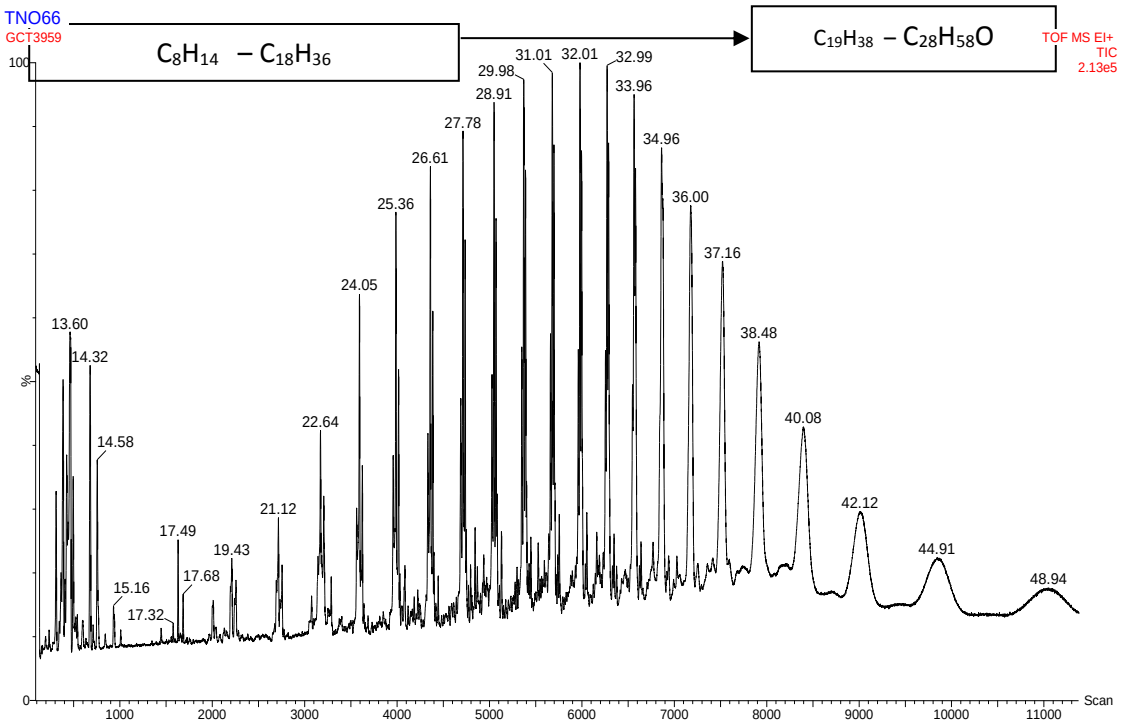

Figure 76: GC- MS results for wax sample produced from Tk feedstock under pyrolysis conditions of 500^{o}C – 20 L.min-1.

In Figure 76, the wax produced from Tk feedstock under the run conditions: 500^{o}C – 20 L.min^{-1} illustrates the following properties including the identified peaks from the GC- MS:

- Solubility of the sample in Toluene and 2 propanol was 82.95%
- Melting point temperature: 61.33^{o}C
- DSC: 56.5^{o}C /58.5^{o}C
- C_8 – C_{23}: 69.2%
- Total alcohol and carboxylic acids: 42.17%
- Paraffin/Olefin ratio: 0.54

For this run the average residence time was controlled via flowrate and it was at the highest selected value (20 $L.min^{-1}$) resulting in lower residence time 1.81 s (Table 25). These conditions, were expected to not favour secondary thermal cracking therefore resulting in heavier components in the wax fraction and subsequently in a higher melting point. Such an assumption is verified from this analysis. There is a significant alcohol and carboxylic acid total percentage measured as well as the heaviest identified component being octacosanol ($C_{28}H_{56}O$) at 42.13 retention time. All major peaks, prior to the last one were identified alcohols ranging from tetracosanol (34.96 retention time) up to octacosanol. However, the P/O ratio is low indicating that less termination and hydrogen transfer reactions take place and the scission and propagation reaction are predominant which result in higher alkene content, supported by the subsequent formation of alcohols and carboxylic acids that ultimately affect the overall melting point as well.

The presence of only one light aromatic hydrocarbon, at 14.32 retention time in 2.35% concentration identified from the GC – MS analysis and library search based on the component structure, is indicative that secondary cracking has not affected the wax product composition significantly. Increase of aromatics in the composition is indicative of thermal secondary cracking (Kaminsky and Kim 1999, Li, Li et al. 1999). The melting point was tested with DSC to validate the results and there appears an 8.5^{o}C variation. Correlating the melting point with the average molecular weight of the sample from Figure 74, and the melting point curve it would coincide with an average chain length of $C_{28}H_{58}$.

Table 25: Summary of analysed wax samples for GC-MS, including the pyrolysis conditions, original feedstock, melting temperatures and grouped GC- MS component concentrations.

Feedstock	Flowrate ($L.min^{-1}$)	Residence time (s)	Temperature (°C)	Wax Melting Temperature (°C)	Solubility (%)	Lighter fractions ($C_8 – C_{23}$%)	Polar components (%)*	P/O ratio
Tk	20	1.81	500	61.33	82.95	69.20	42.17	0.545
Tk	16	2.23	530	60.00	88.31	63.15	40.49	0.535
Tk	18	1.98	530	63.00	86.95	65.20	42.62	0.660
Tk	16	2.18	550	58.60	88.96	64.00	45.69	0.350
Tk	20	1.74	550	72.33	80.67	-	-	-
Gr	16	2.18	550	57.66	87.40	64.15	37.52	0.382
Gr	18	1.98	530	67.50	80.89	-	-	-

*Polar components include alcohols and carboxylic acids

Table 25, summarises the results of all wax samples analysed with GC – MS and provides the pyrolysis conditions under which they were produced as well. Two additional samples (rows 5 and 7) have been added for comparison that have been analysed with GC – MS, with identified peaks but for which the relative area has not been calculated. These results are discussed in detail in this section. In Figure 77, from GC – MS results for the wax sample produced from Tk under the following run conditions: 530.0°C – 18 $L.min^{-1}$ (residence time of 1.98 s) the following properties describe the sample:

- Solubility of the sample in Toluene and 2 propanol was 86.95%
- Melting point temperature: 63.0°C
- DSC: 66.0°C
- $C_8 – C_{23}$: 65.2%
- Total alcohol and carboxylic acids: 42.62%
- P/O ratio: 0.66

For this run, a higher residence time in combination with higher temperature was expected to produce a wax with lower melting point than the sample described previously from Figure 76, (melting point of 61.33ºC), and promote thermal cracking of the primary pyrolysis products. Although, the measured melting point is higher than expected the solubility improved in comparison with the previous sample of lower temperature and residence time. Possibly, at this conditions thermal cracking in not the driving force and re – combinations or re – polymerisation reactions take effect.

The percentage of the lighter fractions < C_{23} decreased proving that the distribution of heavier components in the product might be the one affecting the melting point value. In contrary to, what was expected this temperature range and residence time did not have much influence in secondary cracking of the primary products and instead repolimerisation reaction might have taken place instead resulting in heavier components in the end product or reactions combining free radicals towards naphtene production (López, de Marco et al. 2011). Higher percentage of saturated alkanes are indicative of hydrogen transfer reactions taking place leading to saturation of free radicals.

The total naphtene percentage amounts to 12.31% whereas there is only one aromatic component, ethybenzene (2.01%) that is indicating less secondary reactions taking place (Cunliffe and Williams 1998, Aylón, Fernández-Colino et al. 2008). The total alcohol and carboxylic acid percentage remained in similar levels as before (42.62%) with the heavier component identified as triacontanol ($C_{30}H_{62}O$). The comparison of the melting point with DSC was close with a 3.0ºC difference. The increased soluble part needs to be considered in terms of the identified components since a larger percentage dissolves in the organic solvent.

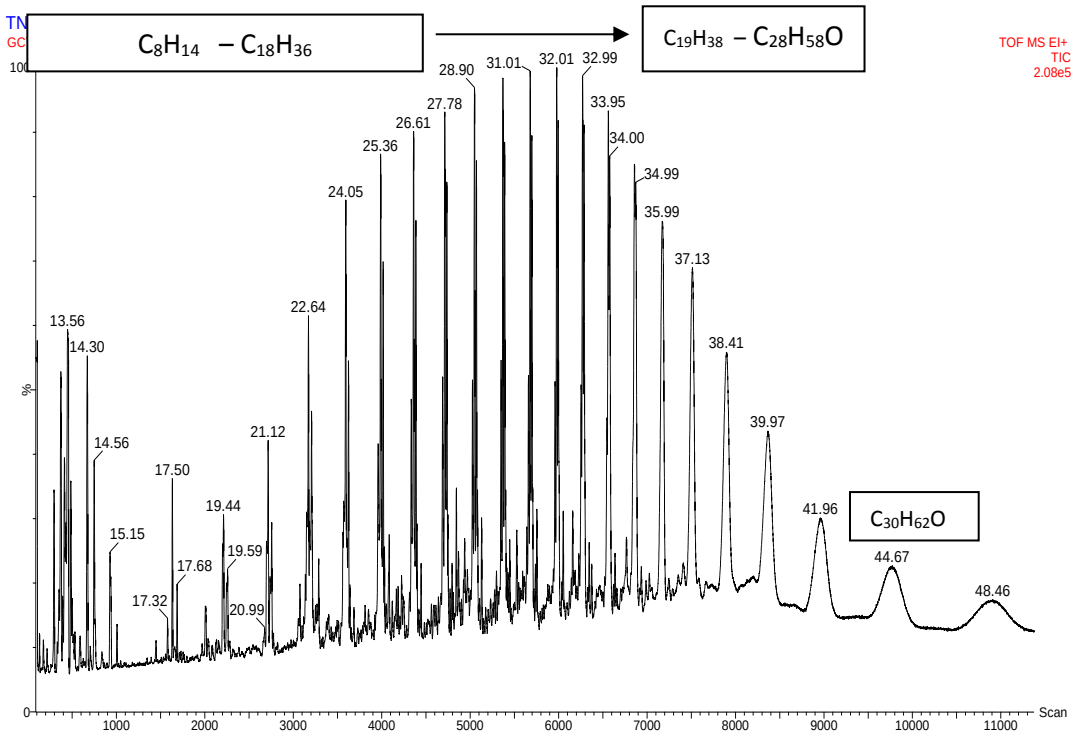

Figure 77: GC-MS results for wax sample produced from Tk feedstock under run conditions of 530°C – 18L.min^{-1}.

The P/O ratio increased comparatively indicating a shift in the pyrolysis reactions favouring more alkane production. Correlating the melting point, with the average molecular weight of the sample from Figure 74, and the melting point curve it would coincide with an average chain length of $C_{29}H_{60}$ (melting point of 63°C).

Additional Tk samples have been analysed with different conditions: 530°C and 16 L.min^{-1} and 550°C and 16 L.min^{-1}. The additional GC – MS spectra, are provided in Appendix B, but the results are discussed here. Also for wax samples produced from: Tk feedstock at run conditions 550°C and 20 L.min^{-1} and Gr feedstock at run conditions 532°C and 18 L.min^{-1} as outlined in Table 25 the results are discussed comparatively in the current section and the spectra is also provided in Appendix B.

The wax sample from Tk feedstock, produced under pyrolysis conditions: 530.0^{o}C – 16 L.min^{-1} is described with the following:

- Solubility of the sample in Toluene and 2 propanol was 88.31 %
- MP: 60.0 ^{o} C
- DSC: 62.0 ^{o} C
- C_8 – C_{23}: 63.15 %
- Total alcohol and carboxylic acids: 40.49%
- P/O ration: 0.535

For this run the average residence time was controlled via flowrate and it was at the lowest selected value (16 L.min^{-1}) resulting in higher residence time (2.23 s) and for the same reaction temperature with the previous sample therefore any changes in the sample consistency can be purely attribute to the effect of residence time. The combination of process parameters resulted in the lowest melting point combined with a slight decrease of 2% in the alcohol and carboxylic acid percentage.

The comparison of the melting point with DSC was close with a 2.0^{o}C difference. The soluble part increased slightly by 1.4% indicative that the sample contained lighter fractions in comparison to the wax sample produced at 1.98 s residence time. The percentage of hydrocarbons <C_{23} decreased marginally by 2% with the last peak identified as pentatriacontene ($C_{35}H_{70}$). The P/O ratio decreased though slightly indicating a shift in the pyrolysis reactions favouring more alkene production. Presence of similar molecular weight hydrocarbons was previously found (up to C_{30}) from the pyrolysis of LDPE and HDPE, identifying alkane components as products of LDPE/HDPE thermal degradation as well(Ballice 2001) .

The total naphthene percentage amounts to 16.07% higher by 4% compared to the lower residence time wax sample whereas there is only one aromatic component, ethybenzene (2.38%) that is indicating that secondary reactions are having a slightly increased effect. So even though the product distribution has shifted in a lower overall M.W. product these conditions favour alkene production linked with higher residence time and lighter molecular weight hydrocarbon production (Gao 2010). Correlating the melting point with the average molecular weight of the sample from Figure 74, and the melting point curve it would coincide with an average chain length of $C_{27}H_{56}$.

From the Tk feedstock and under pyrolysis conditions: 550.0^{o}C – 16 L.min^{-1} a wax sample with the following properties was produced:

- Solubility of the sample in Toluene and 2 propanol was 88.96 %
- MP: 58.6^{o}C
- DSC: 55.0^{o}C
- C_8 – C_{23}: 64.0 %
- Total alcohol and carboxylic acids: 45.69%
- P/O ratio: 0.35

For this run the average residence time was the highest (2.18 s) for the lowest flowrate value (16 L.min^{-1}) for the higher reaction temperature than all analysed therefore any changes in the sample consistency can be purely attribute to the effect of reaction temperature. The combination of process parameters resulted in the lowest melting point combined with a significant increase in the alcohol and carboxylic acid percentage. The comparison of the melting point with DSC was close with a 3.6^{o}C difference.

The soluble part increased slightly by <1%. The percentage of hydrocarbons <C_{23} increased marginally with the highest molecular weight observed component being cyclohexane, 1 – (1- tetradecylpentadecyl) ($C_{35}H_{70}$) in the identified peaks. The P/O ratio decreased though comparatively indicating a shift in the pyrolysis reactions favouring more alkene production.

Total naphtene percentage amounts to 20.03% increased by 4% compared to the higher residence (2.23 s) of the wax sample at the lower temperature indicating that there is a combined cracking effect of higher reaction temperature and residence time. There is only one aromatic component, ethybenzene (1.99%) that is indicating that secondary reactions not favouring production of aromatics. Correlating the melting point with the average molecular weight of the sample from Figure 74, and the melting point curve it would coincide with an average chain length of $C_{26}H_{54}$.

In comparison for Tk, (at pyrolysis conditions of 550^{o}C reaction temperature and 1.74 s residence time) the highest observed component in the wax distribution was Tetratetracontane ($C_{44}H_{90}$) with the highest melting point of 72.33^{o}C and lowest solubility of 80.67% relating to an average chain length of $C_{33}H_{68}$.The overall shift for the melting point of the wax samples produced from Tk feedstock with the current design of experiments has moved the average chain length from $C_{29}H_{60}$ (at pyrolysis conditions of 500^{o}C reaction temperature and 1.81 s residence time) to $C_{26}H_{54}$ (at 550^{o}C reaction temperature and 2.18 s residence time). The latter can be considered the optimum conditions to consider for further fuel wax upgrading.

Table 26: Major component identification for the wax samples analysed with GC –MS analysis produced from different feedstocks and under varying pyrolysis conditions.

Retention time (min)	Molecular Formula	Tk (500°C -20L.min^{-1}) 1.81 s	Tk (530°C - 18 L.min^{-1}) 1.98 s	Tk (530°C -16L.min^{-1}) 2.23 s	Tk (550°C -16L.min^{-1}) 2.18 s	Gr (550°C - 16 L.min^{-1}) 2.18 s
12.90	C_8H_{14} / C_8H_{16}		0.14%	1.12%	0.23%	1.14%
13.56	C_8H_{16}	2.31%	3.34%	3.81%	1.88%	4.03%
14.30	C_8H_{10}	2.35%	2.01%	2.38%	1.99%	2.53%
14.56	C_8H_{14}	1.78%	1.52%	1.64%	1.44%	1.79%
17.50	$C_{10}H_{20}$	0.44%	0.62%	0.66%	0.33%	0.41%
19.44	$C_{11}H_{22}$	0.80%	0.92%	0.94%	0.57%	0.74%
21.12	$C_{12}H_{24}$	1.10%	1.19%	1.12%	0.89%	0.99%
22.64	$C_{13}H_{26}$	0.29%	1.62%	1.88%	1.09%	1.58%
24.05	$C_{14}H_{28}$	1.28%	1.42%	1.98%	1.60%	1.70%
25.36	$C_{15}H_{30}$	1.26%	1.43%	1.26%	2.09%	1.58%
26.60	$C_{16}H_{32}$	1.62%			1.78%	1.67%
27.79	$C_{17}H_{34}$	1.46%	1.52%	1.81%	1.47%	1.50%
28.90	$C_{18}H_{36}$	1.62%	1.40%	1.49%		1.54%
29.98	$C_{19}H_{38}$	1.48%	1.30%	1.49%	1.50%	1.50%
31.01	$C_{20}H_{42}$	1.56%	1.27%	1.54%	1.38%	

32.01	$C_{21}H_{44}$	1.57%	1.39%	1.51%	1.39%	1.32%
32.98	$C_{22}H_{44}$	1.62%	1.30%	1.34%		1.45%
33.96	$C_{23}H_{46}$	1.41%	1.17%	1.47%	1.31%	1.46%
34.95	$C_{24}H_{50}O$	4.18%	3.4%	3.78%	3.58%	3.37%
36.01	$C_{25}H_{52}O$	4.54%	3.66%	3.84%	3.71%	3.50%
37.13	$C_{26}H_{54}O$	4.82%	3.87%	4.27%	4.31%	3.91%
38.40	$C_{27}H_{56}O$	5.25%	4.46%	6.97%	4.99%	4.23%
40.01	$C_{28}H_{58}O$	5.93%	6.89%		5.48%	4.62%

Comparatively for the wax sample produced from Gr feedstock, under pyrolysis conditions: 550.0^{o}C – 16 L.min^{-1} (residence time 2.18 s) the values retrieved from previous analysis and the GC – MS are:

- Solubility of the sample in Toluene and 2 propanol was 87.4 %
- MP: 57.6^{o}C
- DSC: 56.0 ^{o} C
- C_8 – C_{23}: 64.15 %
- Total alcohol and carboxylic acids: 37.52%
- P/O ratio: 0.382

The optimal conditions that were established for both feedstocks were used for the GC- MS analysis of the wax samples to detect changes in the wax composition that would be specific attributes of the feedstock effect on the end wax product while maintaining the pyrolysis conditions the same. The comparison of the melting point

with DSC was close with a 1.6°C difference. The soluble part was at similar values with Tk. The percentage of hydrocarbons <C_{23} was at the same levels however the alcohol and carboxylic acids percentage was much lower which could account for the fact that the end sample had a lower melting point. This could be attributed to the effect of feedstock resulting in a different end product. The P/O ratio was nearly at the same levels indicating that the pyrolysis reactions taking place for the same conditions result in the same end product towards favouring more alkene production. The identified peak with the highest molecular weight component was triacosanol ($C_{30}H_{62}O$).

Total naphtene percentage amounts to 20.31% remaining at the same levels with Tk supporting the case that reactor conditions and the thermal cracking affects both feedstocks in a comparative way in a combined way of cracking effect at higher reaction temperature and residence time. There is only one aromatic component, ethybenzene (2.53%) slightly higher than Tk (1.99%) for the same conditions which again can be related to the effect of feedstock. Correlating the melting point with the average molecular weight of the sample from Figure 74 and the melting point curve it would coincide with an average chain length of $C_{26}H_{54}$.

In comparison, for Gr feedstock produced from pyrolysis conditions of 530°C reaction temperature and 1.98s residence time (Table 25) the highest observed component in the wax distribution was Tetratetracontane ($C_{44}H_{90}$) with the highest melting point of 72.33°C and lowest solubility of 80.67% relating to an average chain length of $C_{33}H_{68}$. In general, increasing the residence time results in further thermal cracking of the primary pyrolysis products with a subsequent wax sample of lower melting point and lighter hydrocarbon distribution in the analysed wax composition.

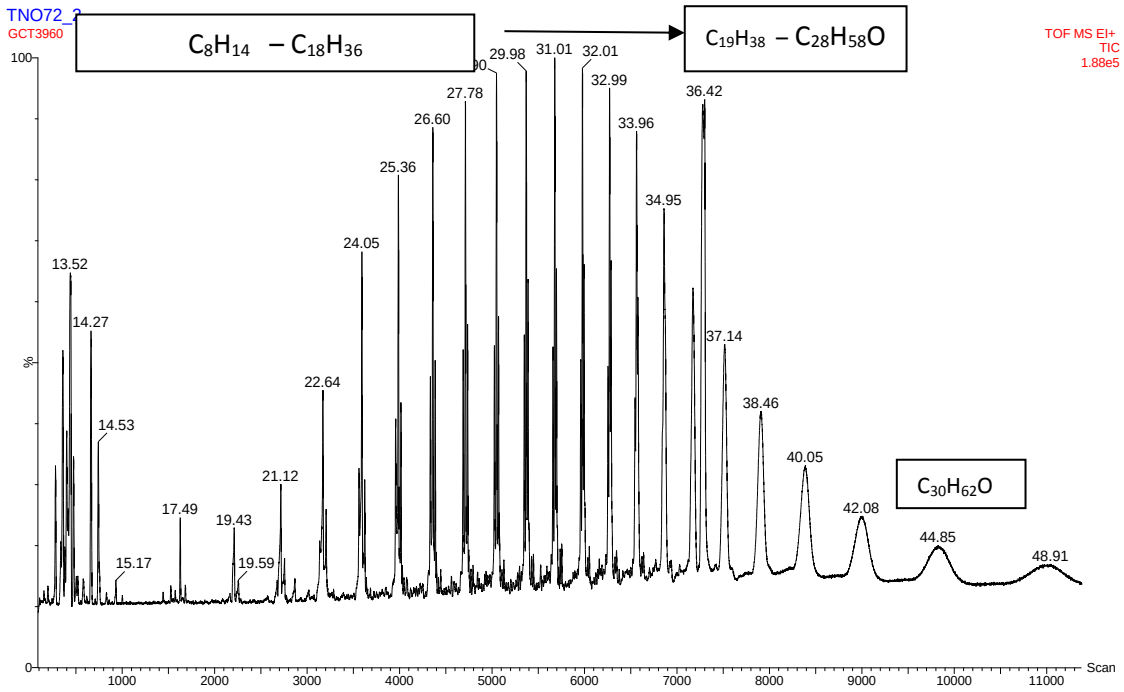

Figure 78: GC-MS results for wax sample produced from Gr feedstock under run conditions of 550°C – 16L.min^{-1}.

The most significant components and peaks identified with GC – MS analysis for all the above mentioned wax samples produced under different pyrolysis conditions and from different feedstocks are summarised in Table 26 including the relative area percentage. From this Table, key observations can be drawn:

- Higher residence time yields higher percentage of lower and medium molecular weight hydrocarbons with a respective reduction in the hydrocarbons > C_{21}, which is indicative of more severe thermal or secondary cracking,
- Lower residence time yields lower percentages of lower and medium molecular weight hydrocarbons with a respective increased percentage of hydrocarbons > C_{21} which shows that less thermal cracking primary and secondary has taken place.

The presence of alkenes in all of the GC – MS analysis components is indicative of thermal pyrolysis due to the fact that less termination reactions and β- scission take place thus increasing the unsaturated hydrocarbon content in the final product (Gao 2010) (Zeaiter 2014). With increasing residence time it can be seen that heavier components C_{18} –C_{26} decrease favoring the production of lighter hydrocarbons in the range of C_{10} –C_{15} where there is an observed increase in the respective percentages moving from a residence time of 1.81s to 2.23s. This could be explained with thermal cracking of heavier components via secondary reactions and cracking related with increased residence time.

5.4.6 Viscosity

To analyse and test the flow characteristics of the wax blends as well as the pure solid wax sample the three samples were tested in the rheometer. The wax samples are in solid state when in ambient temperature and have a soft consistency with a yellow towards brown colour. At temperature around 50 – 60^{o}C they start softening, eventually melt and have a liquid consistency from > 60^{o}C. The standard method for calculation of kinematic viscosity of diesel, transparent is ASTM D445/ISO 3104 which determines the reference temperature to measure kinematic viscosity at 40°C since this is used as the basis for the ISO viscosity grading system (ISO 3448). For the oils that do not have proper fluid characteristics at 40°C the option of 60°C can be used and for petroleum wax 100°C is used. The results for the pure sample as well as the blends are presented in Table 27. Furthermore, tests on pure wax samples were added and the results are also discussed in terms of change in viscosity.

The results presented in Figure 79, are for a wax sample produced from Cr feedstock and comparative 5 wt.% and 10 wt.% blends with diesel. At every temperature step 10 measurements were obtained. At 60^{o}C viscosity values ranged from 1 – 16 Pa.s. With temperature increase the values dropped up to 0.0075 Pa.s at 80^{o}C indicating that the pure wax sample becomes less viscous with temperature increase.

At 100^{o}C viscosity values appeared to be increasing significantly however this can be related to loss of volatile components in the sample is also supported from observations in DSC apparatus and seta flash point value for wax at 108^{o}C carried out in an external testing laboratory (Services 2015) and therefore should not be taken into consideration in connection to the accuracy of viscosity values at that temperature.

Table 27: Summary of viscosity results for pure wax sample and blends with diesel at different temperatures.

Viscosity / Sample	Pa.s (60^{o}C)	Pa.s (65^{o}C)	Pa.s (70^{o}C)	Pa.s (75^{o}C)	Pa.s (80^{o}C)
Pure wax	2.5000	0.5000	0.03500	0.02000	0.0075
5% wax w/w with diesel	0.00200	0.00175	0.00175	0.00175	0.00160
10% wax w/w with diesel	0.00150	0.00150	0.00137	0.00130	0.00120

The same method was applied to the blend of the wax sample with diesel 5% in 95 % USDL diesel w/w. Viscosity values at 60ºC viscosity were lower than the pure wax sample with a strong coherence at 0.002 Pa.s. With temperature increase the values dropped up to 0.00175 Pa.s at 80ºC showing a similar though with a smaller value effect variation with the pure wax sample.

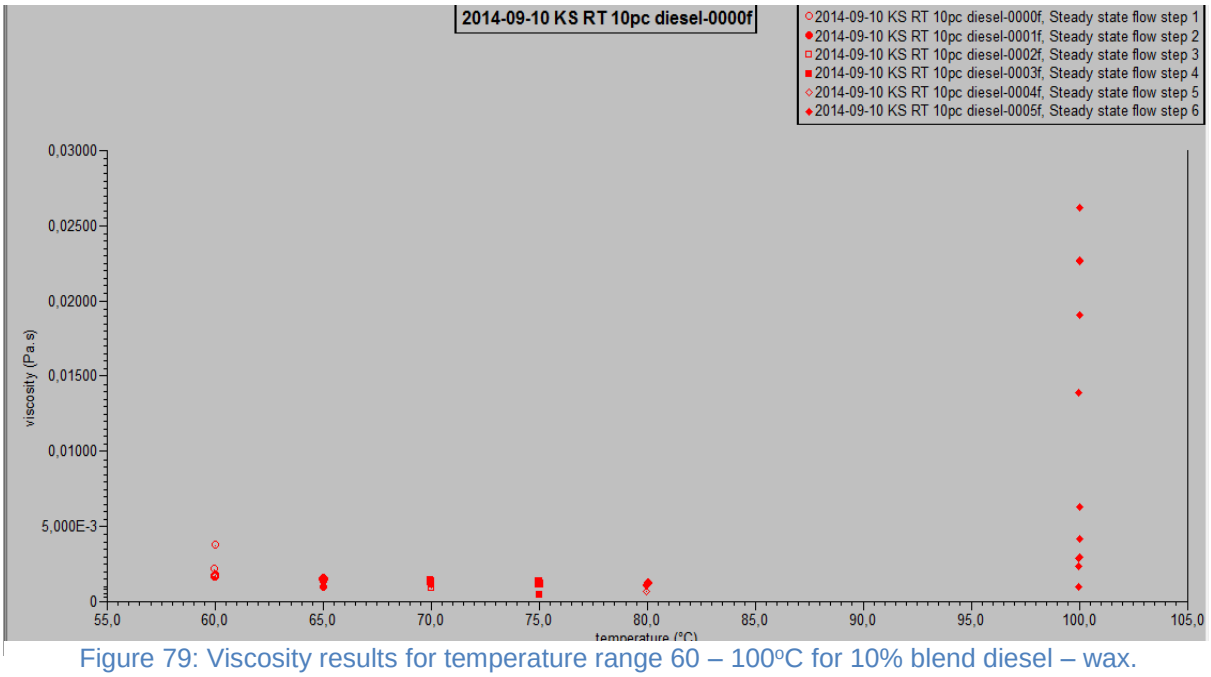

Figure 79: Viscosity results for temperature range 60 – 100ºC for 10% blend diesel – wax.

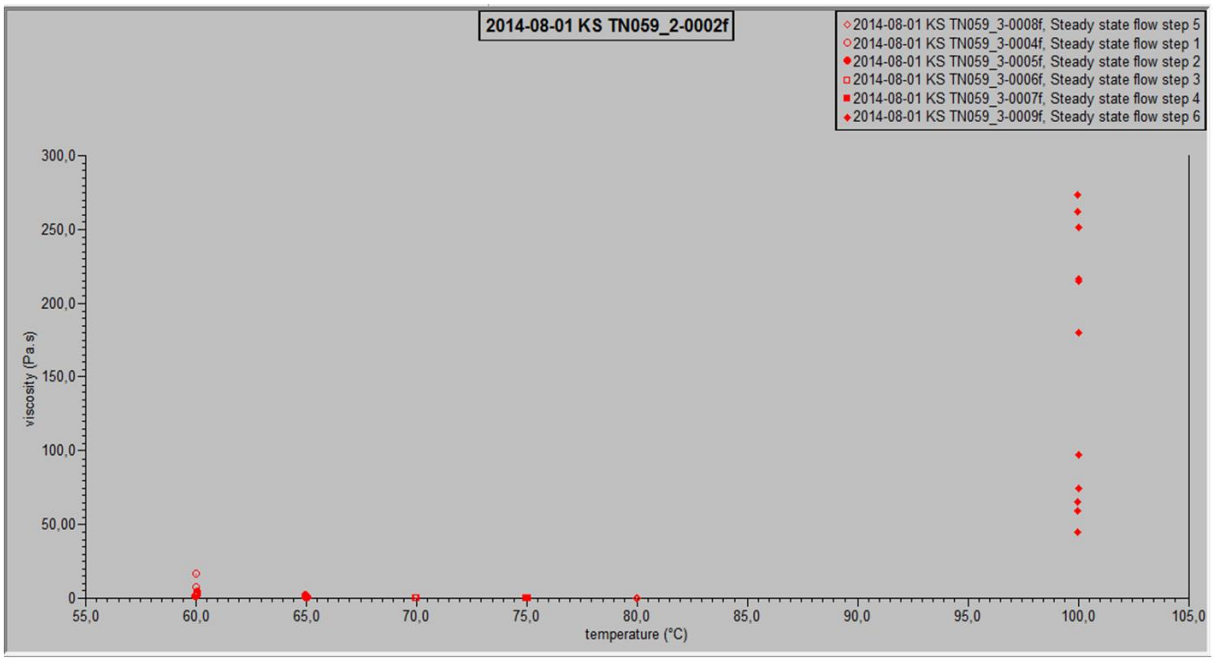

Figure 80: Viscosity measurements for temperature range 60ºC – 100ºC for pure wax sample.

By using the same method four more samples were analysed in their pure state from different experimental conditions that were expected to have different consistencies and viscosity values. The aim for the sample selection was to detect any change in viscosity when the wax was produced under different reaction conditions and see how these affected the viscosity values with increasing temperature.

The wax samples were produced from both Gr and Tk feedstocks and exhibited a significant difference in the reported melting point values. These wax samples were produced from the following feedstocks under the referred pyrolysis conditions: Tk, at 550.0^{o}C and 20 L.min^{-1}, Gr at 530.0^{o}C and 18 L.min^{-1}, Tk at 500.0^{o}C and 16 L.min^{-1}, Gr, at 500.0^{o}C and 16 L.min^{-1}. All of these samples have, also been analysed for their density values and the results are presented in comparison with their average melting point value in §5.4.7.

In Table 28, the summarised results for the viscosity values are presented for all the tested temperatures. Indicatively, in Figure 81 and Figure 82 the viscosity results for two samples are shown in the graphs for the tested temperature steps.

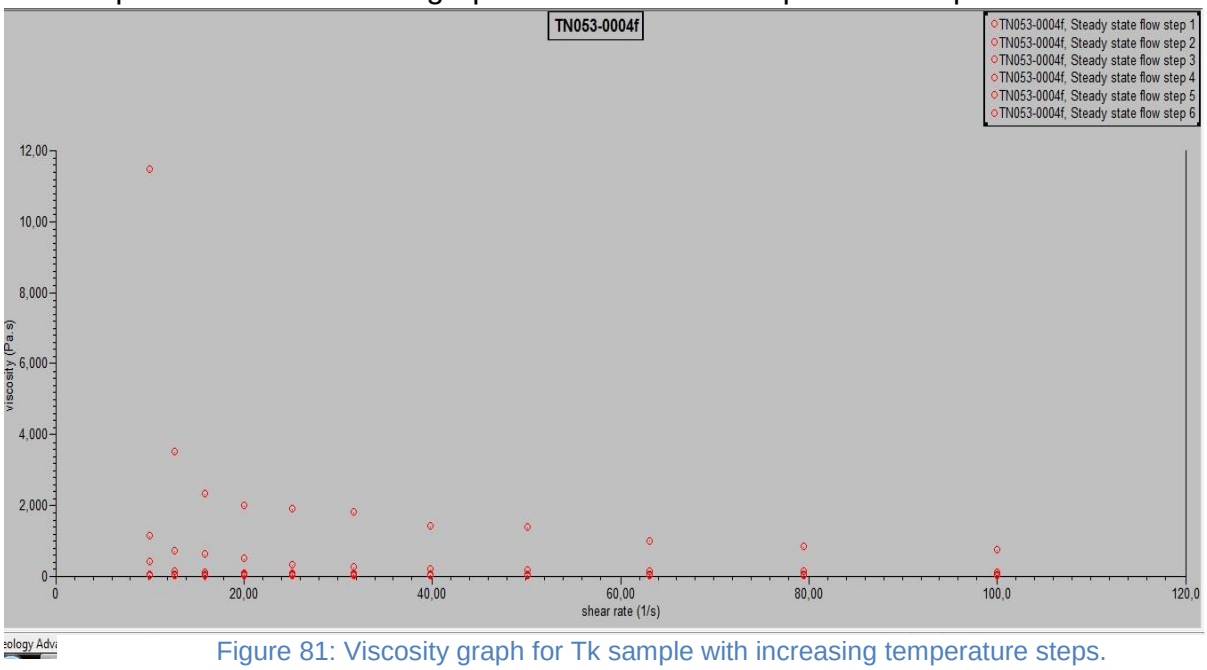

Figure 81: Viscosity graph for Tk sample with increasing temperature steps.

As it can be seen from Figure 81, a similar pattern of decreasing viscosity with increasing temperature appears for Tk feedstock with the only difference being that at 100^{o}C point there is no disturbed distribution of the values as previously observed in Figure 80.

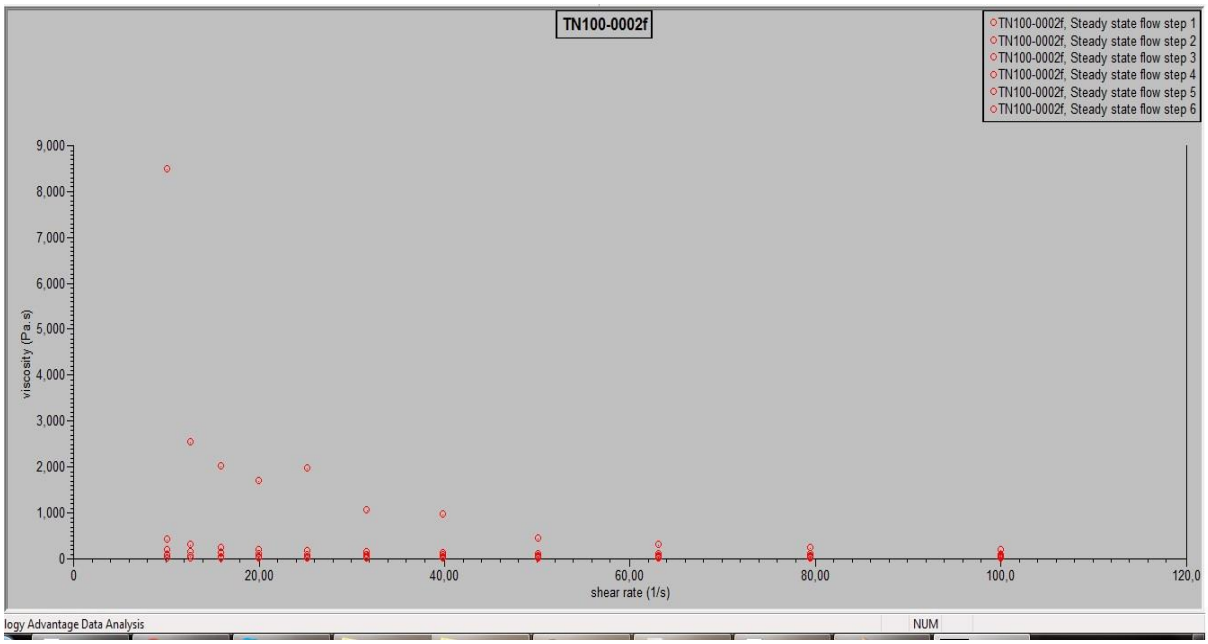

Figure 82: Viscosity graph for Gr feedstock with 5^{o}C temperature increment.

From the above graph and for Gr feedstock a consistent behaviour of the sample can be observed similar to the observations made for Cr and Tk feedstocks before. A summary of all average viscosity values is given in Table 28 below. The average value was calculated from ten point measurements for each temperature step.

There is a considerable difference between the measured viscosities of Tk sample at 40^{o}C produced at different conditions. When the sample was produced at lower residence time (Tk, 1.74s) it resulted in a more viscous wax that the one produced at higher residence time (Tk, 2.27s) which is expected. This coincides with a significant difference it their respective melting point values in Table 29.

Table 28: Viscosity values at different temperatures for Tk and Gr feedstocks.

Sample	Pa.s(60°C)	Pa.s(65°C)	Pa.s(70°C)	Pa.s(75°C)	Pa.s(80°C)	Pa.s(100°C)
Tk (550°C,1.74s)	2.5640	0.3789	0.0874	0.0236	0.0097	0.0048
Gr (530°C,1.98s)	1.1660	0.1491	0.0190	0.0074	0.0062	0.00645
Tk (500°C,2.27s)	1.2213	0.1142	0.0339	0.0116	0.0061	0.0036
Gr (500°C,2.27s)	1.8013	0.1683	0.0821	0.0278	0.0093	0.0041

Viscosity is a parameters, affected from the inter – molecular forces in the material and therefore affected directly from the molecule shape. Such an effect is not consistent as expected for the Gr feedstock where the opposite observations can be made at 60°C the wax produced at higher residence time (2.27s) shows the higher viscosity values. Decreasing viscosity values are consistent for all samples but for the Gr feedstock the lower viscosity does not coincide with the lower melting point value and the change between the 60°C and 100°C steps is more dramatic for Gr which was again for the wax sample produced at higher residence time (2.27s). Syamsiro et al., reported similar range values (0.001739 – 0.0023 Pa.s) for the viscosity of the liquids produced from pyrolysis of PE bags and Miandad et al. measured viscosity values of

0.00177Pa.s with a density of 0.92g.cm^{-3} from the batch pyrolysis of PS at 450^{o}C (Syamsiro, Saptoadi et al. 2014, Miandad, Nizami et al. 2016). When comparing the results with other studies Lopez et al., found that liquids produced at lower reaction temperature (460^{o}C) produced more viscous liquids(López, de Marco et al. 2011).

5.4.7 Density

Fuel Density was measured for wax sample produced from Cr feedstock under pyrolysis conditions (530^{o}C reaction temperature and 18 L.min^{-1} nitrogen flowrate). The measurement was carried in ambient temperature (23^{o}C) with a pycnometer and water as the reference substance. Density was calculated to 0.6988 g/mL or 698.80 kg/m^{3} whereas the average density diesel values for density is: 833 at 15 ^{o} C (ISO3675). In addition, with the method described in §3.4.8 additional measurements for density were taken for the following samples that represented a variety of different feedstocks and run conditions and the results including density as summarised in Table .

The aim was to detect any changes in the density of the sample that would reflect change in composition and viscosity due to alteration of the run conditions. However, for the Tk feedstock with the results in the first two rows of it is shown that the sample with the lowest melting point value has the higher density.

For Tk sample, although the viscosity is lower for the higher residence time (500^{o}C, 2.27s) the density shows slightly lower values for the sample produced at the higher reaction temperature and lower residence time. This could be attributed to the thermal cracking of heavier components resulting in a lighter sample. The same effect applies

to Gr feedstock where the thermal cracking effect appears to impact both density values.

Table 29: Density measurements for Tk and Gr feedstocks from different experimental conditions.

Parameter / Sample	Density (g/cm^3)	Standard deviation (g/cm^3)	Melting point (°C)
Tk (550°C, 1.74s)	0.9076	0.0021	72.33
Tk (500°C, 2.27s)	0.9154	0.0011	62.50
Gr (530°C, 1.98s)	0.8908	0.0004	67.50
Gr (500°C, 2.27s)	0.9089	0.0005	59.75

5.4.9 FTIR spectra on product fuel samples

A complementary method to evaluate the solid wax samples and detect any acidic functional groups such as carboxylic acids was attempted via FTIR and could be used as a faster screening method to detect any changes in fuel – wax composition.

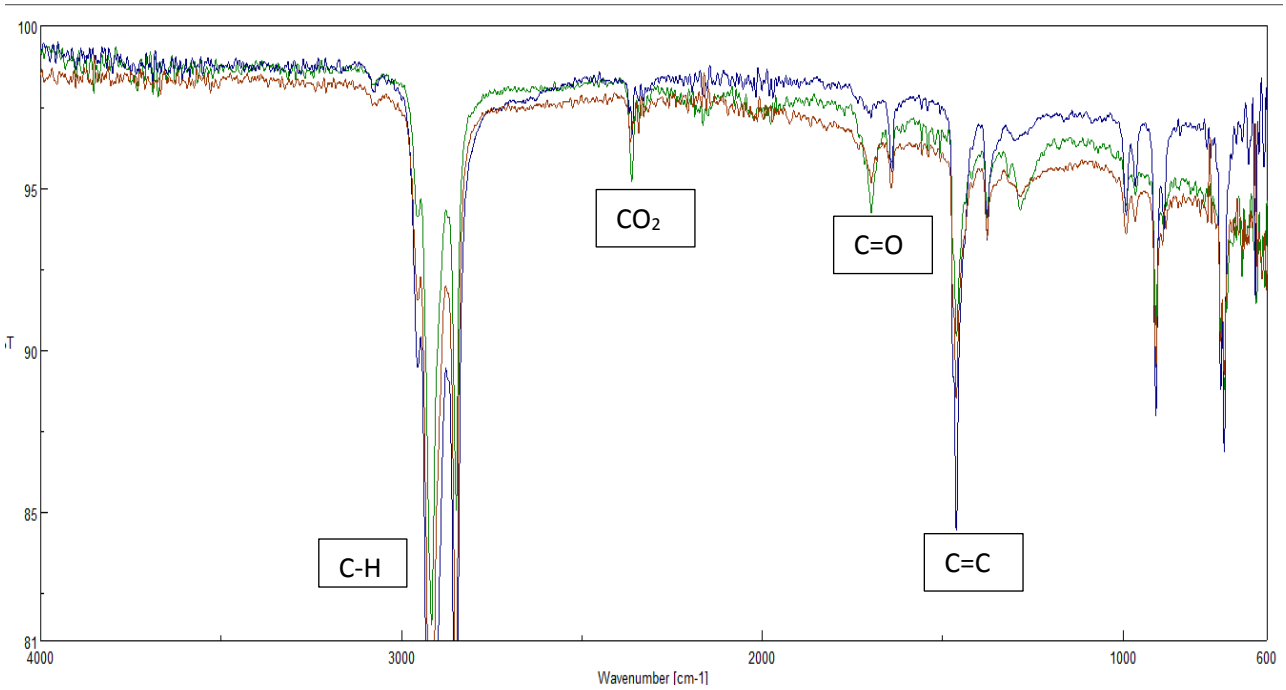

Figure 83: FTIR spectra for wax samples produced from Tk feedstock under different pyrolysis conditions and reactor setups: Green (550°C, 26L.min-1), Blue (530°C, 26L.min-1), Brown (530°C, 20L.min-1).

Figure 83, shows that the comparative results for three different samples, produced from Tk feedstock under different pyrolysis conditions. The intensity of the peak is different for all samples in the region of 2800 – 3000 cm^{-1} wavenumber where the C - H stretch functional group appear (Banar, Akyıldız et al. 2012). The aromatic C=C ring stretch appears in the region of 1500 – 1600 cm^{-1} wavenumber where only one sample has the strongest peak (green colour) whereas in the region of 1650 – 1700 cm^{-1} the strong peak of alkene C=C appears. Two samples have peaks in that region. At 2350 – 2360 cm-1, presence of carbon dioxide is detected and two samples (brown and green) appear to have peaks in this region. This method could be utilised in the future for quick recovery of initial results. The key functional groups and the relative regions that are relevant for the wax sample analyses have been identified and included in Table 29.

Table 29: Basic functional group identification with respective wavenumber (cm^{-1}) from FTIR spectra.

Wavenumber (cm^{-1})	Peak type	Functional group
700 – 800	strong	C – Cl stretch
835	-	C – H stretch
1460 – 1470	Weak	C – H deformation
1500 – 1600	-	Aromatic, C=C ring stretch
1602	Strong very sharp	Polystyrene
1650 – 1700	Strong	Alkene, C=C ring stretch
1700 – 1730	Strong	Carboxylic acids, C=O ring stretch
2100 – 2150	-	Terminal alkynes, C – H stretch
2150 – 2250	-	Non terminal alkynes, C – H stretch
2200 – 2270	Weak	Nitriles, C – N stretch
2350 – 2360	-	Atmospheric CO_2
2800 – 3000	-	C – H stretch C – H deformation

Carboxylic acids and aromatic components that have been identified in the wax components can be viewed in distinctive wavenumbers in the spectra as well. For

example from in the aromatic ring region (C=C ring stretch) peaks at different intensities can be identified for all wax samples from Figure 83 but for the C=O stretch only the green and brown spectra have identified peaks indicating less acidic components for the wax sample produced under pyrolysis conditions of 530^{o}C, 26L.min^{-1} in the blue colour.

5.5 Statistical analysis of melting point results with the Taguchi method

For the three melting point measurements per sample and the calculated average value the results were also processed using the Taguchi design method of experiments for LDPE and Tk. Two signal values were chosen (temperature and flowrate) which were the controlled variables of the pyrolysis process. The levels for each factor were three identified for both signal values:

1. Temperature (500^{o}C - 530^{o}C - 550^{o}C) and,
2. Flowrate (16 – 18 – 20 L.min^{-1}).

The response of this process was selected as the melting point value. The signal to response ratio was selected as the smaller the better since the objective of the project is to produce a sample with a lighter molecular weight which corresponds to lower melting point values. In Figure 84 to Figure 85, the main effect plots for data means for both selected factors are shown. Each graph, plots the response mean for each factor level and connects all levels by a line. The lowest observed value corresponds to the subsequent optimal process conditions. When the line in the produced graph in not horizontal it means that a main effect is observed which translates into that process

parameter actually affecting the process output. The more vertical the line the greater the effect of the main observed. In Figure 84, it can be observed that the smallest signal to noise ratio is for 500°C and for the 16 L.min^{-1} flowrate. This finding coincides with the actual lowest measured value for LDPE which was at the same conditions and was 58.00°C. Furthermore, the effect of the flow rate from the processed results appears to have the most significant effect in the response of the experiments.

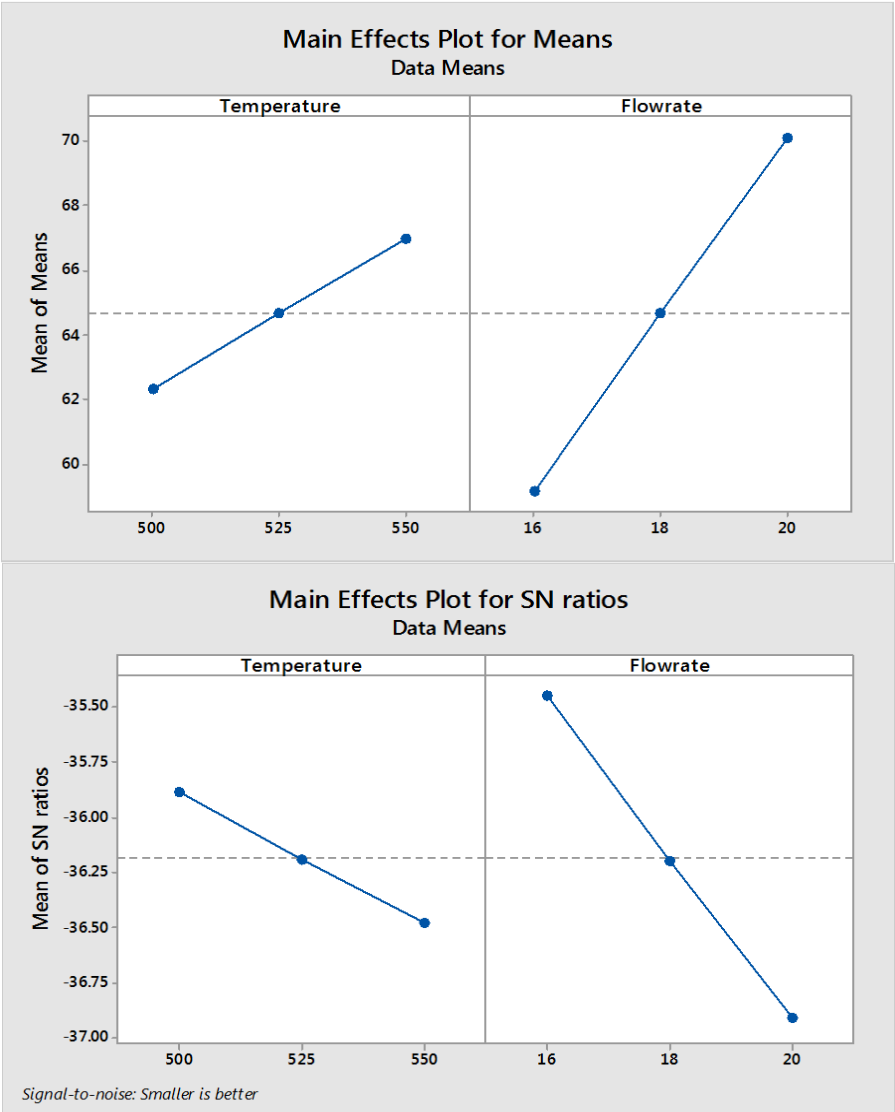

Figure 84: Taguchi results for LDPE: temperature and flowrate with melting point.

From Figure 85, for the Tk results it can be observed that the smallest signal to noise ratio is for 500^{o}C and for the 16 L.min^{-1} flowrate both of which should be considered the optimal design conditions. However, this finding is contradicting with the actual lowest measured value for Tk which was 550.00^{o}C and 16 L.min^{-1} flowrate. It would be expected at the higher temperatures more cracking of the polymer chains to occur thus producing a lighter product.

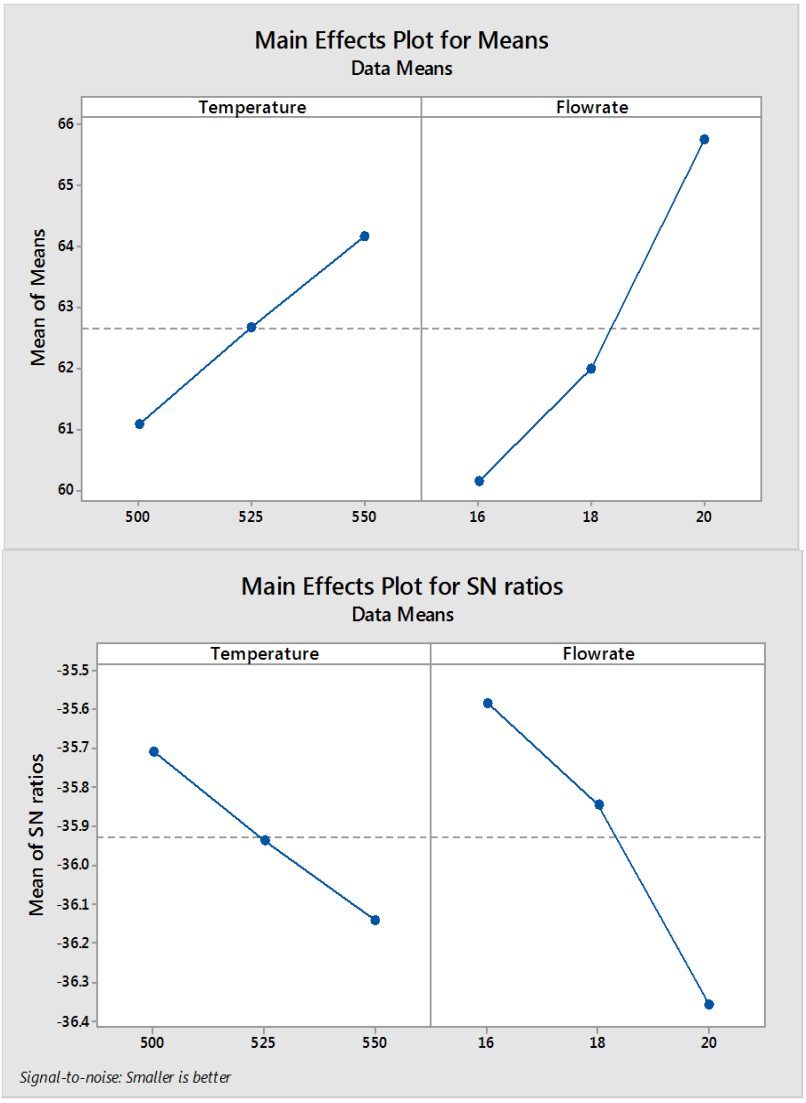

Figure 85: Taguchi results for Tk: temperature and flowrate with melting point.

Apparently, when taking into consideration the average of the averages the optimal area is within a different temperature range. Furthermore, the effect of the flow rate from the processed results appears to have the most significant effect in the response of the experiments which is the case as well with LDPE thus strengthening the observation that residence time via control of the flowrate is the driving factor in the quality of the product. This can be observed from both graphs. The plotted graphs for Gr feedstock are given in the Appendix C.

5.5.1 Effect of temperature

Temperature, is one of the main process parameters in the pyrolysis process which has been both studied and severely reported to have a significant impact and effect through thermal cracking both on fuel quality and composition but also on the mass balance and product yields however through the current study temperature had a varying effect on different feedstocks and optimal conditions were different for different feedstocks. In addition the impact on actual mass balance due to the variability of the feedstock could not be quantified. Specific optimal conditions have been identified for all feedstocks. As a result, of the experimental outputs and the processed results with the Taguchi method in the previous section temperature has been found to have an effect in the means plot. Both for LDPE and Tk the optimal process temperature was identified as the 500^{o}C and for Gr the 550^{o}C value.

5.5.2 Effect of flowrate

Although, flowrate and subsequently residence time has been reported to have an effect on the actual fuel quality and composition identifying the optimal conditions for the specific studied feedstocks with the current fluidised bed reactor setup was one of the main achievements of this section. In addition to that but for the particular analysis residence showed the strongest correlation to actually reducing the melting point and affecting the fuel composition through the Taguchi analysis. In contrast to, the effect of temperature that was variable depending on the feedstock flowrate produced consistent response across all feedstocks with the optimum value being 16 $L.min^{-1}$ and has been shown to have the most significant effect due to the steepness of the slope from the produced graphs. Furthermore, understanding and quantifying how to drive the optimisation of the process in terms of fuel quality were a secondary gain as well as considerations to include for further improvement in the design.

5.6 Results and discussion

5.6.1 Correlation of melting point with average chain length – melting point curve

After completing the set of experiments, comparing these against the melting point curve and linking the outputs with and an average carbon chain length in previously compiled melting point curve can illustrate the actual effect of the optimal process conditions in terms of improving and moving the average feedstock composition along the curve. The actual shift achieved within the operating limits of

the equipment is visually depicted in Figure 86, for the wax samples produced from the three feedstocks. Analytically, the arrows shown, relate to the feedstocks that were used in the pyrolysis process using the experimental conditions described in steps 1 - 3 to produce wax samples. The melting point values of these samples are relating to the shift depicted in Figure 86. The experimental conditions were:

1. LDPE has a shift of 9.00^{o}C in total moving from 67.00^{o}C (highest melting point at 550^{o}C and 20 L.min^{-1}) down to 58.00^{o}C (lowest melting point at 500^{o}C and 16 L.min^{-1}). This change corresponds to moving from a hentriacontane ($C_{31}H_{64}$ – melting point range of 67.00 – 69.00^{o}C) hydrocarbon chain length to heptacosane ($C_{27}H_{56}$ – melting point range of 58.00 – 60.00^{o}C).
2. Tk has a shift of 14.05^{o}C in total moving from 72.30^{o}C (highest melting point at 550^{o}C and 20 L.min^{-1}) down to 58.25^{o}C (lowest melting point at 500^{o}C and 18 L.min^{-1}). This change corresponds to moving from a tritriacontane ($C_{33}H_{68}$ – melting point range of 71.00 – 73.00^{o}C) hydrocarbon chain length to heptacosane ($C_{27}H_{56}$ – melting point range of 58.00 – 60.00^{o}C).
3. Gr has a shift of 9.90^{o}C in total moving from 67.50^{o}C (highest melting point at 530^{o}C and 18 L.min^{-1}) down to 57.66^{o}C (lowest melting point at 550^{o}C and 16 L.min^{-1}). This change corresponds to moving from a hentriacontane ($C_{31}H_{64}$ – melting point range of 67.00 – 69.00^{o}C) hydrocarbon chain length to hexacosane ($C_{26}H_{54}$ – melting point range of 56.00 – 58.00^{o}C).

Although, the biggest shift is observed for the Tk feedstock, noticeable shifts in the melting point are observed for the other two feedstocks as well moving down in the curve from four up to six stages.

This is a significant accomplishment although still away from the initial target to move towards the diesel range of hydrocarbons which is a range from $C_{10}H_{20}$ up to $C_{15}H_{28}$. Within the current reactor setup and process conditions the limits along to which the optimisation possibilities could be explored have been exhausted.

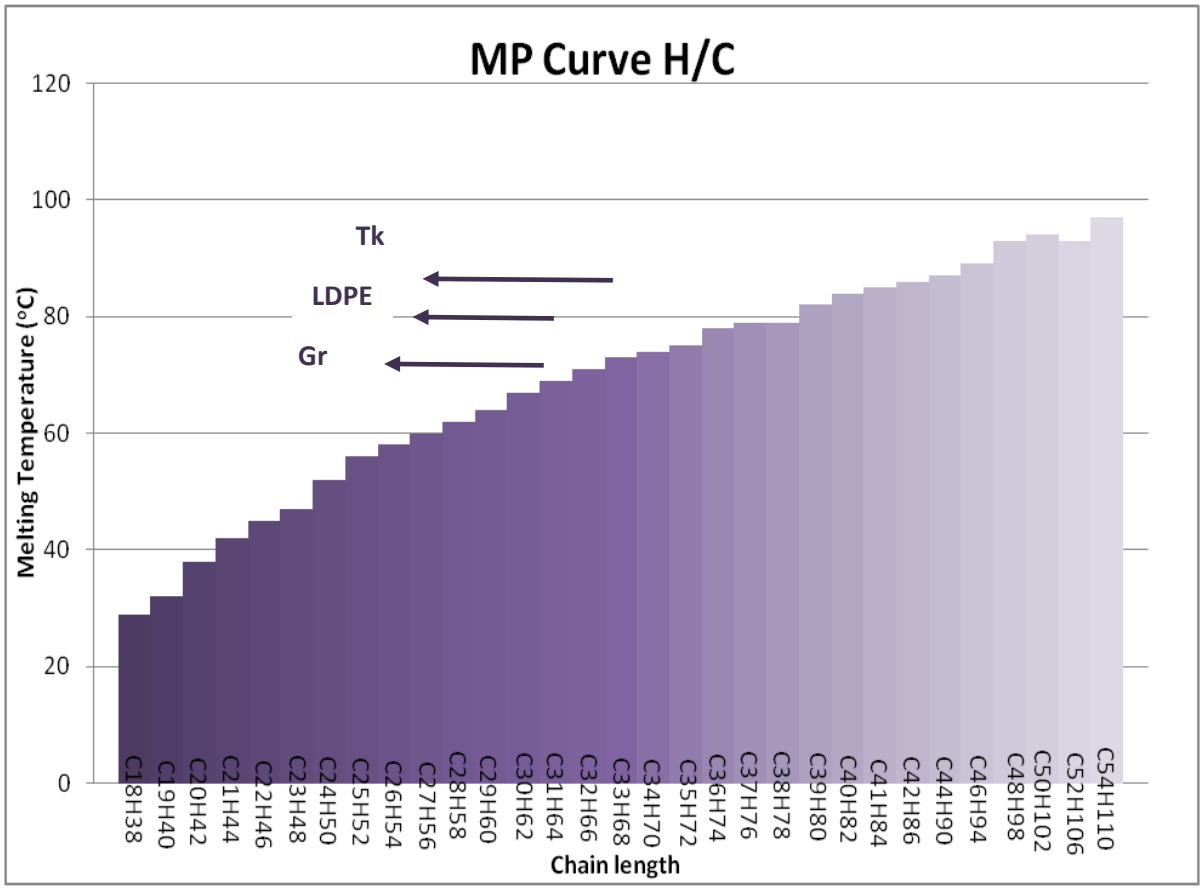

Figure 86: Comparison of process conditions with melting point curve.

Key areas to investigate further for improvement are, increasing the residence time with a variety of works that will be commented in future work suggestions or secondly with the use of catalyst in a fixed catalytic bed that was manufactured.

True boiling point distribution

Using the simulated distillation software with gas chromatography described in §3.4.7 the true boiling point range was obtained for the Tk sample produced under

optimal conditions of 500°C and 18 L.min^{-1}. From the distilled cumulative fractions yields were: 8 vol%, 45 vol% and 99 vol% at respective temperatures of 179°C, 334°C and 500°C. These yield reflect the recovered yields for light naphtha compounds (8 vol % at 179°C), diesel range fractions (37 vol % at 334°C) and heavy fuel oil (55 vol % at 500°C). Any future fuel upgrading method would have to shift this curve towards lighter distillate fractions and reduce the yield of the heavier fractions which would have a corresponding effect in the viscosity values of the fuel, thus reducing it (Hart 2014).

5.6.2 Optimal process conditions for the studied feedstocks

In Table 30 the summary of the outcome from the initial design of experiment is provided in terms of the lowest yielding melting point conditions for all samples. Two of the studied feedstocks, LDPE and Tk, are in the lower end of the reactor temperature whereas, Gr is in the upper limit of the reactor thermal conditions. All samples, are illustrating the lowest melting points for the lower flowrates and higher residence times. Also for Tk the results for the second lowest melting value at 550°C and 16L.min^{-1} with a melting point value of 58.66°C are very close with the value shown in Table 30.

Table 30: Optimal process conditions with relation to melting point for LDPE, Tk, Gr.

Temperature / **Residence time**	500°C	530°C	550°C
16 L.min^{-1}	**LDPE (58.00°C)**		**Gr(58.33°C)**
18 L.min^{-1}	**Tk (58.25°C)**		
20 L.min^{-1}			

5.7 Conclusions

Identifying the driving process factor in relation to the optimisation of the fuel quality and the subsequent effect this has on the process overall yield and mass balance was the main objective of the current study. Residence time has been identified as a factor with a very strong correlation and in combination with temperature has resulted in sufficient results. The produced fuel is in a wax state with melting points starting from as low as 60^{o}C. In order to further improve the quality and composition the focus needs to be on increasing residence time either by controlling the flowrate, the feed rate or increasing the total length of the reactor. Additional considerations include use of catalyst either inside the reactor bed or in a secondary downstream fixed catalytic bed. The latter is considered for future work suggestions. A more in depth understanding of the produced main fuel qualities and characteristics and the effect of altering reactor parameters this had has also been achieved.

Chapter 6

Catalytic study for fuel upgrading

6.1 Catalyst suggestions

Incorporating a catalyst in the existing pilot system was given serious consideration following the completion of the experiments and investigation on optimisation of the fuel. Even though, specific achievements have been completed all produced fuels were in solid state and could not be used for the original intended use in an internal combustion engine. Catalytic upgrading of the wax fuel produced under the optimal conditions, was the next step in selectively improving the qualities of the fuel. Both in situ and secondary downstream positions of the catalyst were considered. To avoid coke deposition and poisoning of the catalyst, it was decided to construct a secondary fixed catalytic bed reactor that would be positioned downstream in the vapours direction towards the condensers after the hot vapours filter (HVF) in the reactor (operating temperature 490^{o}C). In order to perform any tests faster a down scale version of this catalytic bed was constructed in collaboration with University of Birmingham and commissioned in the Chemical Engineering department. Details for the scale and design of the reactor are provided in section 6.3.

As a result of the literature review acid based zeolite catalysts like ZSM – 5 and HZSM – 5 that have been studied extensively, have been proven to have little effect on actually improving the characteristics of the liquid product in terms of its average

carbon number distribution, viscosity and melting point. They had however a positive impact on further cracking the heavier hydrocarbon molecules towards lighter gas products thus reducing the overall liquid yield (Marcilla, Gómez-Siurana et al. 2007, Artetxe, Lopez et al. 2013, Al-Salem, Antelava et al. 2017).

Taking into account, that the objective of the current project was to improve the quality characteristics of the liquid product rather than diminish it; hydro treating catalysts such as NiMo and CoMo were considered instead, to promote hydrogen transfer reactions and created saturated hydrocarbons of lower molecular weight with an expected reduction in the resulting viscosity values (Ateş, Miskolczi et al. 2013, Bezergianni, Dimitriadis et al. 2014, Hart 2014). In addition, acid doped zirconia pellets (ZrO_2) were also considered for their reported vis – breaking and depolimerisation properties resulting in increased saturated hydrocarbons (Jing, Li et al. 2008). Specific limitations due to costs for commercial reasons, also did not allow to consider specific catalysts for the current study.

6.2 Characterisation of catalysts

The selected catalysts were analysed for the BET surface area and the dimensions and remaining characteristics were provided from the supplier (AkzoNobel). All parameters and characteristics are provided in section 3.6, in Table 16. In addition, a controlled regeneration experiment was carried out for both catalysts under a flow of 5.7% H_2/N_2 with a flowrate of 40ml/min and heating rate of 10^oC/min to heat the catalysts up to 950^oC.The resulting data is shown in Figure 88 and Figure 87.

As shown from Figure 88 and Figure 87, the catalyst mass stabilises for NiMo after 500ºC and for CoMo after 530ºC.

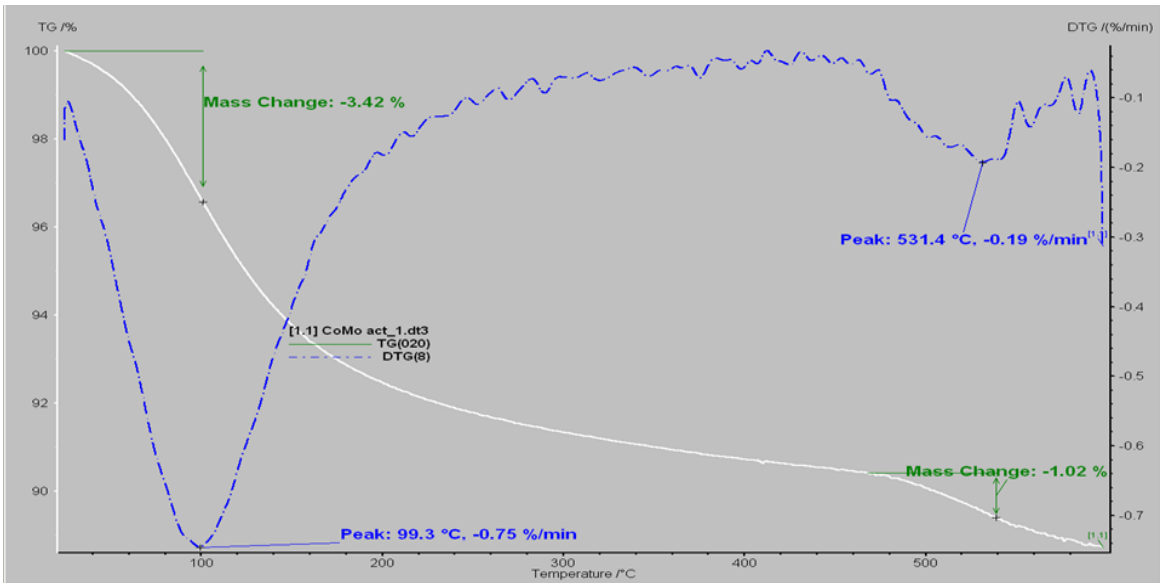

Figure 88: Catalyst reduction for CoMo catalyst.

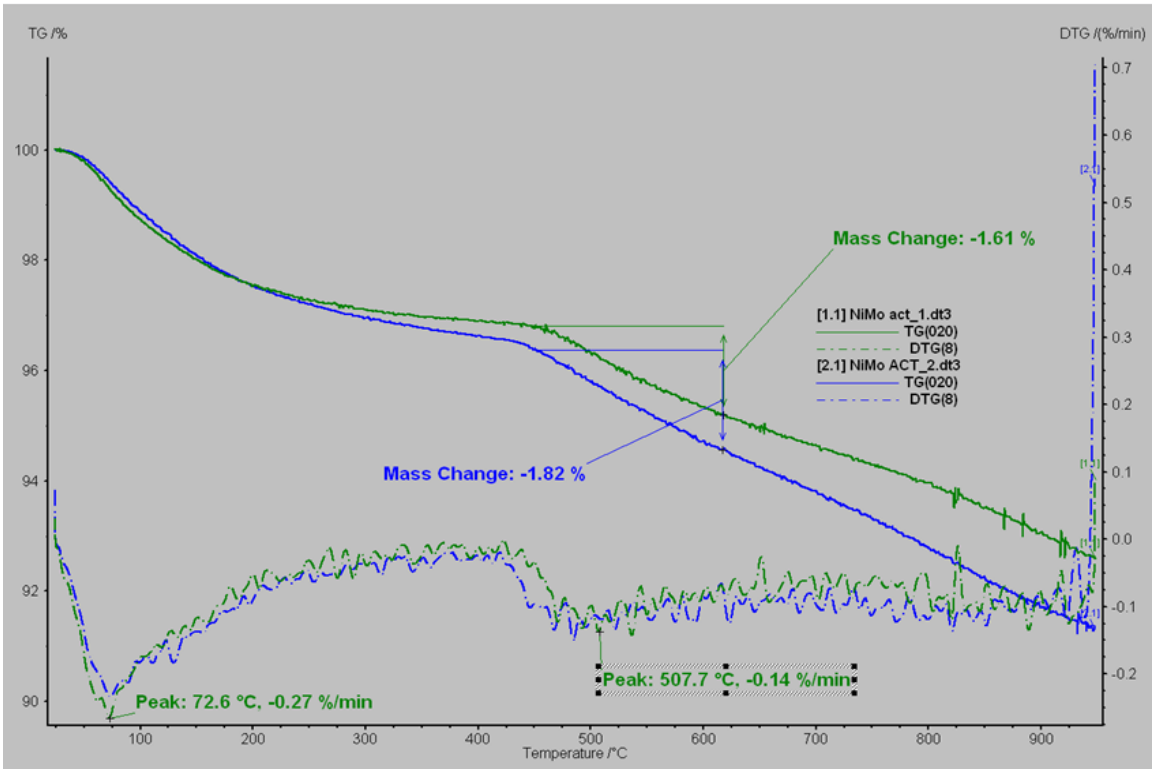

Figure 87: Catalyst reduction for NiMo catalyst.

These values were utilised when designing the activation process for the catalytic fixed bed, where the activation temperatures were taken into consideration for both

catalysts. With the small activated catalyst samples two experiments were run with Tk sample, essentially, in situ, where the pure feedstock and the activated catalyst were placed in the same crucible and heated up to 500^{o}C with a heating rate of 10^{o}C/min. This process was more of slow pyrolysis process however no major shift or effect was observed in terms of thermal decomposition temperature.

6.3 Design of catalytic fixed bed reactor

Following the assessment with the analytical equipment a smaller scale (feed rate of 0.490 g.min^{-1}) fixed catalytic bed was manufactured in School of Chemical Engineering at University of Birmingham to perform tests on the actual wax product. The wax sample was re heated at high temperatures in order to return in vapour state and with a Nitrogen carrier gas to pass through the catalytic bed and down to a water cooled metallic condenser. The concept served for economy of scale and time with the intention to position a fixed catalytic bed downstream after the hot vapours filter (before the condensers) in the actual pilot scale pyrolysis experimental rig once optimal conditions had been established. The temperature at this point would be 500^{o}C. Selection of the position downstream in a secondary fixed bed was considered to enhance the reaction in the vapour phase and avoid coke deposition on the catalyst with potential fast de – activation. Essentially, as a catalytic bed was a stainless steel tube with a suspended container inside at the appropriated height. The suspended container was made of stainless steel mesh.

Using the set fuel feed rate of 0.10 g.min^{-1} and assuming a WHSV of 2 h^{-1}, different lengths of the catalytic bed, were calculated for the two selected catalysts and the longest was selected to accommodate for both trials. The mass flowrate of the sample was calculated assuming a vapour ratio of the fuel of 70 wt.% (from the maximum yields taken from the experiments carried out in the FB reactor).

$$\dot{m} = \text{feed rate} * 0.7 \qquad (6.1)$$

Where:

$\dot{m}$= mass flowrate

0.7 = conversion ratio to vapours

$$W = \frac{\dot{m}}{WHSV} \qquad (6.2)$$

Where:

W = weight of the catalyst

WHSV = Height Hour Space Velocity

$$L_R = \frac{V_R}{A_{cross}}$$

Where:

L_R = the length of the reactor,

A_{cross} = the cross sectional area of the reactor,

And V_R is the required volume of the reactor taking into account voidage, the density of the catalyst and a known diameter of the tube d_R which was 2 cm. The length of the catalytic bed reactor with a diameter of 2cm was:

1. for CoMo L_R= 2.65cm ,
2. and for NiMo the L_R= 2.20cm

To build the reactor the reactor length of 2.65cm was chosen and the pressure drop across the reactor. A schematic and photos of the installed reactor can be seen in Figure 89. A three way valve was installed to allow to switch carrier gases from hydrogen/nitrogen ratio for the catalyst activation to nitrogen for the catalytic experiments. The carrier gas was pre – heated in an oven at 600^{o}C and the connecting piperwork was heated with heater tapes with capacity up to 550^{o}C.

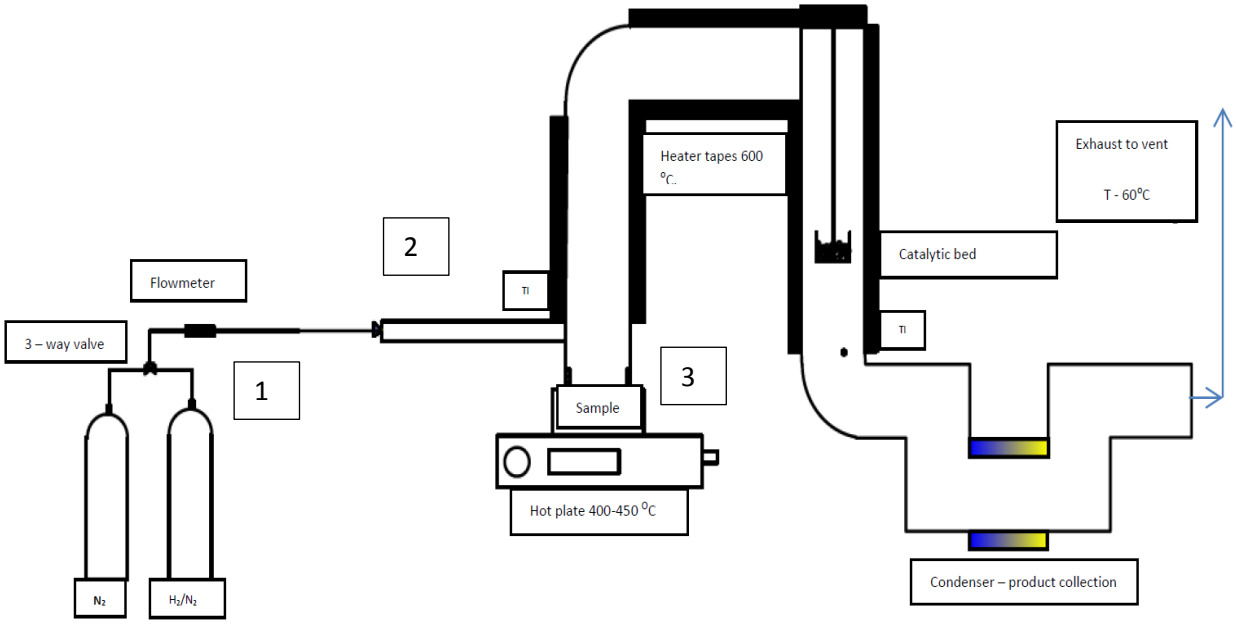

Figure 89: Diagram of the catalytic fixed bed experimental setup: 1) Nitrogen and Hydrogen supply for catalyst activation, 2) pre – heating of the carrier gas in furnace, 3) sample container for re – vaporisation with hot plate and heater tapes.

Finally, the sample container was heated additionally from the bottom with a hot plate that could reach 450^{o}C, and all heated elements were insulated.

Operational issues

Due to a number of issues encountered with the above described apparatus no conclusive results could be derived for the catalytic upgrading. A few of the issues included:

- insufficient heating of the sample not allowing it to vaporise,
- electrical issues with the heater tapes and the furnace leading to tripping of the equipment,
- insufficient heating of the catalytic bed

Based on the observations and lessons from this process a more simple alternative suggestion considered in § 7.2 for future work.

Chapter 7

Conclusions and Future work

7.1 Conclusions

The outcome of the current study, which was focused on obtaining the optimal product from a pilot scale pyrolysis process, utilising a variety of commercial mixed plastic waste feedstocks, was achieved by utilising a fluidised bed reactor and investigating the effect of specific process parameters. With the existing equipment the range of the reactor temperature was between 400 – 670^{o}C. As result a set of defining values for the main process parameters were identified for each feedstock that served as guidelines for a scheduled commercial pyrolysis plant. Based on the outcome, the optimal conditions were established. The optimal conditions were different for each waste stream. After processing the overall results the main factor of the process which had the major effect on improving the fuel quality was identified.

The inherent variability of mixed plastic waste poses not only an opportunity for future development but also a challenge that remains to be fully addressed. Specifically when considering pyrolysis as the main process, the very sensitive response to feedstock variation that will affect the end product needs to be taken into serious consideration when planning a commercial plant that will take into account overall products yields and quality. Variations in the feedstock that are inevitable will change the design,

assumptions and calculation and can alter an expected positive outcome. Therefore characterisation of the Mixed Plastic waste feedstock is crucial, prior to it being introduced in the reactor. In addition identifying and excluding unsuitable plastic materials such as polyvinyl chloride that could produce dangerous chemicals or monitoring polymers with oxygen in their structure that can affect product quality is another significant factor that can be addressed and utilised by their characterisation and quantification. A series of analytical techniques, such as TGA, DSC and FTIR have been employed to thermally decompose and characterise the five different mixed plastic feedstocks and it was possible to identify and quantify the components present in each waste stream. The main components identified included, LDPE, HDPE, PP, PS, cardboard (biomass), PET and aluminium for one feedstock in different percentages. Furthermore, a comprehensive understanding of how cracking temperature and melting phase change can be combined in plastics that might have overlapping decomposition range. Finally, identification of the evolved vapour streams from different feedstocks (in micro scale, mg) has provided the additional proof that the variation in the feedstock results in a varied gas stream which will affect the condensed liquid product. Materials that contain polymers with oxygen in their structure could results in a vapour stream with carboxylic acids affecting the acidity of the product.

All these factors have been taken into consideration during the next stage pyrolysis experiments and fuel analysis especially when considering the reaction temperature range and the minimum limits to achieve maximum conversion. This value was established to be at least above 450^{o}C. Expected yields, including liquid and gas products, from the slow pyrolysis with TGA were a complimentary achievement. Again

feedstock variation affected the mass balance in a scale of up to 17% difference between feedstocks.

From the pyrolysis experiments with the pilot scale fluidised bed reactor very interesting conclusions have been drawn. Firstly, identifying the driving process factor in relation to the optimisation of the fuel quality and the subsequent effect this has on the overall yield and mass balance was the main objective of the current study. As expected, the liquid yields, for example, not only varied between different feedstocks but also within the same feedstock from one run to another (from 4% up to 17%). This is attributed to inherent variation of the mixed plastic waste, however in continuous operation this effect is expected to even out. Adding to these observations the key process parameters studied; reaction temperature and residence time have also had a significant impact on the product quality and overall yields.

Prior to the pyrolysis experiments the product was anticipated to be liquid, however this was not the case since it was in recovered initially in a liquid state and solidified at ambient temperatures with a waxy yellow to brown consistency. This causes an issue when the end application is to burn the product in an internal combustion engine that is designed to run on liquid fuels of specific consistency. Therefore modifying the process parameters to optimise the consistency and quality of the fuel as well as characterising it was set as the immediate goal. A key property of the wax was its melting point which correlates to the carbon number distribution and average molecular weight. Reducing the melting point and characterising the feedstock at the optimal conditions was achieved through residence time variation which has been identified as a factor with the strongest correlation in reducing the average melting point. As result the range of achieved shift (reduction) in the melting point was from 9^{o}C until 14^{o}C

depending on the feedstock. Independent of the feedstock composition analysis of the results proved that increasing the residence time reduced the average melting point of all samples produced from all feedstocks whereas this was not the case for reaction temperature. These observations come in contrast with what was previously reported in literature where reaction temperature was considered to be the factor having the major effect of product yields and quality. A supporting study on the blending potential of the produced waxes with diesel resulted in identifying hydrocarbon components that inhibit the smooth blending of the wax samples. Alcohols, carboxylic acids and alkanes with a molecular formula of Hexacosane ($C_{26}H_{54}$) and above are the compounds that need to be removed, treated or cracked further.

Furthermore utilising the melting point to assess and optimise the fuel quality was not found in any previous studies and positive results were supported from GC – MS analysis and viscosity measurements. The recovered fuel with the existing pilot plant produced an acceptable quality fuel in respectable yields that has the potential to be utilised either for energy generation or further improved.

7.2 Future work

- In order to further improve the quality and composition the focus needs to be on increasing residence time either by controlling the flowrate, the feed rate or increasing the total length of the reactor.

- Additional considerations include the use of a suggested acid based hydrotreating catalyst either, inside the reactor bed or in a secondary downstream fixed catalytic bed.
- Suggestions with regards to the use of catalyst include; suggested position in the vapour stream of the process at a point where temperatures of >450^{o}C are achievable to avoid any heating issues. A secondary downstream fixed catalytic bed is the preferred option to avoid potential issues with catalyst deactivation, poisoning and carbon deposition.
- Product acidity through the presence of oxygenated compounds needs also to be addressed either by introducing neutralising agents in the process or via strict monitoring of the introduced feedstock.
- Blends of the produced fuel with diesel could be an option or alternatively the wax product could be considered and fractional distillation to recover diesel, naphtene and heavy fuel oil fractions.
- Process scale – up of the system is possible when taking into consideration the feedstock variability and the specific process parameters associated with it. Expected differences in the outcome product are another key area that needs to be taken into account when designing an industrial version with the aim to maximise product yield and the recovered gas yields should be considered as an alternative fuel route for utilisation.

Appendix A

Calculation of residence time and effect of flowrate on melting point

Residence time is depended on feedstock flowrate, carrier gas flowrate and the reactor volume (Conesa, Font et al. 1994) . Specifically when the feed rate is constant in a continuous fluidised bed reactor then the carrier gas flowrate and the reactor volume are considered to calculate the residence time using equation A.1.

$$\tau = \frac{V_r}{\dot{V}} \qquad \text{(A.1)}$$

For a variety of different reaction temperatures the change in the gas volume needs to be accounted for therefore different calculations have been completed for the selected flowrates and reaction temperatures. An example of the calculations that were presented in §5.3.2 is provided here:

For reaction temperature of 500^{o}C

Nitrogen flowrate of 16 L.min^{-1} at 20 ^{o}C

The nitrogen density at 500^{o}C (kg/m^{3}) is 0.4356 kg.m^{3}

The nitrogen flowrate at 500^{o}C is 42 L.min^{-1}

$$V_r = \pi * r^2 * h \qquad \text{(A.2)}$$

Reactor volume for a cylindrical reactor bed of Ø 10.16 cm and reactor height of 20.32 cm is calculated using eq. A.2:

V_r = 1.63 L,

Therefore using equation A.1: $\tau = 0.038\,\text{min}$ or $\tau = 2.34\,s$

In Figure 109 the effect of different residence times for two feedstocks is illustrated. For 18L.min^{-1} and for decreasing reactor temperature corresponding to 1.94 to 2.01s residence times and 20 L.min^{-1} and for decreasing reactor temperature corresponding

to 1.74 to 1.81s respectively it can be seen that lower residence times for the higher flowrate correspond to increased melting points that is a clear indication of less secondary thermal cracking taking place which results in an overall higher melting point for both samples.

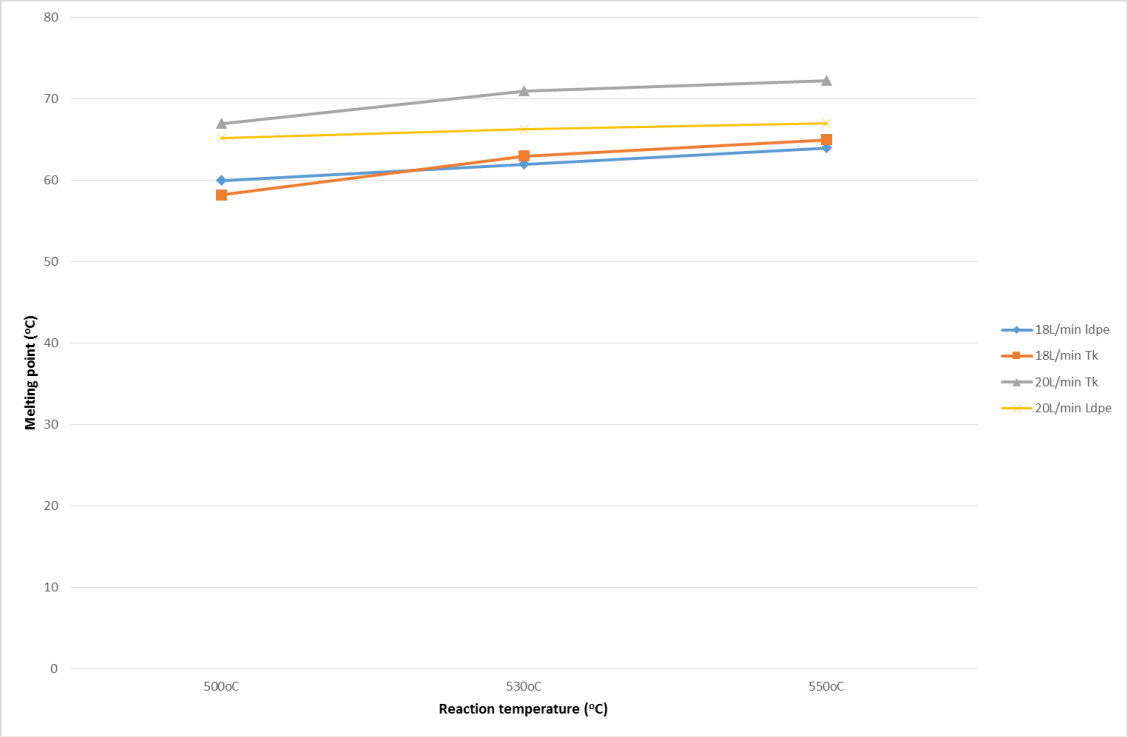

Figure 90: Effect of higher (20 L.min-1) and lower (18 L.min-1) flowrate on average melting point for LDPE and Tk feedstocks.

Appendix B: GC – MS spectra

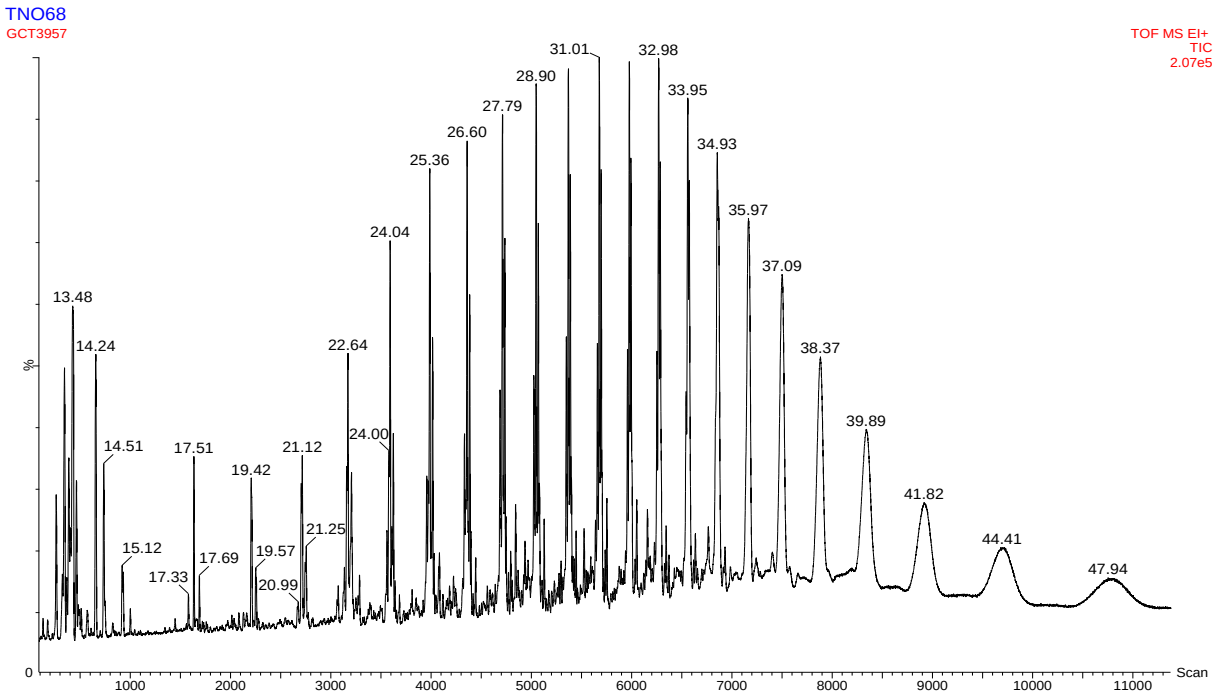

Figure 91: GC - MS spectra for wax sample produced from Tk feedstock under pyrolysis conditions of 530°C and 16L.min-1 flowrate.

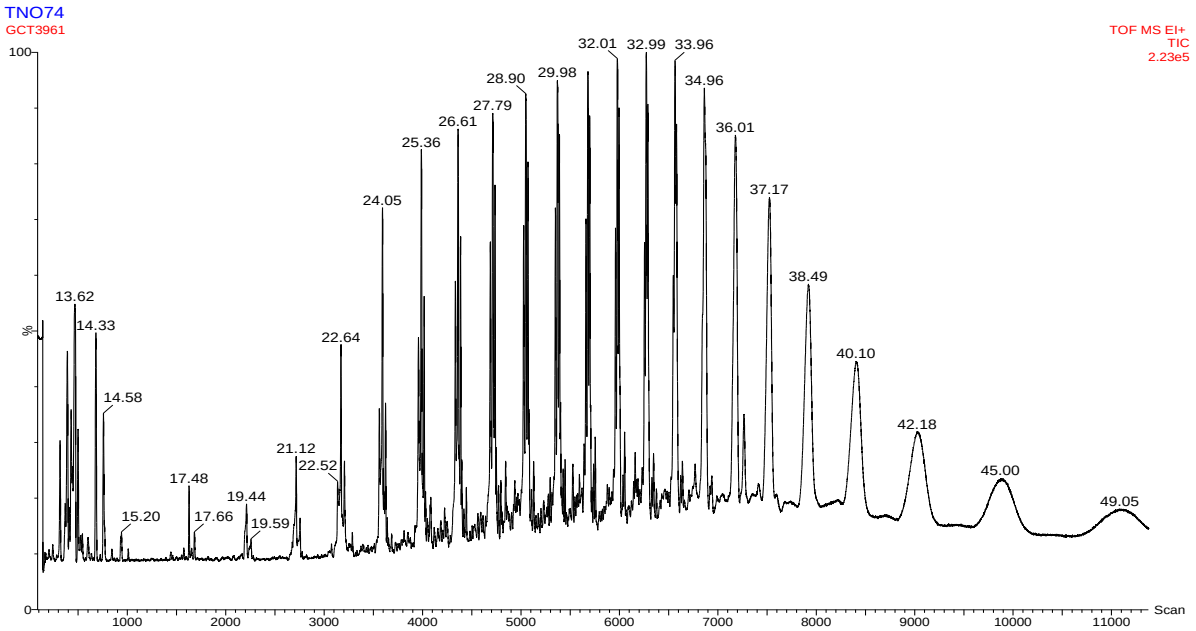

Figure 92: GC - MS spectra for wax sample produced from Tk feedstock under pyrolysis conditions of 550°C and 16L.min-1 flowrate.

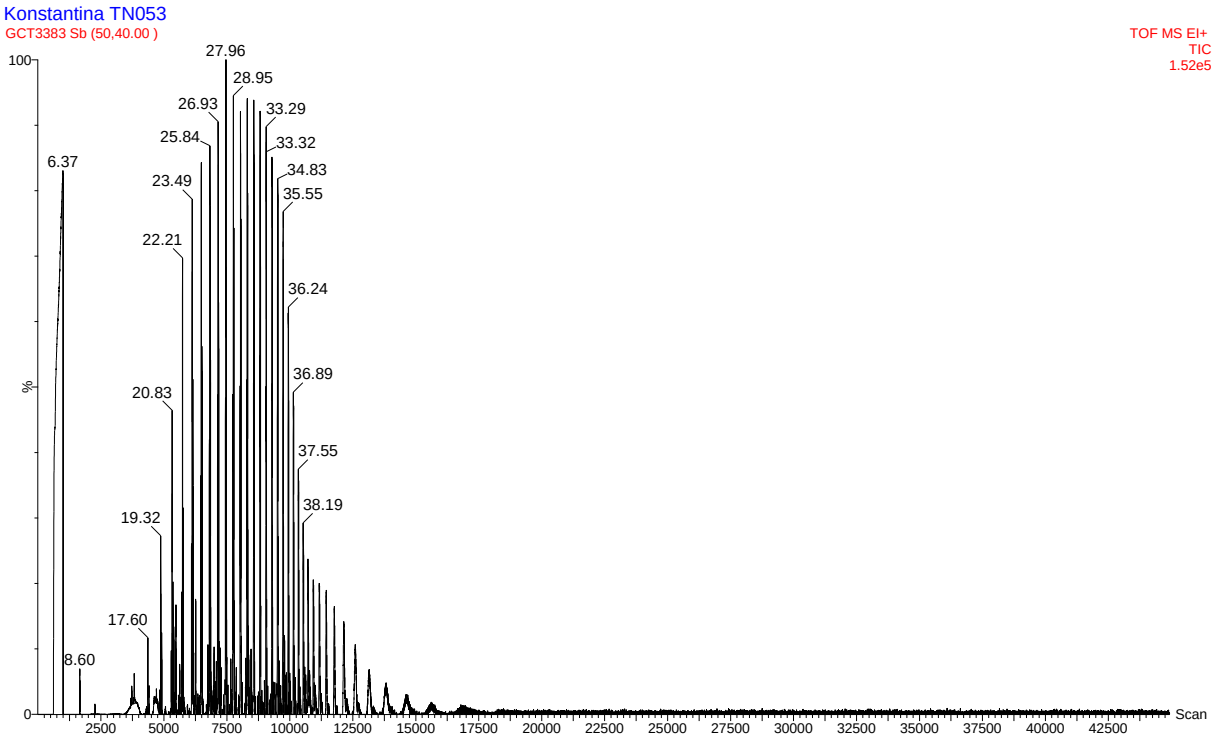

Figure 94: GC - MS spectra for wax sample produced from Tk feedstock under pyrolysis conditions of 550°C and 20L.min-1 flowrate.

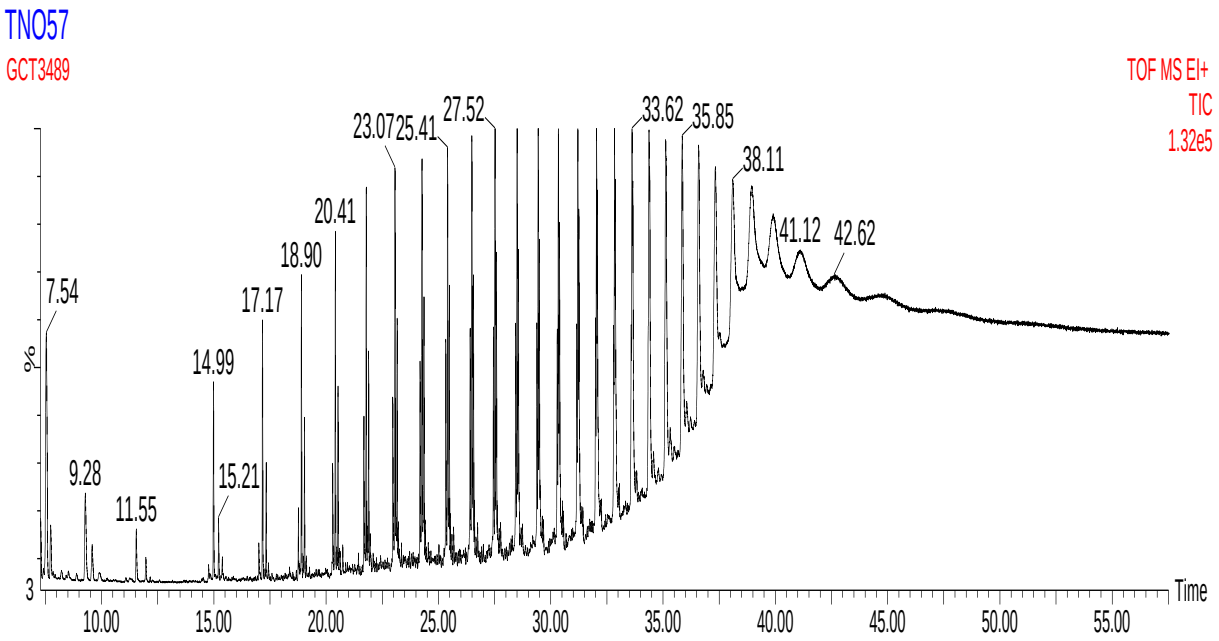

Figure 93: GC - MS spectra for wax sample produced from Gr feedstock under pyrolysis conditions of 530°C and 18L.min-1 flowrate.

Appendix C – Taguchi results for Gr feedstock

The results presented in Figure 95,for temperature and residence time as the signal values and melting point as the response are non linear for the temperature results since there is a peak at 530ºC which was not apparent in Tk and LDPE. However the optimal conditions correspond to the lowest observed value which is the melting point measurement.

These observations are consistent with the ones previously commented for Tk feedstock in §5.5 illustrating the strong effect that residence time in combination with high reaction temperatures have in the recovered wax product even when taking into considering feedstock composition variation which was expected to result in irreguralities in the resulting product quality.

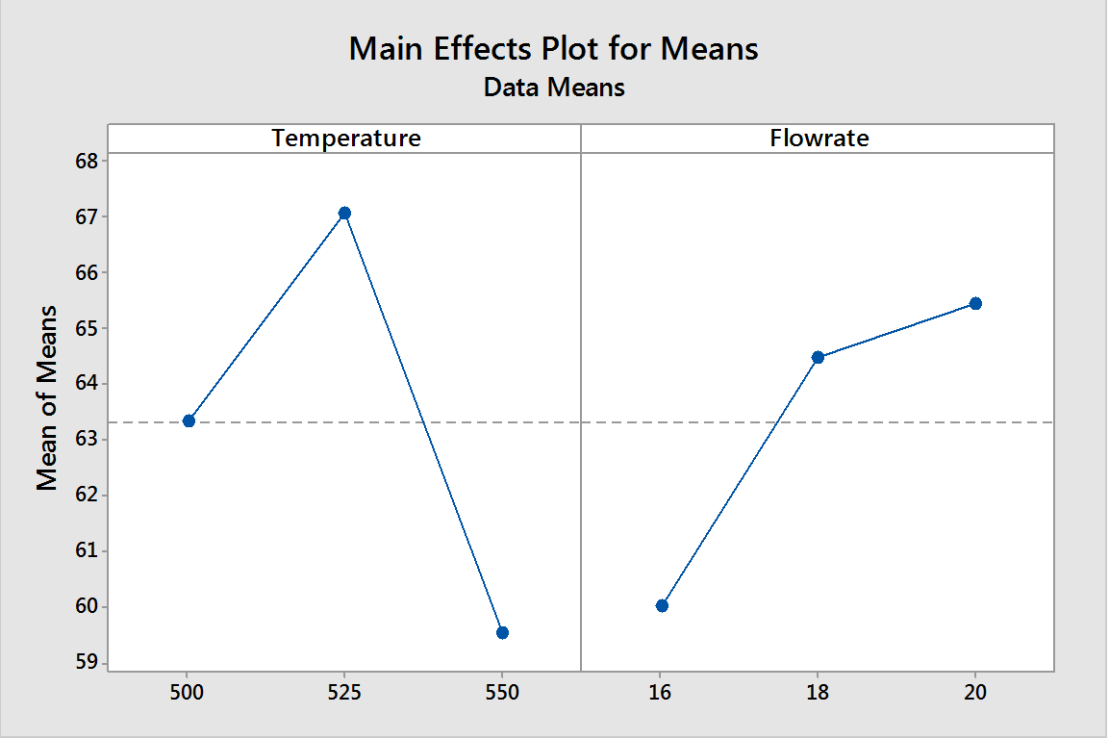

Figure 95: Taguchi results for Gr: temperature and flowrate with melting point.

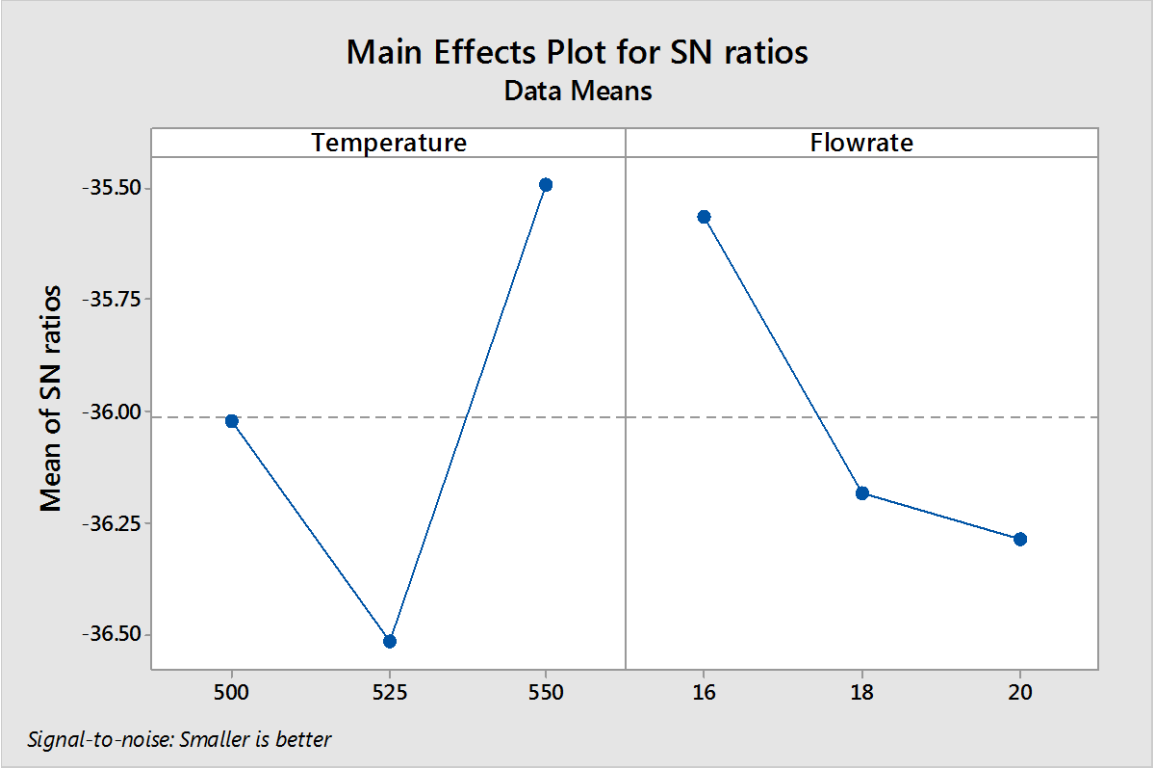

Figure 96: Taguchi results for Gr: temperature and flowrate with melting point (signal to noise ratio).

Appendix D – Analytical equipment used for feedstock characterisation

Figure 97: FTIR connected with the Exstar 6000 TGA with heated transfer line.

Figure 98: Plaxx blends with ULSD diesel in 5% and 10% w/w.

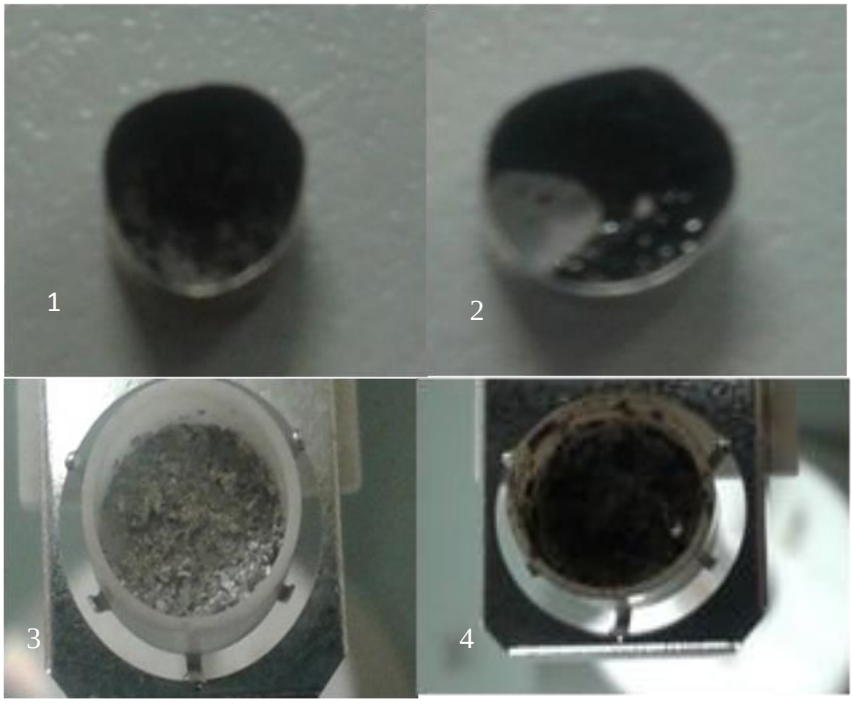

Figure 99: Solid residue from TGA for 1.PS, 2.PET, 3.Tk, 4.Tc.

References

(ATSDR), A. f. T. S. a. D. R. (2017). "Toxicological profile for fuel oils." from https://www.atsdr.cdc.gov/toxprofiles/tp75-c3.pdf.

Aldrich, S. (2015). "MSDS." from http://www.sigmaaldrich.com/safety-center.html.

ASTM (2012). Standard Test Method for Acid and Base Number by Color -Indicator Titration. Standard Test Method for Acid and Base Number by Color -Indicator Titration. United States, ASTM International.

Aylón, E., A. Fernández-Colino, M. V. Navarro, R. Murillo, T. García and A. M. Mastral (2008). "Waste Tire Pyrolysis: Comparison between Fixed Bed Reactor and Moving Bed Reactor." Industrial & Engineering Chemistry Research **47**(12): 4029-4033.

Azinfar, B., M. Zirrahi, H. Hassanzadeh and J. Abedi (2015). "A method for characterization of bitumen." Fuel **153**: 240-248.

Banar, M., V. Akyıldız, A. Özkan, Z. Çokaygil and Ö. Onay (2012). "Characterization of pyrolytic oil obtained from pyrolysis of TDF (Tire Derived Fuel)." Energy Conversion and Management **62**: 22-30.

Bockhorn, H., A. Hornung and U. Hornung (1998). "Stepwise pyrolysis for raw material recovery from plastic waste." Journal of Analytical and Applied Pyrolysis **46**(1): 1-13.

Buah, W. K., A. M. Cunliffe and P. T. Williams (2007). "Characterization of Products from the Pyrolysis of Municipal Solid Waste." Process Safety and Environmental Protection **85**(5): 450-457.

Conesa, J. A., R. Font, A. Gomis and A. N. Garcia (1994). Pyrolysis of Polyethylene in a Fluidized Bed Reactor.

Cunliffe, A. M. and P. T. Williams (1998). "Composition of oils derived from the batch pyrolysis of tyres." Journal of Analytical and Applied Pyrolysis **44**(2): 131-152.

de Marco, I., B. M. Caballero, A. López, M. F. Laresgoiti, A. Torres and M. J. Chomón (2009). "Pyrolysis of the rejects of a waste packaging separation and classification plant." Journal of Analytical and Applied Pyrolysis **85**(1–2): 384-391.

Gao, F. (2010). Pyrolysis of waste plastics into fuels.

Hartulistiyoso, E., F. A. P. A. G. Sigiro and M. Yulianto (2015). "Temperature Distribution of the Plastics Pyrolysis Process to Produce Fuel at 450oC." Procedia Environmental Sciences **28**: 234-241.

Jung, S.-H., M.-H. Cho, B.-S. Kang and J.-S. Kim (2010). "Pyrolysis of a fraction of waste polypropylene and polyethylene for the recovery of BTX aromatics using a fluidized bed reactor." Fuel Processing Technology **91**(3): 277-284.

Kaminsky, W. (1993). "Recycling of polymers by pyrolysis." Journal de Physique IV Colloque **03**(C7): C7-1543-C1547-1552.

Kaminsky, W. and J.-S. Kim (1999). "Pyrolysis of mixed plastics into aromatics." Journal of Analytical and Applied Pyrolysis **51**(1–2): 127-134.

Kaminsky, W., M. Predel and A. Sadiki (2004). "Feedstock recycling of polymers by pyrolysis in a fluidised bed." Polymer Degradation and Stability **85**(3): 1045-1050.

Li, A. M., X. D. Li, S. Q. Li, Y. Ren, Y. Chi, J. H. Yan and K. F. Cen (1999). "Pyrolysis of solid waste in a rotary kiln: influence of final pyrolysis temperature on the pyrolysis products." Journal of Analytical and Applied Pyrolysis **50**(2): 149-162.

Liu, Y., J. Qian and J. Wang (2000). "Pyrolysis of polystyrene waste in a fluidized-bed reactor to obtain styrene monomer and gasoline fraction." Fuel Processing Technology **63**(1): 45-55.

López, A., I. de Marco, B. M. Caballero, M. F. Laresgoiti and A. Adrados (2011). "Influence of time and temperature on pyrolysis of plastic wastes in a semi-batch reactor." Chemical Engineering Journal **173**(1): 62-71.

Mastral, F. J., E. Esperanza, P. García and M. Juste (2002). "Pyrolysis of high-density polyethylene in a fluidised bed reactor. Influence of the temperature and residence time." Journal of Analytical and Applied Pyrolysis **63**(1): 1-15.

Mastral, J. F., C. Berrueco and J. Ceamanos (2007). "Modelling of the pyrolysis of high density polyethylene: Product distribution in a fluidized bed reactor." Journal of Analytical and Applied Pyrolysis **79**(1–2): 313-322.
Miskolczi, N. and R. Nagy (2012). "Hydrocarbons obtained by waste plastic pyrolysis: Comparative analysis of decomposition described by different kinetic models." Fuel Processing Technology **104**(0): 96-104.
Net, D. (1998-1999). "98/69/EC (Euro 3) & 99/96/EC (Euro III) Reference Diesel Fuel ", 1999, from https://www.dieselnet.com/standards/eu/fuel_reference.php.
Oils, F. (2008). "Specification Data Sheet U.L.S. Derv." from http://www.fueloils.co.uk/index.asp?id=3&doc=40.
Park, S. S., D. K. Seo, S. H. Lee, T.-U. Yu and J. Hwang (2012). "Study on pyrolysis characteristics of refuse plastic fuel using lab-scale tube furnace and thermogravimetric analysis reactor." Journal of Analytical and Applied Pyrolysis **97**(0): 29-38.
Pinto, F., P. Costa, I. Gulyurtlu and I. Cabrita (1999). "Pyrolysis of plastic wastes. 1. Effect of plastic waste composition on product yield." Journal of Analytical and Applied Pyrolysis **51**(1–2): 39-55.
Scott, D. S., S. R. Czernik, J. Piskorz and D. S. A. G. Radlein (1990). "Fast pyrolysis of plastic wastes." Energy & Fuels **4**(4): 407-411.
Services, I. I. T. (2015). Analysis of Waste Derived Fuel, ITS Testing Services (UK) Ltd**:** 4.
Singh, R. K. and B. Ruj (2016). "Time and temperature depended fuel gas generation from pyrolysis of real world municipal plastic waste." Fuel **174**: 164-171.
Williams, E. A. and P. T. Williams (1997). "Analysis of products derived from the fast pyrolysis of plastic waste." Journal of Analytical and Applied Pyrolysis **40**: 347-363.
Williams, P. T. and E. A. Williams (1999). "Fluidised bed pyrolysis of low density polyethylene to produce petrochemical feedstock." Journal of Analytical and Applied Pyrolysis **51**(1–2): 107-126.
Wright, M. C., R. W. Court, F.-C. A. Kafantaris, F. Spathopoulos and M. A. Sephton (2015). "A new rapid method for shale oil and shale gas assessment." Fuel **153**: 231-239.
Zeaiter, J. (2014). "A process study on the pyrolysis of waste polyethylene." Fuel **133**: 276-282.

Cafiero, L., D. Fabbri, E. Trinca, R. Tuffi and S. Vecchio Ciprioti (2015). "Thermal and spectroscopic (TG/DSC–FTIR) characterization of mixed plastics for materials and energy recovery under pyrolytic conditions." Journal of Thermal Analysis and Calorimetry **121**(3): 1111-1119.

Camacho, W. and S. Karlsson (2001). "NIR, DSC, and FTIR as quantitative methods for compositional analysis of blends of polymers obtained from recycled mixed plastic waste." Polymer Engineering & Science **41**(9): 1626-1635.
Camposo, A., F. M. Margem, R. L. Loiola and S. N. Monteiro (2013). Evaluation of Sisal Fibers Components by Infrared Spectroscopy. Characterization of Minerals, Metals, and Materials 2013, John Wiley & Sons, Inc.**:** 153-158.
Chattopadhyay, J., C. Kim, R. Kim and D. Pak (2009). "Thermogravimetric characteristics and kinetic study of biomass co-pyrolysis with plastics." Korean Journal of Chemical Engineering **25**(5): 1047.
Colthup, N. B., L. H. Daly and S. E. Wiberley (1990). CHAPTER 9 - CARBONYL COMPOUNDS. Introduction to Infrared and Raman Spectroscopy (Third Edition). San Diego, Academic Press**:** 289-325.
Colthup, N. B., L. H. Daly and S. E. Wiberley (1990). CHAPTER 13 - MAJOR SPECTRA–STRUCTURE CORRELATIONS BY SPECTRAL REGIONS. Introduction to Infrared and Raman Spectroscopy (Third Edition). San Diego, Academic Press**:** 387-481.

Colthup, N. B., L. H. Daly and S. E. Wiberley (1990). CHAPTER 14 - THE THEORETICAL ANALYSIS OF MOLECULAR VIBRATIONS. Introduction to Infrared and Raman Spectroscopy (Third Edition). San Diego, Academic Press**:** 483-542.
Europe, P. (2106). Plastics the Facts 2016. Dusseldorf, Plastics Europe Deutschland e.V.**:** 38.
Gao, F. (2010). Pyrolysis of waste plastics into fuels.
Heikkinen, J. M., J. C. Hordijk, W. de Jong and H. Spliethoff (2004). "Thermogravimetry as a tool to classify waste components to be used for energy generation." Journal of Analytical and Applied Pyrolysis **71**(2): 883-900.
Jung, S.-H., M.-H. Cho, B.-S. Kang and J.-S. Kim (2010). "Pyrolysis of a fraction of waste polypropylene and polyethylene for the recovery of BTX aromatics using a fluidized bed reactor." Fuel Processing Technology **91**(3): 277-284.
López, A., I. de Marco, B. M. Caballero, M. F. Laresgoiti and A. Adrados (2010). "Pyrolysis of municipal plastic wastes: Influence of raw material composition." Waste Management **30**(4): 620-627.
Marongiu, A., T. Faravelli, G. Bozzano, M. Dente and E. Ranzi (2003). "Thermal degradation of poly(vinyl chloride)." Journal of Analytical and Applied Pyrolysis **70**(2): 519-553.
Odochian, L., C. Moldoveanu, A. M. Mocanu and G. Carja (2011). "Contributions to the thermal degradation mechanism under nitrogen atmosphere of PTFE by TG-FTIR analysis. Influence of the additive nature." Thermochimica Acta **526**(1–2): 205-212.
Reyes-Labarta, J. A., M. M. Olaya and A. Marcilla (2006). "DSC and TGA study of the transitions involved in the thermal treatment of binary mixtures of PE and EVA copolymer with a crosslinking agent." Polymer **47**(24): 8194-8202.
Robert M. Silverstein, F. X. W., David J. Kiemle (2005). Spectrometric Identification of Organic Compounds USA, John Wiley & Sons, Inc.
Salman, M., Nisar, S. , Hussain, Z. , Salman, H. and Kazimi, M. ((2015)). "TGA-DSC: A Screening Tool for the Evaluation of Hydrocracking Catalyst Performance." American Journal of Analytical Chemistry, **6**: 364-375.
Sharma, B. K., B. R. Moser, K. E. Vermillion, K. M. Doll and N. Rajagopalan (2014). "Production, characterization and fuel properties of alternative diesel fuel from pyrolysis of waste plastic grocery bags." Fuel Processing Technology **122**: 79-90.
Singh, S., C. Wu and P. T. Williams (2012). "Pyrolysis of waste materials using TGA-MS and TGA-FTIR as complementary characterisation techniques." Journal of Analytical and Applied Pyrolysis **94**: 99-107.
Sørum, L., M. G. Grønli and J. E. Hustad (2001). "Pyrolysis characteristics and kinetics of municipal solid wastes." Fuel **80**(9): 1217-1227.
Zhu, H. M., X. G. Jiang, J. H. Yan, Y. Chi and K. F. Cen (2008). "TG-FTIR analysis of PVC thermal degradation and HCl removal." Journal of Analytical and Applied Pyrolysis **82**(1): 1-9.

Aldrich, S. (2015). "MSDS." from http://www.sigmaaldrich.com/safety-center.html.

Equipment, S. (2017). "Melting point apparatus, Digital, SMP10 and SMP20." Retrieved 16/06/2107, 2017, from http://www.stuart-equipment.com/product.asp?dsl=114.
Hitachi, H. (2017). "Tabletop Microscope TM3030." Retrieved 18/06/2017, 2017, from http://www.hitachi-hightech.com/eu/product_detail/?pn=em-tm3030&version=.
Jasco, A. I. (2107). "FT/IR - 6600 Fourier Transform Infrared Spectroscopy ". Retrieved 16/6/2017, 2017, from http://www.jascoint.co.jp/asia/products/spectroscopy/ftir/ftir6600.html.
K. Smolders, J. B. (1997). " Powder Handling and Processing." **9 (2)**: 123.
Micromeritics (2017). "AccuPyc II 1340 Pycnometer." Retrieved 16/06/2017, 2017, from http://www.micromeritics.com/Product-Showcase/AccuPyc-II-1340.aspx.
Netzsch, T. A. (2017). "STA 449 F3 Jupiter." Retrieved 10/04/2017, 2017, from https://www.netzsch-thermal-analysis.com/us/products-solutions/simultaneous-thermogravimetry-differential-scanning-calorimetry/sta-449-f3-jupiter/.

Oils, F. (2008). "Specification Data Sheet U.L.S. Derv." from http://www.fueloils.co.uk/index.asp?id=3&doc=40.
Scientific and Medical Products Ltd, S. (2017). "EXSTAR 6000 TG/DTA Series." Retrieved 16/06/2017, 2017, from http://www.scimed.co.uk/product/exstar-6000-tgdta-series/.
Wang, F.-J., et al. (2007). "Effects of pressure drop and superficial velocity on the bubbling fluidized bed incinerator." Journal of Environmental Science and Health, Part A **42**(14): 2147-2158.
Wen, C. Y. and Y. H. Yu (1966). "A generalized method for predicting the minimum fluidization velocity." AIChE Journal **12**(3): 610-612.

(CROW), C. D. R. o. t. W. (2015). Polymer database. www.polymerdatabase.com.

(PEMRG), P. E. M. R. a. S. G. (2016). Plastics the Facts 2016. Dusseldorf, Plastics Europe Deutschland e.V.**:** 38.
Abbas-Abadi, M. S., M. N. Haghighi and H. Yeganeh (2013). "Evaluation of pyrolysis product of virgin high density polyethylene degradation using different process parameters in a stirred reactor." Fuel Processing Technology **109**: 90-95.
Abbas-Abadi, M. S., M. N. Haghighi, H. Yeganeh and A. G. McDonald (2014). "Evaluation of pyrolysis process parameters on polypropylene degradation products." Journal of Analytical and Applied Pyrolysis **109**: 272-277.
Abnisa, F., W. M. A. W. Daud and J. N. Sahu (2014). "Pyrolysis of mixtures of palm shell and polystyrene: An optional method to produce a high-grade of pyrolysis oil." Environmental Progress & Sustainable Energy **33**(3): 1026-1033.
Aboulkas, A., K. El harfi and A. El Bouadili (2010). "Thermal degradation behaviors of polyethylene and polypropylene. Part I: Pyrolysis kinetics and mechanisms." Energy Conversion and Management **51**(7): 1363-1369.
Acevedo, B., A. M. Fernández and C. Barriocanal (2015). "Identification of polymers in waste tyre reinforcing fibre by thermal analysis and pyrolysis." Journal of Analytical and Applied Pyrolysis **111**: 224-232.
Adrados, A., I. de Marco, B. M. Caballero, A. López, M. F. Laresgoiti and A. Torres (2012). "Pyrolysis of plastic packaging waste: A comparison of plastic residuals from material recovery facilities with simulated plastic waste." Waste Management **32**(5): 826-832.
Aguado, J., D. P. Serrano, G. San Miguel, M. C. Castro and S. Madrid (2007). "Feedstock recycling of polyethylene in a two-step thermo-catalytic reaction system." Journal of Analytical and Applied Pyrolysis **79**(1–2): 415-423.
Aguado, R., M. Olazar, B. Gaisán, R. Prieto and J. Bilbao (2002). "Kinetic Study of Polyolefin Pyrolysis in a Conical Spouted Bed Reactor." Industrial & Engineering Chemistry Research **41**(18): 4559-4566.
Ahmad, I., M. Ismail Khan, M. Ishaq, H. Khan, K. Gul and W. Ahmad (2013). "Catalytic efficiency of some novel nanostructured heterogeneous solid catalysts in pyrolysis of HDPE." Polymer Degradation and Stability **98**(12): 2512-2519.
Ahmad, I., M. I. Khan, H. Khan, M. Ishaq, R. Tariq, K. Gul and W. Ahmad (2015). "Pyrolysis Study of Polypropylene and Polyethylene Into Premium Oil Products." International Journal of Green Energy **12**(7): 663-671.
Ahmad, Z., F. Al-Sagheer and N. A. Al-Awadi (2010). "Pyro-GC/MS and thermal degradation studies in polystyrene–poly(vinyl chloride) blends." Journal of Analytical and Applied Pyrolysis **87**(1): 99-107.
Akpanudoh, N. S., K. Gobin and G. Manos (2005). "Catalytic degradation of plastic waste to liquid fuel over commercial cracking catalysts." Journal of Molecular Catalysis A: Chemical **235**(1): 67-73.

Al-Salem, S. M., A. Antelava, A. Constantinou, G. Manos and A. Dutta (2017). "A review on thermal and catalytic pyrolysis of plastic solid waste (PSW)." Journal of Environmental Management **197**: 177-198.
Al-Salem, S. M. and A. R. Khan (2014). "On the degradation kinetics of poly(ethylene terephthalate) (PET)/poly(methyl methacrylate) (PMMA) blends in dynamic thermogravimetry." Polymer Degradation and Stability **104**: 28-32.
Al-Salem, S. M. and P. Lettieri (2010). "Kinetic study of high density polyethylene (HDPE) pyrolysis." Chemical Engineering Research and Design **88**(12): 1599-1606.
Al-Salem, S. M., P. Lettieri and J. Baeyens (2009). "Recycling and recovery routes of plastic solid waste (PSW): A review." Waste Management **29**(10): 2625-2643.
Arabiourrutia, M., G. Elordi, G. Lopez, E. Borsella, J. Bilbao and M. Olazar (2012). "Characterization of the waxes obtained by the pyrolysis of polyolefin plastics in a conical spouted bed reactor." Journal of Analytical and Applied Pyrolysis **94**: 230-237.
Arenillas, A., C. Pevida, F. Rubiera, R. García and J. J. Pis (2004). "Characterisation of model compounds and a synthetic coal by TG/MS/FTIR to represent the pyrolysis behaviour of coal." Journal of Analytical and Applied Pyrolysis **71**(2): 747-763.
Artetxe, M., G. Lopez, M. Amutio, G. Elordi, J. Bilbao and M. Olazar (2013). "Cracking of High Density Polyethylene Pyrolysis Waxes on HZSM-5 Catalysts of Different Acidity." Industrial & Engineering Chemistry Research **52**(31): 10637-10645.
Ateş, F., N. Miskolczi and N. Borsodi (2013). "Comparision of real waste (MSW and MPW) pyrolysis in batch reactor over different catalysts. Part I: Product yields, gas and pyrolysis oil properties." Bioresource Technology **133**: 443-454.
Aydın, H. and C. İlkılıç (2012). "Optimization of fuel production from waste vehicle tires by pyrolysis and resembling to diesel fuel by various desulfurization methods." Fuel **102**: 605-612.
Aylón, E., A. Fernández-Colino, M. V. Navarro, R. Murillo, T. García and A. M. Mastral (2008). "Waste Tire Pyrolysis: Comparison between Fixed Bed Reactor and Moving Bed Reactor." Industrial & Engineering Chemistry Research **47**(12): 4029-4033.
Bagri, R. and P. T. Williams (2002). "Catalytic pyrolysis of polyethylene." Journal of Analytical and Applied Pyrolysis **63**(1): 29-41.
Bains, M., S. T. Balke, D. Reck and J. Horn (1994). "The compatibility of linear low density polyethylene-polypropylene blends: Viscosity ratio plots." Polymer Engineering & Science **34**(16): 1260-1268.
Ballice, L. (2001). "A kinetic approach to the temperature-programmed pyrolysis of low- and high-density polyethylene in a fixed bed reactor: determination of kinetic parameters for the evolution of n-paraffins and 1-olefins." Fuel **80**(13): 1923-1935.
Banar, M., V. Akyıldız, A. Özkan, Z. Çokaygil and Ö. Onay (2012). "Characterization of pyrolytic oil obtained from pyrolysis of TDF (Tire Derived Fuel)." Energy Conversion and Management **62**: 22-30.
Barbooti, M. M., T. J. Mohamed, A. A. Hussain and F. O. Abas (2004). "Optimization of pyrolysis conditions of scrap tires under inert gas atmosphere." Journal of Analytical and Applied Pyrolysis **72**(1): 165-170.
Basu, P. (2010). Chapter 1 - Introduction. Biomass Gasification and Pyrolysis. Boston, Academic Press**:** 1-25.
Basu, P. (2010). Chapter 3 - Pyrolysis and Torrefaction. Biomass Gasification and Pyrolysis. Boston, Academic Press**:** 65-96.
Basu, P. (2013). Chapter 5 - Pyrolysis. Biomass Gasification, Pyrolysis and Torrefaction: Practical Design and Theory. Saint Louis, UNITED STATES, Elsevier Science.
Basu, P. (2013). Chapter 13 - Analytical Techniques. Biomass Gasification, Pyrolysis and Torrefaction : Practical Design and Theory. San Diego, UNITED STATES, Elsevier Science**:** 439-452.
Bernardo, M., N. Lapa, M. Gonçalves, B. Mendes, F. Pinto, I. Fonseca and H. Lopes (2012). Physico-chemical properties of chars obtained in the co-pyrolysis of waste mixtures.

Berrueco, C., E. Esperanza, F. J. Mastral, J. Ceamanos and P. García-Bacaicoa (2005). "Pyrolysis of waste tyres in an atmospheric static-bed batch reactor: Analysis of the gases obtained." Journal of Analytical and Applied Pyrolysis **74**(1): 245-253.
Bezergianni, S., A. Dimitriadis and G. Meletidis (2014). "Effectiveness of CoMo and NiMo catalysts on co-hydroprocessing of heavy atmospheric gas oil–waste cooking oil mixtures." Fuel **125**(Supplement C): 129-136.
Bhadury, P. S., S. Singh, M. Sharma and M. Palit (2007). "Flash pyrolysis of polytetrafluoroethylene (teflon) in a quartz assembly." Journal of Analytical and Applied Pyrolysis **78**(2): 288-290.
Bhaskar, T., J. Kaneko, A. Muto, Y. Sakata, E. Jakab, T. Matsui and M. A. Uddin (2004). "Pyrolysis studies of PP/PE/PS/PVC/HIPS-Br plastics mixed with PET and dehalogenation (Br, Cl) of the liquid products." Journal of Analytical and Applied Pyrolysis **72**(1): 27-33.
Bhaskar, T., M. Tanabe, A. Muto, Y. Sakata, C.-F. Liu, M.-D. Chen and C. C. Chao (2005). "Analysis of chlorine distribution in the pyrolysis products of poly(vinylidene chloride) mixed with polyethylene, polypropylene or polystyrene." Polymer Degradation and Stability **89**(1): 38-42.
Biswas, S. and D. K. Sharma (2013). "Co-cracking of jatropha oil, vacuum residue and HDPE and characterization of liquid, gaseous and char products obtained." Journal of Analytical and Applied Pyrolysis **101**: 17-27.
Blazsó, M. (1997). "Recent trends in analytical and applied pyrolysis of polymers." Journal of Analytical and Applied Pyrolysis **39**(1): 1-25.
Blazsó, M. (2006). "Composition of liquid fuels derived from the pyrolysis of plastics." Feedstock recycling and pyrolysis of waste plastics: converting waste plastics into diesel and other fuels: 315-344.
Bockhorn, H., S. Donner, M. Gernsbeck, A. Hornung and U. Hornung (2001). "Pyrolysis of polyamide 6 under catalytic conditions and its application to reutilization of carpets." Journal of Analytical and Applied Pyrolysis **58**: 79-94.
Bockhorn, H., A. Hornung and U. Hornung (1998). "Stepwise pyrolysis for raw material recovery from plastic waste." Journal of Analytical and Applied Pyrolysis **46**(1): 1-13.
Brebu, M., T. Bhaskar, K. Murai, A. Muto, Y. Sakata and M. A. Uddin (2005). "Removal of nitrogen, bromine, and chlorine from PP/PE/PS/PVC/ABS–Br pyrolysis liquid products using Fe- and Ca-based catalysts." Polymer Degradation and Stability **87**(2): 225-230.
Brems, A., J. Baeyens, J. Beerlandt and R. Dewil (2011). "Thermogravimetric pyrolysis of waste polyethylene-terephthalate and polystyrene: A critical assessment of kinetics modelling." Resources, Conservation and Recycling **55**(8): 772-781.
Bridgwater, A. V. (2012). "Review of fast pyrolysis of biomass and product upgrading." Biomass and Bioenergy **38**: 68-94.
Brydson, J. (1999). Chapter 4 - Relation of structure to Thermal and Mechanical Properties. Plastics Materials (7th Edition)

Elsevier**:** 59-74.
Brydson, J. (1999). Chapter 5 - Relation of Structure to Chemical Properties Plastics Materials (7th Edition), Elsevier**:** 76-87.
Brydson, J. A. (1999). 2 - The Chemical Nature of Plastics. Plastics Materials (Seventh Edition). Oxford, Butterworth-Heinemann**:** 19-42.
Buah, W. K., A. M. Cunliffe and P. T. Williams (2007). "Characterization of Products from the Pyrolysis of Municipal Solid Waste." Process Safety and Environmental Protection **85**(5): 450-457.
Buekens, A. (2006). Introduction to Feedstock Recycling of Plastics. Feedstock Recycling and Pyrolysis of Waste Plastics, John Wiley & Sons, Ltd**:** 1-41.
Cafiero, L., D. Fabbri, E. Trinca, R. Tuffi and S. Vecchio Ciprioti (2015). "Thermal and spectroscopic (TG/DSC–FTIR) characterization of mixed plastics for materials and energy

recovery under pyrolytic conditions." Journal of Thermal Analysis and Calorimetry **121**(3): 1111-1119.
Camacho, W. and S. Karlsson (2001). "NIR, DSC, and FTIR as quantitative methods for compositional analysis of blends of polymers obtained from recycled mixed plastic waste." Polymer Engineering & Science **41**(9): 1626-1635.
Ceamanos, J., J. F. Mastral, A. Millera and M. E. Aldea (2002). "Kinetics of pyrolysis of high density polyethylene. Comparison of isothermal and dynamic experiments." Journal of Analytical and Applied Pyrolysis **65**(2): 93-110.
Çepelioğullar, Ö. and A. E. Pütün (2013). "Thermal and kinetic behaviors of biomass and plastic wastes in co-pyrolysis." Energy Conversion and Management **75**: 263-270.
Chao-Hsiung, W., C. Ching-Yuan, H. Jwo-Luen, S. Shin-Min, C. Leo-Wang and C. Feng-Wen (1993). "On the thermal treatment of plastic mixtures of MSW: Pyrolysis kinetics." Waste Management **13**(3): 221-235.
Chao, K., Y. Chen, J. Li, X. Zhang and B. Dong (2012). "Upgrading and visbreaking of super-heavy oil by catalytic aquathermolysis with aromatic sulfonic copper." Fuel Processing Technology **104**: 174-180.
Chattopadhyay, J., C. Kim, R. Kim and D. Pak (2009). "Thermogravimetric characteristics and kinetic study of biomass co-pyrolysis with plastics." Korean Journal of Chemical Engineering **25**(5): 1047.
Chen, X., J. Zhuo and C. Jiao (2012). "Thermal degradation characteristics of flame retardant polylactide using TG-IR." Polymer Degradation and Stability **97**(11): 2143-2147.
Chin, B. L. F., S. Yusup, A. Al Shoaibi, P. Kannan, C. Srinivasakannan and S. A. Sulaiman (2014). "Kinetic studies of co-pyrolysis of rubber seed shell with high density polyethylene." Energy Conversion and Management **87**: 746-753.
Choi, G.-G., S.-H. Jung, S.-J. Oh and J.-S. Kim (2014). "Total utilization of waste tire rubber through pyrolysis to obtain oils and CO2 activation of pyrolysis char." Fuel Processing Technology **123**: 57-64.
Churkunti, P. R., J. Mattson, C. Depcik and G. Devlin (2016). "Combustion analysis of pyrolysis end of life plastic fuel blended with ultra low sulfur diesel." Fuel Processing Technology **142**: 212-218.
Collins, R. D., P. Fiveash and L. Holland (1969). "A mass spectrometry study of the evaporation and pyrolysis of polytetrafluorethylene." Vacuum **19**(3): 113-116.
Colthup, N. B., L. H. Daly and S. E. Wiberley (1990). CHAPTER 2 - IR EXPERIMENTAL CONSIDERATIONS. Introduction to Infrared and Raman Spectroscopy (Third Edition). San Diego, Academic Press**:** 75-107.
Conesa, J. A., R. Font, A. Gomis and A. N. Garcia (1994). Pyrolysis of Polyethylene in a Fluidized Bed Reactor.
Conesa, J. A., A. Marcilla, R. Font and J. A. Caballero (1996). "Thermogravimetric studies on the thermal decomposition of polyethylene." Journal of Analytical and Applied Pyrolysis **36**(1): 1-15.
Cozzani, V., L. Petarca and L. Tognotti (1995). "Devolatilization and pyrolysis of refuse derived fuels: characterization and kinetic modelling by a thermogravimetric and calorimetric approach." Fuel **74**(6): 903-912.
Cunliffe, A. M., N. Jones and P. T. Williams (2003). "Pyrolysis of composite plastic waste." Environmental Technology **24**(5): 653-663.
Czégény, Z., E. Jakab, M. Blazsó, T. Bhaskar and Y. Sakata (2012). "Thermal decomposition of polymer mixtures of PVC, PET and ABS containing brominated flame retardant: Formation of chlorinated and brominated organic compounds." Journal of Analytical and Applied Pyrolysis **96**(0): 69-77.
Dai, X., X. Yin, C. Wu, W. Zhang and Y. Chen (2001). "Pyrolysis of waste tires in a circulating fluidized-bed reactor." Energy **26**(4): 385-399.
Degnan, T. F. (2000). "Applications of zeolites in petroleum refining." Topics in Catalysis **13**(4): 349-356

Demirbas, A. (2004). "Effects of temperature and particle size on bio-char yield from pyrolysis of agricultural residues." Journal of Analytical and Applied Pyrolysis **72**(2): 243-248.
Demirbas, A. (2004). "Pyrolysis of municipal plastic wastes for recovery of gasoline-range hydrocarbons." Journal of Analytical and Applied Pyrolysis **72**(1): 97-102.
Dimitrov, N., L. Kratofil Krehula, A. Ptiček Siročić and Z. Hrnjak-Murgić (2013). "Analysis of recycled PET bottles products by pyrolysis-gas chromatography." Polymer Degradation and Stability **98**(5): 972-979.
Donaj, P. J., W. Kaminsky, F. Buzeto and W. Yang (2012). "Pyrolysis of polyolefins for increasing the yield of monomers' recovery." Waste Management **32**(5): 840-846.
Efika, E. C., J. A. Onwudili and P. T. Williams (2015). "Products from the high temperature pyrolysis of RDF at slow and rapid heating rates." Journal of Analytical and Applied Pyrolysis **112**: 14-22.
Elordi, G., M. Olazar, P. Castaño, M. Artetxe and J. Bilbao (2012). "Polyethylene Cracking on a Spent FCC Catalyst in a Conical Spouted Bed." Industrial & Engineering Chemistry Research **51**(43): 14008-14017.
FakhrHoseini, S. M. and M. Dastanian (2013). "Predicting Pyrolysis Products of PE, PP, and PET Using NRTL Activity Coefficient Model." Journal of Chemistry **2013**: 5.
Faravelli, T., G. Bozzano, M. Colombo, E. Ranzi and M. Dente (2003). "Kinetic modeling of the thermal degradation of polyethylene and polystyrene mixtures." Journal of Analytical and Applied Pyrolysis **70**(2): 761-777.
Frigo, S., M. Seggiani, M. Puccini and S. Vitolo (2014). "Liquid fuel production from waste tyre pyrolysis and its utilisation in a Diesel engine." Fuel **116**: 399-408.
Gao, F. (2010). Pyrolysis of waste plastics into fuels.
Garcia, A. N., R. Font and A. Marcilla (1995). "Gas Production by Pyrolysis of Municipal Solid Waste at High Temperature in a Fluidized Bed Reactor." Energy & Fuels **9**(4): 648-658.
Garforth, A. A., Y. H. Lin, P. N. Sharratt and J. Dwyer (1998). "Production of hydrocarbons by catalytic degradation of high density polyethylene in a laboratory fluidised-bed reactor." Applied Catalysis A: General **169**(2): 331-342.
Grammelis, P., P. Basinas, A. Malliopoulou and G. Sakellaropoulos (2009). "Pyrolysis kinetics and combustion characteristics of waste recovered fuels." Fuel **88**(1): 195-205.
Gulab, H., M. R. Jan, J. Shah and G. Manos (2010). "Plastic catalytic pyrolysis to fuels as tertiary polymer recycling method: Effect of process conditions." Journal of Environmental Science and Health, Part A **45**(7): 908-915.
Hall, W. J. and P. T. Williams (2007). "Analysis of products from the pyrolysis of plastics recovered from the commercial scale recycling of waste electrical and electronic equipment." Journal of Analytical and Applied Pyrolysis **79**(1): 375-386.
Hart, A. (2014). Advanced studies of catalytic upgrading of heavy oils, University of Birmingham.
Hassan, E. B., I. Elsayed and A. Eseyin (2016). "Production high yields of aromatic hydrocarbons through catalytic fast pyrolysis of torrefied wood and polystyrene." Fuel **174**: 317-324.
Heikkinen, J. M., J. C. Hordijk, W. de Jong and H. Spliethoff (2004). "Thermogravimetry as a tool to classify waste components to be used for energy generation." Journal of Analytical and Applied Pyrolysis **71**(2): 883-900.
Hernández, M. d. R., A. Gómez, Á. N. García, J. Agulló and A. Marcilla (2007). "Effect of the temperature in the nature and extension of the primary and secondary reactions in the thermal and HZSM-5 catalytic pyrolysis of HDPE." Applied Catalysis A: General **317**(2): 183-194.
Hujuri, U., A. K. Ghoshal and S. Gumma (2008). "Modeling pyrolysis kinetics of plastic mixtures." Polymer Degradation and Stability **93**(10): 1832-1837.
Islam, M., M. Islam and M. Beg (2004). "Fixed bed pyrolysis of waste plastic for alternative fuel production." Journal of Energy and Environment **3**: 69-80.

Jamradloedluk, J. and C. Lertsatitthanakorn (2014). "Characterization and Utilization of Char Derived from Fast Pyrolysis of Plastic Wastes." Procedia Engineering **69**: 1437-1442.
Jing, P., Q. Li, M. Han, D. Sun, L. Jia and W. Fang (2008). "Visbreaking of heavy petroleum oil catalyzed by SO 4 2− /ZrO2 solid super-acid doped with Ni2+ or Sn2+." Frontiers of Chemical Engineering in China **2**(2): 186-190.
Jung, S.-H., M.-H. Cho, B.-S. Kang and J.-S. Kim (2010). "Pyrolysis of a fraction of waste polypropylene and polyethylene for the recovery of BTX aromatics using a fluidized bed reactor." Fuel Processing Technology **91**(3): 277-284.
Kaminsky, W. and J.-S. Kim (1999). "Pyrolysis of mixed plastics into aromatics." Journal of Analytical and Applied Pyrolysis **51**(1–2): 127-134.
Kaminsky, W., C. Mennerich and Z. Zhang (2009). "Feedstock recycling of synthetic and natural rubber by pyrolysis in a fluidized bed." Journal of Analytical and Applied Pyrolysis **85**(1): 334-337.
Kaminsky, W., M. Predel and A. Sadiki (2004). "Feedstock recycling of polymers by pyrolysis in a fluidised bed." Polymer Degradation and Stability **85**(3): 1045-1050.
Kaminsky, W., B. Schlesselmann and C. Simon (1995). "Olefins from polyolefins and mixed plastics by pyrolysis." Journal of Analytical and Applied Pyrolysis **32**: 19-27.
Kaminsky, W., B. Schlesselmann and C. M. Simon (1996). "Thermal degradation of mixed plastic waste to aromatics and gas." Polymer Degradation and Stability **53**(2): 189-197.
Kan, T., V. Strezov and T. J. Evans (2016). "Lignocellulosic biomass pyrolysis: A review of product properties and effects of pyrolysis parameters." Renewable and Sustainable Energy Reviews **57**: 1126-1140.
Kim, S.-S. and S. Kim (2004). "Pyrolysis characteristics of polystyrene and polypropylene in a stirred batch reactor." Chemical Engineering Journal **98**(1): 53-60.
Kiran Ciliz, N., E. Ekinci and C. E. Snape (2004). "Pyrolysis of virgin and waste polypropylene and its mixtures with waste polyethylene and polystyrene." Waste Management **24**(2): 173-181.
Kissel, T. (2002). "Advanced polymer chemistry - a problem solving guide Manas Chanda Marcel Dekker Inc., New York, USA; 2000, ISBN: 0-8247-0257-3." EUROPEAN JOURNAL OF PHARMACEUTICS AND BIOPHARMACEUTICS **53**(1): 133.
Kluska, J., M. Klein, P. Kazimierski and D. Kardaś (2014). Pyrolysis of biomass and refuse-derived fuel performance in laboratory scale batch reactor. Archives of Thermodynamics. **35:** 141.
Kong, Y. and J. N. Hay (2002). "The measurement of the crystallinity of polymers by DSC." Polymer **43**(14): 3873-3878.
Kruse, T. M., S. E. Levine, H.-W. Wong, E. Duoss, A. H. Lebovitz, J. M. Torkelson and L. J. Broadbelt (2005). "Binary mixture pyrolysis of polypropylene and polystyrene: A modeling and experimental study." Journal of Analytical and Applied Pyrolysis **73**(2): 342-354.
Kumar, S., R. Prakash, S. Murugan and R. K. Singh (2013). "Performance and emission analysis of blends of waste plastic oil obtained by catalytic pyrolysis of waste HDPE with diesel in a CI engine." Energy Conversion and Management **74**: 323-331.
Kumar, S. and R. K. Singh (2011). "Recovery of hydrocarbon liquid from waste high density polyethylene by thermal pyrolysis." Brazilian Journal of Chemical Engineering **28**: 659-667.
Lee, K.-H. (2006). Thermal and Catalytic Degradation of Waste HDPE. Feedstock Recycling and Pyrolysis of Waste Plastics, John Wiley & Sons, Ltd**:** 129-160.
Lee, K.-H., N.-S. Noh, D.-H. Shin and Y. Seo (2002). "Comparison of plastic types for catalytic degradation of waste plastics into liquid product with spent FCC catalyst." Polymer Degradation and Stability **78**(3): 539-544.
Lee, K.-H. and D.-H. Shin (2007). "Characteristics of liquid product from the pyrolysis of waste plastic mixture at low and high temperatures: Influence of lapse time of reaction." Waste Management **27**(2): 168-176.

Levine, S. E. and L. J. Broadbelt (2009). "Detailed mechanistic modeling of high-density polyethylene pyrolysis: Low molecular weight product evolution." Polymer Degradation and Stability **94**(5): 810-822.
Li, A. M., X. D. Li, S. Q. Li, Y. Ren, Y. Chi, J. H. Yan and K. F. Cen (1999). "Pyrolysis of solid waste in a rotary kiln: influence of final pyrolysis temperature on the pyrolysis products." Journal of Analytical and Applied Pyrolysis **50**(2): 149-162.
Lin, Y. H. and M. H. Yang (2007). "Catalytic pyrolysis of polyolefin waste into valuable hydrocarbons over reused catalyst from refinery FCC units." Applied Catalysis A: General **328**(2): 132-139.
Lin, Y. H., M. H. Yang, T. F. Yeh and M. D. Ger (2004). "Catalytic degradation of high density polyethylene over mesoporous and microporous catalysts in a fluidised-bed reactor." Polymer Degradation and Stability **86**(1): 121-128.
Lin, Y. H. and H. Y. Yen (2005). "Fluidised bed pyrolysis of polypropylene over cracking catalysts for producing hydrocarbons." Polymer Degradation and Stability **89**(1): 101-108.
Lonfei, J., W. Jingling and X. Shuman (1986). "Mechanisms of pyrolysis of fluoropolymers." Journal of Analytical and Applied Pyrolysis **10**(2): 99-106.
López, A., I. de Marco, B. M. Caballero, M. F. Laresgoiti and A. Adrados (2010). "Pyrolysis of municipal plastic wastes: Influence of raw material composition." Waste Management **30**(4): 620-627.
López, A., I. de Marco, B. M. Caballero, M. F. Laresgoiti and A. Adrados (2011). "Dechlorination of fuels in pyrolysis of PVC containing plastic wastes." Fuel Processing Technology **92**(2): 253-260.
López, A., I. de Marco, B. M. Caballero, M. F. Laresgoiti and A. Adrados (2011). "Influence of time and temperature on pyrolysis of plastic wastes in a semi-batch reactor." Chemical Engineering Journal **173**(1): 62-71.
López, G., M. Olazar, R. Aguado and J. Bilbao (2010). "Continuous pyrolysis of waste tyres in a conical spouted bed reactor." Fuel **89**(8): 1946-1952.
Ludlow-Palafox, C. and H. A. Chase (2001). "Microwave-Induced Pyrolysis of Plastic Wastes." Industrial & Engineering Chemistry Research **40**(22): 4749-4756.
Luo, G., T. Suto, S. Yasu and K. Kato (2000). "Catalytic degradation of high density polyethylene and polypropylene into liquid fuel in a powder-particle fluidized bed." Polymer Degradation and Stability **70**(1): 97-102.
Ma, S., J. Lu and J. Gao (2002). "Study of the Low Temperature Pyrolysis of PVC." Energy & Fuels **16**(2): 338-342.
Magdziarz, A. and S. Werle (2014). "Analysis of the combustion and pyrolysis of dried sewage sludge by TGA and MS." Waste Management **34**(1): 174-179.
Mani, M., G. Nagarajan and S. Sampath (2011). "Characterisation and effect of using waste plastic oil and diesel fuel blends in compression ignition engine." Energy **36**(1): 212-219.
Manos, G., A. Garforth and J. Dwyer (2000). "Catalytic Degradation of High-Density Polyethylene over Different Zeolitic Structures." Industrial & Engineering Chemistry Research **39**(5): 1198-1202.
Marcilla, A., J. C. García-Quesada, S. Sánchez and R. Ruiz (2005). "Study of the catalytic pyrolysis behaviour of polyethylene–polypropylene mixtures." Journal of Analytical and Applied Pyrolysis **74**(1): 387-392.
Marcilla, A., A. Gómez-Siurana and F. Valdés (2007). "Catalytic pyrolysis of LDPE over H-beta and HZSM-5 zeolites in dynamic conditions: Study of the evolution of the process." Journal of Analytical and Applied Pyrolysis **79**(1–2): 433-442.
Marcilla, A., M. d. R. Hernández and Á. N. García (2007). "Study of the polymer–catalyst contact effectivity and the heating rate influence on the HDPE pyrolysis." Journal of Analytical and Applied Pyrolysis **79**(1): 424-432.
Marongiu, A., T. Faravelli, G. Bozzano, M. Dente and E. Ranzi (2003). "Thermal degradation of poly(vinyl chloride)." Journal of Analytical and Applied Pyrolysis **70**(2): 519-553.

Marongiu, A., T. Faravelli and E. Ranzi (2007). "Detailed kinetic modeling of the thermal degradation of vinyl polymers." Journal of Analytical and Applied Pyrolysis **78**(2): 343-362.
Martínez, J. D., R. Murillo, T. García and A. Veses (2013). "Demonstration of the waste tire pyrolysis process on pilot scale in a continuous auger reactor." Journal of Hazardous Materials **261**: 637-645.
Martínez, J. D., A. Veses, A. M. Mastral, R. Murillo, M. V. Navarro, N. Puy, A. Artigues, J. Bartrolí and T. García (2014). "Co-pyrolysis of biomass with waste tyres: Upgrading of liquid bio-fuel." Fuel Processing Technology **119**: 263-271.
Mastral, F. J., E. Esperanza, P. García and M. Juste (2002). "Pyrolysis of high-density polyethylene in a fluidised bed reactor. Influence of the temperature and residence time." Journal of Analytical and Applied Pyrolysis **63**(1): 1-15.
Mastral, J. F., C. Berrueco and J. Ceamanos (2007). "Theoretical prediction of product distribution of the pyrolysis of high density polyethylene." Journal of Analytical and Applied Pyrolysis **80**(2): 427-438.
Mastral, J. F., C. Berrueco, M. Gea and J. Ceamanos (2006). "Catalytic degradation of high density polyethylene over nanocrystalline HZSM-5 zeolite." Polymer Degradation and Stability **91**(12): 3330-3338.
Meade, A.-M. B. a. J. (1999). Thermoplastics, in Modern Plastics Handbook. Modern plastics handbook. C. A. Harper. United States of America, McGraw - Hill: Lutherville.
Mehl, M., A. Marongiu, T. Faravelli, G. Bozzano, M. Dente and E. Ranzi (2004). "A kinetic modeling study of the thermal degradation of halogenated polymers." Journal of Analytical and Applied Pyrolysis **72**(2): 253-272.
Meissner, E., A. Wróblewska and E. Milchert (2004). "Technological parameters of pyrolysis of waste polytetrafluoroethylene." Polymer Degradation and Stability **83**(1): 163-172.
Miandad, R., A. S. Nizami, M. Rehan, M. A. Barakat, M. I. Khan, A. Mustafa, I. M. I. Ismail and J. D. Murphy (2016). "Influence of temperature and reaction time on the conversion of polystyrene waste to pyrolysis liquid oil." Waste Management **58**: 250-259.
Miranda, R., J. Yang, C. Roy and C. Vasile (2001). Vacuum pyrolysis of commingled plastics containing PVC I. Kinetic study.
Miskolczi, N., A. Angyal, L. Bartha and I. Valkai (2009). "Fuels by pyrolysis of waste plastics from agricultural and packaging sectors in a pilot scale reactor." Fuel Processing Technology **90**(7): 1032-1040.
Miskolczi, N., L. Bartha, G. Deák, B. Jóver and D. Kalló (2004). "Thermal and thermo-catalytic degradation of high-density polyethylene waste." Journal of Analytical and Applied Pyrolysis **72**(2): 235-242.
Miskolczi, N. and R. Nagy (2012). "Hydrocarbons obtained by waste plastic pyrolysis: Comparative analysis of decomposition described by different kinetic models." Fuel Processing Technology **104**(0): 96-104.
Miskolczi, N., L. Prof. Bartha and A. Angyal (2009). Pyrolysis of Polyvinyl Chloride (PVC)-Containing Mixed Plastic Wastes for Recovery of Hydrocarbons.
Muhammad, C., J. A. Onwudili and P. T. Williams (2015). "Catalytic pyrolysis of waste plastic from electrical and electronic equipment." Journal of Analytical and Applied Pyrolysis **113**(Supplement C): 332-339.
Murata, K., K. Sato and Y. Sakata (2004). "Effect of pressure on thermal degradation of polyethylene." Journal of Analytical and Applied Pyrolysis **71**(2): 569-589.
Murty, M. V. S., P. Rangarajan, E. A. Grulke and D. Bhattacharyya (1996). "Thermal degradation/hydrogenation of commodity plastics and characterization of their liquefaction products." Fuel Processing Technology **49**(1): 75-90.
N.J. Themelis, M. J. C., J. Bhatti, and L. Arsova (2011). Energy and economic value of non - recycled plastics (NRP) and municipal solid wastes (MSW) that are currently landfilled in the fifity states.

. E. E. Center, Columbia University**:** 33.

Obeid, F., J. Zeaiter, A. a. H. Al-Muhtaseb and K. Bouhadir (2014). "Thermo-catalytic pyrolysis of waste polyethylene bottles in a packed bed reactor with different bed materials and catalysts." Energy Conversion and Management **85**: 1-6.
Odochian, L., C. Moldoveanu, A. M. Mocanu and G. Carja (2011). "Contributions to the thermal degradation mechanism under nitrogen atmosphere of PTFE by TG-FTIR analysis. Influence of the additive nature." Thermochimica Acta **526**(1–2): 205-212.
Olazar, M., G. Lopez, M. Amutio, G. Elordi, R. Aguado and J. Bilbao (2009). "Influence of FCC catalyst steaming on HDPE pyrolysis product distribution." Journal of Analytical and Applied Pyrolysis **85**(1): 359-365.
Onwudili, J. A., N. Insura and P. T. Williams (2009). "Composition of products from the pyrolysis of polyethylene and polystyrene in a closed batch reactor: Effects of temperature and residence time." Journal of Analytical and Applied Pyrolysis **86**(2): 293-303.
Ouadi, M., J. G. Brammer, Y. Yang, A. Hornung and M. Kay (2013). "The intermediate pyrolysis of de-inking sludge to produce a sustainable liquid fuel." Journal of Analytical and Applied Pyrolysis **102**: 24-32.
Park, J. W., S. C. Oh, H. P. Lee, H. T. Kim and K. O. Yoo (2000). "Kinetic analysis of thermal decomposition of polymer using a dynamic model." Korean Journal of Chemical Engineering **17**(5): 489-496.
Park, S. S., D. K. Seo, S. H. Lee, T.-U. Yu and J. Hwang (2012). "Study on pyrolysis characteristics of refuse plastic fuel using lab-scale tube furnace and thermogravimetric analysis reactor." Journal of Analytical and Applied Pyrolysis **97**(0): 29-38.
Patra, C. N. and A. Yethiraj (2000). "Generalized van der Waals density functional theory for nonuniform polymers." The Journal of Chemical Physics **112**(3): 1579-1584.
Perret, B. and B. Schartel (2009). "The effect of different impact modifiers in halogen-free flame retarded polycarbonate blends – II. Fire behaviour." Polymer Degradation and Stability **94**(12): 2204-2212.
Pinto, F., P. Costa, I. Gulyurtlu and I. Cabrita (1999). "Pyrolysis of plastic wastes. 1. Effect of plastic waste composition on product yield." Journal of Analytical and Applied Pyrolysis **51**(1–2): 39-55.
Radhakrishnan Nair, M. N. and M. R. Gopinathan Nair (2011). "Thermogravimetric analysis of PVC/NR-b-PU blends." Journal of Thermal Analysis and Calorimetry **103**(3): 863-872.
Ranzi, E., M. Dente, T. Faravelli, G. Bozzano, S. Fabini, R. Nava, V. Cozzani and L. Tognotti (1997). "Kinetic modeling of polyethylene and polypropylene thermal degradation." Journal of Analytical and Applied Pyrolysis **40**: 305-319.
Reeves, W. P. (1996). "Organic Chemistry, Third Edition (Wade, Jr., L.G.)." Journal of Chemical Education **73**(1): A13.
Reyes-Labarta, J. A., M. M. Olaya and A. Marcilla (2006). "DSC and TGA study of the transitions involved in the thermal treatment of binary mixtures of PE and EVA copolymer with a crosslinking agent." Polymer **47**(24): 8194-8202.
Sáez, I. A., A. F. Font, J. A. C. Ferrer and S. S. Sidhu (2005). "Influence of chlorine and oxygen on the formation of chlorobenzenes during PVC thermal decomposition."
Saha, B. and A. K. Ghoshal (2005). "Thermal degradation kinetics of poly(ethylene terephthalate) from waste soft drinks bottles." Chemical Engineering Journal **111**(1): 39-43.
Salman, M., S. Nisar, Z. Hussain, H. Salman and M. R. Kazimi (2015). "TGA-DSC: A Screening Tool for the Evaluation of Hydrocracking Catalyst Performance." American Journal of Analytical Chemistry **Vol.06No.04**: 12.
Salman, M., Nisar, S. , Hussain, Z. , Salman, H. and Kazimi, M. ((2015)). "TGA-DSC: A Screening Tool for the Evaluation of Hydrocracking Catalyst Performance." American Journal of Analytical Chemistry, **6**: 364-375.
Scott, D. S., S. R. Czernik, J. Piskorz and D. S. A. G. Radlein (1990). "Fast pyrolysis of plastic wastes." Energy & Fuels **4**(4): 407-411.

Seo, Y.-H., K.-H. Lee and D.-H. Shin (2003). "Investigation of catalytic degradation of high-density polyethylene by hydrocarbon group type analysis." Journal of Analytical and Applied Pyrolysis **70**(2): 383-398.
Shah, J., M. R. Jan, F. Mabood and F. Jabeen (2010). "Catalytic pyrolysis of LDPE leads to valuable resource recovery and reduction of waste problems." Energy Conversion and Management **51**(12): 2791-2801.
Sharma, B. K., B. R. Moser, K. E. Vermillion, K. M. Doll and N. Rajagopalan (2014). "Production, characterization and fuel properties of alternative diesel fuel from pyrolysis of waste plastic grocery bags." Fuel Processing Technology **122**: 79-90.
Sharratt, P. N., Y. H. Lin, A. A. Garforth and J. Dwyer (1997). "Investigation of the Catalytic Pyrolysis of High-Density Polyethylene over a HZSM-5 Catalyst in a Laboratory Fluidized-Bed Reactor." Industrial & Engineering Chemistry Research **36**(12): 5118-5124.
Silva, R. B., S. Martins-Dias, C. Arnal, M. U. Alzueta and M. Costa (2015). "Pyrolysis and Char Characterization of Refuse-Derived Fuel Components." Energy & Fuels **29**(3): 1997-2005.
Simon, C. M. and W. Kaminsky (1998). "Chemical recycling of polytetrafluoroethylene by pyrolysis." Polymer Degradation and Stability **62**(1): 1-7.
Singh, R. K. and B. Ruj (2016). "Time and temperature depended fuel gas generation from pyrolysis of real world municipal plastic waste." Fuel **174**: 164-171.
Singh, S., C. Wu and P. T. Williams (2012). "Pyrolysis of waste materials using TGA-MS and TGA-FTIR as complementary characterisation techniques." Journal of Analytical and Applied Pyrolysis **94**: 99-107.
Sobko, A. (2008). Generalized van der Waals-Berthelot equation of state.
Sørum, L., M. G. Grønli and J. E. Hustad (2001). "Pyrolysis characteristics and kinetics of municipal solid wastes." Fuel **80**(9): 1217-1227.
Strezov, V. and T. J. Evans (2009). "Thermal processing of paper sludge and characterisation of its pyrolysis products." Waste Management **29**(5): 1644-1648.
Stuart, B. H. (2005). Spectral Analysis. Infrared Spectroscopy: Fundamentals and Applications, John Wiley & Sons, Ltd**:** 45-70.
Syamsiro, M., H. Saptoadi, T. Norsujianto, P. Noviasri, S. Cheng, Z. Alimuddin and K. Yoshikawa (2014). "Fuel Oil Production from Municipal Plastic Wastes in Sequential Pyrolysis and Catalytic Reforming Reactors." Energy Procedia **47**: 180-188.
Szabo, E., M. Olah, F. Ronkay, N. Miskolczi and M. Blazso (2011). "Characterization of the liquid product recovered through pyrolysis of PMMA–ABS waste." Journal of Analytical and Applied Pyrolysis **92**(1): 19-24.
Uemura, Y., M. Azeura, Y. Ohzuno and Y. Hatate (1999). Products from flash pyrolysis of plastics.
Vasile, C., H. Pakdel, B. Mihai, P. Onu, H. Darie and S. Ciocâlteu (2001). "Thermal and catalytic decomposition of mixed plastics." Journal of Analytical and Applied Pyrolysis **57**(2): 287-303.
Westerhout, R. W. J., J. A. M. Kuipers and W. P. M. van Swaaij (1998). "Experimental Determination of the Yield of Pyrolysis Products of Polyethene and Polypropene. Influence of Reaction Conditions." Industrial & Engineering Chemistry Research **37**(3): 841-847.
Westerhout, R. W. J., J. Waanders, J. A. M. Kuipers and W. P. M. van Swaaij (1997). "Kinetics of the Low-Temperature Pyrolysis of Polyethene, Polypropene, and Polystyrene Modeling, Experimental Determination, and Comparison with Literature Models and Data." Industrial & Engineering Chemistry Research **36**(6): 1955-1964.
Williams, E. A. and P. T. Williams (1997). "Analysis of products derived from the fast pyrolysis of plastic waste." Journal of Analytical and Applied Pyrolysis **40**: 347-363.
Williams, E. A. and P. T. Williams (1997). "The pyrolysis of individual plastics and a plastic mixture in a fixed bed reactor." Journal of Chemical Technology and Biotechnology **70**(1): 9-20.

Williams, P. T. and E. Slaney (2007). "Analysis of products from the pyrolysis and liquefaction of single plastics and waste plastic mixtures." Resources, Conservation and Recycling **51**(4): 754-769.
Williams, P. T. and E. A. Williams (1999). "Fluidised bed pyrolysis of low density polyethylene to produce petrochemical feedstock." Journal of Analytical and Applied Pyrolysis **51**(1–2): 107-126.
Williams, P. T. and E. A. Williams (1999). "Interaction of Plastics in Mixed-Plastics Pyrolysis." Energy & Fuels **13**(1): 188-196.
Wu, C.-H., C.-Y. Chang, J.-L. Hor, S.-M. Shih, L.-W. Chen and F.-W. Chang (1993). "On the thermal treatment of plastic mixtures of MSW: pyrolysis kinetics." Waste Management **13**(3): 221-235.
Xue, Y., S. Zhou, R. C. Brown, A. Kelkar and X. Bai (2015). "Fast pyrolysis of biomass and waste plastic in a fluidized bed reactor." Fuel **156**: 40-46.
Yan, R., D. T. Liang and L. Tsen (2005). "Case studies—Problem solving in fluidized bed waste fuel incineration." Energy Conversion and Management **46**(7): 1165-1178.
Yang, Y., J. G. Brammer, A. S. N. Mahmood and A. Hornung (2014). "Intermediate pyrolysis of biomass energy pellets for producing sustainable liquid, gaseous and solid fuels." Bioresource Technology **169**: 794-799.
Yang, Y., J. G. Brammer, M. Ouadi, J. Samanya, A. Hornung, H. M. Xu and Y. Li (2013). "Characterisation of waste derived intermediate pyrolysis oils for use as diesel engine fuels." Fuel **103**: 247-257.
Yang, Y., J. G. Brammer, J. Samanya, A. K. Hossain and A. Hornung (2013). "Investigation into the performance and emissions of a stationary diesel engine fuelled by sewage sludge intermediate pyrolysis oil and biodiesel blends." Energy **62**: 269-276.
Yoshioka, T., G. Grause, C. Eger, W. Kaminsky and A. Okuwaki (2004). "Pyrolysis of poly(ethylene terephthalate) in a fluidised bed plant." Polymer Degradation and Stability **86**(3): 499-504.
Yuan, G., D. Chen, L. Yin, Z. Wang, L. Zhao and J. Y. Wang (2014). "High efficiency chlorine removal from polyvinyl chloride (PVC) pyrolysis with a gas–liquid fluidized bed reactor." Waste Management **34**(6): 1045-1050.
Zeaiter, J. (2014). "A process study on the pyrolysis of waste polyethylene." Fuel **133**: 276-282.
Zhu, H. M., X. G. Jiang, J. H. Yan, Y. Chi and K. F. Cen (2008). "TG-FTIR analysis of PVC thermal degradation and HCl removal." Journal of Analytical and Applied Pyrolysis **82**(1): 1-9.